

Electronic Thesis and Dissertation Repository

7-8-2015 12:00 AM

Hydrotreatment of Lignin into Green Fuels and Chemicals

Matthew Tymchyshyn
The University of Western Ontario

Supervisor
Dr. Chunbao (Charles) Xu
The University of Western Ontario

Graduate Program in Chemical and Biochemical Engineering
A thesis submitted in partial fulfillment of the requirements for the degree in Doctor of
Philosophy
© Matthew Tymchyshyn 2015

Follow this and additional works at: <https://ir.lib.uwo.ca/etd>

 Part of the [Catalysis and Reaction Engineering Commons](#)

Recommended Citation

Tymchyshyn, Matthew, "Hydrotreatment of Lignin into Green Fuels and Chemicals" (2015). *Electronic Thesis and Dissertation Repository*. 2979.
<https://ir.lib.uwo.ca/etd/2979>

This Dissertation/Thesis is brought to you for free and open access by Scholarship@Western. It has been accepted for inclusion in Electronic Thesis and Dissertation Repository by an authorized administrator of Scholarship@Western. For more information, please contact wlsadmin@uwo.ca.

HYDROTREATMENT OF LIGNIN INTO GREEN FUELS AND CHEMICALS

(Thesis format: Integrated Article)

by

Matthew Alexander Tymchyshyn

Graduate Program in Chemical and Biochemical Engineering

A thesis submitted in partial fulfillment
of the requirements for the degree of
Doctor of Philosophy

The School of Graduate and Postdoctoral Studies
The University of Western Ontario
London, Ontario, Canada

© Matthew Tymchyshyn 2015

Abstract

Concerns about declining non-renewable fossil resources, energy security, climate change and sustainability are increasing worldwide. This has resulted in an increased interest in the development of alternatives to fossil resources not only for energy, but particularly for chemical production on a global level. There are a number of promising alternatives to fossil resources, however, lignocellulosic biomass such as forestry residues and wood waste (bark, sawdust, etc.) seem to be the most promising. They are widely available, renewable and a non-food resource. Therefore woody biomass holds the promise of being a sustainable resource for both energy and chemical production.

The lignin component of woody biomass is of particular interest as it comprises the world's largest natural source of aromatic compounds and is produced in large quantities as a by-product of pulp and paper processing. The main challenge in lignin utilization for fuels and chemicals is that it is composed of very large molecules with low heating values (due to high oxygen content) and low reactivity. Accordingly, the overall objective of this work is the production of chemicals and fuels by the catalytic hydroprocessing of lignin and lignin-derived bio-oils aiming to reduce their molecular weights and oxygen contents.

This work investigated the catalytic hydrotreatment (hydroprocessing) of a number of different lignins as well as depolymerized hydrolysis lignin for the production of fuels and chemicals. Several supported metal hydrogenation catalysts were investigated for the depolymerization, deoxygenation and desulfurization of Kraft lignin (KL) organosolv lignin (OL) and hydrolysis lignin (HL) under hydrogen atmospheres to produce depolymerized lignins. All of the catalysts tested were effective in depolymerizing the lignin feedstocks, however, the alumina-supported catalysts and the carbon-supported Ni catalyst did not perform as well as the carbon-supported Ru catalyst and FHUDS-2 (an industrial HDS catalyst). The molecular weights of the depolymerized lignins using these last two catalysts at 300 °C were markedly lower than the OL and KL feeds (~1,000 vs. 2,600 and 10,200 g/mol, respectively). In addition, the sulfur contents of the depolymerized Kraft lignins were drastically reduced.

Targeting the development of effective and inexpensive catalysts for the hydrotreatment of lignin and lignin-derived bio-oils to produce chemicals and fuels, screening of catalysts was

performed using guaiacol as model compound. The most effective catalyst under the conditions tested was found to be 1 wt.% Mo-doped 5 wt.% Ru supported on activated charcoal (MoRu/AC). The selected catalyst proved to be very effective for hydrotreatment of organosolv lignin ($M_W \approx 2,600$ g/mol) into a liquid product comprising >85% phenolic compounds with a M_W of 460 g/mol at ~70% yield at 340 °C. This catalyst was also successfully employed in the hydroprocessing of hydrolysis lignin (HL) and depolymerized hydrolysis lignin (DHL).

Keywords

Hydrotreatment, hydroprocessing, catalysts, carbon-supported catalyst, MoRu, Kraft lignin, organosolv lignin, hydrolysis lignin, depolymerized lignin, fuels, chemicals

Co-Authorship Statement

Chapter 3: Reductive depolymerization of Kraft and organosolv lignin for aromatic chemicals and materials

Authors: Matthew Tymchyshyn, Zhongshun Yuan, and Chunbao (Charles) Xu

The experimental work was performed by Matthew Tymchyshyn and Zhongshun Yuan who also analyzed the results and wrote the paper. The work was performed under the supervision of Charles Xu who reviewed and revised the paper which has been submitted for publication.

Chapter 4: Catalyst screening for the hydrotreatment of lignin using guaiacol as a model compound

Authors: Matthew Tymchyshyn, Zhongshun Yuan, and Chunbao (Charles) Xu

The experimental work was performed by Matthew Tymchyshyn under the guidance of Zhongshun Yuan. The results were interpreted by Matthew Tymchyshyn with Zhongshun Yuan. The work was performed under the supervision of Charles Xu who reviewed and revised the paper which is to be submitted for publication.

Chapter 5: Hydrotreatment of organosolv lignin using carbon-based catalysts

Authors: Matthew Tymchyshyn, Zhongshun Yuan, and Chunbao (Charles) Xu

The experimental work was performed by Matthew Tymchyshyn under the guidance of Zhongshun Yuan. The results were interpreted by Matthew Tymchyshyn and Zhongshun Yuan. The work was performed under the supervision of Charles Xu who reviewed and revised the paper which is to be submitted for publication.

Chapter 6: Reductive depolymerization of hydrolysis lignin for aromatic chemicals and fuels

Authors: Matthew Tymchyshyn, Malaya Nanda, Zhongshun Yuan, and Chunbao (Charles) Xu

The experimental work was performed by Matthew Tymchyshyn with the assistance of Malaya Nanda under the guidance of Zhongshun Yuan. The results were interpreted by Matthew Tymchyshyn and Zhongshun Yuan. The work was performed under the supervision of Charles Xu who reviewed and revised the paper which is to be submitted for publication.

Chapter 7: Hydrotreatment of depolymerized hydrolysis lignin

Authors: Matthew Tymchyshyn, Malaya Nanda, Nubla Mahmood, Zhongshun Yuan, and Chunbao (Charles) Xu

The experimental work was performed by Matthew Tymchyshyn with the assistance of Nubla Mahmood and Malaya Nanda under the guidance of Zhongshun Yuan. The results were interpreted by Matthew Tymchyshyn and Zhongshun Yuan. The work was performed under the supervision of Charles Xu who reviewed and revised the paper which is to be submitted for publication.

Acknowledgments

Many people have contributed to this body of work, without whose assistance and support, it would not have been completed.

First, I would like to express my special appreciation and deepest gratitude to Dr. Chunbao (Charles) Xu for providing me with the opportunity to pursue my doctoral degree under his supervision. His encouragement, expert guidance, and advice were invaluable. Without his continuous support, this thesis could not have been realized.

My sincere thanks also go to Dr. Zhongshun (Sean) Yuan, for his helpful discussions, suggestions, instruction, and assistance over the course of my research. I also extend my appreciation to Dr. Franco Berruti for acting as my co-supervisor until Dr. Xu effected his transfer to the University of Western Ontario from Lakehead University as well as serving as a member of my advisory committee along with Dr. Cedric Briens. Their encouragement and suggestions were much valued.

I would also like to thank Ms. Caitlin Marshall, Ms. Fang (Flora) Cao, Mr. Rob Taylor, and Mr. Thomas Johnston for their contributions and assistance in sample analysis and characterization as well as equipment construction and maintenance.

I wish to express my gratitude to my colleagues at Western's Institute of Chemicals and Fuels from Alternative Resources (ICFAR), past and present, for their assistance and friendship. In particular, I wish to thank Nick Prociw, Clayton Stanlick, Dr. Francisco Sanchez, Ehsan Reyhanitash, Izad Behnia, Alejandro Costa, Nubla Mahmood, Sadra Souzanchi, Fatemeh Ferdosian, Dr. Shuna Cheng, and Dr. Shanghuan Feng. They could always be counted on to lend an ear, offer a suggestion, or brighten my day when a particular day's experiment had gone awry. A very special thanks goes to Malaya Nanda, with whom I spent two and a half years at the Sarnia-Western Research Park, for his suggestions and questions and putting up with me in general.

I also extend my gratitude to my examination board: Mr. Douglas C. Elliott from Pacific Northwest National Laboratory and Drs. Mita Ray, Shahzad Barghi and Zhifeng Deng from the University of Western Ontario, for their efforts in reviewing my thesis. Their comments and suggestions have greatly improved this work.

Financial support from NSERC under the auspices of the Lignoworks project is gratefully acknowledged. Additional funding was provided by the Government of Ontario via an NSERC Discovery Grant, the NSERC/FPInnovations Industrial Research Chair program and an ORF-RE grant in Forest Biorefinery, awarded to my supervisor, Prof. Charles Xu. I also recognize financial support provided by the Mitacs Accelerate internship program.

Finally, I would like to thank my family and friends outside of school for their support and encouragement.

Dedication

This work is dedicated to my family.

To my sister, uncles, aunts and cousins whose encouragement throughout helped to keep me going. I'm going to hold you to your word regarding that party you promised!

To my nephews, Kaleb and Sebastian, and later, Simon, whose boundless curiosity reminded me of what it was like to be a child again, and whose antics could divert me from the mountain of work yet to be done, if only for a little while.

And last, but not least, to my parents for their inexhaustible love, patience and support.

Table of Contents

Abstract.....	ii
Co-Authorship Statement.....	iv
Acknowledgments.....	vi
Dedication.....	viii
Table of Contents.....	ix
List of Tables.....	xv
List of Figures.....	xviii
List of Schemes.....	xxii
List of Abbreviations and Symbols.....	xxiii
Chapter 1	1
1 General Introduction.....	1
1.1 Introduction.....	1
1.2 Background.....	1
1.3 Research Objectives.....	6
1.4 Approaches and Methodology.....	7
1.5 Thesis Overview.....	9
1.6 References.....	11
Chapter 2	15
2 Literature Review.....	15
2.1 Thermochemical Conversion of Biomass.....	16
2.1.1 Fast Pyrolysis.....	16
2.1.2 High-pressure Liquefaction.....	19
2.2 Bio-oil Upgrading.....	20

2.3	Hydroprocessing of Model Compounds.....	23
2.4	Hydroprocessing of Bio-oils.....	24
2.5	Lignin	26
2.5.1	Lignin Production	27
2.6	Lignin Decomposition.....	28
2.6.1	Lignin Pyrolysis	29
2.6.2	Lignin Hydrogenolysis.....	30
2.6.3	Lignin Oxidation	32
2.7	Catalysts	33
2.7.1	Acid Catalysts	34
2.7.2	Alkali-Catalyzed Depolymerization	36
2.8	Solvents	37
2.8.1	Hydrogen-donating Solvents.....	37
2.8.2	Supercritical Solvents.....	40
2.9	Summary.....	41
2.9.1	Model Compounds.....	43
2.9.2	Catalysts.....	43
2.9.3	Catalyst Support.....	44
2.9.4	Solvents.....	44
2.10	References	46
Chapter 3		63
3	Reductive depolymerization of Kraft and organosolv lignin for aromatic chemicals and materials.....	63
3.1	Introduction	63
3.2	Experimental.....	66
3.2.1	Materials.....	66

3.2.2	Experimental apparatus and procedure	66
3.2.3	Product Characterization	67
3.3	Results and discussion	67
3.3.1	Effect of catalyst	67
3.3.2	Effect of catalyst loading	71
3.3.3	Effect of reaction temperature.....	72
3.3.4	Effect of reaction time.....	75
3.3.5	Effect of solvent	76
3.4	Product characterization	76
3.5	Conclusions	81
3.6	References	82
Chapter 4	84
4	Catalyst screening for the hydroprocessing of lignin using guaiacol as a model compound	84
4.1	Introduction	84
4.2	Experimental.....	87
4.2.1	Materials.....	87
4.2.2	Experimental apparatus and procedure	88
4.3	Results and Discussion	89
4.3.1	Fresh catalyst characterization	89
4.3.2	Catalyst screening	90
4.3.3	Process Optimization	97
4.3.4	Spent catalyst characterization.....	101
4.4	Conclusions	105
4.5	References	106

Chapter 5	109
5 Hydroprocessing of organosolv lignin for aromatic chemicals and materials using carbon-based catalysts	109
5.1 Introduction	109
5.2 Experimental.....	111
5.2.1 Materials.....	111
5.2.2 Experimental apparatus and procedure	113
5.3 Results and Discussion	114
5.3.1 Catalyst characterization	114
5.3.2 DOL Yields	114
5.3.3 Hydrogen consumption during OL hydroprocessing.....	120
5.3.4 DOL product characterization.....	121
5.3.5 Elemental analysis of DOL	124
5.3.6 GC/MS analysis of DOL.....	127
5.3.7 FTIR analysis of DOL.....	129
5.3.8 NMR analysis of DOL	131
5.4 Conclusions	133
5.5 References	134
Chapter 6	137
6 Reductive depolymerization of hydrolysis lignin for aromatic chemicals and fuels.....	137
6.1 Introduction	137
6.2 Experimental.....	140
6.2.1 Materials.....	140
6.2.2 Method and apparatus	142
6.3 Results and Discussion	143
6.3.1 Effect of catalyst and temperature on HL bio-oil yields	143

6.3.2	Elemental analysis of HL bio-oils.....	147
6.3.3	Formation of gaseous products and hydrogen consumption during HL hydroprocessing	150
6.3.4	GPC analysis of HL bio-oils	153
6.3.5	FTIR analysis of HL bio-oils	156
6.3.6	GC/MS analysis of HL bio-oils	159
6.3.7	NMR analysis of HL-derived bio-oils	162
6.4	Conclusions	164
6.5	References	165
Chapter 7	168
7	Hydroprocessing of depolymerized hydrolysis lignin.....	168
7.1	Introduction	168
7.2	Experimental.....	170
7.2.1	Materials.....	170
7.2.2	Method and apparatus	171
7.3	Results and Discussion	172
7.3.1	Catalyst characterization	172
7.3.2	Effect of catalyst and temperature.....	173
7.3.3	DHL gasification.....	176
7.3.4	DHL hydrogen consumption.....	177
7.3.5	Elemental analysis of hydroprocessed DHL.....	179
7.3.6	GPC analysis of hydroprocessed DHL	182
7.3.7	GC/MS analysis of hydroprocessed DHL.....	186
7.3.8	FTIR analysis of hydroprocessed DHL	187
7.3.9	NMR analysis of hydroprocessed DHL.....	190
7.4	Conclusions	193

7.5	References	194
Chapter 8	197
8	Conclusions and Future Work	197
8.1	Conclusions	197
8.2	Future Work.....	201
Curriculum Vitae	203

List of Tables

Table 2.1	Typical properties of pyrolysis bio-oil (before upgrading) and of a petroleum-based heavy fuel oil (Czernik and Bridgwater, 2004)	17
Table 2.2	Elemental composition of bio-oil from wood and of a heavy fuel oil (Şenol, 2007b)	21
Table 3.1	Catalyst screening	68
Table 3.2	Temperature effect on yield and M_w	72
Table 3.3	KL and DKL hydroxyl groups	80
Table 3.4	Elemental analysis (CHNSO) of KL and DKL.....	81
Table 4.1	Textural analysis of fresh catalysts	90
Table 4.2	Guaiacol conversion and product yields from the guaiacol hydroprocessing experiments with various catalysts (2 h, 350°C with neat guaiacol, 9 MPa H ₂) ..	92
Table 4.3	Molar yields of main gas species and total molar C yield in gas from the guaiacol hydroprocessing experiments.....	95
Table 4.4	Guaiacol conversion and product yields from the guaiacol hydroprocessing experiments with MoRu/C catalyst at selected conditions	100
Table 5.1	Textural analysis of the carbon-supported catalysts	114
Table 5.2	DOL and product yields.....	116
Table 5.3	Comparison of textural properties of MoRu/AC catalyst after reaction at different temperatures	118
Table 5.4	Comparison of textural properties of fresh and spent catalysts at 300 °C	118
Table 5.5	Composition of gaseous products (vol. %) from OL hydroprocessing with different catalysts and at different temperatures	119

Table 5.6	Gasification of OL	120
Table 5.7	DOL molecular weight as a function of catalyst and reaction temperature.....	122
Table 5.8	Elemental analysis of DOL produced using different catalysts at 300 °C.....	125
Table 5.9	Elemental analysis of DOL produced at different temperatures using different catalysts.....	126
Table 5.10	Comparison of compounds found in DOL with MoRu/AC and Ru/C at different temperatures	128
Table 6.1	Chemical and elemental composition (d.a.f) of hydrolysis lignin (HL).....	140
Table 6.2	Textural properties of the carbon-supported catalysts and activated charcoal support.....	142
Table 6.3	Elemental composition of HL-derived bio-oils	148
Table 6.4	Composition of gaseous products (vol.%) from experiments with different catalysts and temperatures	151
Table 6.5	Effects of reaction time and temperature on molecular weight and distribution of bio-oils from the hydroprocessing of HL in the presence of MoRu/AC catalyst	155
Table 6.6	Composition of HL bio-oils produced at 340 °C with different catalysts	160
Table 6.7	Composition of HL bio-oils produced with MoRu/AC catalyst at different temperatures	161
Table 7.1	Catalyst textural properties	173
Table 7.2	DHL hydrotreatment product yields	175
Table 7.3	Typical DHL hydroprocessing gas composition (mol%) vs. temperature and catalyst	176
Table 7.4	DHL gasification during hydroprocessing vs. temperature and catalyst	177

Table 7.5	Elemental composition of DHL and DHL-derived bio-oils	180
Table 7.6	Hydroprocessed DHL molecular weights	183
Table 7.7	Comparison of hydroprocessed DHL composition vs. temperature	187

List of Figures

Figure 1.1	Typical composition of woody biomass	5
Figure 1.2	Structure of lignin	6
Figure 1.3	Schematic and photos of the mini-reactor system	8
Figure 3.1	Molecular weight of depolymerized lignin using different catalysts.....	69
Figure 3.2	Yields of depolymerized product and solid residue for Kraft lignin (a) and organosolv lignin (b).....	70
Figure 3.3	Effect of temperature on DKL and DOL yields.....	73
Figure 3.4	Effect of temperature on DKL and DOL MW using Ru catalyst	74
Figure 3.5	Effect of temperature on DKL and DOL MW using FHUDES-2 catalyst	75
Figure 3.6	Effect of reaction time on DKL MW	76
Figure 3.7	GPC curves of the original and depolymerized lignin products from KL.....	77
Figure 3.8	GPC curves of the original and depolymerized lignin products from OL.....	77
Figure 3.9	IR spectra of KL and DKL.....	78
Figure 3.10	NMR spectrum of acetylated DKL	79
Figure 4.1	Conversion of guaiacol during hydroprocessing at 9 MPa cold hydrogen pressure, 350 °C, and 2 h reaction time	91
Figure 4.2	Molar yield of the liquid products after guaiacol hydroprocessing at 9 MPa cold hydrogen pressure, 350°C, and 2 h reaction time	94
Figure 4.3	Hydrogen consumption during guaiacol hydroprocessing at 9 MPa cold hydrogen pressure, 350°C, and 2 h reaction time	96

Figure 4.4	Cumulative carbon balances for the guaiacol hydroprocessing tests with various catalysts (2 h, 350°C, 9 MPa H ₂)	97
Figure 4.5	Guaiacol conversion as a function of reaction time, temperature and initial H ₂ pressure with MoRu/C catalyst.....	99
Figure 4.6	TGA plots for fresh (a) and spent (b) Ru/AC and MoRu/AC catalysts from the guaiacol hydroprocessing tests (2 h, 350°C, 9 MPa H ₂).....	101
Figure 4.7	dTGA plots for fresh and spent Ru/AC and MoRu/AC catalysts from the guaiacol hydroprocessing tests (2 h, 350°C, 9 MPa H ₂).....	103
Figure 4.8	XRD spectra of selected fresh and spent catalysts.....	104
Figure 5.1	Yield of DOL as a function of reaction temperature	115
Figure 5.2	Cumulative DOL Product Yields.....	117
Figure 5.3	Hydrogen consumption during OL hydroprocessing.....	121
Figure 5.4	GPC curves for DOL obtained at 300 °C using different catalysts	123
Figure 5.5	GPC curves for DOL obtained at different temperatures using MoRu/AC (a) and Ru/C (b)	124
Figure 5.6	van Krevelen plot for DOL produced by different catalysts at 300 °C	125
Figure 5.7	van Krevelen plot for DOL produced by different catalysts at different temperatures.....	127
Figure 5.8	GC/MS plots for DOL obtained at 250 °C (bottom), 300 °C (middle) and 340 °C (top)	129
Figure 5.9	FTIR spectra of OL feed and DOL products obtained at different temperatures with MoRu/AC and the expanded fingerprint region (top).	130
Figure 5.10	NMR spectra for OL feed (bottom) and MoRu/AC DOL at 300 °C (middle) and 340 °C (top)	132

Figure 6.1	HL bio-oil yields as a function of temperature	144
Figure 6.2	HL bio-oil yields as a function of soaking time at reaction temperature.....	145
Figure 6.3	Cumulative product yields as a function of reaction temperature and catalyst	146
Figure 6.4	Photographs of solid residue from HL depolymerization at 200 °C with MoRu/AC catalyst (left) and HL feed before reaction (right)	147
Figure 6.5	Hydrogen and oxygen contents in HL bio-oils produced at different temperatures	148
Figure 6.6	van Krevelen plot for HL bio-oils obtained at 340 °C.....	149
Figure 6.7	van Krevelen plot for HL bio-oils obtained at different temperatures.....	150
Figure 6.8	HL hydrogen consumption vs. temperature.....	152
Figure 6.9	Hydrogen consumption vs. reaction time and temperature during hydroprocessing of HL with MoRu/AC catalyst	153
Figure 6.10	GPC curves for bio-oils obtained at 340 °C and different catalysts	154
Figure 6.11	GPC curves for HL at different reaction times	154
Figure 6.12	Normalized FTIR spectra for HL bio-oils as a function of reaction temperature with the fingerprint region expanded.....	157
Figure 6.13	Normalized FTIR spectra (expanded fingerprint region) for HL-derived bio-oils obtained at 340 °C with different catalysts	158
Figure 6.14	GC/MS plots for HL bio-oils produced at 340 °C with different catalysts	159
Figure 6.15	GC/MS plots for HL bio-oils produced with MoRu/AC catalyst at different temperatures.....	161
Figure 6.16	H-NMR spectra of HL bio-oil obtained after 1 h reaction using MoRu/AC at 200 °C (top) and 340 °C (bottom)	163

Figure 7.1	Yields of DHL bio-oil vs. temperature and catalyst	174
Figure 7.2	Cumulative product yields for hydroprocessed DHL	175
Figure 7.3	DHL gasification during hydroprocessing.....	177
Figure 7.4	Hydrogen consumption during DHL hydroprocessing vs. reaction temperature and time.....	178
Figure 7.5	van Krevelen plot of DHL hydroprocessed at different temperatures	181
Figure 7.6	van Krevelen plot of DHL and DHL hydroprocessed with different catalysts	182
Figure 7.7	GPC curves for DHL at different reaction temperatures for Ru/C (top) and MoRu/AC catalyst (bottom)	184
Figure 7.8	GPC curves of MoRu/AC-derived DHL bio-oil at different reaction times....	185
Figure 7.9	Comparison of the GC spectra for hydroprocessed DHL obtained with MoRu/AC catalyst at different temperatures	186
Figure 7.10	FTIR spectra of DHL bio-oils obtained using MoRu/C catalyst at different temperatures.....	188
Figure 7.11	H-NMR spectra of DHL (bottom) and DHL bio-oils obtained at 250 (middle) and 340 °C (top).....	192

List of Schemes

Scheme 1.1	Product separation scheme	8
Scheme 3.1	Routes of lignin valorization	65

List of Abbreviations and Symbols

ATR	attenuated total reflectance
BCD	base-catalyzed depolymerization
BET	Brunauer-Emmett-Teller surface area analysis
C	carbon
¹³ C-NMR	carbon 13 nuclear magnetic resonance spectroscopy
C/L	catalyst to lignin mass ratio
CHNS	carbon, hydrogen, nitrogen and sulfur elemental analysis
d.a.f.	dry, ash-free basis
d.b.	dry basis
DHL	depolymerized hydrolysis lignin
DKL	depolymerized Kraft lignin
DMSO-d ₆	deuterated dimethylsulfoxide
DOL	depolymerized organosolv lignin
FCC	fluid catalyzed cracking
FTIR	Fourier transform infrared spectroscopy
GC/FID	gas chromatography/flame ionization detector
GC/MS	gas chromatography/mass spectroscopy
GC/TCD	gas chromatography/thermal conductivity detector
GPC	gel permeation chromatography
H	hydrogen

$^1\text{H-NMR}$	proton nuclear magnetic resonance spectroscopy
H/C	molar ratio of H to C in a material
HDS	hydrodesulfurization
HDO	hydrodeoxygenation
HL	hydrolysis lignin
HPLC	high performance liquid chromatography
KL	Kraft lignin
KOH	potassium hydroxide
MW	molecular weight, in g/mole
M_n	number average molecular weight, in g/mole
M_w	weight average molecular weight, in g/mole
NaOH	sodium hydroxide
O	oxygen
O/C	molar ratio of O to C in a material
OL	organosolv lignin
S	sulfur
SEC	size exclusion chromatography
SR	solid residue
Temp	temperature
TGA	thermogravimetric analysis
THF	tetrahydrofuran
UV	ultraviolet

Chapter 1

1 General Introduction

1.1 Introduction

The main objective of this project was to investigate and develop effective carbon-supported hydroprocessing catalysts for the depolymerization of lignin as well as the upgrading of lignin-derived bio-oil. The chemical and physical properties of the resulting products were analyzed to demonstrate the effectiveness of these catalysts.

1.2 Background

Over the past century a majority of the world's energy demands was met by fossil fuels, comprising: 30% petroleum, 23% natural gas, 22% coal, 6% nuclear, and 19% renewable (Song, 2002). Chemical industries and energy production based on fossil fuel resources are expected to gradually phase out over the course of the 21st century due to the depletion of the fossil resources that these industries rely on (Okkerse and Van Bakkum, 1999). Biomass feedstocks such as agricultural/forestry residues and wood wastes (harvest residues, slash, sawdust, bark, etc.) have the potential to be a large source for energy, fuels, chemicals and materials (Karagoz *et al.*, 2005; Ogi and Yokohama, 1993). Many countries have legislation set in place to promote the use of biomass energy and bio-fuels. For example, the Canadian federal government has enacted a target of 5% ethanol in gasoline by 2010, which will require the production of more than 300 million litres of cellulosic ethanol per year to meet this target. The European Union has set an objective to substitute conventional fuels with biomass-derived fuels (bio-fuels) in the transport sector with a market share of 5.75% by the end of 2010 (EU Directive 2003/30/EC). In December 2007, then President Bush of the U.S.A. signed into law a Renewable Fuels Standard (RFS) that called for at least 36 billion gallons of ethanol and other bio-fuels to be used nationwide by 2022, including a minimum of 9 billion gallons in 2008, and 20.5 billion gallons by 2015 or about 15% replacement of the U.S.A.'s gasoline consumption.

Bio-energy is a blanket term that refers to all forms of renewable energy that are derived from biomass feedstocks. Biomass feedstocks typically have a heating value comparable to that of low rank coal (lignite and sub-bituminous coals). The heating values range from 8 MJ/kg for green matter to between 17-23 MJ/kg for dry plant matter. The Earth's natural biomass of 150 billion metric tonnes of dry biomass replacement represents an energy supply of around 3000 EJ (3×10^{21} J) per year, or about 6 times the world's total energy consumption. Although these resources are renewable, carbon-neutral, and remarkably abundant, they are also very bulky and difficult to transport, handle, and store. In order to make use of these resources it is, therefore, necessary to develop cost-effective technologies to convert them into liquid bio-fuels of a higher energy density and other valuable chemicals (Yamazaki *et al.*, 2006).

Biomass conversion technologies may be classified into two major categories: bio-chemical processes and thermo-chemical processes (Sharma and Bakshi, 1991; Bridgwater, 1991; Holt and Van der Burgt, 1998). Biologically-based technologies use acid/engineered enzymes to break down lignocellulosic materials with the aim of hydrolyzing the cellulose into glucose that can be fermented into ethanol or other chemicals. The development of new enzymes is still at the research stage, and most of the enzymes and the microorganisms that have been developed are strongly dependent on the chemical composition of the feedstocks, and are therefore applicable only to specific homogenous feedstocks. In addition, enzymatic processes are quite slow. As a result, current fermentation-based technology does not make the cellulosic ethanol production economically viable. In addition, the blending of high ratios of fuel alcohol into gasoline would require the modification of existing engines and delivery systems (Holt and Van der Burgt, 1998).

Thermo-chemical processes for the production of liquid bio-fuels include indirect liquefaction processes e.g. gasification combined with various catalytic processes for production of synthetic fuels (e.g., methanol, ethanol and high quality diesel), and direct liquefaction technologies mainly pyrolysis and high pressure liquefaction processes.

Direct liquefaction of biomass followed by upgrading and refining is regarded as a promising approach in addition to indirect liquefaction processes such as the MTG (Mobil methanol to gasoline) and the SMDS (Shell middle distillate synthesis) processes currently under devel-

opment. Direct liquefaction of biomass for the production of bio-oil/bio-crude has attracted increasing interest in recent years due to increasing crude oil price and increasing concerns over greenhouse gas emissions. The bio-oil/bio-crude products from direct liquefaction can be upgraded into high quality liquid transportation fuels (Sharma and Bakshi, 1991).

Fast pyrolysis (operating at low pressures of 0.1-0.5 MPa but high temperatures >500 °C) is currently the only industrially realized technology for production of bio-oils from biomass. However, pyrolysis oils have high oxygen and water contents and only about half the caloric content of petroleum (<20 MJ/kg).

High-pressure liquefaction technology, on the other hand, normally operates at moderate temperatures (<400 °C) but higher pressures of 5-20 MPa in the presence of suitable solvents (water or organics) with or without catalysts and has the potential for producing liquid oils (also called bio-oils or bio-crudes) with much higher caloric values (25-35 MJ/kg) (Yamazaki *et al.*, 2006; Xu and Etcheverry, 2008).

Two typical technologies for upgrading of bio-oils include catalytic cracking and catalytic hydrotreating. Note that the term 'hydrotreatment' has a specific meaning in petroleum processing operations: namely it is a blanket term for the removal of heteroatoms (specifically S, N and metals) from petroleum feeds using hydrogen. This term has carried over to bio-oil upgrading and refers to the HDO and hydrogenation of bio-oil (as well as the HDS of sulfur-containing lignins and bio-oils derived from these feeds). Some researchers have instead used the term 'hydroprocessing' to differentiate these processes from those found in petroleum operations. In this work, the terms are used interchangeably.

Catalytic cracking processes, using cracking catalysts (zeolites, silica-alumina and molecular sieves), are performed at or near atmospheric pressure without the addition of hydrogen. The advantages of low-pressure operation without the need of hydrogen, i.e. lower equipment costs and lack of expensive hydrogen, have attracted much interest in the literature on the upgrading of bio-oils (Adjave and Bakhshi, 1995a and 1995b; Katikaneni *et al.*, 1995; Williams and Horne, 1995; Adjave *et al.*, 1996; Graça *et al.*, 2011). However, the yield of hydrocarbon oils is very low because of high yields of both char/coke and tars. In addition, the deposition of these undesirable products on the catalyst results in gradual catalyst deactivation and necessitates periodical or continual regeneration of the catalysts. In contrast, cata-

lytic hydrotreating processes operate at high pressures under a hydrogen atmosphere and/or in the presence of hydrogen donor solvents (Craig and Coxworth, 1987; Maggi and Delmon, 1993; Baker and Elliott, 1996; Kleinert *et al.*, 2009; Li *et al.*, 2012; Huang *et al.*, 2014). Over the past 30 years, significant efforts have been made in hydrodeoxygenation (HDO) of biomass-derived oils. Research into the catalytic chemistry and kinetics of the hydroprocessing of various model compounds containing oxygen, such as phenolic compounds and aromatic ethers, have been reviewed by Furimsky (2000) and Elliott (2007).

The bio-oils/bio-crudes produced by the pyrolysis or liquefaction of biomass are a complex mixture of oxygen-containing compounds in the form of phenol and benzene derivatives, hydroxyketones, carboxylic acids and esters, and aliphatic and aromatic alcohols which all contribute to the oxygen content of the oil (Appell *et al.*, 1969; Minowa *et al.*, 1998; Qu *et al.*, 2003). In addition, water originating from both the moisture originally present in the feedstock as well as water produced during the pyrolysis and direct liquefaction processes adds to the oxygen content in bio-oil or bio-crude (Bridgwater, 2003; Czernik and Bridgwater, 2004). The total oxygen content of bio-oils can be as high as 40-50 wt.% for pyrolysis oils and 20-30 wt.% for bio-crudes from high-pressure liquefaction processes, depending on the origin of the biomass and the process conditions, e.g. temperature, residence time, heating rate and the catalysts used (Bridgwater, 1994; Furimsky, 2000). The presence of high levels of oxygen in bio-oils is a limitation in their use as liquid transportation fuels since high oxygen contents result in high viscosity, low heating value, poor thermal and chemical stability, corrosivity (due to organic acids present) and immiscibility with hydrocarbon fuels (Bridgwater, 2003; Czernik and Bridgwater, 2004; Yaman, 2004). The bio-crudes/bio-oils must therefore be upgraded by reducing or completely eliminating their oxygen content (Bridgwater, 1994; Bridgwater, 1996).

A potentially more profitable exercise is the production of chemicals from only the lignin component of biomass. Biomass is, for the most part, composed of cellulose, hemicelluloses and lignin with very small amounts of other components such as ash and extractives. The typical composition of woody biomass is shown in Figure 1.1 below.

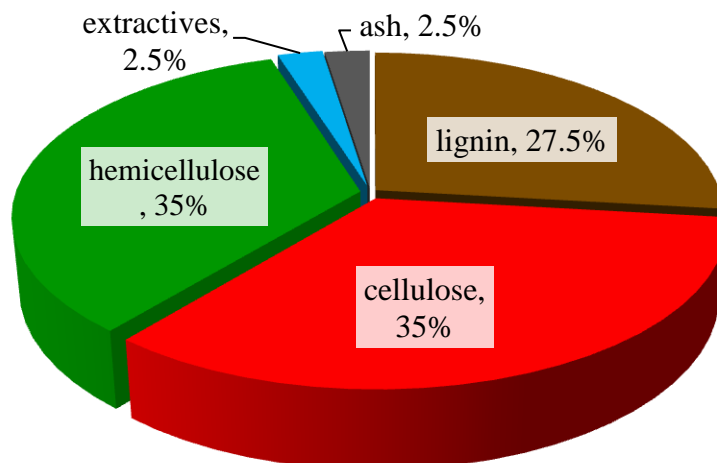


Figure 1.1 Typical composition of woody biomass

Currently the lignin component in biomass is mainly utilized for process heat by direct combustion. The large amounts of lignin produced in pulp mills are problematic in that the recovery boilers present a bottleneck. A recent study by FPIinnovations determined that a significant fraction of the lignin produced in a pulp mill could be removed without unduly affecting the unit's material and energy balances. It was calculated that, on average, North American pulp mills could produce 30 tonnes/day of lignin and that for each tonne of lignin removed from the process, a mill could process an additional tonne of pulp.

Lignin is an amorphous polymer (Figure 1.2) comprised of three types of phenyl propane derivatives: guaiacyl alcohol, syringyl alcohol, and *p*-coumaryl alcohol (Mohan *et al.* 2006). It provides support and rigidity to the cell walls and is more resistant to most forms of biological attack in comparison with cellulose and other polysaccharides (Akin and Benner, 1988; Baurhoo *et al.*, 2008; Kirk, 1971) and is the largest natural source of aromatic compounds.

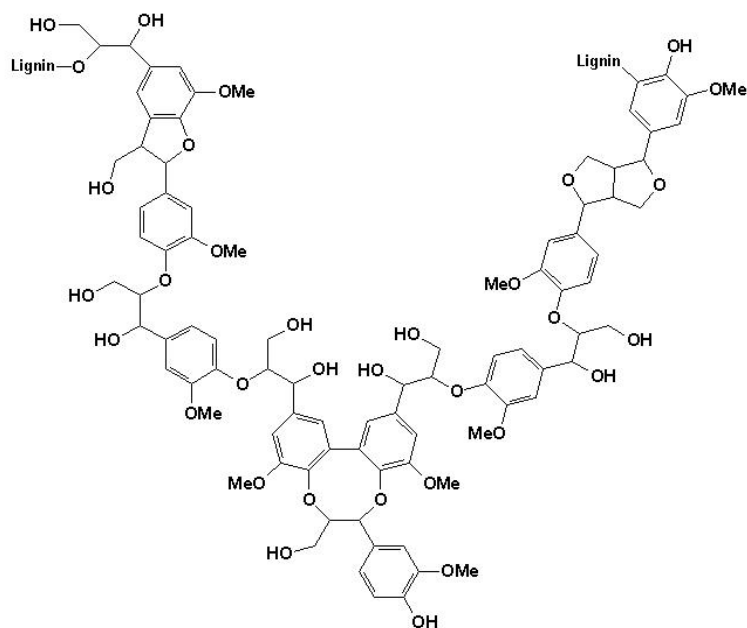


Figure 1.2 Structure of lignin

Due to its chemical composition, lignin is a promising source for chemicals and fuels such as phenols and aromatics via thermochemical and/or catalytic decomposition of the lignin macromolecule into mono-lignols and other compounds followed by hydroprocessing to remove oxygen. While the removal of oxygen is necessary to minimize re-condensation of the depolymerized lignin and to decrease acidity, the hydrodeoxygenation and hydrogenation of lignin and lignin-derived bio-oils under less severe conditions than those required to upgrade whole biomass-derived bio-oil can produce both high value oxygenated and deoxygenated compounds from the lignin precursor.

1.3 Research Objectives

As discussed above, biomass is an abundant and renewable resource that can be exploited for the production of aromatic compounds and fuels. However, effective utilization of this resource is complicated by the presence of the carbohydrate fraction of biomass which decomposes into oxygen-rich compounds upon thermal degradation. Lignin is produced in mass quantity by pulp and paper manufacturing, as well as by solvolytic and enzymatic extraction.

It comprises the world's largest natural source of aromatic compounds. Effective utilization of this resource by depolymerization and hydroprocessing, thus avoid the challenges of whole biomass degradation, is one way of reducing our dependence on dwindling petroleum reserves for aromatics as well as increasing the economics of the pulp mills as well as the development of extractive lignin processes. Accordingly, the overall objective of this work is the production of chemicals and fuels by the catalytic hydroprocessing of lignin and lignin-derived bio-oils.

1.4 Approaches and Methodology

Technical lignin is a complex polymer with a high average molecular weight and some types of lignin such as Kraft lignin and hydrolysis lignin are not soluble in common organic solvents, which prevents their direct use as a substitute for petroleum-based chemicals in the synthesis of bio-based polymer materials, e.g., PF and epoxy resins. Therefore, samples of these lignins including organosolv lignin, Kraft lignin and hydrolysis lignin were depolymerized into the lower molecular weight products.

The depolymerization was conducted concurrently with hydrogenation/hydrodeoxygenation of the lignins and the overall process has been termed hydroprocessing instead of hydrotreatment to avoid confusion, as hydrotreatment has a specific meaning in the petroleum industry. The hydroprocessing reactions were conducted in several different reactors. The depolymerization of larger quantities of lignin was carried out in a 500 mL Parr stirred autoclave reactor. Subsequent reactions were conducted in both a 100 mL Parr stirred autoclave reactor and a mini-reactor constructed in-house with an effective volume of 13 mL (Figure 1.3). The lignins and depolymerized lignins were reacted in the presence of various catalysts under hydrogen at different temperatures, pressures and reaction times.

Where possible, the chemical and physical structure of the catalysts, feed and depolymerized products was measured. Typical analyses included: BET, XRD and TGA for the fresh and spent catalysts; GPC, GC/MS, CHNS, $^1\text{H-NMR}$, and FTIR for the lignin and depolymerized lignin products and Micro-GC for the gaseous products. The product separation scheme is shown in Figure 1.4.

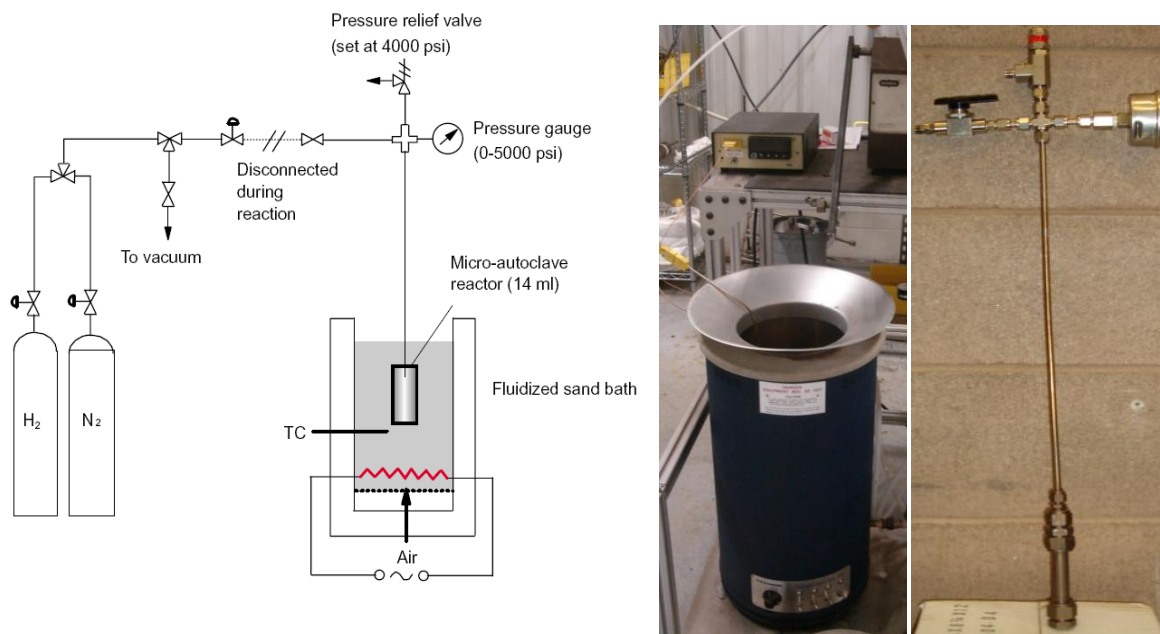
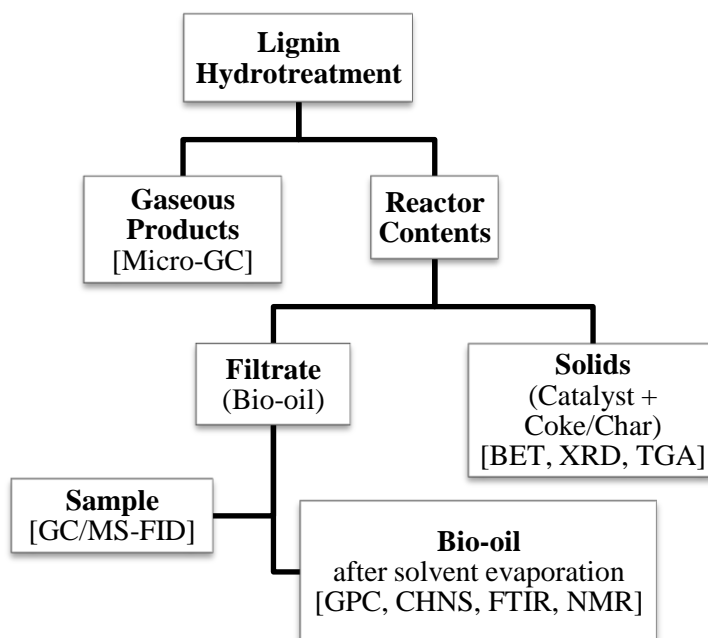


Figure 1.3 Schematic and photos of the mini-reactor system



Scheme 1.1 Product separation scheme

1.5 Thesis Overview

Chapter 1 provides a general introduction to the importance of the use of lignin derived from biomass as a feedstock for fuels and aromatic compounds rather than using whole biomass, highlighting the economic and environmental potential of this abundant and renewable resource. The research objectives, approach and methodology and thesis structure are outlined.

Chapter 2 presents a detailed overview of the available literature on the production of lignin and the various technologies used in the production of bio-oil from both whole biomass and lignin. The technologies and methods used to upgrade and hydroprocess these bio-oils are also discussed along with the effects of process variables (e.g. reaction environment, temperature and time, catalyst metals and support materials, solvents and promoters).

Chapter 3 details the investigation of the depolymerization of Kraft and organosolv lignin under reducing conditions using a number of different catalysts. The effects of catalyst loading, reaction temperature and time were studied and the properties of the reaction products were compared to the feed.

Chapter 4 presents results of a study on the effectiveness of MoRu carbon-supported catalysts in the hydroprocessing of guaiacol as a model compound for lignin. Catalysts supported by different carbon materials were prepared and their effectiveness in guaiacol conversion was evaluated. Process parameters were adjusted to determine the optimum reaction conditions.

Chapter 5 focuses on the hydroprocessing of organosolv lignin using MoRu carbon-supported catalysts. The effects of reaction time and reaction temperature were investigated to determine the most effective depolymerization conditions.

Chapter 6 describes the hydroprocessing of hydrolysis lignin using carbon-supported MoRu catalysts. The effects of reaction time and temperature on depolymerization effectiveness were examined.

Chapter 7 describes the hydroprocessing of depolymerized hydrolysis lignin using carbon-supported MoRu catalysts. The effects of reaction time and temperature on upgrading effectiveness were examined.

Chapter 8 presents the main conclusions obtained from the present research and suggests future work.

1.6 References

- Adjave JD, Bakhshi NN. (a) Production of hydrocarbons by catalytic upgrading of a fast pyrolysis bio-oil. Part I: Conversion over various catalysts. *Fuel Process. Technol.* 45 (1995) 161-183.
- Adjave JD, Bakhshi NN. (b) Production of hydrocarbons by catalytic upgrading of a fast pyrolysis bio-oil. Part II: Comparative catalyst performance and reaction pathways. *Fuel Process. Technol.* 45 (1995) 185-202.
- Adjave JD, Katikaneni SPR, Bakhshi NN. Catalytic conversion of a biofuel to hydrocarbons: effect of mixtures of HZSM-5 and silica-alumina catalysts on product distribution. *Fuel Process. Technol.* 48 (1996) 115-143.
- Akin DE, Benner R. Degradation of polysaccharides and lignin by ruminal bacteria and fungi. *Applied and Environmental Microbiology*, 54 (1988) 1117-1125.
- Appell HR, Wender I, Miller RD. Conversion of urban refuse to oil. US Bureau of Mines, Technical Progress Report (1969) No. 25.
- Baker EG, Elliott DC. Research in thermochemical biomass conversion. London: Elsevier Applied Science (1988) 883.
- Baurhoo B, Ruiz-Feria CA, Zhao X., Purified lignin: nutritional and health impacts on farm animals-a review. *Animal Feed Science and Technology* 144 (2008) 175-184.
- Bridgwater AV, Double JM. Production costs of liquid fuels from biomass. *Fuel* 70 (1991) 1209-1224.
- Bridgwater AV. Catalysis in thermal biomass conversion. *Appl. Catal. A: Gen.* 116 (1994) 5-47.
- Bridgwater AV. Production of high grade fuels and chemicals from catalytic pyrolysis of biomass. *Catal. Today* 29 (1996) 285-295.
- Bridgwater AV. Renewable fuels and chemicals by thermal processing of biomass. *Chem. Eng. J.* 91 (2003) 87-102.

Canadian Renewable Fuels Association, Manitoba Fuels Change with New Biodiesel Mandate (2009).

Craig W, Coxworth E. Proceedings of the sixth Canadian bioenergy R&D seminar. London: Elsevier Applied Science (1987) 407.

Czernik S, Bridgwater AV. Overview of applications of biomass fast pyrolysis oil. *Energy Fuels* 18 (2004) 590-598.

Dasari MA, Kiatsimkula P-P, Sutterlin WR, Suppes GJ. Low-pressure hydrogenolysis of glycerol to propylene glycol. *Appl. Catal. A: Gen.* 281 (2005) 225-231.

Elliott DC. Historical developments in hydroprocessing bio-oils. *Energy Fuels* 21 (2007) 1792-1815.

EU Directive 2003/30/EC, The promotion of the use of biofuels and other renewable fuels for transport. (2003).

Furimsky E. Review: catalytic hydrodeoxygenation. *Appl. Catal. A: Gen.* 199 (2000) 147-190.

Graça I, Lopes JM, Ribeiro M., Ramôa Ribeiro F, Cerqueira HS, de Almeida MBB. Catalytic cracking in the presence of guaiacol *Applied Catalysis B: Environmental* 101 (2011) 613-621.

Holt NA, Van Der Burgt MJ. Proceedings of power production from biomass III, gasification and pyrolysis R&D&D for industry (VTT Symposium 192). Espoo, Finland, 14-15 September (1998) 163-177.

<http://www.lignoworks.ca/content/what-lignin>. No copyright permission is needed

Huang, S., Mahmood, N., Tymchyshyn, M., Yuan, Z., Xu, C. Reductive De-polymerization of Kraft Lignin for Chemicals and Fuels using Formic Acid as an In-situ Hydrogen Source, *Bioresource Tech.* 171 (2014) 95-102.

Karagoz S, Bhaskar T, Muto A, Sakata Y, Oshiki T, Kishimoto T. Low-temperature catalytic hydrothermal treatment of wood biomass: analysis of liquid products. *Chem. Eng. J.* 108 (2005) 127-137.

Katikaneni SPR, Adjave JD, Bakhshi NN. Performance of aluminophosphate molecular sieve catalysts for the production of hydrocarbons from wood-derived and vegetable oils. *Energy Fuels* 9 (1995) 1065-1078.

Kirk TK. Effects of microorganisms on lignin. *Annual Review Phytopathology.* 9 (1971) 185-210.

Kleinert M, Gasson JR, Barth T. Optimizing solvolysis conditions for integrated depolymerisation and hydrodeoxygenation of lignin to produce liquid biofuel *J. Anal. Appl. Pyrolysis* 85 (2009) 108-117.

Li X, Su L, Wang Y, Yu Y, Wang C, Li X, Wang Z. Catalytic fast pyrolysis of Kraft lignin with HZSM-5 zeolite for producing aromatic hydrocarbons *Front. Environ. Sci. Eng.* 6 (2012) 295-303.

Maggi R, Delmon B. Advances in thermochemical biomass conversion. London: Elsevier Applied Science (1993) 1185.

Minowa T, Kondo T, Sudirjo ST. Thermochemical liquefaction of Indonesia biomass residues. *Biomass Bioenergy* 14 (1998) 517-524.

Mohan D, Pittman CU Jr., Steele PH. Pyrolysis of wood/biomass for bio-oil: a critical review. *Energy Fuels* 20 (2006) 848-889.

Murata K, Liu Y, Inaba M, Takahara I. Production of Synthetic Diesel by Hydroprocessing of Jatropha Oils Using Pt-Re/H-ZSM-5 Catalyst *Energy Fuels* 24 (2010) 2404-2409.

Ogi T, Yokoyama S. Liquid fuel production from woody biomass by direct liquefaction. *Journal of The Japan Petroleum Institute* 36 (1993) 73-84.

Okkerse C, Van Bekkum H. Fossil to green. *Green Chem.* 1 (1999) 107-114.

Pagliari M, Ciriminna R, Kimura H, Rossi M, Della Pina C. From Glycerol to Value-Added Products. *Angew. Chem. Int. Ed.* 46 (2007) 4434-4440.

Qu Y, Wei X, Zhong C. Experimental study on the direct liquefaction of *Cunninghamia Lanceolata* in water. *Energy* 28 (2003) 597-606.

Sharma RK, Bakhshi NN. Catalytic upgrading of biomass-derived oils to transportation fuels and chemical. *Can. J. Chem. Eng.* 69 (1991) 1071-1108.

Song C. Fuel processing for low-temperature and high-temperature fuel cells: challenges and opportunities for sustainable development in the 21st century. *Catal. Today* 77 (2002) 17-49.

Valliyappan T, Bakhshi NN, Dalai AK Pyrolysis of glycerol for the production of hydrogen or syn gas. *Bioresource Technology* 99 (2008) 4476-4483.

Williams PT, Horne PA. The influence of catalyst regeneration on the composition of zeolite-upgraded biomass pyrolysis oils. *Fuel* 74 (1995) 1839-1851.

Xu C, Etcheverry T. Hydro-liquefaction of woody biomass in sub- and super-critical ethanol with iron-based catalysts. *Fuel* 87 (2008) 335-345.

Yamazaki J, Minami E, Saka S. Liquefaction of beech wood in various supercritical alcohols. *J. Wood Sci.* 52 (2006) 527-532.

Yazdani SS, Gonzalez R. Anaerobic fermentation of glycerol: a path to economic viability for the biofuels industry. *Current Opinion in Biotechnology* 18 (2007) 213-219.

Chapter 2

2 Literature Review

Direct liquefaction of biomass for the production of bio-oil/bio-crude has attracted increasing interest in recent years due to rising crude oil prices, diminishing supply and increasing concerns over greenhouse gas emissions as well as energy security. Pyrolysis and high pressure liquefaction are the two main thermo-chemical technologies that have been developed for the direct liquefaction of biomass into bio-oil or bio-crude products. Fast pyrolysis (operated at moderate pressures of 0.1-0.5 MPa and temperatures >500 °C) is, so far, the only industrially realized technology for production of bio-oils from biomass. However, pyrolysis oils contain high levels of oxygenated compounds and water and therefore have only about half of the caloric value (<20 MJ/kg) of petroleum. High-pressure liquefaction technology with a suitable solvent (water or organic) plus catalyst, operating at moderate temperatures (<400 °C) but higher pressures of 5-20 MPa, has the potential to produce liquid oils (also called bio-oils or bio-crudes) with much higher caloric values (25-35 MJ/kg).

Pyrolysis oils and bio-oils/bio-crudes are composed of a complex mixture of oxygen-containing compounds in the form of phenol and benzene derivatives, hydroxyketones, carboxylic acids and esters, aldehydes as well as aliphatic and aromatic alcohols. These compounds contribute to the high oxygen content of bio-oil (up to 30-50 wt.%), and result in not only a lower calorific value, but increased viscosity, poor thermal and chemical stability, corrosivity (due to organic acids) and immiscibility with hydrocarbon fuels. To produce high-quality bio-oils for use as liquid transportation fuels, pyrolysis oils/bio-crudes must be upgraded by various means to reduce their oxygen content.

The objective of this review is to provide an overview of direct thermo-chemical liquefaction technologies used in the production of bio-oils/bio-crudes from biomass, the development of the upgrading technologies to produce high quality liquid transport fuels and chemicals from bio-oils/bio-crudes, as well as the current research into the utilization of lignin as a feedstock for the production of chemicals and fuels.

2.1 Thermochemical Conversion of Biomass

Thermochemical conversion of biomass into liquid fuels and valuable chemicals can be achieved by either pyrolysis or high-pressure liquefaction (Demirbas, 2000; Molton *et al.*, 1978).

2.1.1 Fast Pyrolysis

Pyrolysis of biomass is performed in an inert atmosphere at high temperatures, typically 400-800°C, and at low pressures around 0.1-0.5 MPa without the addition of any catalyst. At these high temperatures, solid lignocellulosic materials thermally decompose into smaller fragments which combine to produce oily compounds, yielding about 50-75 wt.% liquid products (pyrolysis oil or bio-oil). As a side note, the yield of bio-oil (or other liquid or solid products) is usually presented as wt.%, i.e. mass of product as a fraction of the mass of feedstock. In the case of gaseous products, the yield is usually expressed as mol%. Heat is usually added indirectly, although partial gasification and combustion of the feedstock may be employed to give direct heating. Gas and char are produced in addition to the liquid products. The relative proportions of gas, liquid and solid products depend on the pyrolysis parameters specifically heating rate and final temperature. Fast or flash pyrolysis (with a high heating rate and short vapour residence time) is used to maximize liquid products (Bridgwater, 1991). Flash pyrolysis produces liquid yields up to 75 wt.% at relatively low temperatures, typically 500 °C but less than 650 °C, and at very high heating rates of 1,000 °C/s, or even 10,000 °C/s, and very short residence times of typically less than 1 s. The rapid heating and rapid quenching in fast pyrolysis processes produces intermediate liquid products, which condense to form liquid oil products before they are further broken down into gaseous products. The high heating rates also minimize char formation, and no char is formed under some conditions (Demirbas, 2005). Increasing flash pyrolysis temperature above 700°C leads to still higher heating and reaction rates but results in very high gas product yields of up to 80 wt.% (Bridgwater, 1992).

Over the past thirty years, research into fast or flash pyrolysis has shown that high yields of liquid and gas products, including valuable chemicals or chemical intermediates and fuels,

can be obtained from various biomass feedstocks including agricultural/forest residues and waste streams (Bridgwater *et al.*, 2001). Fast pyrolysis bio-oils are complex mixtures of compounds derived from the depolymerization and degradation of cellulose, hemi-cellulose and lignin (Czernik and Bridgwater, 2004; Zhang *et al.*, 2007; Oasmaa *et al.*, 2010). The typical properties of pyrolysis bio-oils and of a petroleum-based heavy fuel oil are shown in Table 2-1.

Table 2.1 Typical properties of pyrolysis bio-oil (before upgrading) and of a petroleum-based heavy fuel oil (Czernik and Bridgwater, 2004)

Physical property	Bio-oil	Heavy fuel oil
Moisture content (wt.%)	15-30	0.1
pH	2.5	-
Specific gravity	1.2	0.94
Viscosity (cP , at 50 °C)	40-100	180
Elemental composition (wt.%)		
C	54-58	85
H	5.5-7.0	11
O	35-40	1.0
N	0-0.2	0.3
Ash	0-0.2	0.1
HHV (MJ/kg)	16-19	40

Bio-oil from fast pyrolysis is a complex mixture composed of acids, alcohols, aldehydes, esters, furans, guaiacols, ketones, sugars, syringols, lignin-derived phenols and extractible terpenes (Guo *et al.*, 2001). Zhang *et al.* (2001) separated the bio-oil into four fractions: aliphatic, aromatic, and polar compounds as well as non-volatiles by using solvent extraction and liquid chromatography on an aluminum column. Analysis of the fractions indicated the presence of high levels of acetic acid and hydroxyacetones in the aqueous phase, with aromatic hydrocarbons and less polar components in the oil phase. In general, fast pyrolysis bio-

oils are a complex mixture of highly oxygenated compounds with a broad distribution of oxygenated organics, such as esters, ethers, aldehydes, ketones, phenols, carboxylic acids and alcohols (Peng and Wu, 2000).

Fast pyrolysis is, so far, the only industrially realized technology for the production of bio-oils from biomass. A fast pyrolysis process employing circulating fluidized beds, originally developed at the University of Western Ontario, is now commercialized by Ensyn Technologies in Renfrew, Ontario (RTP, rapid thermal processing). Also in Canada, another fast pyrolysis technology based on a fluidized bed has been commercialized by Dynamotive Energy Systems Corp., which has a demonstration project at Erie Flooring and Wood Products in Ontario. However, pyrolysis oils contain high levels of oxygen/water and therefore have a caloric value only about half of that of petroleum (<20 MJ/kg). In addition, the presence of organic acids makes them strongly acidic and corrosive. As a result, pyrolysis oils are not regarded as an ideal liquid fuel for heat or power generation, and without upgrading, cannot be used as a liquid transportation fuels.

The water content of bio-oil can be as high as 15-30 wt.% and comes from moisture initially present in the feedstock and also as the product of dehydration reactions during pyrolysis and later storage. The presence of water decreases the heating value of the oil as well as the combustion flame temperature of the fuel (Scholze and Meier, 2001). The removal of water from pyrolysis oil by evaporation is problematic, because heating bio-oil results in the rapid polymerization of components in the bio-oil and an associated increase in viscosity.

It is the presence of high levels of oxygen in bio-oils that is the principal difference between bio-oils and hydrocarbon fuels. The high oxygen content of bio-oil results in its lower energy density compared to conventional fossil fuels and is responsible for its immiscibility with hydrocarbon fuels. In addition, the presence of substantial amounts of carboxylic acids, such as formic and acetic acid, contributes to bio-oil pH values as low as 2-3 (Sipilae *et al.*, 1998). This makes bio-oils corrosive and the problem is exacerbated at elevated temperatures. This imposes more stringent requirements in the choice of construction materials of bio-oil storage vessels and necessitates significant upgrading before it can be used as a transportation fuel (Zhang *et al.*, 2007).

2.1.2 High-pressure Liquefaction

In contrast to fast pyrolysis, high-pressure liquefaction is performed under an inert or, preferably, a reducing atmosphere at moderate temperatures less than 400°C, but higher pressures ranging between 5 and 20 MPa. In high-pressure liquefaction processes, the macro-molecular compounds in the feedstock are decomposed into small fragments in the presence of suitable solvent(s) (i.e. water, alcohols, alkanes, phenols, or tetralin, etc.) and a catalyst. The molecular fragments produced in the reaction are unstable and reactive, and tend to re-polymerize into oily compounds having various molecular weights (Molten, 1983). The presence of a suitable solvent is critical for a direct liquefaction process as the solvent can act a diluting agent for the products formed and/or as a fragment stabilization agent to prevent re-polymerization/condensation reactions from forming char or a heavy residuum.

High-pressure liquefaction is a superior direct liquefaction technology compared with fast pyrolysis, in that it produces higher quality bio-oil with more desirable chemical and physical properties. High-pressure liquefaction technology also has the potential for producing heavy liquid oils or bio-crudes with increased heating values and a range of other value-added chemicals including vanillin, phenols, aldehydes, and acetic acid etc. Research at the Pittsburgh Energy Technology Center (PETC) reported effective high-pressure liquefaction of a variety of lignocellulosic materials into oily products in water at an elevated temperature in the presence of a CO atmosphere and Na₂CO₃ catalyst (Appell *et al.*, 1971). The PETC's research into direct liquefaction of biomass was further advanced by the research group at the Pacific Northwest National Laboratory (PNNL) in the U.S.A. led by Dr. D. Elliott. During the 1980's, much work on scaling up the pioneer work by Appell *et al.* and on utilizing the direct liquefaction oil products was done at PNNL. (Elliott, 1980; Schirmer *et al.*, 1984)

High-pressure direct liquefaction processes are normally operated at moderate temperatures (200-450 °C), pressures greater than 1 MPa and using longer residence times (10-60 min) in hot compressed water (Boocock *et al.*, 1979; Yokohama *et al.*, 1984; Minowa *et al.*, 1998; Qu *et al.*, 2003; Karagoz *et al.*, 2004; Nguyen *et al.*, 2014) or organic solvents such as anthracene oil (Appell *et al.*, 1969; Crofcheck *et al.*, 2005), alcohols (methanol, ethanol, propanol and butanol) and acetone, etc. (Miller *et al.*, 1999; Cemek and Kucuk, 2001; EU Directive 2003/30/EC; Tang *et al.*, 2010; Song *et al.*, 2013; Warner *et al.*, 2014). Typical yields of

liquid products for high-pressure liquefaction processes are in the range of 20-60 wt.%. Although high-pressure liquefaction processes produce lower yields of heavy oil (bio-crude) compared with fast pyrolysis processes (which yield 40-75 wt.% bio-oil with a HHV of about 20 MJ/kg), the bio-crude products have much higher caloric values (HHV = ~30 MJ/kg) (Minowa *et al.*, 1998; Qu *et al.*, 2003). Higher heating value (HHV) is also known as the gross calorific value or gross energy of a fuel. It is defined as the amount of heat released by a specified quantity of fuel (initially at 25 °C) once it is combusted and the products have returned to a temperature of 25°C. This takes into account the latent heat of vaporization of any water that is produced during combustion. When comparing the gross energy yield (oil yield × HHV), the two types of direct liquefaction processes are comparable. The yields of bio-crude depend on many operating parameters including reaction temperature, pressure, residence time, type of solvents and the catalysts employed.

Yan *et al.* (2008) reported by that pine and birch wood can be effectively degraded in hot-compressed water at 200 °C for 4 h under 4 MPa (cold pressure) H₂ in the presence of carbon-supported Pt or Ru catalysts. The products were a mixture of phenolic monomers of guaiacyl propane, guaiacyl propanol, syringyl propane and syringyl propanol. Yields of mono-phenolic compounds were as high as 45% of the total number of C₉ units in the lignin were obtained in a 50:50 wt.% mixture of dioxane/H₂O (1:1 wt/wt) with 1 wt.% H₃PO₄ and in the presence of Pt/C catalyst (5 wt.% of the sawdust).

2.2 Bio-oil Upgrading

Biomass-derived oils are very different from crude oils obtained from petroleum sources; the sulfur and nitrogen content of bio-crudes is negligible, but they are rich in oxygen-containing molecules (see Table 2-2). (Georget *et al.*, 1999; Şenol, 2007a,b) Bio-oils/bio-crudes are comprised of a complex mixture of oxygen-containing compounds in the form of phenol and benzene derivatives, hydroxyketones, carboxylic acids and esters, and aliphatic and aromatic alcohols (Xu and Lad, 2008; Yang *et al.*, 2009a). These compounds contribute to the oxygen content of the oil. In addition, water originating from both moisture initially present in the feedstock and as a pyrolytic product in pyrolysis and direct liquefaction processes adds to the oxygen content in bio-oil or bio-crude (Bridgwater, 2003; Czernik and Bridgwater, 2004).

The total oxygen content of bio-crudes can be as high as 40-50 wt.% for pyrolysis oils, and 20-30 wt.% for heavy oils from high-pressure direct liquefaction process, depending on the origin of the biomass and liquefaction conditions, e.g. temperature, residence time, heating rate and different catalysts used (Bridgwater, 1994; Furimsky, 2000). The high oxygen content is a limitation in the utilization of bio-crude as liquid transportation fuel since the high oxygen content of the oils causes high viscosity, poor thermal and chemical stability, corrosivity (due to the organic acids present) and immiscibility with hydrocarbon fuels (Bridgwater, 2003; Czernik and Bridgwater, 2004; Yaman, 2004).

Table 2.2 Elemental composition of bio-oil from wood and of a heavy fuel oil (Şenol, 2007b)

Composition (wt.%)	Bio-crude/Bio-oil		Heavy Fuel Oil
	High-pressure liquefaction	Pyrolysis	
Carbon	74.8	45.3	85.0
Hydrogen	8.0	7.5	11.0
Oxygen	16.6	46.9	1.0
Nitrogen	<0.1	<0.1	0.3
Sulfur	<0.1	<0.1	0.5-3.0
HHV (MJ/kg)	~30	~20	~40

Bio-crude/bio-oils therefore need to be upgraded by reducing their oxygen content (Bridgwater, 1994; Bridgwater, 1996).

Technologies for upgrading of bio-oils for fuel applications include physical and chemical/catalytic approaches (Czernik *et al.*, 2002; Zhang *et al.*, 2007). Techniques, such as emulsification and solvent extraction are physical methods in which bio-oils are mixed with diesel oil and solvents, respectively, to extract lower oxygen-containing components from the original bio-oil (Czernik *et al.*, 2002). Although the physical mixing of bio-oils with diesel fuel directly, aided by the addition of a surfactant, may be the simplest way to use bio-oil as a liquid transportation fuel, the associated problem of corrosion to the engine and related com-

ponents limits its application.

Currently, two main chemical approaches have been proposed and tested for the upgrading of both pyrolysis oils and bio-crudes from high-pressure direct liquefaction processes. These are catalytic cracking and catalytic hydrotreating and are analogous to the upgrading of heavy oils in a petroleum refinery.

Catalytic cracking processes, using various cracking catalysts (e.g. zeolites, silica-alumina and molecular sieves), are performed at atmospheric pressure without the requirement of added hydrogen. The advantages of low-pressure operation without the need of hydrogen have attracted much interest of studies on upgrading of bio-oils as reported in the literature (Adjave and Bakhshi, 1995; Katikaneni *et al.*, 1995; Williams and Horne, 1995; Adjave *et al.*, 1996; Gerber, 2007; Yoshikawa *et al.*, 2013). The yield of desired fuel hydrocarbons however is typically very low because of the high yields of char/coke and tar. Deposition of these undesired products on the catalyst results in the serious problem of rapid catalyst deactivation. As a result, periodic or continual regeneration of the catalysts becomes necessary.

In contrast to catalytic cracking, catalytic hydroprocessing processes operate at high pressures in the presence of hydrogen and/or hydrogen donor solvents (Craig and Coxworth, 1987; Baker and Elliott, 1988; Maggi and Delmon, 1993; Kleinert *et al.*, 2008; Huang *et al.*, 2014).

Significant efforts have been made over the past 20 years to study the hydrodeoxygenation (HDO) of biomass-derived oils. The catalysts used in the hydrotreatment (hydroprocessing) of bio-oils have been studied extensively and fall into two general categories: Al₂O₃-supported catalysts, typically loaded with NiMo or CoMo, (Baker and Elliott, 1988; Sheu *et al.*, 1988; Gevert *et al.*, 1990; Sharma and Bakshi, 1993; Jongerius *et al.*, 2013) or noble metals (Lee *et al.*, 2012) and zeolite catalysts (e.g. H-ZSM-5) (Baker and Elliott, 1988; Furrier and Bakshi, 1988; Sharma and Bakshi, 1991; Li *et al.*, 2012). The supported metal catalysts are more active in hydrogenation and deoxygenation reactions while the zeolite and similar acidic catalysts are used to enhance cracking reactions (Pindoria *et al.*, 1998).

2.3 Hydroprocessing of Model Compounds

Review of research efforts to study the catalytic chemistry and kinetics of hydroprocessing have focused on various model compounds containing oxygen, such as phenolic compounds and aromatic ethers, as well as various bio-oils (fast pyrolysis oils and bio-crudes from high-pressure liquefaction processes) (Furimsky, 2000; Elliott 2007). Pacific Northwest National Laboratory (PNL/PNNL) employed a batch reactor to test hydrotreating of phenolic model compounds with various catalysts (Elliott, 1983). Some key results are summarized as follows: commercially available catalysts (Al_2O_3 -supported CoMo, NiMo, NiW, Ni, Co, Pd, and CuCrO) were used to hydrogenate phenol at 300 °C or 400 °C for 1 h. Of the catalysts tested, the sulfided form of CoMo was found to be most active, producing a product containing 33.8% benzene and 3.6% cyclohexane at 400°C, while the sulfided Ni catalyst produced 8.0% cyclohexane but only 0.4% benzene. On the basis of other model compound studies involving o-cresol and naphthalene, Elliott, *et al.* (1995) concluded that NiMo with a phosphated alumina support was the most active for oxygen removal and hydrogen addition, but CoMo catalyst should be considered if hydrodeoxygenation is the main goal due to its much higher selectivity.

The addition of a small amount of phosphorus to sulfided NiMo/ Al_2O_3 catalyst has been shown to enhance both hydrodenitrogenation (HDN) and hydrodesulfurization (HDS) activities, with less susceptibility to coke formation (DeCanio *et al.*, 1991). The presence of phosphorus was found to induce the formation of new Brønsted and Lewis acid sites with intermediate strength as was evidenced by FTIR analysis (Ferdous *et al.*, 2004).

One of the key parameters determining the hydrodeoxygenation (HDO) activity of Mo, CoMo or NiMo catalysts is the type of support material used. The most common and conventional support is solid acid Al_2O_3 , which has been widely used in hydrotreating catalysts on an industrial scale (Zdrazil, 2003). Extensive studies have been undertaken on CoMo and NiMo catalysts supported on alternative materials such as SiO_2 , activated carbon, TiO_2 , ZrO_2 , zeolites and various mixed oxides (Breyesse *et al.*, 1991; Luck, 1991; Topsøe *et al.*, 1996; Vasudevan and Fierro, 1996; Radovic and Rodriguez-Reinoso, 1997). Centeno, *et al.* (1995) compared the hydroprocessing abilities with carbon-supported and alumina-supported CoMo and NiMo catalysts using various oxygen-containing and phenolic model compounds includ-

ing guaiacol, catechol, phenol, 4-methyl acetophenone and *para*-cresol, in a *para*-xylene medium. Their studies showed that coke formation was an important cause of catalyst deactivation where alumina supports are used, especially with compounds containing two oxygen atoms such as guaiacols or catechols.

The use of MgO as a basic support material has attracted much less attention. Basic supports however are interesting for two main reasons as stated by Klicpera and Zdrzil (2002). First, the acid-base interaction between acidic MoO₃ and a basic support in the oxide precursors of the sulfided catalyst may promote dispersion of the Mo species in the catalyst. Second, the basic character of the support may inhibit coking which is rather intensive for conventional Al₂O₃-supported catalysts. It was not until recently that MgO-supported catalysts have been used to upgrade bio-oil. Sulfided MgO-supported CoMoP catalyst was used to successfully upgrade both phenol (as a model compound) and bio-oil in supercritical hexane. After 1 h at optimum reaction conditions of 450 °C and 5.0 MPa hydrogen, the phenol had been converted to reduced products comprising ~65 wt.% benzene and >10 wt.% cyclohexyl compounds (Yang *et al.*, 2009b).

2.4 Hydroprocessing of Bio-oils

Studies on the hydroprocessing of bio-oils have mostly focused on conventional petroleum hydrotreating catalysts, i.e., sulfided CoMo and NiMo. Elliott and Baker (1984) and Soltes *et al.* (1987) examined hydrocatalytic reactions of bio-oils obtained from a high-pressure liquefaction process using a continuously fed fixed bed reactors. Their results showed the sulfided form of the CoMo catalyst to be much more active than the oxide form. The sulfided nickel catalyst exhibited similar activity to the sulfided CoMo catalyst except that the nickel catalyst led to a much higher gas yield and much greater hydrogen consumption. More than 95% oxygen removal from the wood-derived bio-crude, initially containing about 15 wt.% O, was achieved with the sulfided CoMo/Al₂O₃ catalyst at 573 K (Gevert, 1988). Using the same bio-oil, Gevert *et al.* (1990) studied the effect of pore diameter of a sulfided CoMo/Al₂O₃ catalyst on the overall hydroprocessing. The best performance was achieved at 623 K for a catalyst with narrow pores. A two-step hydroprocessing process for upgrading of pyrolysis oils developed was developed at the PNNL (Elliott and Neuenschwander, 1996; Elliott *et al.*,

1988; Elliot and Oasmaa, 1991). The first step involves a low temperature and high pressure (270 °C, 136 atm) catalytic treatment that hydrogenates the thermally unstable bio-oil compounds. The second step involves catalytic hydrogenation at higher temperature and the same pressure (400 °C, 136 atm). The same catalyst, a sulfided CoMo/Al₂O₃ or sulfided NiMo/Al₂O₃, was used for both steps. This process produced 40 wt.% yields of refined oil containing less than 1 wt.% oxygen from raw pyrolysis oil. Catalyst deactivation and gum formation in the lines were found to be the major process challenges. Churin *et al.* (1988 and 1989) conducted upgrading experiments on pyrolysis oil produced from olive oil. The authors reported that using sulfided NiMo or CoMo catalysts on alumina or silica-alumina supports perform better than noble metal catalysts which were found to be more readily deactivated by poisoning, sintering, and fouling. The use of a hydrogen donor solvent (e.g. tetrahydronaphthalene also known as tetralin) was found to lead to a marked improvement in the quality of the hydrotreated product and a reduction in catalyst deactivation by coke deposition. Zhang *et al.* (2005) hydrotreated a pyrolysis oil using sulfided CoMoP/γ-Al₂O₃, in tetralin under the optimum conditions of 360 °C and 2 MPa of cold hydrogen pressure. The oxygen content of the oil was reduced from 41.8 wt.% for the crude oil to 3 wt.% for the upgraded product. A pyrolytic lignin, extracted from softwood fast pyrolysis bio-oil, was catalytic hydrotreated by Piskorz *et al.* (1989) using pelletized sulfided CoMo catalyst. The process produced a light organic oil with 0.46% oxygen content.

Soltes *et al.* (1987) and Sheu *et al.* (1988) upgraded pyrolytic oils obtained from pine. Twenty catalyst formulations were tested in a batch reactor and an alumina-supported Pd catalyst was determined to be most effective with the highest yield of liquid oil at 400 °C for 1 h. Alumina-supported Pt or Re catalyst were found to produce higher gas yields, while Ru and Rh were found to be most active in gas formation. Sulfided CoMo, NiMo, and NiW catalysts were found to be of much lower activity for bio-oil hydrotreating compared to the precious metal catalysts, and the Pt catalyst was found to be the most active for oxygen removal.

Although sulfided CoMo and NiMo catalysts are traditionally used in petroleum and bio-oil hydrotreatment and have received much of the focus in hydroprocessing processes, other types of catalysts, including solid acids, solid bases and precious metal catalysts, have also been used. Upgrading of fast pyrolysis oil using solid acid (40SiO₂/TiO₂-SO₄²⁻) and solid base (30K₂CO₃/Al₂O₃-NaOH) catalysts at 50 °C for 5 h was investigated by Zhang *et al.*

(2006) in which the dynamic viscosity of the bio-oil was markedly decreased. The density of the upgraded bio-oil was decreased from 1,240 to 960 kg/m³, and the gross calorific value increased by 50% from 16 MJ/kg for the original bio-oil to 24 MJ/kg for the upgraded bio-oil. The results of GC/MS analysis showed that decarboxylation of the bio-oil was promoted by both the solid acid and solid base catalysts.

A longstanding problem for hydroprocessing of bio-oils was associated with catalyst deactivation due to coke formation, particularly for alumina-supported catalysts. Gagnon and Kaliaguine (1988) reported that bio-oil polymerization occurred during the upgrading of the vacuum pyrolysis bio-oil. The polymerization was more evident during bio-oil upgrading in the presence of NiWO/Al₂O₃ catalyst at 598 K and about 18 MPa H₂, although significant oxygen removal was achieved.

The development of highly active and stable catalysts for the hydroprocessing of bio-oils/bio-crudes will continue to be the great challenge in the advancement of bio-oils and the focus of much future study.

Regardless of which process is used to decompose biomass and upgrade the resulting bio-oil, the issue remains that the presence of cellulose and hemicelluloses is undesirable since they are the precursors to the water and many of the oxygenated compounds found in conventional bio-oil which decrease the heating value of the bio-oil, can cause corrosion problems due to the formation of organic acids. They also present problems of long-term stability and miscibility with conventional fuels. Thus the use of lignin alone as a feedstock for bio-oil production would be an improvement over the use of whole biomass as it avoids many of the challenges that are encountered in the utilization of conventional bio-oil.

2.5 Lignin

Lignin is a complex amorphous polymer composed of phenyl propane units that comprises ~25-30% of wood by weight. Three related compounds make up the polymer. These are guaiacyl alcohol, syringyl alcohol, and *p*-coumaryl alcohol. The ratio of these units within the lignin polymer varies depending on the source of the lignin. For example, softwood lignin

is composed almost entirely of guaiacyl units derived from coniferyl alcohol while hardwood lignins are comprised of different ratios of guaiacyl and syringyl units (Rohella *et al.*, 1997). In contrast, lignin from grassy biomass is a mixture of all three types of monomers.

To complicate matters, the different monomers making up the structure of lignin are linked via a number of different types of chemical bonds comprising α -O-4 aryl ether, β -O-4 aryl ether, 4-O-5 diaryl ether, 5-5 biphenyl, β -5 phenylcoumaran, β - β -(resinol) and β -1-(1,2-diaryl-propane) linkages. The numbers and types of these bonds in a particular sample of lignin depend on the source of the lignin (hardwood vs. softwood) as well as environmental factors including stresses experienced by the trees as they grew. Thus the structure and chemical composition of lignin can vary significantly even within the same tree (Pandey and Kim, 2011).

2.5.1 Lignin Production

Crude lignin is generated in large amounts as a by-product of the pulp and paper industry. This lignin is currently utilized mainly by direct combustion in the recovery boilers for heat generation. Over the past 30 years there has been increasing interest in the production of potentially higher value chemicals and fuels from lignin.

The lignin produced from lignocellulosic materials can be classified into two categories: sulfur-containing lignins and sulfur-free lignins. The sulfur-containing lignins, Kraft lignin and lignosulfonates, are produced as by-products of the Kraft and sulfonate pulping processes. Sulfur-free lignins include soda, organosolv, steam-explosion, oxygen delignification and hydrolysis lignins. Approximately 80% of lignins come from the widely used Kraft process, which is known for air/water pollution and the odour issues related to sulfur. Furthermore, extraction of the lignin from the black liquor is necessary in order to maintain a closed cycle of pulping chemicals within the pulp mills. Olivares *et al.* (1988) proposed a lignin extraction procedure involving a 2-stage acidification followed by filtration to produce high quality lignin from Kraft black liquor with the added benefit of recycling the Na and sulfate-rich filtrates back into the process. A fraction of the sulfur in the Kraft pulping process ends up in the lignin.

The α - and β -ether linkages in the lignin polymer are easily cleaved, but the 5-5 biphenyl-type bonds and aromatic ring structures are much more stable and resistant to chemical degradation. The ether linkages make up 56-72% of the bonds in lignin depending on the source (Pandey & Kim, 2011). Therefore a significant portion of the bonds in lignin are refractory to degradation. In addition, the recombination of highly reactive radicals obtained from the degradation these bonds can result in the production of condensed structures or coke.

The recent increase in the conversion of agricultural residues into bio-ethanol, functional polysaccharides or bio-gas by means of enzymatic conversion has attracted much attention in many countries and increased the availability of sulfur-free lignins. (Champagne, 2007; Demirbas *et al.*, 2006) One such lignin comprises the solid residues remaining after the enzymatic hydrolysis of lignocellulosic feedstocks and is known as hydrolysis lignin (HL) or hydrolyzed wood biomass. It is composed of unreacted cellulose, mono and oligosaccharides, and lignin, with lignin comprising 50 to 55% of the mass. (Dahlman *et al.*, 2000; Santos *et al.*, 2012) Hydrolysis lignin is expected to be produced in large quantities as projects producing cellulosic sugar-based chemicals or ethanol are realized. For now, it is mainly utilized as a low-value fuel and large-scale development of these biomass conversion projects is limited by the high cost of cellulose enzymes and process equipment. (Jin *et al.*, 2011) Finding effective ways to make full use of the lignin present in the process residues for value-added energy and chemical products is critical in improving bio-ethanol process economics.

2.6 Lignin Decomposition

A review of available literature shows that much research has been done on degradation of lignin into aromatic and other compounds. In addition, many more papers have been published on the use of phenol as a model compound for lignin degradation/upgrading. The use of guaiacol, veratrole, 2,6-dimethoxyphenol, 1,2,3-trimethoxybenzene, guaiacol- β -guaiacol, diphenyl ether, biphenyl and similar chemicals as model compounds has been reported less often and few papers have been published on the upgrading of degraded lignin itself. In addition, most of these studies have investigated the reactions of these model compounds in the gas phase.

2.6.1 Lignin Pyrolysis

Pyrolysis is the most studied method for the conversion of biomass to lower-molecular-weight liquid or gaseous products. Pyrolysis is the rapid heating of an organic substance in the absence of air so that the large macromolecular structure is broken down into smaller units (thermolysis). The absence of air limits the amount of oxygen that is available for combustion. The resulting products from the pyrolysis of biomass or lignin depend on the reaction temperature and time. As might be expected, lower temperatures and shorter reaction times produce more liquid products and higher temperatures tend to produce more gaseous products. In addition, increasing the severity of the treatment results in the formation of simpler lower-molecular-weight components (Barth and Kleinert, 2008). The pyrolysis of lignin is highly complex and is affected by several factors including: type of lignin, reaction temperature, heating rate, catalysts etc. (Ferdous *et al.*, 2002; Várhegyi *et al.*, 1997) It is further complicated by the tendency of lignin to form a foam during heating. (Palmisano *et al.*, 2012) The major products of lignin pyrolysis include gaseous hydrocarbons along with carbon monoxide and carbon dioxide, volatile liquids such as methanol, acetone, and acetaldehyde, phenolic compounds including phenol, guaiacol, syringol, and catechol and other substituted phenols such as lignols. A fraction of lignin is converted to thermally stable products called char. Char yields are higher at lower pyrolysis temperatures (Sharma *et al.*, 2004). At high temperatures, gasification of lignin yields hydrogen (by cracking of aromatic rings), CO₂ (by reformation of C=O and COOH functional groups), CO (by cracking of C-O-C and C=O functional groups), and CH₄ (by cracking of methoxy groups) (Yang *et al.*, 2007).

Lignin pyrolysis covers a rather wide range of temperatures in comparison to cellulose pyrolysis (Yang *et al.*, 2007). At lower temperatures the weaker bonds in lignin are cleaved. As the temperature increases progressively stronger bonds are broken and at significantly high temperature (>500 °C), aromatic ring cracking and condensation occur, releasing hydrogen. In the first step (120-300 °C), typical products include formic acid, formaldehyde, CO₂, CO, and water. The water is produced by the cleavage of OH functional groups linked to b or c carbons in aliphatic side chains, while formaldehyde is released by the breaking of the b-c carbon bonds in alkyl side chains. Aryl ether linkages (α - or β -O-4-bonds) are also relatively easy to break. Ether linkages at c-carbons are relatively more resistant, and methoxy groups are even more resistant to thermal treatment. Although the general trend in degradation is

similar, the yield of particular products and the specific temperature for bond breakage varies according to the lignin type (Ferdous *et al.*, 2002).

Liu *et al.* (2008) analyzed the pyrolysis products of lignin from birch and fir using a thermogravimetric analyzer along with Fourier transform infrared spectrometry (TGA-FTIR). H₂O and CO₂ were the primary products produced at temperatures around 100 °C. At around 225 °C, the presence of CO, aldehydes, formic acid, and phenols was observed. The presence of CO₂ was more obvious in the birch lignin decomposition products. The presence of monomeric phenol indicated the breaking of ether linkages at these temperatures. At temperatures around 425 °C for fir and 375 °C for birch, gaseous products such as CO, CO₂, and hydrocarbons (mainly methane) became dominant. Significant amounts of methanol were also observed. Ferdous *et al.* (2002) studied the pyrolysis of Alcell lignin (a type of organosolv lignin) and Kraft lignin (produced using a sulfate pulping process) at different heating rates and temperatures of up to 800 °C using a fixed-bed micro reactor. At 800 °C, the gaseous products were mainly H₂, CO, CO₂, CH₄, and C₂₊. Overall conversion was observed to increase with increasing temperature. At lower temperatures, conversion was higher at lower heating rates. However, as the pyrolysis temperature increased, conversion started to level off and, eventually, at temperatures above ~700 °C, conversion was higher at higher heating rates. For example, the conversion of Alcell and Kraft lignin increased to 65 and 57 wt.% from 56 and 52 wt.%, respectively, when the heating rate was increased from 5 to 15 °C min⁻¹ at 800 °C. Fast pyrolysis of various technical lignins by Windt *et al.* (2009) also showed that fast pyrolysis results in higher conversion than lower heating rates because lower temperatures and longer residence times favor the formation of coke and char.

2.6.2 Lignin Hydrogenolysis

Hydrogenation of the radical compounds produced by the decomposition of lignin is one solution to prevent recondensation reactions. Kleinert's work (2008) suggests that hydrogenation leads to higher yields of monomeric phenols and less char formation. The reactive hydrogen can be obtained from the liquefaction solvent(s) or gaseous hydrogen in combination with suitable catalysts.

Pyrolysis of neat lignin is not ideal for converting lignin into liquid fuels or chemicals since it results mainly in the production of solid coke and gas (Kleinert and Barth, 2008). Pyrolysis may be performed in the presence of hydrogen rather than nitrogen, resulting in hydrogenation or hydrogenolysis. In addition, the addition of suitable solvents and catalysts can speed up the reaction and increase the product yield (Okuda *et al.*, 2004). Pyrolytic oils contain a significant fraction of lignin-derived oligomers. Catalytic hydroprocessing can convert them to more useful and stable lower-molecular-weight monomeric compounds (Tang *et al.*, 2010). Hydrogenolysis is one of the most promising methods for producing phenols from lignin. Compared to pyrolysis (thermolysis), or pyrolysis in the presence of a solvent, hydrogenolysis leads to higher net conversion, higher yields of monophenols, and less char formation (Windt *et al.*, 2009; Connors *et al.*, 1980). Microwave and ultrasound pre-treatment methods prior to hydrogenolysis lead to higher conversion and oil yields (Gonçalves and Schuchardt, 2002). In addition, the reaction temperature required is in the range of 300-600 °C, which is lower than the temperature typical of thermolysis (Dorrestijin *et al.*, 2000).

Hydrogenation is performed either by reacting lignin in the presence an active hydrogen-donating solvent, such as tetralin (Connors *et al.*, 1980; Davoudzadeh *et al.*, 1985; Vuori and Bredenberg, 1988; Kudsy *et al.*, 1995; Thring *et al.*, 2003, Sales *et al.*, 2006) or formic acid (Kleinert and Barth, 2008; Huang *et al.* 2014), or in the presence of gaseous (molecular) hydrogen and a catalyst (Piskorz *et al.*, 1989; Meier *et al.*, 1992; Elliott *et al.*, 2009; Joshi and Lawal, 2012).

A lignin hydroprocessing system in a packed-bed catalytic reactor supplied with a constant flow of hydrogen was proposed by Piskorz *et al.*, (1989). Experiments with pyrolytic lignin resulted in high conversion with a light organic liquid yield of 65 wt.% and a total liquid yield of around 85 wt.%. Meier *et al.* (1992) studied catalytic hydrogenolysis of lignin in the presence of a NiMo aluminosilica catalyst and obtained a liquid oil yield of around 65 wt.%. The partial pressure of hydrogen had a significant influence on the conversion. Similar results were obtained during hydroprocessing of organocell lignin. The yield of light oil increased from 20 to 57 wt.% accompanied by an almost doubling of the phenolic fraction from 7 to 12.3wt.%, when the hydrogen pressure was increased from 5 to 14 MPa (Meier *et al.*, 1994). Oasmaa and Johansson (1993) achieved an oil yield of 61 wt.% during the hydroprocessing of Kraft lignin at 10 MPa hydrogen and in the presence of a water-soluble molyb-

denum catalyst. Experiments without the catalyst produced a condensed coke-like product instead of oil.

Wild *et al.* (2009) hydrotreated pyrolytic oil produced by the pyrolytic depolymerization of lignin as separate processes. The pyrolytic oil was reacted with molecular hydrogen at 350 °C and 10 MPa for 1 h in the presence of a Ru/C catalyst. GC-MS and NMR analysis showed that the hydroprocessing oil differed significantly from the pyrolytic oil feed, comprising mainly cycloalkanes and alkyl-substituted cyclohexanols.

The presence of hydrogen appears to suppress the formation of char. Thring and Breau (1996) observed that the addition of hydrogen up to a pressure of 1MPa increased the net conversion, and significantly reduced solid residue yield from 40 to 11 wt.%. Meier *et al.* (2004) obtained an even greater reduction in char yield (from 32 to 1.9 wt.%) after increasing the pressure from 5 to 14 MPa.

2.6.3 Lignin Oxidation

Due to the presence of numerous hydroxyl groups, lignin can be oxidized or undergo oxidative cracking. Oxidative cracking involves the cleavage of the aromatic ring structures, aryl ether bonds and other linkages within the lignin. The oxidation of lignin has been achieved using nitrobenzene, metal oxides, and hydrogen peroxide as oxidants for lignin. A cheaper alternative is catalytic oxidation with gaseous oxygen. Work at the University of Ottawa, Canada, has investigated the aerobic oxidation of lignin and lignin model compounds using copper and oxovanadium catalysts. (Sedai *et al.*, 2011; Sedai *et al.*, 2013) The products of lignin oxidation range from aromatic aldehydes to carboxylic acids, depending on the severity of the reaction conditions (Xiang and Lee, 2001). Oxidation of softwood lignin under alkaline conditions produces vanillin and vanillic acid while syringaldehyde and syringic acid are obtained from hardwood lignin. Vanillin is, in fact, one of the few low-molecular-weight chemicals that has been produced industrially in large quantities from lignin by alkaline oxidation in air. As late as the mid 1980s, a single pulp mill employing the soda pulping process in Thorold, ON, Canada produced ~60% of the world's artificial vanillin. The production of acetic acid by wet oxidation of lignin has been studied using model compounds. (Suzuki *et*

al., 2006) However, the wet oxidation of guaiacol, syringol, and phenol as lignin model compounds resulted in low yields of acetic acid.

2.7 Catalysts

Catalysis is an important technology in biomass and lignin conversion. Catalysts are used in lignin depolymerization to promote high conversion and suppress char formation and condensation reactions. In many cases, catalysts participate in selective bond cleavage, thus increasing the yields of particular compounds or types of compounds. Many types of catalysts have been tested for different processes and substrates including both model compounds and various types of lignin. Zakzeski *et al.* (2010) have published an exhaustive review of catalytic lignin valorization. Typically, zeolite and amorphous silica-alumina catalysts have been employed in the cracking of lignin (Thring and Breau, 1996; Li *et al.*, 2012) and upgrading of pyrolysis oils (Sheu *et al.*, 1988; Sharma and Bakhshi, 1993; Joshi and Lawal, 2012). H-ZSM-5 zeolite has been found to be more selective for aromatic hydrocarbons while amorphous silica-alumina catalysts favour the production of aliphatic hydrocarbons (Adjave and Bakhshi, 1995). Alkaline catalysts such as KOH and NaOH have been found to be effective in the hydrolysis of lignin in a process known as base-catalyzed decomposition or depolymerization (BCD) (Shabtai *et al.*, 1999; Miller *et al.*, 1999; Watanabe *et al.*, 2003; Nenkova *et al.*, 2008).

The use of catalysts in the hydroprocessing of lignin increases product yields and promotes hydrodeoxygenation (Oasmaa and Johansson, 1993). Commonly studied hydrogenation catalysts are typically composed of transition metals (e.g. cobalt, nickel and molybdenum) or noble metals (e.g. palladium). (Thring and Breau, 1996) The most studied catalysts have been cobalt- or nickel-promoted molybdenum (Ratcliff *et al.*, 1988; Meier, *et al.*, 1992; Meier *et al.*, 1994; Shabtai *et al.*, 1999; Okuda *et al.*, 2004; Matsumura *et al.*, 2006; Tang *et al.*, 2010; Jongorius *et al.*, 2012; Yoshikawa *et al.*, 2013).

Oasmaa and Johansson (1993) reported high yields of lignin oils from the hydroprocessing of Kraft lignin in the presence of a water-soluble molybdenum catalyst. Other catalysts used in the hydroprocessing of lignin include Ni-W (Thring and Breau, 1996), carbon-supported Pd

and Ru catalysts (Wild *et al.*, 2009; Yan *et al.*, 2008) and Ru(PPh₃)₃Cl₂ (Nagy *et al.*, 2009). Catalysts have been found to increase the yield of aldehydes during oxidation under both acidic and alkaline conditions (Xiang and Lee, 2001). The catalysts used in lignin oxidation range from metal-supported alumina catalysts such as Pd/Al₂O₃ (Sales *et al.*, 2006) and Cu-Ni/Al₂O₃ (Bhargava *et al.*, 2007) to a wide variety of homogenous catalysts (Voitl and von Rohr, 2010; Chen *et al.*, 2003). Lignin oxidation using molecular oxygen as the oxidant has been most frequently reported using metal salt-based catalysts such as CuO, CuSO₄, FeCl₃, and MnSO₄ (Xiang and Lee, 2001; Partenheimer, 2009)

Other catalysts used in the hydroprocessing of lignin and lignin model compounds belong to the family of catalysts used in the petrochemical industry. Typically these comprise Mo and Co, usually in sulfide form. Yang *et al.*, (2008) for example, reported on the HDO activity of exfoliated and crystalline MoS₂, using phenol, 4-methylphenol and 4-methoxyphenol. They found that hydrogenolysis of the C-OH bond of 4-methylphenol was favored over MoS₂ with a lower degree of stacking, while aromatic ring hydrogenation of phenol was favored over MoS₂ with a higher degree of stacking (exfoliated MoS₂).

2.7.1 Acid Catalysts

Most catalysts used in the hydroprocessing of lignin and its model compounds are supported by acid materials such as alumina (e.g. alumina-supported NiMo and CoMo), silica, and more recently, zeolites. Bui *et al.*, (2011a) hydrotreated guaiacol over alumina-supported and unsupported MoS₂ and CoMoS catalysts. The presence of Co was found to greatly increase the direct deoxygenation pathway in guaiacol conversion, similar to the well-known increase of direct desulfurization of refractory sulfur compounds over cobalt promoted molybdenum sulfide catalysts of in the hydrodesulfurization (HDS). Guaiacol hydroprocessing using the same metals but supported on zirconia (ZrO₂) (Bui *et al.*, 2011b) was very effective but different spectrum of products indicating that the support material can have a great effect on product selectivity.

The same group also studied the co- processing of guaiacol, as an oxygenated molecule representative of pyrolytic bio oils, with a straight run gas oil (Bui *et al.*, 2009). The presence of

guaiacol was found to decrease the HDS performance of a reference CoMo/Al₂O₃ catalyst at low temperatures, but above 320 °C, HDS could proceed without any further inhibition.

Similarly, Graca *et al.* (2011) found that the presence of guaiacol had a negative impact on the conversion of both n-heptane and gasoil in a simulated fluid catalyzed cracking (FCC) operation using HY, HZSM-5 and an industrial FCC equilibrium catalyst (E-CAT). This was found to be due to deposition of condensed material on the catalyst surface and was more pronounced with HZSM-5. This phenomenon was also observed by Graca *et al.*, (2009; 2010) who investigated the effects of phenol on the FCC of n-heptane and methylcyclohexane over an HY zeolite. Phenol was found to deactivate the zeolite by adsorbing onto the Brönsted and Lewis acid sites of the zeolite along with coke molecules from condensation of the reaction intermediates. Higher temperatures decreased phenol adsorption but did not prevent it.

Olcese *et al.*, (2010) investigated catalytic hydrodeoxygenation (HDO) of guaiacol, a model for lignin pyrolysis vapours, over Fe/SiO₂. They found that the Fe catalyst produced less methane than the reference Co catalyst with a good selectivity for benzene and toluene. Temperature and reaction time were found to influence the aromatic carbon-oxygen bond hydrogenolysis reaction whereas hydrogen partial pressure had a minor influence.

Gas phase hydrodeoxygenation (HDO) of guaiacol, as a model compound for pyrolysis oil, was tested on a series of transition metal phosphides which included Ni₂P/SiO₂, Fe₂P/SiO₂, MoP/SiO₂, Co₂P/SiO₂ and WP/SiO₂ (Zhao *et al.*, 2011). A commercial CoMoS/Al₂O₃ deactivated quickly and showed little activity for the HDO of guaiacol at the conditions tested while the most active phosphides were able to produce benzene and phenol with a small amount of methoxybenzene. A commercial catalyst 5% Pd/Al₂O₃ was more active than the metal phosphides.

Popov *et al.* (2011) studied the details of phenol adsorption on various catalysts and support materials. On silica, phenol was found to mainly interact via hydrogen-bonding while on alumina it was found to dissociate on the acid-base pairs leading to the formation of strongly adsorbed phenolate species. Similarly, phenol dissociates on alumina-supported sulfided CoMo but does not interact strongly with the sulfide phase. The adsorption of the phenolate was found to decrease the accessibility of reactive catalyst sites and they proposed that de-

creasing the number or strength of the acid-base paired sites of the support should be a way to limit catalyst deactivation.

2.7.2 Alkali-Catalyzed Depolymerization

As mentioned previously, one means of depolymerizing lignin is to use alkali as a catalyst. Shabtai *et al.* (1999) proposed a three-step process for converting lignin into reformulated gasoline which involves base-catalyzed depolymerization (BCD) followed by hydrodeoxygenation and hydrocracking steps. The BCD process uses a catalyst-solvent system of an alkali hydroxide e.g. NaOH and a supercritical alcohol such as methanol or ethanol and is performed at a temperature of about 270 °C. The reaction produces a pressure of around 140 bar after ~5 min and results in depolymerized lignin with about a 50% decrease in oxygen content as compared to the lignin feed. In the second step of the process, the depolymerized lignin was subjected to hydrodeoxygenation (HDO) in the presence of sulfided CoMo/Al₂O₃. Phenolic chemicals can be extracted from the product stream after this step if they are desired. The final step involved mild catalytic hydrocracking resulting in partial ring hydrogenation and a final product comparable to reformulated gasoline. These experiments were performed on three different types of lignin including Kraft lignin, organosolv lignin, and National Renewable Energy Laboratory (NREL) ethanol lignin. The lignins produced a wide range of compounds with little difference between the feed stocks and only small differences in reactivity were observed. The hydroprocessing of base-catalyzed depolymerized Kraft lignin yielded 73.5 wt.% of alkylated phenols and methoxyphenols.

In other work, Shabtai *et al.* (2001) proposed a different three-step process for converting lignin into partially oxygenated gasoline additives. The first stage of this process was also base-catalyzed depolymerization but was followed by selective hydrocracking using a superacid catalyst rather than HDO. This produced a depolymerized lignin product with a higher oxygen content and composed mainly of alkylated phenols, alkylated alkoxyphenols, and alkyl benzenes. In a final step, the depolymerized lignin underwent etherification and partial ring hydrogenation, producing a reformulated, partially oxygenated/etherified gasoline.

An enhanced catalytic lignin to liquid bio-fuels process involving BCD has been proposed by

Zmierzczak and Miller (2006). This method involves a similar three-step conversion process resulting in the production of either gasoline or aromatic ethers. An alternative one-step method to convert lignin into liquid fuels was also proposed.

Miller *et al.* (1999) also studied BCD of both lignin and lignin model compounds in a micro reactor. The lignin model compounds included anisole, guaiacol, phenyl ether, biphenyl, and benzyl phenyl ether. These compounds and lignin were depolymerized in a fluidized-bed reactor at 290 °C for up to 1 h using 10% KOH and an ethanol or methanol solvent. Kinetic studies showed that BCD occurs rapidly within 15 min. Ethanol was a better solvent than methanol and organosolv lignin resulted in the highest conversion. It was also observed that the excess amounts of alkali catalyst are required to achieve the greatest conversion. As has been reported in other literature, the analysis of model compound decomposition products revealed that phenyl ether linkages were relatively easily broken during BCD but the carbon-carbon linkages were more refractory. The ethanol solvent was found to react with phenyl ethers to form phenols and ethyl ethers as well as to participate in the alkylation of phenols and catechols.

More recent work by Nguyen (2014), investigated the depolymerization of a Kraft lignin slurry dispersed in aqueous K_2CO_3 and phenol and decomposed over ZrO_2 in a fixed-bed reactor at near critical conditions. A large fraction of the product stream was recycled to pre-heat the feed. The process produces an aqueous phase containing phenolics and a bio-oil phase exhibiting an increased heating value around 32 MJ/kg. The monoaromatic compounds produced consisted mainly of anisoles, alkyl phenols, guaiacols and catechols, with yields increasing (from 17 to 27%) with increased K_2CO_3 concentration.

2.8 Solvents

2.8.1 Hydrogen-donating Solvents

Hydrogen-donor solvents such as tetralin, 9,10-dihydroanthracene (AnH_2) and their derivatives and 1,4,5,8,9,10-hexahydroanthracene, have proven to be effective hydrogen donors for the liquefaction of coal. It was found that the quantity of hydrogen transferred from the solvent to the coal had a significant effect on the liquefaction reactions (Arends and Mulder,

1996).

Thring *et al.* (1993) reacted hardwood solvolytic lignin in the presence of tetralin and studied the effects of process severity on lignin conversion. Upon dehydrogenation at hydrocracking temperatures and pressures, tetralin was found to readily release four hydrogen atoms and was converted primarily to naphthalene. The hydrogen that was released was able to cap the highly reactive allyl- and vinyl-substituted intermediates resulting from lignin depolymerization. Conversion was found to increase monotonically with increased process severity and char formation was low under all reaction conditions. A maximum conversion of ~68% was observed and was essentially constant at low concentrations of lignin in tetralin. Conversion decreased with higher concentrations of lignin. The decomposition products resulting from neat pyrolysis of the lignin feed showed a similar trend: at low severity, syringols, guaiacols, and aromatic ketones were the most common products. With increased process severity, further decomposition of lignin into phenol and alkyl derivatives of phenol was observed.

Davoudzadeh *et al.* (1985) performed lignin hydrogenolysis using tetralin with phenol as a solvent. They observed an increase in liquid yield compared to neat pyrolysis. Vuori and Bredenberg (1988) reported a maximum yield of phenol around 20 wt.% for lignin pyrolysis under hydrogen in the presence of tetralin and *m*-cresol solvents. The presence of tetralin at longer reaction times was found to decrease guaiacol yield considerably while increasing the yields of phenol and their derivatives (Jegers and Klein, 1985). Kudsy *et al.* (1995) analyzed the role of tetralin in hydrogenolysis. The addition of tetralin was found to increase the yield of phenolic compounds but did not have a significant effect on gas yield.

Although these solvents are effective in increasing the hydrogenation of lignin they are relative expensive and hard to recover. There is another family of solvents such as formic acid and 2-propanol, which are thermally unstable and will decompose to give hydrogen upon being heated at elevated temperatures. For example, formic acid decomposes completely into hydrogen and carbon dioxide, and 2-propanol can decompose into hydrogen and acetone upon heating. Recently, these types of hydrogen-donating solvents have found special applications in the hydroprocessing of both biomass and lignin.

As reported by Kleinert *et al.* (2008), formic acid and 2-propanol were used as hydrogen donor solvents in the depolymerization and hydrogenation of lignin. The solvolysis products of

weak acid hydrolysis lignin (WAHL), strong acid hydrolysis lignin (SAHL), and enzymatic hydrolysis lignin (EHL) were analyzed for the presence of phenolic compounds. A well-separated mixture of an organic top layer and an aqueous bottom layer with a total liquid yield of up to 90 wt.% was obtained. The GC-MS spectrum of the liquid organic fraction clearly showed a significant presence of phenols, although their yield varied considerably depending on the feed. In general, the yield of the isolated phenolic fraction was reported to be within 25-35 wt.% of the lignin feedstock and was composed exclusively of monoaromatic phenols with alkylation ranging from C1-C7 in the side chain(s), in a one-step conversion of lignin to oxygen-depleted bio-fuels and phenols using a co-solvent mixture of formic acid and ethanol at about 400°C. The yield was 2 or 3 times that of an earlier work by Dorrestijn *et al.* (1999) using AnH_2 for de-polymerization of wood lignin at 352°C.

Kleinert and Barth (2008) performed solvolysis of steam explosion lignin, organosolv lignin, and hydrolysis lignin using formic acid in a non-stirred batch reactor. A reaction temperature around 380 °C was maintained for reaction times up to 17 h. Satisfactory conversion was achieved at temperatures of 350 °C and above with a minimum reaction time of 3-4 h. Analysis of the products revealed predominantly alkyl chains, although lignin monomers were still present. More recently, the results of a study on a one-step alternative for the conversion of lignin into low-oxygen content fuel and monomeric phenols have been published (Huang *et al.*, 2014). The proposed novel solvolytic method involves thermal treatment of lignin in a high pressure reactor with formic acid as an active hydrogen donor and water/ethanol as the solvent. On heating, formic acid decomposes completely into CO_2 and active hydrogen, which combines with oxygen from the methoxy groups of lignin to form water. Since both depolymerization and hydrodeoxygenation occur simultaneously, such solvolytic reactions can result in monomers with low oxygen contents in a single step.

A detailed analysis of characteristic properties of the solvolysis product oils from different sources of lignin by Gellerstedt *et al.* (2008) has shown similarities in composition, with nearly the same O/C and H/C ratios. FTIR analysis of lignin oil showed strong signals around 1200 and 1710 cm^{-1} , indicating the presence of isopropyl and/or tert-butyl groups and carboxyl groups, respectively. Characteristic peaks indicating the hydroxyl group and the aromatic ring were also observed. The strong presence of phenolic structures was confirmed by the signal cluster at 150 ppm in ^{13}C -NMR analysis. A peak mass weight of around 300 mass

units was calculated from size exclusion chromatography (SEC). Determination of optimum process conditions with a high yield of the desired chemicals, with a minimum use of solvents as well as acceptable ranges of temperature and pressure in the solvolysis reaction is very important for the method to be technologically acceptable. This, however, is very complex due to the interactions between the different parameters. Optimizing experiments show that high-pressure conditions give high yields. In addition, for high yield, the liquid loading of the reactor should be increased while keeping the amount of lignin and formic acid low (Kleinert *et al.*, 2009).

2.8.2 Supercritical Solvents

Supercritical solvents have also been used in the depolymerization of lignin. Supercriticality is a unique phase of matter wherein there is no differentiation between the liquid and gas phases of a solvent. Solvents in the supercritical state, that is, above their critical temperature and pressure, exhibit gas-like diffusivity, which facilitates mass transfer, at liquid-like densities, which facilitates heat transfer. Many researchers have studied the conversion of biomass, lignin, and lignin model compounds in supercritical water ($T_c = 374.15$ °C and $P_c = 22.1$ MPa). These studies have shown that hydrolysis in supercritical water is a viable means of lignin depolymerization. However, the yields of phenolic monomers are not as high as in other methods, likely due to the re-polymerization of reactive intermediates forming char. Aida *et al.*, (2002) suggested that the presence of phenol in could minimize the formation of char.

In related research, Saisu *et al.* (2003) depolymerized organosolv lignin in supercritical water in a stainless-steel tube reactor at 400 °C, with and without phenol. A comparison of the yields of tetrahydrofuran-soluble and -insoluble fractions of the depolymerized lignin demonstrated that the insoluble fraction increased with increased reaction time. Conversely, the THF-insoluble fraction decreased with increasing phenol/lignin ratio. The mechanism of the decomposition of lignin in supercritical water was proposed to be hydrolysis followed by dealkylation, yielding low-molecular-weight fragments and that cross-linking reactions between the depolymerized fragments gives rise to higher-molecular-weight fragments that deposit as char. The presence of phenol prevents the cross-linking reactions by interacting with

reactive sites of the decomposed fragments and so capping the molecules. In the presence of sufficient phenol, the formation of char can be significantly reduced. Okuda *et al.*, (2004b) obtained residual solid yields of ~1 wt.% when depolymerizing lignin a 1:1.4 (v/v) mixture of water and phenol. Similar experiments using *p*-cresol and water as the solvent in supercritical conditions also resulted in very low yields of solid residue. In addition, the molecular weight distribution shifted to remarkably lower values as compared to the original lignin feedstock (Okuda *et al.*, 2004a). A study of the depolymerization of lignin in a supercritical water/phenol mixture by Fang *et al.* (2008) also confirmed that addition of phenol inhibits repolymerization reactions. Lignin depolymerization in the presence of supercritical methanol instead of water was studied by Saka and his group. Their experiments using lignin model compounds showed that depolymerization of lignin in a batch reactor at 270 °C proceeds rapidly due to the cleavage of β -O-4 linkages (Tsujino *et al.*, 2003).

2.9 Summary

1. Fast pyrolysis is the only industrially realized technology for production of bio-oils from biomass. However, pyrolysis oils contain high levels of oxygenated compounds and water, and therefore have lower caloric values than petroleum oils.
2. High-pressure liquefaction technology which uses moderate temperatures <400 °C but higher pressures of 5-20 MPa has the potential to produce superior quality bio-oils with much higher caloric values (25-35 MJ/kg).
3. The bio-oils/bio-crudes produced by biomass liquefaction are composed of a complex mixture of oxygen-containing compounds in the form of phenol and benzene derivatives, hydroxyketones, carboxylic acids and esters, and aliphatic and aromatic alcohols. The high oxygen content of the bio-oils limits their usefulness as liquid transportation fuels since the high oxygen content results in increased viscosity, poor thermal and chemical stability, corrosivity (due to the organic acids present) and immiscibility with hydrocarbon fuels. Pyrolysis oils/bio-crudes, therefore, need to be upgraded to reduce their oxygen content in order to convert them into useful fuels.

4. Catalytic cracking and catalytic hydrotreating are the two typical technologies used in the upgrading of bio-oils for fuel applications. Catalytic cracking processes, which use cracking catalysts (e.g. zeolites, silica-alumina and molecular sieves), operate at atmospheric pressure without the requirement of additional hydrogen. In contrast, catalytic hydrotreating processes operate at higher pressures (2-20 MPa) in the presence of hydrogen and/or in the presence of hydrogen donor solvents.
5. Commercially available sulfided catalysts (Al_2O_3 -supported CoMo, NiMo, NiW, Ni, Co, Pd, and CuCrO) have been widely used for hydrodeoxygenation (HDO) of both bio-oils and model compounds. Alumina-supported Pd catalysts have been found to be the most effective catalysts, producing higher bio-oil yields than conventional Mo-based catalysts. Catalyst deactivation due to the formation of coke and tars has been identified as the major issue with the conventional alumina-supported catalysts.
6. Lignin can be extracted from woody biomass thereby reducing the amount of oxygen that needs to be removed from the resulting bio-oil since the oxygen-containing cellulose breakdown products are not present.
7. Some of the chemical bonds in lignin are more refractive to hydroprocessing than others.
8. Kraft lignin (alkali lignin) is widely available. However it presents a challenge in processing. During degradation, the sulfur present in the alkali lignin can become incorporated into the degradation products (as sulfides and thiols). The sulfur present will also, over time, poison any catalysts used. As a side note, the presence of sulfur also imparts a very strong unpleasant odour to the bio-oil, further limiting its utility.
9. Organosolv and hydrolysis lignin are an alternative to Kraft lignin, though they are not available in as large abundance. They are extracted without the use of sulfur compounds and are therefore sulfur-free. As such, the degradation of these lignins produces sulfur-free bio-oil - a benefit in terms of catalyst longevity (due to the absence of catalytic poisons) and odour during processing.
10. Lignin can be degraded by various means including; cracking or hydrolysis reactions, catalytic reduction reactions, and catalytic oxidation reactions.

11. Much literature has been published on whole bio-oil and lignin model compound upgrading (hydroprocessing) rather than the upgrading of lignin and degraded lignin.
12. Lignin degradation is complicated by the different types of bonds that make up the polymer.

2.9.1 Model Compounds

13. Model compounds allow researchers to determine reaction mechanisms and kinetics in simpler systems.
14. Phenol and guaiacol are the most studied lignin model compounds.
15. Guaiacol, and other di-oxygenates, are susceptible to coke formation and can be used to determine the ratio of coke (on the catalyst) to char (re-polymerization solids) production.
16. A large fraction of the model compound studies have investigated gas phase hydrodeoxygenation rather than liquid phase reactions.

2.9.2 Catalysts

17. Noble metals (e.g. Pt, Re, Rh) are effective hydroprocessing catalysts but are very expensive especially if they have are subjected to conditions where they have a short lifetime and cannot be regenerated effectively.
18. Transition metals are also active in bio-oil and model compound hydroprocessing but are generally not as active as noble metals catalysts.
19. The effectiveness of transition metal catalysts can be increased by the addition of promoters and/or additives.
20. Transition metal catalysts are usually used in reduced or sulfided forms.

21. Much research has been reported on hydroprocessing using sulfided catalysts (e.g. CoMo/alumina) similar to those used in petroleum processing
22. Conventional sulfided hydrodeoxygenation catalysts can give rise to products incorporating sulfur, are subject to rapid deactivation by coke formation, and can potentially become poisoning by water produced as a by-product of oxygen removal.
23. Ru/C may be too active a catalyst for the conversion of pyrolytic lignin oil to low molecular weight phenolics, but may be suitable for the production of fuels.

2.9.3 Catalyst Support

24. Acidic support materials such as alumina and zeolites are known to catalyze condensation reactions and quickly become deactivated by coke deposition.
25. Some of the catalyst deactivation observed in bio-oil upgrading using zeolites is due to adsorption of phenolic compounds on both Brønsted and Lewis acid sites
26. Catalyst supports also affect model compound adsorption mechanisms.
27. Support materials influence the selectivity of hydroprocessing products.
28. Catalyst morphology can affect hydroprocessing product selectivity as well.

2.9.4 Solvents

29. Solvents can enhance the hydroprocessing of bio-oils and model compounds either by dilution of the reactive coke precursors or by actively participating in the reactions as hydrogen donors.
30. Hydrogen donor solvents include isopropanol and formic acid which decompose upon heating while tetralin and similar compounds which have been used in coal liquefaction.
31. Hydrogen donor solvents produce reactive hydrogen species that cap highly reactive in-

intermediates

32. The use of co-solvents can improve product yields.
33. Supercritical solvents including water, CO₂, and alcohols have been used to produce and upgrade bio-oil.

2.10 References

- Adjave JD, Bakhshi NN. Production of hydrocarbons by catalytic upgrading of a fast pyrolysis bio-oil. Part I: Conversion over various catalysts. *Fuel Process. Technol.* 45 (1995) 161-183.
- Adjave JD, Katikaneni SPR, Bakhshi NN. Catalytic conversion of a biofuel to hydrocarbons: effect of mixtures of HZSM-5 and silica-alumina catalysts on product distribution. *Fuel Process. Technol.* 48 (1996) 115-143.
- Adschiri T, Hirose S, Malaluan R, Arai K. Noncatalytic conversion of cellulose in supercritical and subcritical water. *J. Chem. Eng. Jpn.* 26 (1993) 676-680.
- Aida TM, Sato T, Sekiguchi G, Adschiri T, Arai K, Extraction of Taiheiyo coal with supercritical water-phenol mixtures *Fuel* 81 (2002) 1453-1461.
- Appell HR, Fu YC, Friedman S, Yavorsky PM, Wender I. Converting organic wastes to oil. US Bureau of Mines, Report of Investigation No. 7560 (1971).
- Appell HR, Wender I, Miller RD. Conversion of urban refuse to oil. US Bureau of Mines, Technical Progress Report No. 25 (1969).
- Appell HR. Fuels from waste. New York: Academic Press (1967).
- Arechederra R, Treu BL, Minter SD. Development of glycerol/O₂ biofuel cell, *Journal of Power Sources* 173 (2007) 156-161.
- Arends IWCE, Mulder P. Study of Hydrogen Shuttling Reactions in Anthracene/9,10-dihydroanthracene-Naphthyl-X Mixtures. *Energy Fuels*, 10 (1996) 235-242.
- Baker EG, Elliott DC. Research in thermochemical biomass conversion. London: Elsevier Applied Science (1988) 883.
- Barth T, Kleinert M, Phenols from Lignin. *Chem. Eng. Technol.* 31 (2008) 736-745.

Bhargava S, Jani H, Tardio J, Akolekar D, Hoang M, Catalytic Wet Oxidation of Ferulic Acid (A Model Lignin Compound) Using Heterogeneous Copper Catalysts *Ind. Eng. Chem. Res.* 46 (2007) 8652-8656.

Boocock DGB, Mackay D, McPherson M, Nadeau S, Thurier R. Direct hydrogenation of hybrid poplar wood to liquid and gaseous fuels. *Can. J. Chem. Eng.* 57 (1979) 98-101.

Breysse M, Portefaix JL, Vrinat M. Support effects on hydrotreating catalysts. *Catal. Today* 10 (1991) 489-505.

Bridgwater AV, Bridge SA. Review of biomass pyrolysis processes. In *Biomass Pyrolysis Liquids Upgrading and Utilisation*; Elsevier: New York (1991) 11-92.

Bridgwater AV, Cottam ML. Opportunities for biomass pyrolysis liquids production and upgrading. *Energy Fuels* 6 (1992) 113-120.

Bridgwater AV, Czernik S, Piskorz, J. An overview of fast pyrolysis. *Progress in thermochemical biomass conversion, Volume 2*; Blackwell Science: London (2001) 977- 997.

Bridgwater AV. Catalysis in thermal biomass conversion. *Appl. Catal. A: Gen.* 116 (1994) 5-47.

Bridgwater AV. Production of high grade fuels and chemicals from catalytic pyrolysis of biomass. *Catal. Today* 29 (1996) 285-295.

Bridgwater AV. Renewable fuels and chemicals by thermal processing of biomass. *Chem. Eng. J.* 91 (2003) 87-102.

Bui VN, Laurenti D, Afanasiev P, Geantet C. Hydrodeoxygenation of guaiacol with CoMo catalysts. Part I: Promoting effect of cobalt on HDO selectivity and activity *Appl. Catal. B: Environmental* 101 (2011) 239-245.

Bui VN, Laurenti D, Delichère P, Geantet C. Hydrodeoxygenation of guaiacol : Part II: Support effect for CoMoS catalysts on HDO activity and selectivity *Appl. Catal. B: Environmental* 101 (2011) 246-255.

Bui VN, Laurenti D, Mirodatos C, Geantet C. Co-processing of pyrolysis bio oils and gas oil for new generation of bio-fuels: Hydrodeoxygenation of guaiacol and SRGO mixed feed *Catal. Today* 143 (2009) 172-178.

Butt DAE. Formation of phenols from the low-temperature fast pyrolysis of Radiata pine (*Pinus radiata*): Part I. Influence of molecular oxygen *J. Anal. Appl. Pyrolysis* 76 (2006) 38-47.

Cemek M, Kucuk MM. Liquid products from *Verbascum* stalk by supercritical fluid extraction. *Energy Convers. Manage.* 42 (2001) 125-130.

Centeno A, Laurent E, Delmon B. Influence of the support of CoMo sulfide catalysts and of the addition of potassium and platinum on the catalytic performances for the hydrodeoxygenation of carbonyl, carboxyl, and guaiacol-type molecules. *J. Catal.* 154 (1995) 288-298.

Champagne, P. *Resources, Conservation and Recycling* 50 (2007) 211-230.

Chen CL, Capanema EA, Gracz HS. Comparative studies on the delignification of pine kraft-anthraquinone pulp with hydrogen peroxide by binucleus Mn(IV) complex catalysis. *J. Agric. Food Chem.* 51 (2003) 6223-6232.

Chornet E, Overend RP. *Fundamentals of thermochemical biomass conversion*. Amsterdam: Elsevier (1985) 65.

Churin E, Grange P, Delmon B. Quality improvement of pyrolysis oils. Final report on contract no. EN3B-0097-B for the Directorate-General Science, Research and Development, Commission of the European Communities (1989).

Churin E, Maggi R, Grange P, Delmon B. Characterization and upgrading of a bio-oil produced by pyrolysis of biomass. *Research in thermochemical biomass conversion*, Elsevier Science Publishers, Ltd. (1988) 896-909.

Connors WJ, Johanson LN, Sarkanen KV, Winslow P. Thermal Degradation of Kraft Lignin in Tetralin *Holzforschung* 34 (1980) 29-37.

Corma A, Huber GW, Sauvinaud L, O'Connor P. Biomass to chemicals: catalytic conversion of glycerol/water mixtures into acrolein, reaction network. *J Catal* 257 (2008) 163-171.

Craig W, Coxworth E. Proceedings of the sixth Canadian bioenergy R&D seminar. London: Elsevier Applied Science (1987) 407.

Crofcheck C, Montross MD, Berkovich A, Andrews R. The effect of temperature on the mild solvent extraction of white and red oak. *Biomass Bioenergy* 28 (2005) 572-578.

Czernik S, Bridgwater AV. Overview of applications of biomass fast pyrolysis oil. *Energy Fuels* 18 (2004) 590-598.

Czernik S, Maggi R, Peacocke GVC. Review of methods for upgrading biomass-derived fast pyrolysis oils. *Fast Pyrolysis of Biomass: A handbook* (2002) 141-145.

Dahlman O, Jacobs A, Liljenberg A, Olsson AI. Analysis of carbohydrates in wood and pulps employing enzymatic hydrolysis and subsequent capillary zone electrophoresis. *Journal of Chromatography A* 891 (2000) 157-174.

Davoudzadeh F, Smith B, Avni E, Coughlin RW. Depolymerization of Lignin at Low Pressure Using Lewis Acid Catalysts and under High Pressure Using Hydrogen Donor Solvents *Holzforschung* 39 (1985) 159-164.

Davoudzadeh F, Coughlin RW. Coliquefaction of lignin and bituminous coal. *Fuel* 65 (1986) 95-106.

De Wild P, Van der Laan R, Kloekhorst A, Heeres HJ. Lignin valorisation for chemicals and (transportation) fuels via (catalytic) pyrolysis and hydrodeoxygenation. *Environ. Progr. Sust. Energy* 28 (2009) 461-469.

Decanio EC, Edwards JC, Scalzo TR, Storm DA, Bruno JW. FT-IR and solid-state NMR investigation of phosphorus promoted hydrotreating catalyst precursors. *J. Catal.* 132 (1991) 498-511.

Demirbas A. (a) Mechanism of liquefaction and pyrolysis reactions of biomass. *Energy Convers. Manage.* 41 (2000) 633-646.

Demirbas A. (b) Conversion of biomass using glycerin to liquid fuel for blending gasoline as alternative engine fuel. *Energy Convers. Manage.* 41 (2000) 1741-1748.

Demirbas A. Supercritical fluid extraction and chemicals from biomass with supercritical fluids. *Energy Convers. Manage.* 42 (2001) 279-294.

Demirbas A. Pyrolysis of ground beech wood in irregular heating rate conditions. *J. Anal. Appl. Pyrolysis* 73 (2005) 39-43.

Demirbas A, Pehlivan E, Altun T. Potential evolution of Turkish agricultural residues as bio-gas, bio-char and bio-oil sources. *Int. J. of Hydro. Energy* 31 (2006) 613-620.

Dorrestijn E, Kranenburg M, Poinot D, Mulder P, Lignin depolymerization in hydrogen-donor solvents, *Holzforschung*, 53 (1999) 611-616.

Dorrestijn E, Laarhoven LJJ, Arends IWCE, Mulder P, The occurrence and reactivity of phenoxy linkages in lignin and low rank coal. *J. Anal. Appl. Pyrolysis* 54 (2000) 153-192.

Elliott DC, Baker EG, Piskorz J, Scott DS, Solantausta Y. Production of liquid hydrocarbon fuels from peat. *Energy Fuels* 2 (1988) 234-235.

Elliott DC, Baker EG. Upgrading biomass liquefaction products through hydrodeoxygenation. *Biotechnol. Bioeng. Symp.* 14 (1984) 159-174.

Elliott DC, Hart TR, Neuenschwander GG, McKinney MD, Norton MV, Abrams CW. Environmental impacts of thermochemical biomass conversion. NREL/TP-433-7867, National Renewable Energy Laboratory: Golden, Colorado (1995).

Elliott DC, Neuenschwander GG, Hart TR, Hu J, Solana AE, Cao C. Hydrogenation of bio-oil for chemical and fuel production. *Science in Thermal and Chemical Biomass Conversion*, CPL Press: Newbury Berks, UK (2006) 1536-1546.

Elliott DC, Neuenschwander GG. Developments in thermochemical biomass conversion. Blackie Academic and Professional: London (1996).

Elliott DC, Oasmaa A. Catalytic hydrotreating of black liquor oils. *Energy Fuels* 5 (1991) 102-109.

Elliott DC. Bench-scale research in biomass liquefaction by the CO-steam process. *Can. J. Chem. Eng.* 58 (1980) 730-734.

Elliott DC. Historical developments in hydroprocessing bio-oils. *Energy Fuels* 21 (2007) 1792-1815.

Elliott DC. Hydrodeoxygenation of phenolic components of wood-derived oil. *Am. Chem. Soc., Div. Pet. Chem. Prepr.* 28 (1983) 185.

EU Directive 2003/30/EC, The promotion of the use of biofuels and other renewable fuels for transport, (2003).

Fang Z, Sato T, Smith Jr. RL, Inomata H, Arai K, Kozinski JA. Reaction chemistry and phase behavior of lignin in high-temperature and supercritical water. *Bioresour. Technol.* 99 (2008) 3424-3430.

Ferdous D, Dalai AK, Adjaye JD. A series of NiMo/Al₂O₃ catalysts containing boron and phosphorus Part I. synthesis and characterization. *Appl. Catal. A: Gen.* 260 (2004) 137-151.

Ferdous D, Dalai AK, Bej SK, Thring RW. Pyrolysis of lignins: experimental and kinetics studies *Energy Fuels*, 16 (2002) 1405-1142.

Furimsky E. Review: catalytic hydrodeoxygenation. *Appl. Catal. A: Gen.* 199 (2000) 147-190.

Furrer RM and Bakhshi NN in *Research in Thermochemical Biomass Conversion*, eds A. V. Bridgewater and J. L. Kuester. Elsevier Applied Science, London and New York (1988) 956.

Gagnon J, Kaliaguine S. Catalytic hydroprocessing of vacuum pyrolysis oils from wood. *Ind. Eng. Chem. Res.* 27 (1988) 1783-1788.

Gellerstedt G, Li J, Eide I, Kleinert M, Barth T, Chemical Structures Present in Biofuel Obtained from Lignin. *Energy Fuels* 22 (2008) 4240-4244.

Gerber MA. Review of Novel Catalysts for Biomass Tar Cracking and Methane Reforming, PNNL-16950 (2007).

Georget DMR, Cairns P, Smith AC, Waldron KW. Crystallinity of lyophilised carrot cell wall components. *Int. J. Biological Macromolecules* 26 (1999) 325-31.

Gevert SB, Andersson BW, Sandqvist SP, Jaeraas SG, Tokarz MT. Hydroprocessing of directly liquefied biomass with large-pore catalysts. *Energy Fuels* 4 (1990) 78-81.

Gevert SB. Energy from biomass and wastes XI. IGT, Chicago (1988).

Gonçalves AR, Schuchardt U. Hydrogenolysis of lignins: influence of the pretreatment using microwave and ultrasound irradiations. *Appl. Biochem. Biotechnol.* 98-100 (2002) 1211-1219.

Graça I, Fernandes A, Lopes JM, Ribeiro MF, Laforge S, Magnoux P, Ramôa Ribeiro F, Effect of phenol adsorption on HY zeolite for n-heptane cracking: Comparison with methylcyclohexane. *Appl. Catal. A: General* 385 (2010) 178-189.

Graça I, Lopes JM, Ribeiro M, Ramôa Ribeiro F, Cerqueira HS, de Almeida MBB. Catalytic cracking in the presence of guaiacol. *Appl. Catal. B: Environmental* 101 (2011) 613-621.

Graça I, Ramôa-Ribeira F, Cerqueirb HS, Lam YL, de Almeida MBB. Catalytic cracking of mixtures of model bio-oil compounds and gasoil. *Appl. Catal. B: Environmental* 90 (2009) 556-563.

Guo Y, Wang Y, Wei F. Research progress in biomass flash pyrolysis technology for liquids production. *Chem. Ind. Eng. Progr.* 8 (2001) 13-17.

Gutierrez A, Krause O. Production alternatives of biocomponents for diesel. *Laboratory of Industrial Chemistry - TKK* (2008).

Huang S, Mahmood N, Tymchyshyn M, Yuan Z, Xu C. Reductive De-polymerization of Kraft Lignin for Chemicals and Fuels using Formic Acid as an In-situ Hydrogen Source. *Bio-resour. Technol.* 171 (2014) 95-102.

Ishikawa Y, Saka S. Chemical conversion of cellulose as treated in supercritical methanol. *Cellulose* 8 (2001) 189-195.

Jegers HE, Klein MT. Primary and secondary lignin pyrolysis reaction pathways, *Ind. Eng. Chem. Process Des. Dev.* 24 (1985) 173-178.

Jin Y, Ruan X, Cheng X, Lü Q. Liquefaction of lignin by polyethyleneglycol and glycerol. *Bioresour. Technol.* 102 (2011) 3581-3583.

Jongerius AL, Jastrzebski R, Bruijninx PCA, Weckhuysen BM. CoMo sulfide-catalyzed hydrodeoxygenation of lignin model compounds: An extended reaction network for the conversion of monomeric and dimeric substrates. *J. Catal.* 285 (2012) 315-323.

Jongerius AL, Bruijninx PCA, Weckhuysen BM. Liquid-phase reforming and hydrodeoxygenation as a two-step route to aromatics from lignin. *Green Chem.* 15 (2013) 3049-3056.

Joshi N, Lawal A. Hydrodeoxygenation of pyrolysis oil in a microreactor. *Chem. Eng. Sci.* 74 (2012) 1-8.

Karagoz S, Bhaskar T, Muto A, Sakata Y, Oshiki T, Kishimoto T. Low-temperature catalytic hydrothermal treatment of wood biomass: analysis of liquid products. *Chem. Eng. J.* 108 (2005) 127-137.

Karagoz S, Bhaskar T, Muto A, Sakata Y. Effect of Rb and Cs carbonates for production of phenols from liquefaction of wood biomass. *Fuel* 83 (2004) 2293-2299.

Katikaneni SPR, Adjave JD, Bakhshi NN. Performance of aluminophosphate molecular sieve catalysts for the production of hydrocarbons from wood-derived and vegetable oils. *Energy Fuels* 9 (1995) 1065-1078.

Kleinert M, Barth T. Towards a lignocellulosic biorefinery: Direct one-step conversion of lignin to hydrogen-enriched bio-fuel. *Energy Fuels* 22 (2008) 1371-1379.

Kleinert M, Gasson JR, Barth T. Optimizing solvolysis conditions for integrated depolymerisation and hydrodeoxygenation of lignin to produce liquid biofuel. *J. Anal. Appl. Pyrolysis* 85 (2009) 108-117.

Klipcera T, Zdrzil M. Preparation of high activity MgO-supported Co-Mo and Ni-Mo sulfide hydrodesulfurization catalysts. *J. Catal.* 206 (2002) 314-320.

Kudsy M, Kumazawa H, Sada E, Pyrolysis of kraft lignin in molten ZnCl₂-KCl media with tetralin vapor addition. *Can. J. Chem. Eng.* 73 (1995) 411-415.

Lee CR, Yoon JS, Suh YW, Choi JW, Ha JM, Suh DJ, Park YK. Catalytic roles of metals and supports on hydrodeoxygenation of lignin monomer guaiacol. *Catal. Commun.* 17 (2012) 54-58.

Li X, Su L, Wang Y, Yu Y, Wang C, Li X, Wang Z. Catalytic fast pyrolysis of Kraft lignin with HZSM-5 zeolite for producing aromatic hydrocarbons. *Front. Environ. Sci. Eng.* 6 (2012) 295-303.

Liu Q, Wang SR, Zheng Y. Mechanism Study of Wood Lignin Pyrolysis by using TG-FTIR Analysis. *J. Anal. Appl. Pyrolysis* 82 (2008) 170-177.

Luck F. A review of support effects on the activity and selectivity of hydrotreating catalysts. *Bull. Soc. Chim. Belg.* 100 (1991) 781-800.

Maggi R, Delmon B. Advances in thermochemical biomass conversion. London: Elsevier Applied Science (1993) 1185.

Matsumura Y, Nonaka H, Yokura H, Tsutsumi A, Yoshida K. Co-liquefaction of coal and cellulose in supercritical water. *Fuel* 78 (1999) 1049-1056.

Matsumura Y, Sasaki M, Okuda K, Takami S, Ohara S, Umetsu M, Adschiri T. Supercritical water treatment of biomass for energy and material recovery. *Combustion Science and Technology* 178 (2006) 509-536.

McDonald EC, Howard J, Bennett B. Chemicals from forest products by supercritical fluid extraction. *Fluid Phase Equilib.* 10 (1983) 337-344.

Meier D, Ante R, Faix O. Catalytic hydrolysis of lignin: Influence of reaction conditions on the formation and composition of liquid products. *Bioresour. Technol.* 40 (1992) 171-177.

Meier D, Berns J, Faix O, Balfanz U, Baldauf W. Hydrocracking of organocell lignin for phenol production. *Biomass Bioenergy* 7 (1994) 99-105.

Miller JE, Evans L, Littlewolf A, Trudell DE. Batch microreactor studies of lignin and lignin model compound depolymerization by bases in alcohol solvents. *Fuel* 78 (1999) 1363-1366.

Minami E, Kawamoto H, Saka S. Reaction behaviours of lignin in supercritical methanol as studied with lignin model compounds. *J. Wood Sci.* 49 (2003) 158-165.

Minowa T, Kondo T, Sudirjo ST. Thermochemical liquefaction of Indonesia biomass residues. *Biomass Bioenergy* 14 (1998) 517-524.

Molton PM, Demmitt TF, Donovan JM, Miller RK. Mechanism of conversion of cellulose wastes to liquid in alkaline solution. *Symposium on Energy from Biomass and Wastes* Washington, DC (1978) 293-316.

Nagy M, David K, Britovsek GJP, Ragauskas AJ. Catalytic hydrogenolysis of ethanol organosolv lignin. *Holzforschung* 63 (2009) 513-520.

Nenkova S, Vasileva T, Stanulov K. Production of low molecular phenolic compounds from technical hydrolysis lignin and wood biomass. *Chem. Nat. Compd.* 44 (2008) 182-185.

Nguyen TDH, Maschietti M, Belkheiri T, Åmand L-E, Theliander H, Vamling L, Olausson L, Andersson S-I. Catalytic depolymerisation and conversion of Kraft lignin into liquid products using near-critical water *J. of Supercritical Fluids* 86 (2014) 67-75.

Oasmaa A, Czernik S. Fuel oil quality of biomass pyrolysis oils-state of the art for the end users. *Energy Fuels* 13 (1999) 914-921.

Oasmaa A, Johansson A. Catalytic hydrotreating of lignin with water-soluble molybdenum catalyst. *Energy Fuels* 7 (1993) 426-429.

Oasmaa A, Solantausta Y, Arpiainen V, Kuoppala E, Sipila K. Fast pyrolysis bio-oils from wood and agricultural residues. *Energy Fuels* 24 (2010) 1380-1388.

Okuda K, Man X, Umetsu M, Takami S, Adschiri T. (a) Efficient conversion of lignin into single chemical species by solvothermal reaction in water/*p*-cresol solvent. *J. Phys. Condens. Matter* 16 (2004) S1325.

Okuda K, Umetsu M, Takami S, Adschiri T. (b) Disassembly of lignin and chemical recovery—rapid depolymerization of lignin without char formation in water-phenol mixtures. *Fuel Process. Technol.* 85 (2004) 803-813.

Olcese RN, Bettahar M, Petitjean D, Malaman B, Giovanella F, Dufour A. Gas-phase hydrodeoxygenation of guaiacol over Fe/SiO₂ catalyst. *Appl. Catal. B: Environmental* 115-116 (2012) 63-73.

Olivares M, Guzmán JA, Natho A, Saavedra A. Kraft lignin utilization in adhesives. *Wood Sci. Technol.* 22 (1988) 157-165.

Palmisano P, Lago V, Berruti F, Briens C. Fluidized Bed Pyrolysis of Lignin in a Bubbling Bed Reactor. In: *Bioenergy III: Present and New Perspectives on Biorefineries*, ECI Symposium Series, 14 (2012).

Pandey MP, Kim CS. Lignin depolymerization and conversion: a review of thermochemical methods. *Chem. Eng. Technol.* 34 (2011) 29-41.

Partenheimer W. The aerobic oxidative cleavage of lignin to produce hydroxyaromatic benzaldehydes and carboxylic acids via metal/bromide catalysts in acetic acid/water mixtures. *Adv. Synth. Catal.* 351 (2009) 456-466.

Peng WM, Wu QY. Production of fuels from biomass by pyrolysis. *New Energy Sources* 22 (2000) 39-44.

Pindoria RV, Megaritis A, Herod A and Kandiyoti R. A two-stage fixed-bed reactor for direct hydrotreatment of volatiles from the hydrolysis of biomass: effect of catalyst temperature, pressure and catalyst ageing time on product characteristics. *Fuel* 77 (1998) 1715-1726.

Piskorz J, Majerski P, Radlein D, Scott DS. Conversion of lignins to hydrocarbon fuels. *Energy Fuels* 3 (1989) 723-726

Poirier MG, Ahmed A, Grandmaison JL, Kaliaguine CF. Supercritical gas extraction of wood with methanol in a tubular reactor. *Ind. Eng. Chem. Res.* 26 (1987) 1738-1743.

Popov A, Kondratieva E, Gilson J-P, Mariey L, Travert A, Maugé F. IR study of the interaction of phenol with oxides and sulfided CoMo catalysts for bio-fuel hydrodeoxygenation. *Catal. Today* 172 (2011) 132-135.

Qian Y, Zuo C, Tan J, He J. Structural analysis of bio-oils from sub-and supercritical water liquefaction of woody biomass. *Energy* 32 (2007) 196-202.

Qu Y, Wei X, Zhong C. Experimental study on the direct liquefaction of *Cunninghamia Lanceolata* in water. *Energy* 28 (2003) 597-606.

Radovic LR, Rodriguez-Reinoso F. Carbon materials in catalysis. *Chem. Phys. Carbon* 25 (1997) 243-358.

Ratcliff MA, Johnson DK, Posey FL, Chum HL. Hydrodeoxygenation of lignins and model compounds. *Appl. Biochem. Biotechnol.* 17 (1988) 151-160.

Rohella RS, Sahoo N, Chakravorty V. Lignin macromolecule. *Resonance* 2 (1997) 60-66.

Saisu M, Sato T, Adschiri T, Arai K. Conversion of lignin with supercritical water-phenol mixtures. *Energy Fuels* 17 (2003) 922-928.

Saka S, Konishi R. Chemical conversion of biomass resources to useful chemicals and fuels by supercritical water treatment. In: Bridgwater A.V. (ed.), *Progress in Thermochemical Biomass Conversion*. Blackwell Science, Oxford, UK (2000) 1338-48.

Saka S, Ueno T. Chemical conversion of various celluloses to glucose and its derivatives in supercritical water. *Cellulose* 6 (1999) 177-191.

Sakaki T, Shibata M, Sumi T, Yasuda S. Saccharification of cellulose using a hot-compressed water-flow reactor. *Ind. Eng. Chem. Res.* 41 (2002) 661-665.

Sales FG, Maranhão LCA, Lima Filho NM, Abreu CAM. Kinetic Evaluation and Modeling of Lignin Catalytic Wet Oxidation to Selective Production of Aromatic Aldehydes. *Chem. Eng. Sci.* 45 (2006) 6627-6631.

Santos RB, Lee JM, Jameel H, Chang HM, Lucia LA. *Bioresour. Technol.* 110 (2012) 232-238.

Sasaki M, Fang Z, Fukushima Y, Adschiri T, Arai K. Dissolution and hydrolysis of cellulose in subcritical and supercritical water. *Ind. Eng. Chem. Res.* 39 (2000) 2883-2890.

Savage PE. Organic chemical reactions in supercritical water. *Chem. Review* 99 (1999) 603-621.

Schirmer RE, Pahl TR, Elliott DC. Analysis of a thermochemically-derived wood oil. *Fuel* 63 (1984) 368-372.

Scholze B, Meier D. Characterization of the water-insoluble fraction from pyrolysis oil (pyrolytic lignin) Part I. PY-GC/MS, FTIR, and functional groups. *J. Anal. Appl. Pyrol.* 60 (2001) 41-54.

Sedai B, Díaz-Urrutia C, Baker RT, Wu R, Silks LA, Hanson SK. Comparison of Copper and Vanadium Homogeneous Catalysts for Aerobic Oxidation of Lignin Models. *ACS Catalysis* 1 (2011) 794-804

Sedai B, Díaz-Urrutia C, Baker RT, Wu R, Silks LA, Hanson SK. Aerobic Oxidation of β -1 Lignin Model Compounds with Copper and Oxovanadium Catalysts. *ACS Catalysis* 3 (2013) 3111-3122.

Senol OI, Ryymin E-M, Viljava T-R, Krause AOI. Effect of Hydrogen Sulphide on the Hydrodeoxygenation of Aromatic and Aliphatic Oxygenates on Sulphided Catalysts *J. Mol. Catal. A: Chem.* 277 (2007) 107-112.

Şenol Oİ. Hydrodeoxygenation of aliphatic and aromatic oxygenates on sulphided catalysts for production of second generation biofuels. Doctoral Thesis, Helsinki University of Technology, ISBN 978-951-22-9035-2 (2007).

Shabtai JS, Zmierczak WW, Chornet E. US Patent 5959167 (1999).

Shabtai JS, Zmierczak WW, Chornet E. US Patent 6172272 B1 (2001).

Shabtai, JS, Zmierczak WW, Chornet E, Johnson DK. Conversion of lignin. 2. Production of high-octane fuel additives. *Am. Chem. Soc. Div. Fuel. Chem. Prepr.* 44 (1999) 267.

Sharma RK, Bakhshi NN. Catalytic upgrading of fast pyrolysis oil over HZSM-5. *Can. J. Chem. Eng.* 71 (1993) 383-391.

Sharma RK, Bakhshi NN. Catalytic upgrading of pyrolysis oil. *Energy Fuels* 7 (1993) 306-314.

Sharma RK, Bakhshi NN. Catalytic upgrading of biomass-derived oils to transportation fuels and chemical. *Can. J. Chem. Eng.* 69 (1991) 1071-1108.

Sharma RK, Wooten JB, Baliga VL, Lin X, Chan WG, Hajaligol MR. Characterization of chars from pyrolysis of lignin. *Fuel* 83 (2004) 1469-1482.

Sheu Y-H, Anthony RG, Soltes EJ, Kinetic studies of upgrading pine pyrolytic oil by hydro-processing *Fuel Process. Technol.* 19 (1988) 31-50.

Sipilae K, Kuoppala E, Fagermaes L. Characterization of biomass-based flash pyrolysis oils. *Biomass Bioenergy* 14 (1998) 103-113.

Soltes EJ, Lin SCK, Sheu YHE. Catalyst specificities in high pressure hydroprocessing of pyrolysis and gasification tars. *Am. Chem. Soc., Div. Fuel Chem.* 32 (1987) 229-239.

Song Q, Wang F, Cai J, Wang Y, Zhang J, Yua W, Xu J. Lignin depolymerization (LDP) in alcohol over nickel-based catalysts via a fragmentation-hydrogenolysis process. *Energy Environ. Sci.* 6 (2013) 994-1007.

Suzuki H, Cao J, Jin FM, Kishita A, Emonoto H. Wet oxidation of lignin model compounds and acetic acid production. *J. Mater. Sci.* 41 (2006) 1591-1597.

Tang Z, Zhang Y, Guo Q. Catalytic hydrocracking of pyrolytic lignin to liquid fuel in super-critical ethanol *Ind. Eng. Chem. Res.* 49 (2010) 2040-2046.

Thring RW, Breau J. Hydrocracking of solvolysis lignin in a batch reactor. *Fuel* 75 (1996) 795-800.

Thring W, Chornet E, Overend RP. Fractionation of woodmeal by prehydrolysis and thermal organosolv. Process strategy, recovery of constituents, and solvent fractionation of lignins so produced. *Can. J. Chem. Eng.* 71 (1993) 116-123.

Topsøe H, Clausen BS, Massoth FE. Hydrotreating catalysis, science and technology. Springer, Berlin (1996) 1-24.

Tsujino J, Kawamoto H, Saka S. Reactivity of lignin in supercritical methanol studied with various lignin model compounds. *Wood Sci. Technol.* 37 (2003) 299-307.

Várhegyi G, Antal Jr. MJ, Jakab E, Szabó P. Kinetic modeling of biomass pyrolysis. *J. Anal. Appl. Pyrol.* 42 (1997) 73-87.

Vasudevan PT, Fierro JLG. A review of deep hydrodesulfurization catalysis. *Catal. Rev.* 38 (1996) 161-188.

Voitl T, von Rohr PR. Demonstration of a Process for the Conversion of Kraft Lignin into Vanillin and Methyl Vanillate by Acidic Oxidation in Aqueous Methanol. *Ind. Eng. Chem. Res.* 49 (2010) 520-525.

Vuori A, Bredenberg JB. Liquefaction of Kraft Lignin: 1. Primary Reactions under Mild Thermolysis Conditions. *Holzforschung* 42 (1988) 155-161.

Warner G, Hansen TS, Riisager A, Beach ES, Barta K, Anastas PT. Depolymerization of organosolv lignin using doped porous metal oxides in supercritical methanol. *Bioresour. Technol.* 161 (2014) 78-83.

Watanabe M, Inomata H, Osada M, Sato T, Adschiri T, Arai K. Catalytic effects of NaOH and ZrO₂ for partial oxidative gasification of n-hexadecane and lignin in supercritical water. *Fuel* 82 (2003) 545-552.

Williams PT, Horne PA. The influence of catalyst regeneration on the composition of zeolite-upgraded biomass pyrolysis oils. *Fuel* 74 (1995) 1839-1851.

Windt M, Meier D, Marsman JH, Heeres HJ, de Koning S. Micro-pyrolysis of technical lignins in a new modular rig and product analysis by GC-MS/FID and GC × GC-TOFMS/FID. *J. Anal. Appl. Pyrolysis* 85 (2009) 38-46.

Xiang Q, Lee YY. Production of oxychemicals from precipitated hardwood lignin. *Appl. Biochem. Biotechnol.* 91-93 (2001) 71-80.

Xu C, Donald J. Upgrading peat to gas and liquid fuels in supercritical water with catalysts. *Fuel* 102 (2012) 16-25.

Xu C, Etcheverry T. Hydro-liquefaction of woody biomass in sub- and supercritical ethanol with iron-based catalysts. *Fuel* 87 (2008) 335-345.

Xu C, Lad N. Production of heavy oils with high caloric values by direct liquefaction of woody biomass in sub/near-critical water. *Energy Fuels* 22 (2008) 635-642.

Yaman S. Pyrolysis of biomass fuels and chemical feedstocks. *Energy Convers. Manage.* 45 (2004) 651-671.

Yan N, Zhao C, Dyson PJ, Wang C, Liu L, Kou Y. Selective degradation of wood lignin over noble-metal catalysts in a two-step process. *Chem. Sus. Chem.* 1 (2008) 626-629.

Yang H, Yan R, Chen H, Lee DH, Zheng C. Characteristics of hemicellulose, cellulose and lignin pyrolysis. *Fuel* 86 (2007) 1781-8.

Yang Y, Gilbert A, Xu C. (a) Production of bio-crude from forestry waste by hydro-liquefaction in sub-/super-critical methanol. *AIChE J.* 55 (2009) 807-819.

Yang Y, Gilbert A, Xu C. (b) Hydrodeoxygenation of bio-crude in supercritical hexane with sulfided CoMo and CoMoP catalysts supported on MgO: A model compound study using phenol. *Appl. Catal. A: Gen.* 360 (2009) 242-249.

Yang YQ, Tye CT, Smith KJ. Influence of MoS₂ catalyst morphology on the hydrodeoxygenation of phenols. *Catal. Comm.* 9 (2008) 1364-1368.

Yokoyama S, Ogi T, Koguchi K, Nakamura E. Direct liquefaction of wood by catalyst and water. *Liquid Fuels Technol.* 2 (1984) 115-163.

Yoshikawa T, Yagi T, Shinohara S, Fukunaga T, Nakasaka Y, Tago T, Masuda T. Production of phenols from lignin via depolymerization and catalytic cracking. *Fuel Proc. Technol.* 108 (2013) 69-75.

Zakzeski J, Bruijninx PC, Jongerius AL, Weckhuysen BM. The catalytic valorization of lignin for the production of renewable chemicals. *Chem. Rev.* 110 (2010) 3552-3599.

Zdražil M. MgO-supported Mo, CoMo and NiMo sulfide hydrotreating catalysts. *Catal. Today* 86 (2003) 151-171.

Zhang Q, Chang J, Wang T, Xu Y. Upgrading bio-oil over different solid catalysts. *Energy Fuels* 20 (2006) 2717-20.

Zhang Q, Chang J, Wang T, Xu Y. Review of biomass pyrolysis oil properties and upgrading research. *Energy Convers. Manage.* 48 (2007) 87-92.

Zhang Q, Zhao G, Chen J. Effects of inorganic acid catalysts on liquefaction of wood in phenol. *Front. For. China* 2 (2006) 214-218.

Zhang SP, Yan YJ, Li T, Ren Z. Upgrading of liquid fuel from the pyrolysis of biomass. *Bioresour. Technol.* 96 (2005) 545-550.

Zhang SP, Yan YJ, Ren ZW. Analysis of liquid product obtained by the fast pyrolysis of biomass. *J. Chin. Sci. Technol.* 27 (2001) 666-668.

Zhao HY, Li D, Bui P, Oyama ST. Hydrodeoxygenation of guaiacol as model compound for pyrolysis oil on transition metal phosphide hydroprocessing catalysts. *Appl. Catal. A: Gen.* 391 (2011) 305-310.

Zhong C, Wei X. A comparative experimental study on the liquefaction of wood. *Energy* 29 (2004) 1731-1741.

Zmierczak WW, Miller JD. US Patent 119357 (2006).

Chapter 3

3 Reductive depolymerization of Kraft and organosolv lignin for aromatic chemicals and materials

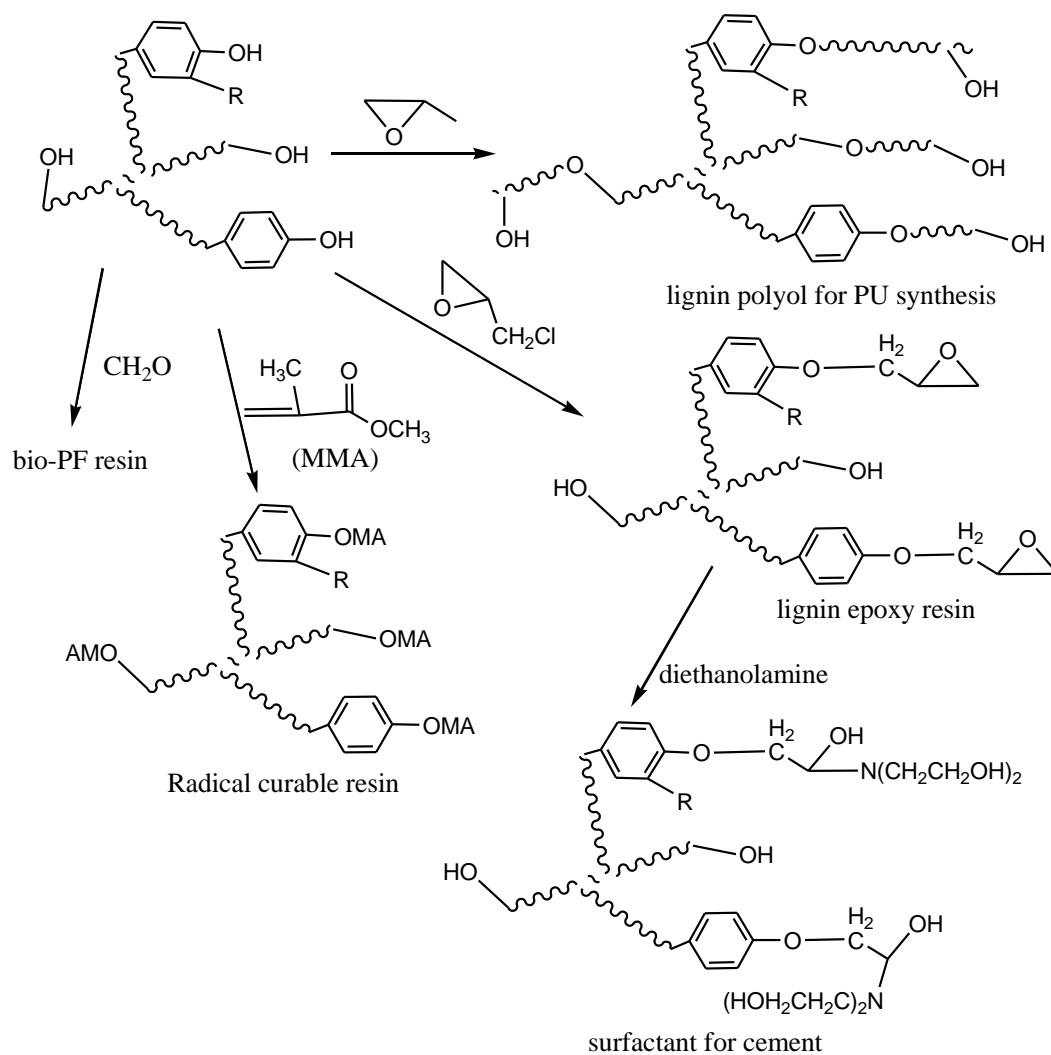
3.1 Introduction

Due to rapid depletion of available petroleum reserves, one of the major priorities of 21st century is to find new resources for fuel and chemicals to replace the fossil deposits as they become exhausted. In this regard, biomass, as an abundant and renewable resource, is certainly the most feasible choice. Lignin is the second most abundant naturally synthesized polymer after cellulose comprising 25-40 % of dry wood and a majority of crop stems. (Tejado *et al.*, 2007) About 70 million tons of Kraft lignin (KL) is generated annually as a by-product in the pulp and paper industry in the form of “black liquor”. Up to now, it has been utilized predominantly as a low-energy content fuel in pulp/paper mill recovery boilers for generation of heat and pulping chemical regeneration. However, in many Kraft mills, the recovery boilers present a bottleneck in the pulping process due to the sheer amounts of lignin produced. In addition, large volumes of organosolv lignin (OL) from the pre-treatment processes in cellulosic ethanol plants are expected to become available as the bio-ethanol industry expands in the near future. (Champagne, 2007) With the increasing interest in developing cellulose-based biodegradable materials and composites, new technologies, such as ionic liquid (Pinkert *et al.*, 2011; Hart and Aldous, 2015; van Spronsen *et al.*, 2014) and organic acid (Vasquez *et al.*, 1995; Hirose *et al.*, 2001) approaches, are being developed to separate lignin from cellulose. All of these methods produce OL.

As a natural polymer of substituted phenyl-propanols, lignin contains many polar hydroxyl groups attached to the polymer chains, making it incompatible with most synthetic polymers due to its high polarity, high degree of crystallinity and wide range of glass transition temperatures. (Chakar and Ragauskas, 2004) In addition, due to its branched structure and naturally limited molecular weight, lignin does not have enough strength to be used as a structural material on its own. However, lignin’s molecular weight is too high and its energy content is too low for fuel applications (due to its high oxygen content). It is commonly accepted that modification of lignin (e.g. via esterification or depolymerization) is needed for utilization of lignin for fuels or chemicals. Most of the research on the applications of lignin has concen-

trated on converting lignin into chemicals and fuels via hydrolytic, (Nadji *et al.*, 2005) oxidative, (El Mansouri *et al.*, 2011) and reductive depolymerization (Doumel *et al.*, 1988) and pyrolysis (Sigoillot *et al.*, 2012) approaches. Most of these destructive approaches suffer from the drawbacks of high energy input, low yields and difficulty in product separation. To overcome these disadvantages, a viable strategy for lignin application might be to perform molecular reconstruction of high molecular weight, low reactivity lignin into moderate molecular weight (e.g. in the range of 1,000-2000 g/mol or lower), more reactive feedstocks through depolymerization then introducing curable functional groups for use in the production of various types of bio-materials. Since lignin contains abundant ether linkages and aliphatic and phenolic hydroxyl groups, depolymerized lignin of moderate molecular weight may directly replace petroleum-based polyether polyols in the synthesis of polyurethane (PU) materials and petroleum-derived phenol (or polyphenol) in the synthesis of phenol-formaldehyde (PF) resins (Mahmood *et al.*, 2013; Liu and Wilson, 2013) or epoxy resins. (Zhang *et al.*, 2011; Yuan *et al.*, 2010) The hydroxyl groups can also undergo a variety of reactions such as oxypropylation (Cateto *et al.*, 2009, Song *et al.*, 2013; Chen and Falconer, 1994) for the synthesis of lignin-based polyols for use as surfactants and PU raw materials, grafting of amines for use as catalysts, (Mahmood *et al.*, 2013) grafting of epichlorohydrin followed by reaction with diethanolamine for use as a surfactant for cement construction materials, and grafting of vinyl monomers for the synthesis of radical curable resins. The above proposed chemical reactions for lignin valorization are shown in Scheme 1.

The original molecular weights of KL and OL, generally >10,000 g/mol and >2,600 g/mol, respectively, are too high for the above applications. Fortunately, the relatively weaker C-O bonds connecting the phenyl-propanol monomers in lignin can be cleaved, resulting in smaller molecules. Fungal bio-depolymerization of lignin has also been investigated intensively, but these biological processes are slow and capital intensive. Hydrolytic depolymerization has shown some promise, but the process leads to low de-polymerized lignin (DL) yields. Recently, reductive depolymerization of lignin in the presence of hydrogen and metal catalysts, especially late 3d and 4d transition metals (Fe, Co, Ni, Cu, Ru, Rh, Pd, and Ag) has been studied (Jin *et al.*, 2014). Laskar *et al.* (2014), used noble-metal (Pt, Ru, Rh) catalysts to hydroprocess lignin into aromatic hydrocarbons for fuel with about 50% yield.



Scheme 3.1 Routes of lignin valorization

To economically utilize lignin and build a sustainable bio-based economy, we are attempting to depolymerize lignin into oligomers of moderate molecular weight at a high yield and reduced sulfur content (sulfur is a detrimental element in fuel applications) by hydrotreatment under milder conditions.

Thus, in this work, several supported metal hydrogenation catalysts were investigated for the depolymerization and desulfurization of KL and OL under hydrogen atmospheres for applications such as fuel additives and intermediates for chemicals and materials.

3.2 Experimental

3.2.1 Materials

The organosolv lignin used in these experiments was provided by Lignol, Canada while the Kraft lignin was provided by FPInnovations, Canada. The activated carbon-supported Ru catalyst was purchased from Sigma-Aldrich. Hydrogen (99.99%) was purchased from Praxair. The solvents (acetone, reagent grade) and ethanol (denatured, reagent grade) were purchased from Caledon Canada. FHUDES-2 (NiMoW-based) catalyst was provided by SINOPEC Fushun Research Institute of Petroleum and Petrochemicals. The activated carbon- and γ -alumina-supported Ni catalysts and the γ -alumina-supported Ru catalyst were prepared by incipient impregnation. All the materials were used as received.

3.2.2 Experimental apparatus and procedure

Lignin depolymerization was conducted in a 500 mL Parr autoclave reactor. In a typical run, 30.0 g lignin, 1.5 g catalyst, and 120 g (150 mL) acetone were added to the reactor. The reactor was evacuated and purged with nitrogen twice, then evacuated and purged with hydrogen twice and finally pressurized with 100 bar hydrogen. After a leak check, the reactor was then heated under stirring to the set temperature (approximately 1 h) and the reaction was continued for 1 h after reaching the set temperature. After the set time had elapsed, the reactor was quenched by cooling the reaction mixture to room temperature by running water through the cooling coil in the reactor. After cooling, the pressure in the reactor was typically in the range of 50-55 bar, suggesting significant hydrogen consumption during the hydroprocessing process. The reaction mixture was rinsed from the reactor with acetone and filtered through a pre-weighed Whatman #5 filter paper to isolate the solid residue and spent catalyst. The solids were then dried in vacuum oven under 50 °C to remove volatile components. Solids yields were calculated by the mass difference between spent catalysts and catalyst loaded into the reactor. An aliquot of the filtrate was taken for GC-MS analysis. The remaining liquid was evaporated under reduced pressure in a rotary evaporator to remove the solvent and obtain depolymerized lignin (DKL and DOL) as the final product. The yields (wt.%) of depolymer-

ized lignin (DKL or DOL) and SR were calculated by weight of DKL, DOL and SR relative to the weight of KL or OL loaded.

3.2.3 Product Characterization

The relative molecular weights and their distributions of the original and de-polymerized lignin samples were measured with a Waters Breeze GPC-HPLC (gel permeation chromatography-high performance liquid chromatography) instrument (1525 binary pump, UV detector at 270 nm; Waters Styrylgel HR1 column at a column temperature of 40 °C) using THF as the eluant at a flow rate of 1 mL/min. Linear polystyrene standards were used to generate a calibration curve for molecular weight estimation. ¹H NMR spectra were obtained on a 500 MHz Unity Inova NMR instrument at room temperature, wherein DMSO-d₆ was used as solvent. FT-IR spectra were collected on a Bruker Tensor 37 FTIR spectrophotometer in the range of 550-4000 cm⁻¹ with ATR accessory. The volatile components of the DOL and DAL were identified by GC-MS (HP 6890 GC and HP 5972 MS) using a silicon column with temperature programming from an initial temperature of 50 °C for 2 min hold at 10 °C/min to a final temperature of 280 °C for 2 min hold. Elemental analysis of CHNS (carbon, hydrogen, nitrogen, and sulfur) was conducted on a Flash EA 1112 Series elemental Analyzer. The BET surface area analysis was performed on a Micrometrics ASAP 2010 instrument. The samples were degassed at 150 °C until a stable static vacuum of less than 5×10⁻³ Torr was achieved prior to analysis.

3.3 Results and discussion

3.3.1 Effect of catalyst

Ru/C (5%), Ru/Al₂O₃ (5%), Ni/Al₂O₃ (10%), Ni/C (10%), FHUDS-2 were used in catalyst screening test for the hydroprocessing of Kraft lignin (KL) and organosolv lignin (OL) with relative weight average molecular weights (M_w, all molecular weights were based on linear polystyrene standards) of 10,200 and 2,600 g/mol, respectively. The objective of the hydroprocessing was to depolymerize the lignin feedstocks into low molecular weight compounds

with high yields of products and low yields of solid residual. The results of the experiments are presented in Table 3.1.

Table 3.1 Catalyst screening

Feed	Catalyst	Catalyst (g)	DL (wt.%)	SR Yield (wt.%)	M _w (g/mol)	M _w /M _n
KL	Original KL				10,200	4.18
KL	None		70.3	28.0	21,400	4.73
KL	Ru/C (5%)	1.5	95.2	1.7	5,300	4.34
KL	Ru/C (5%)	3.0	94.7	3.8	5,200	3.56
KL	Ru/Al ₂ O ₃ (5%)	1.5	94.3	5.9	7,300	5.15
KL	Ni/Al ₂ O ₃ (10%)	1.5	94.5	5.3	8,210	5.03
KL	Ni/C (10%)	1.5	95.0	4.5	6,860	4.55
KL	FHUDS-2	3	97.9	2.3	5,150	4.35
OL	None		102	2.0	6,910	5.43
OL	Ru/C	3	96.9	1.9	1,470	2.61
OL	Ru/C	1.5	103	1.0	1,400	2.66
OL*	Ru/C	1.5	100	1.8	1,730	2.06
OL	Ru/Al ₂ O ₃	1.5	96.8	2.5	2,460	4.06
OL	Ni/C (10%)	1.5	98.8	1.5	1,620	2.81
OL	FHUDS-2	3	98.6	2.3	1,480	3.01

* Ethanol as the solvent

The results for the depolymerization of AL and OL at 300 °C under 100 bar hydrogen using different catalysts are presented in Figures 3.1 and 3.2, showing the molecular weights (Figure 3.1) and yields of DKL, DOL and solid residual (SR) (Figure 3.2). The yields (wt.%) of depolymerized lignin (DAL and DOL) were calculated by dividing the weight of acetone-soluble products by the weight of lignin feed, multiplied by 100%. The yields of char (or solid residual) were calculated by dividing the increased weight of the spent catalyst by the

weight of lignin feed. It is obvious that the catalysts used played a key role in the depolymerization of both types of lignin. Without catalyst, after 1 h treatment under H₂ at 300 °C, the M_w of both types of lignin dramatically increased, being more than double of that of the original lignin. A possible mechanism for this increase in M_w is Friedel-Craft condensation between the aliphatic hydroxyl groups and the *ortho* positions of the phenolic rings in lignin under heating.

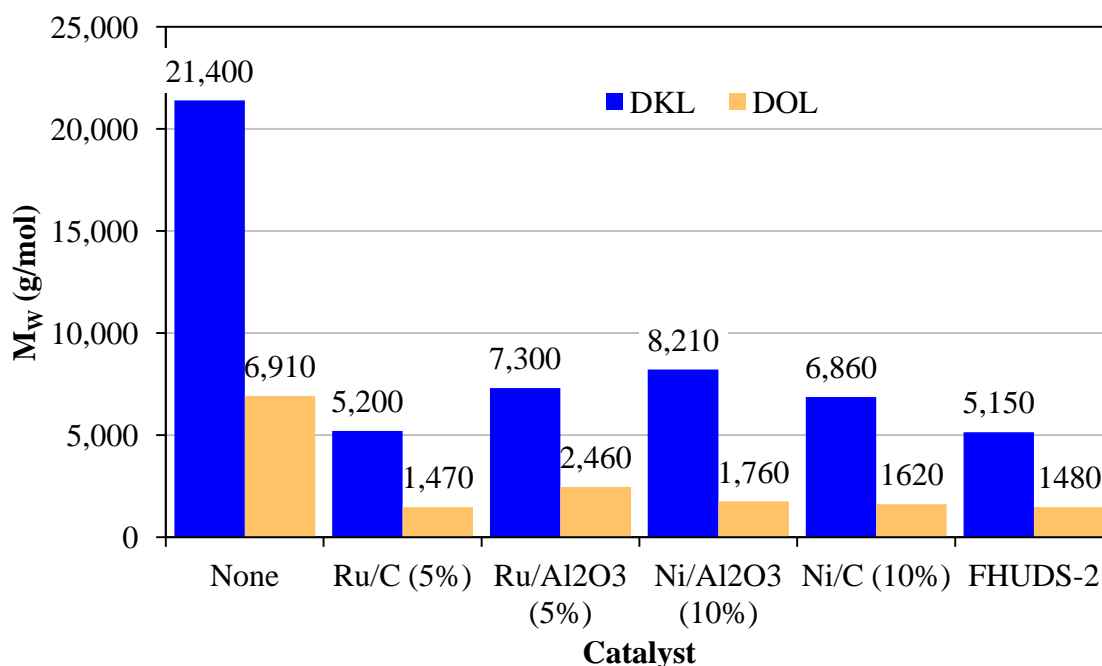


Figure 3.1 Molecular weight of depolymerized lignin using different catalysts

Reaction conditions: 30.0 g lignin, 120 g (150 mL) acetone, initial H₂ pressure 100 bar, reaction time 1 h at 300 °C, the amount of catalysts were 1.5 g except 3.0 g for FHUDES-2 (cheaper with lower metal contents). Catalysts named with percentage of metal on support

The yield of depolymerized KL (DKL) without catalyst was about 70 wt.% with 28 wt.% solid residue or char formation. This may be due to the higher initial M_w of the KL. Thus, when the molecular weight further increased through condensation, the solubility of the higher molecular weight compounds decreased causing some of the lignin precipitate, which greatly increased the local concentration of lignin and expedited condensation and the cross-linking reactions that promote char formation.

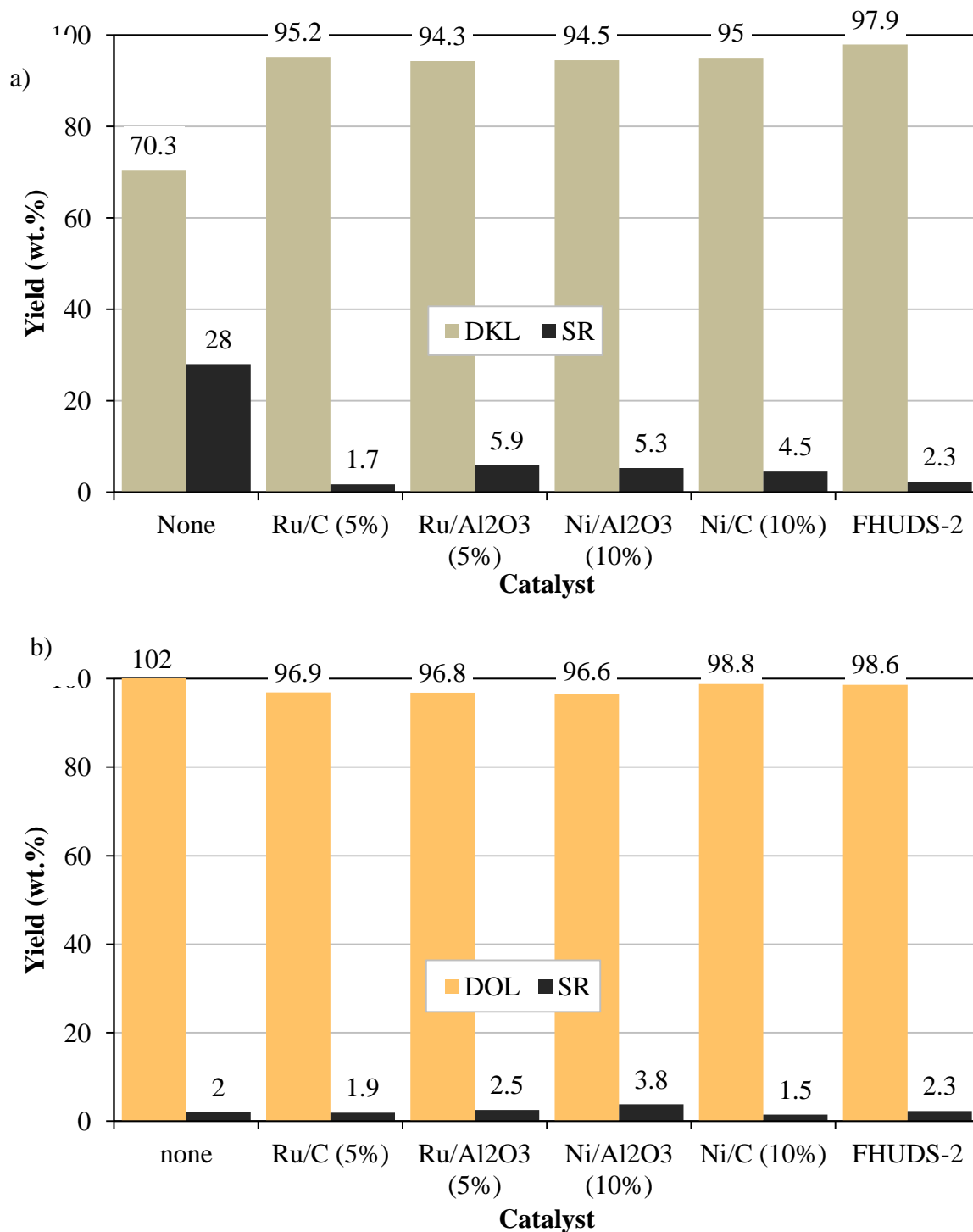


Figure 3.2 Yields of depolymerized product and solid residue for Kraft lignin (a) and organosolv lignin (b)

Reaction conditions: 30.0 g lignin, 120 g (150 mL) acetone, initial H₂ pressure 100 bar, reaction time 1 h at 300 °C, the amount of catalysts were 1.5 g except 3.0 g for FHUDES-2 (cheaper with lower metal contents). Catalysts named with percentage of metal on support.

Two competitive reactions occur in lignin in the presence of catalysts: condensation reactions which increase molecular weight and depolymerization reactions acting on the ether bonds which reduce molecular size. When an effective catalyst was used, depolymerization reactions were dominant, which allowed the depolymerized lignin to dissolve. Therefore all the catalysts gave very good yields of DKL, mostly over 95 wt.%.

Since the M_w of OL was much lower to begin with, even without catalyst, the yield was still very high (close 100%). When Ru/C was used, the molecular weights were significantly reduced to 5,300 g/mol for KL and to 1,400 g/mol for OL. When Ru was supported on Al_2O_3 (5%), catalyst effectiveness was much lower. One reason for this could be that the surface area of Ru/C (over 1200 m^2/g , as measured by BET) was several times higher than the surface area (230 m^2/g) of Ru/ Al_2O_3 . This would increase the distribution of the Ru over the surface of the support, resulting in more active sites. Another reason could be due to the acidic properties of alumina which are known to promote condensation reactions. The Ni-based catalysts have proven to be effective catalysts for the hydrogenation of the ether bonds in lignin. However, even though the Ni/ Al_2O_3 (10%), and Ni/C (10%) also reduced the molecular weight of KL and OL, they were not as effective as Ru/C. FHUDS-2 is a NiMoW-based commercial hydrodesulfurization catalyst. When FHUDS-2 was used, the molecular weights of the lignins were reduced to 5,150 and 1,480 g/mol for DKL and DOL, respectively. Although surface area of the FHUDS-2 catalyst (220 m^2/g) was close to that of the alumina-supported Ru catalyst, its much higher activity indicates that the three metal combination of Ni, Mo, and W has a synergistic effect. Thus, among the catalysts tested, Ru/C and FHUDS-2 were chosen for further evaluation of reaction condition optimization.

3.3.2 Effect of catalyst loading

The results with 1.5 g and 3.0 g Ru/C catalyst (entry 3 and 4 in Table 3.1) at 300 °C for both DKL and DOL show that at a set reaction time, doubling the amount of catalyst used had little difference on the M_w of the DL products and only a small decrease in the amount of char (SR) produced with the DKL. Considering the cost of Ru/C catalyst, using a smaller amount of catalyst in the treatment is more economically viable.

3.3.3 Effect of reaction temperature

The temperature effect on KL and OL depolymerization using Ru/C as a catalyst for 1 h reaction was investigated. The yields of depolymerized product and solid residue are presented in Table 3.2 and Figure 3.3.

Table 3.2 Temperature effect on yield and M_w

Lignin	Temp (°C)	Time (h)	DL yield (%)	Char (%)	M_w (g/mol)	PDI
KL	250	1	73.3	26.9	5530	3.27
KL	275	1	91.4	7.1	5460	6.41
KL	300	1	94.7	3.8	5260	4.55
KL	325	1	97.3	1.6	1980	4.73
KL	350	1	97.7	1.5	1020	2.34
KL	350	0.5	97.2	1.4	1570	2.78
KL	350	1	97.7	1.5	1020	2.34
KL	350	2	95.4	0.93	966	2.24
KL	350	3	96.1	1.23	890	2.24
OL	250	1	96.8	1.9	1970	2.59
OL	275	1	97.3	1.8	1630	2.40
OL	300	1	103	1.0	1400	2.66
OL	325	1	99.7	1.6	1320	2.45
OL	350	1	98.0	1.5	850	2.28

At 250 °C, with Ru/C catalyst, the yield of soluble DKL product was only about 73 wt.% with 27 wt.% solid residue (SR), similar with the results without catalyst at 300 °C, indicating that catalyst activity is not very high at 250 °C. As the reaction temperature was increased to 275 °C the DKL yield improved to greater than 95 wt.%, likely due to increasing lignin solubility and depolymerization reactions counteracting the cross-linking reactions evidenced at 250 °C. The yields of char for OL were much lower than those of KL, likely because the initial M_w of OL was lower and the fact that OL is more soluble in acetone than the KL, therefore the char formation for OL is much less severe.

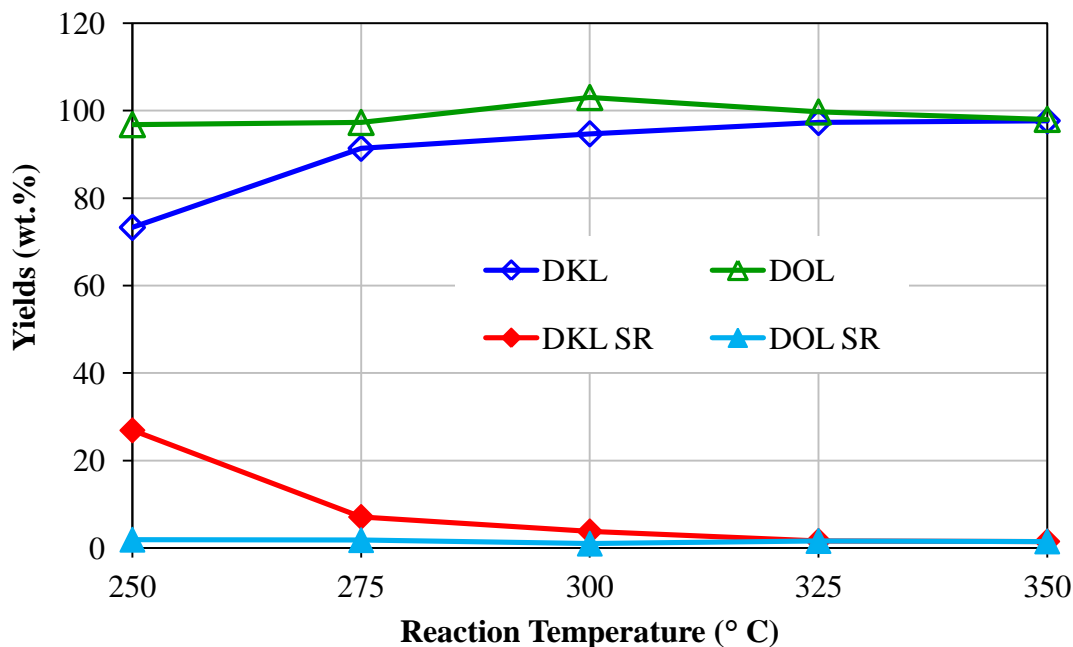


Figure 3.3 Effect of temperature on DKL and DOL yields

Reaction condition: 30.0 g lignin, 120 g (150 mL) acetone, 1.5 g Ru/C, H₂ pressure 100 bar, reaction time 1 h.

The effects of temperature on the Mw's of DKL and DOL using Ru/C catalyst are presented on Figure 3.4. The results show that temperature plays a more important role in product molecular weight than product yields. The Mw's of the DOL decreased monotonically from 1,970 to 850 g/mol over a temperature range of 250 to 350 °C without drastic change due to the initial low Mw of the OL. In contrast, the Mw's of the DKL decreased slightly from 5,530 g/mol at 250 °C to 5,260 g/mol at 300 °C. However, at 325 °C the MW of the DKL decreased dramatically to 1,980 g/mol and reached 1,020 g/mol at 350 °C. As mentioned previously, two main reactions are involved in the process. The energy barrier for condensation reactions is lower than for the depolymerization reactions. Therefore, at a lower temperatures, condensation reactions are dominant leading to products with an increased molecular weight. In contrast, at higher temperatures, condensation reactions are energetically unfavourable since they result in the joining of two large molecules together. In addition, the breaking of ether bonds which results in smaller molecules is favoured at higher temperatures leading to greater conversions. Thus it is possible that 300 °C represents the energy barrier (activation energy) required for ether bond cleavage to occur.

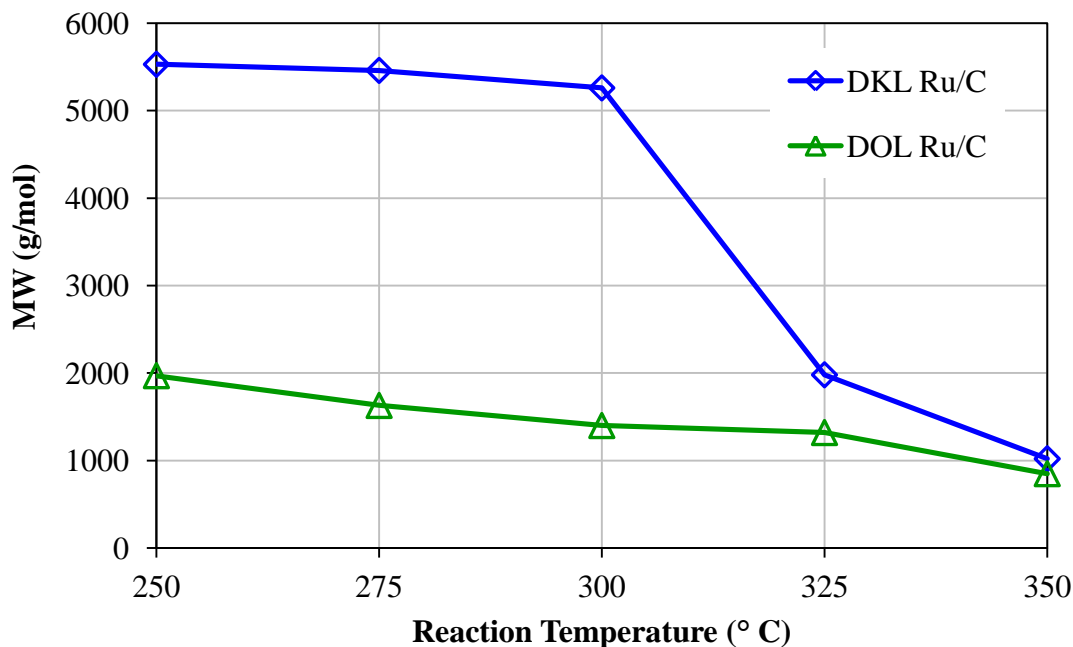


Figure 3.4 Effect of temperature on DKL and DOL MW using Ru catalyst

Reaction condition: 30.0 g lignin, 120 g (150 mL) acetone, 1.5 g Ru/C, initial H₂ pressure 100 bar, reaction time 1 h.

During heating, the reactor pressure was found to increase quickly between 250-300 °C, but the pressure increase slowed at temperatures above 300 °C, suggesting that significant hydrogen consumption was occurring. Thus, the rate of hydrogenation increased slowly at temperatures up to 300 °C and but more rapidly above 300 °C, as evidenced by the decreased M_w's of DKL and DOL in Figure 3.4 as the reaction temperature increased above 300 °C.

The temperature effects for FHUDES-2 catalyst were also investigated from 300 °C to 350 °C. The MW's of DKL and DOL using this catalyst are shown in Figure 3.5. The MW's of DKL drastically decreased from 5,150 g/mol at 300 °C to 2,170 and 1,150 g/mol at 325 °C and 350 °C, respectively. Similarly, though not as great, the Mw's of DOL decreased from 2,200 g/mol at 300 °C to 1,980 and 1,020 g/mol at 325 and 350 °C, respectively. The product yields were all greater than 95 wt.% and SR yields were all less than 2 wt.%.

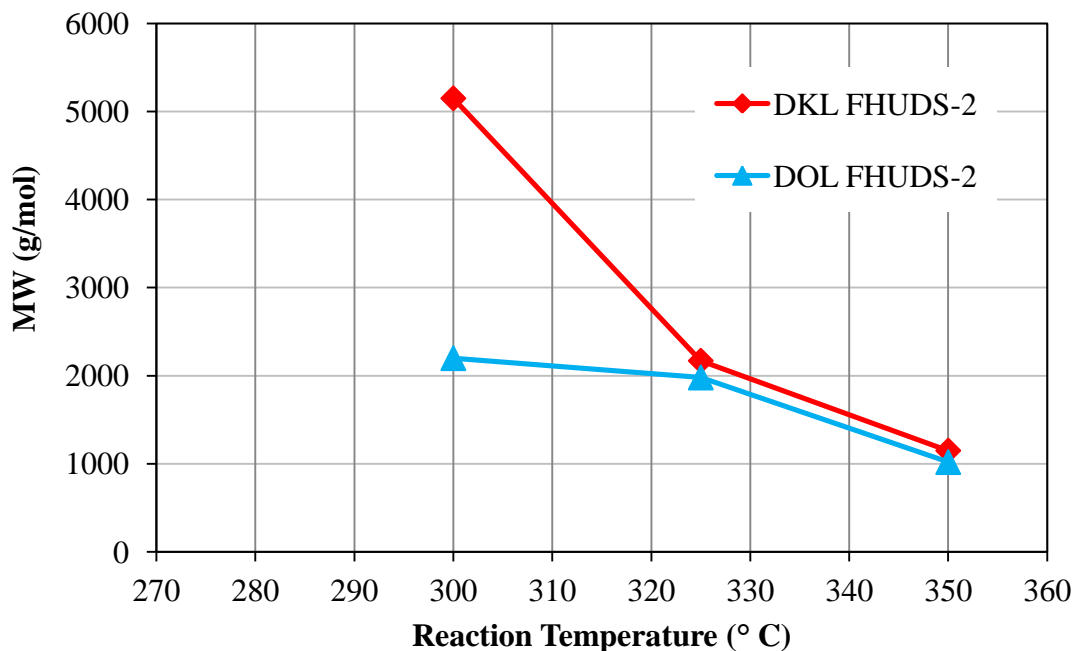


Figure 3.5 Effect of temperature on DKL and DOL MW using FHUDES-2 catalyst

Reaction conditions: 30.0 g lignin, 120 g (150 mL) acetone, 3.0 g FHUDES-2, initial H₂ pressure 100 bar, reaction time 1 h.

3.3.4 Effect of reaction time

The effect of reaction time on product molecular weight was also investigated for the depolymerization of KL using Ru/C as catalyst at 350 °C. Figure 3.6 shows that there was a significant decrease in molecular weight (from 1,570 g/mol to 1,020 g/mol) as reaction time was increased from 0.5 h to 1 h. As the reaction time was increased to 2 h and then 3 h, the molecular weight continued to decrease (to 966 and 890 g/mol, respectively), but the effect was not as great as was seen earlier. Comparing these results with the effect of temperature, it seems that under these conditions there is a limit of around 900 g/mol, beyond which lignin cannot be depolymerized under the conditions used here. When the depolymerization reached a molecular weight of 1,000 g/mol, whether increasing reaction temperature or reaction time, the molecular weight cannot be further reduced. This phenomenon was also found in previous work for catalytic lignin depolymerization in water solution either in the presence of

phenol as capping agent or without capping agent. This is probably because the hydrodeoxygenation reactions occur mostly on the ether linkages, especially β -O-4 structures (Chakar and Ragauskas, 2004). Once these linkages are broken, further reduction in molecular weight requires the breaking of more resistant chemical bonds.

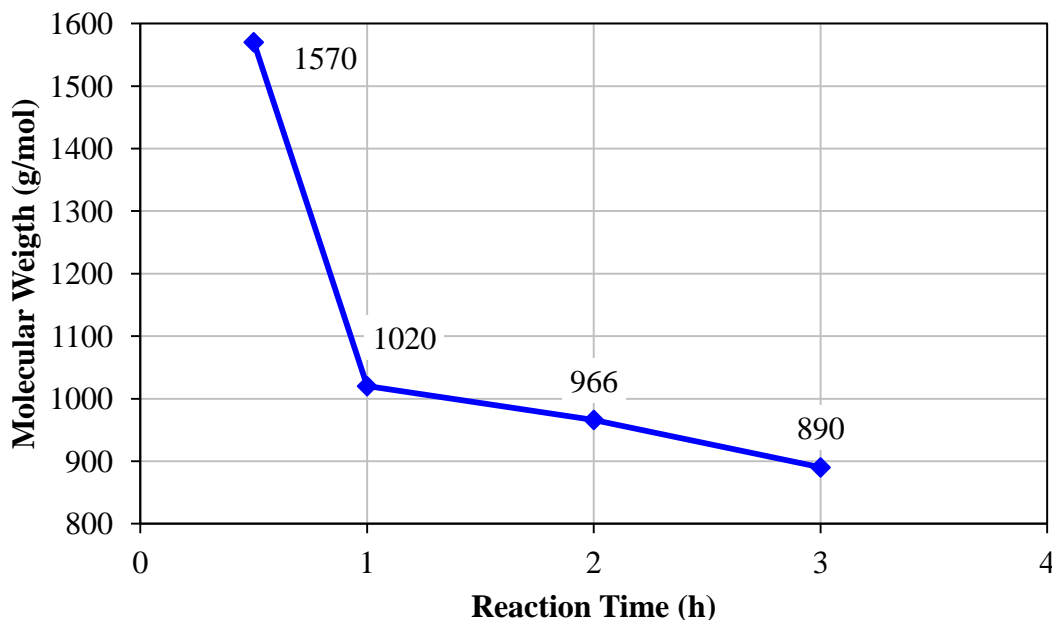


Figure 3.6 Effect of reaction time on DKL MW

Reaction conditions: Ru/C catalyst, 350 °C, 100 bar H₂

3.3.5 Effect of solvent

In addition to acetone, ethanol was also tested for OL hydroprocessing. The results as seen in Table 3.1 above showed that ethanol was not as effective a solvent as acetone, producing lower yields of higher M_w products. This is likely due to the OL lignin being less soluble in ethanol as compared to acetone as well as the possibility of the OH groups of the solvent participating in condensation reactions with the OL.

3.4 Product characterization

The relative molecular weights of original KL and OL as well as product DKLs and DOLs were measured by gel permeation chromatography (GPC). The GPC curves for KL and OL

depolymerization with Ru/C catalyst at different treatment conditions are shown in Figures 3.7 and 3.8.

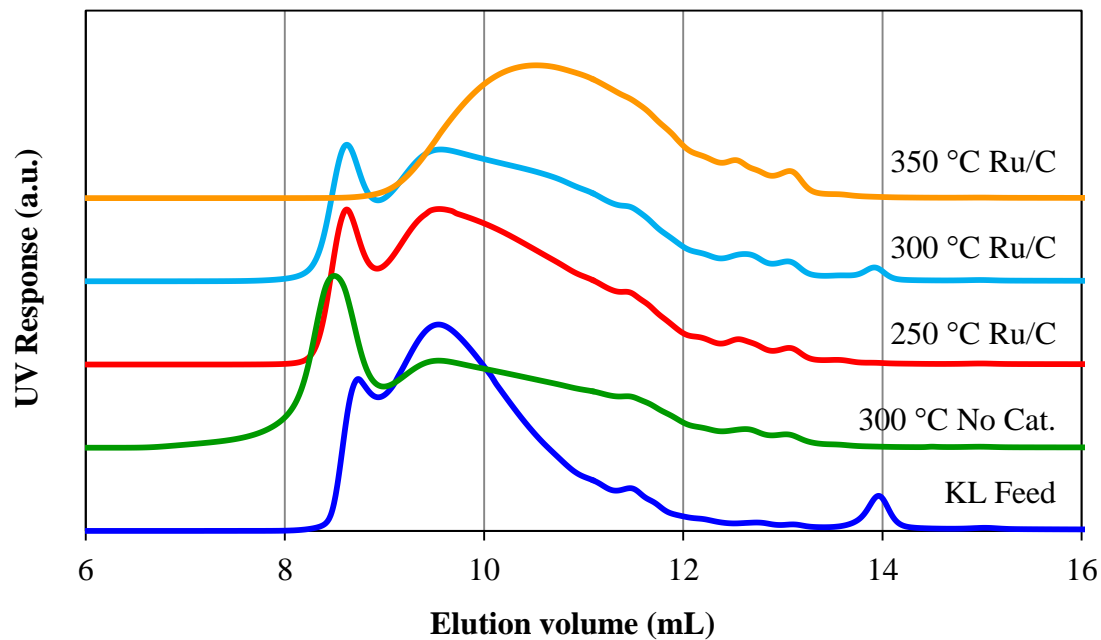


Figure 3.7 GPC curves of the original and depolymerized lignin products from KL

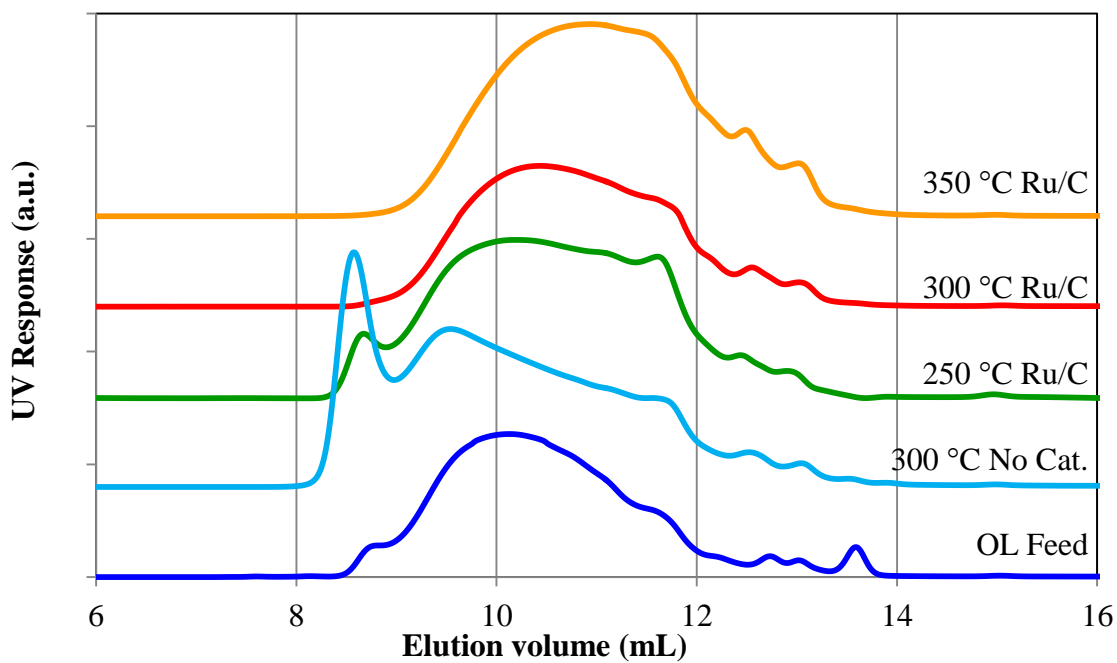


Figure 3.8 GPC curves of the original and depolymerized lignin products from OL

Reaction conditions: 30.0 g lignin, 120 g (150 mL) acetone, initial H₂ pressure 100 bar, 1.5 g 5%Ru/C catalyst.

It can be seen that a new peak at high molecular weight region (low elution volume) appears for the un-catalyzed products of both of DKL and DOL because of condensation reactions. The GPC curves also give a clear illustration of the temperature effects on lignin depolymerization. A new peak in the high molecular region for both DKL and DOL appears on the curves for lignin depolymerization at 250 °C and the peak intensity becomes weaker at a higher temperature and disappears in DOL at 300 °C and in DKL at 350 °C. This again can be explained by lower temperatures favouring condensation reactions while higher temperatures favour depolymerization reactions.

The volatile components (yields below 2% by difference through subtracting 100% with the yield of DL and solid residue) of the reaction mixture were analyzed by GC-MS. The identified compounds are mainly substituted phenolic compounds and aromatic hydrocarbons.

A comparison of the IR spectra of the KL feed and DKL are presented in Figure 3.9. As expected, the spectra are very similar except for relatively stronger absorption in the OH region for the DKL which may attributed to the newly generated OH group from hydrogenation of the ether linkages in the lignin. Similar observations were obtained for the OL and DOL.

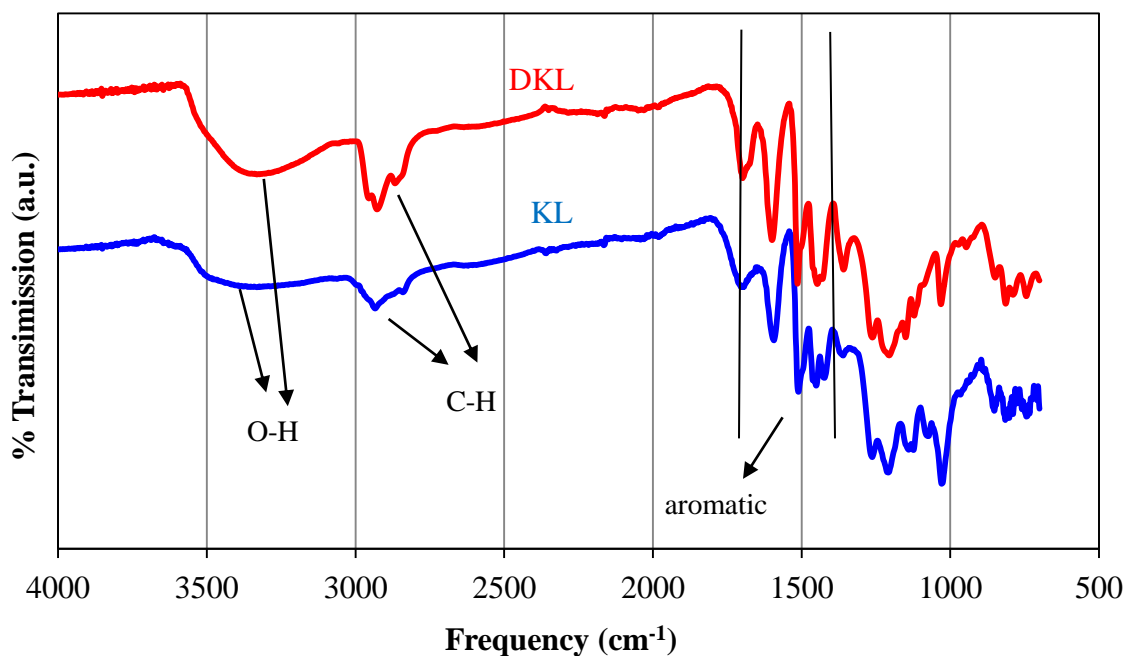


Figure 3.9 IR spectra of KL and DKL

Since lignin has large numbers of OH groups it is a potential feedstock for replacing petroleum-based bisphenol A in the synthesis of epoxy resin and a potential polyol substitute in the synthesis of polyurethane materials. Phenolic hydroxyl groups are more active in the synthesis of epoxy resin while aliphatic hydroxyl groups are more reactive in the synthesis of polyurethane. Furthermore, phenolic hydroxyl groups can easily be modified to aliphatic hydroxyl groups, for use in PU synthesis for example, by oxypropylation using propylene oxide. The average number of hydroxyl groups per lignin monomer unit (supposing the unit molecular weight is 180 g/mol) can be estimated by $^1\text{H-NMR}$ (Figure 3.10) through acetylation with acetic anhydride in the presence of pyridine. Dibromomethane was used as an internal standard for the quantification.

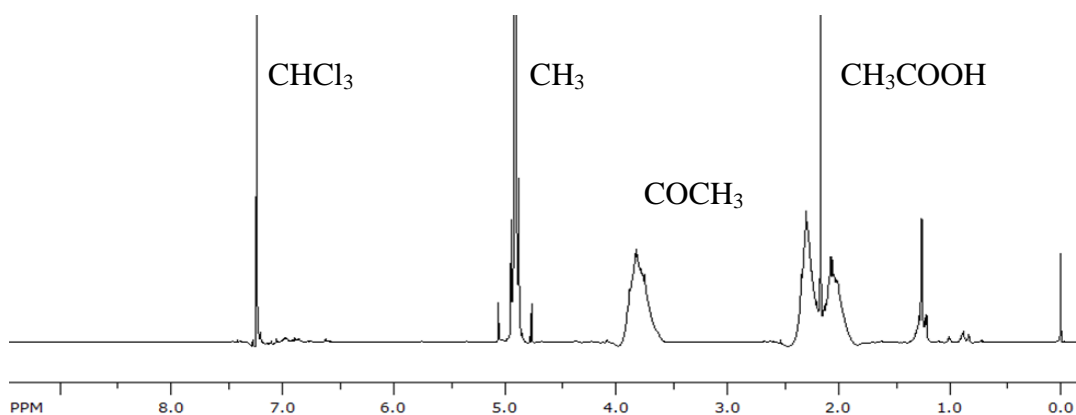


Figure 3.10 NMR spectrum of acetylated DKL

The chemical shifts of the methyl groups on the aliphatic hydroxyl acetyl esters and phenolic hydroxyl acetyl esters appear at 1.6-2.2 and 2.2-2.6 ppm, respectively. The methyl group of methyl-aromatic ethers appears at 3.7 ppm. Table 3.3 shows the estimated number of OH groups per lignin unit for DKL hydroprocessed with FHUDES-2 catalyst at 300 °C and 350 °C for 1h. The average aliphatic and aromatic (phenolic) hydroxyl groups per lignin unit changed from 1.16 and 0.81 of original KL to 0.77 and 0.91 for DKL of 300 °C and 0.54 and 0.99 for DKL of 350 °C. There was almost no change in the number of methyl phenyl ether bonds. The increased phenolic OH was from the cleavage of $\beta\text{-O-4}$ ether linkage producing a phenolic OH and an alkane, which is the main reaction of lignin depolymerization. The decrease in aliphatic OH groups indicates that dehydration (hydrodeoxygenation) of the ali-

phatic OH groups is easier than for phenolic OH groups, which was the main contribution to the overall decrease in oxygen content. This is because phenolic C-OH bonds, with carbon sp^2 hybridization, are much stronger than aliphatic C-OH bonds.

Table 3.3 KL and DKL hydroxyl groups

Sample	OH group/lignin unit		OMe/lignin unit
	Aliphatic	Aromatic	
KL	1.16	0.81	0.69
DKL, 300 °C	0.77	0.91	0.68
DKL, 350 °C	0.54	0.99	0.65

Lignin is viewed as low energy content fuel due to high oxygen content. KL, incorporating sulfur from the pulping process, is even more unsuitable as a fuel. One of the purposes of lignin hydroprocessing is to reduce oxygen and sulfur contents for further upgrading to fuel. Table 3.4 shows the results of elemental analysis for KL and DKL treated with Ru/C and FHUDES-2 catalysts at 300 °C and 350 °C for 1 h. After depolymerization, oxygen contents were reduced by 20-30% for both OL and KL. The sulfur contents of the KL were reduced by 92-96%. Deoxygenation was achieved through dehydration of the hydroxyl groups present. Desulfurization was achieved by rupturing C-S bond to produce hydrogen sulfide and other sulfur compounds which was evidenced by the foul smell of the resulting reaction mixture. As a desulfurization catalyst, FHUDES-2 is also effective in deoxygenation reactions. As a hydrogenation catalyst, Ru/C also has very good activity in deoxygenation and desulfurization. It is interesting to observe that the sulfur in KL did not appear to poison the Ru/C catalyst. The spent Ru/C and FHUDES-2 catalysts could be reused at least two times without obvious decrease their catalytic activity.

Table 3.4 Elemental analysis (CHNSO) of KL and DKL

	C	H	S	O*
KL	64.1	5.60	4.40	25.9
Ru/C, 300 °C	71.6	7.13	0.33	20.9
Ru/C, 350 °C	74.1	7.08	0.29	18.5
FHUDS-2, 300 °C	73.4	7.09	0.30	19.2
FHUDS-2, 350 °C	74.5	7.24	0.18	18.1

Reaction conditions: 30.0 g lignin, 1.5 g catalyst, initial H₂ pressure 100 bar, 120 g acetone.

* determined by mass difference

3.5 Conclusions

All of the catalysts tested were effective in depolymerizing the lignin feedstocks, however, the alumina-supported catalysts and the carbon-supported Ni catalyst did not perform as well as the carbon-supported Ru and FHUDES-2 catalysts. The molecular weights of the depolymerized lignins using these last two catalysts were markedly lower than the lignin feeds (~1,000 vs. 2,600 and 10,000 g/mol). It should be noted that the molecular weight of organosolv lignin decreased monotonically with increased temperature but for Kraft lignin, temperatures greater than 300 °C were required to materially decrease molecular weight. In addition, the sulfur contents of the depolymerized Kraft lignins were drastically reduced (by 92-96%), although the foul odour of the products indicated that the organosulfur compounds remaining present an issue even at low concentrations. Given the effectiveness of sulfur removal, it is somewhat surprising that these catalysts were not particularly effective in deoxygenating the lignin (reduction of 20-30%). This is perhaps due to the strength of C-O bonds (358 kJ/mol) relative to C-S bonds (272 kJ/mol) in addition to difference in bond strength between aromatic and aliphatic C-OH bonds.

3.6 References

- Cateto CA, Barreiro MF, Rodrigues AE, Belgacem MN. *Ind. & Eng. Chem. Research*, 2009, 48, 2583.
- Chakar FS, Ragauskas A. *J. Ind. Crops Prod.*, 2004, 20, 131.
- Chen BS, Falconer JL. *J. Catal.*, 1994, 147, 72.
- Doumel P, Randrianalimanana E, Deffieux A, Fontanille M. *Eur. Polym. J.*, 1988, 24, 843.
- El Mansouri N-E, Yuan Q, Huang F. *BioResources*, 2011, 6, 2492.
- Hart WES, Aldous L. *Green Chem.*, 2015, 17, 214.
- Hirose S, Kobayashi M, Kimura H, Hatakeyama H. In: Kennedy JF, Phillips GO, Williams PA, Hatakeyama H. (Eds.), *Recent advances in environmentally compatible polymers*. Woodhead, Cambridge, 2001, 73.
- Jin S, Xiao Z, Li C, Chen X, Wang L, Xing J, Li W, Liang C. *Catal. Today*, 2014, 234, 125.
- Laskar DD, Tucker MP, Chen X, Helms GL, Yang B. *Green Chem.*, 2014, 16, 897.
- Liu C, Wilson AK. Abstracts of Papers, 245th ACS National Meeting & Exposition, New Orleans, LA, United States, April 7-11, 2013, COMP-278.
- Mahmood N, Yuan Z, Schmidt J, Xu C. *Bioresour. Technol.*, 2013, 139, 13.
- Nadji H, Bruzzese C, Belgacem MN, Benaboura A, Gandini A. *Macromol. Mater. Eng.*, 2005, 290, 1009.
- Pinkert A, Goeke DF, Marsha KN, Pang S. *Green Chem.*, 2011, 13, 3124.
- Sasaki C, Wanaka M, Takagi H, Tamura S, Asada C, Nakamura Y. *Ind. Crops Prod.*, 2013, 43, 757.
- Sigoillot J-C, Berrin J-G, Bey M, Lesage-Meessen L, Levasseur A, Lomascolo A, Record E, Uzan-Boukhris E. *Advances in Botanical Research*, 2012, 61(Lignins), 263.

- Snelders J, Dornez E, Benjelloun-Mlayah B, Huijgen WJJ, de Wild PJ, Gosselink RJA, Geritsma J, Courtin CM. *Bioresour. Technol.*, 2014, 156, 275.
- Song Q, Cai J, Zhang J, Yu W, Wang F, Xu J. *Chin. J. Catal.*, 2013, 34, 651.
- Tejado A, Pena C, Labidi J, Echeverria JM, Mondragon I. *Bioresour. Technol.*, 2007, 98, 1655.
- van Spronsen J, Tavares-Cardoso MA, Witkamp G-J, de Jong W, Kroon MC. *Chemical Engineering and Processing: Process Intensification*, 2011, 50, 196.
- Vázquez G, Antorrena G, González J, Mayor J. *Bioresour. Technol.*, 1995, 51, 187.
- Wang M, Leitch M, Xu, C. *Eur. Polym. J.*, 2009, 45, 3380.
- Yuan Z, Cheng S, Leitch M, Xu C. *Bioresour. Technol.*, 2010, 101, 9308.
- Zhang L, Champagne P, Xu C. *Bioresour. Technol.*, 2011, 102, 8279.

Chapter 4

4 Catalyst screening for the hydrotreatment of lignin using guaiacol as a model compound

4.1 Introduction

The depletion of fossil fuel reserves coupled with increased consumption from rising economies such as China and India in the 21st century, has intensified the interest in the production of chemicals and fuels from alternative resources. Biomass, such as agricultural and forestry wastes, is generally regarded as the most feasible alternative as it is widely available, renewable and generally carbon-neutral.

Lignin is the second most abundant naturally synthesized polymer after cellulose and comprises 25-40 % of dry wood and crop stems. (Tejado *et al.*, 2007) In addition, it is the most abundant natural source of aromatic compounds. About 50 million tons of Kraft lignin (KL) in the form of black liquor is generated annually as a by-product in the pulp and paper industry where it has historically been viewed as a waste material or a low value by-product. Consequently, it has been predominantly used as a low-energy content fuel in the recovery boilers of pulp/paper mills. However, the recovery boilers represent a bottleneck in the many pulping plants in North America.

In addition to Kraft lignin, due to the recent increase and projected growth of bio-ethanol production, it is expected that large quantities of organosolv lignin (OL) and hydrolysis lignin (HL), as by-products of pre-treatment processes in these cellulosic ethanol plants, will become available in the near future.

As an amorphous natural polymer of substituted propyl-phenols, lignin contains many polar hydroxyl groups, making it incompatible with most synthetic polymers due to its high polarity and broad glass transition temperature. (Chakar and Ragauskas, 2004) Since lignin contains abundant ether (e.g. β -O-4) linkages and aliphatic and phenolic hydroxyl groups, lignin depolymerization products of moderate molecular weight could be good candidates for raw materials to replace petroleum-based polyether polyols for the synthesis of polyurethane (PU) materials and replace petroleum phenol for the synthesis of phenol-formaldehyde (PF)

(Wang *et al.*, 2009; Vasquez *et al.*, 1995) and epoxy resins. (Hirose *et al.*, 2001; Sasaki *et al.*, 2013)

Consequently, most of the research on the application of lignin is concentrated on converting lignin into chemicals and fuels via hydrolytic, oxidative and reductive depolymerization and pyrolysis. Most of these destructive methods suffer from the drawbacks of high energy input, low yields and difficulty in product separation. Fungal biodegradation of lignin has been intensively investigated, (Zhang *et al.*, 2011) but this process is slow and time consuming. Hydrolytic depolymerization has also been investigated, (Yuan *et al.*, 2010) but the yield is usually very low. To overcome these disadvantages, a more viable strategy might be moderate depolymerization of lignin under mild conditions to convert the lignin to oxygenated fuel additives and feedstock for various types of bio-materials.

As evidenced by the previous chapter (Chapter 3), lignin in both its untreated form and the depolymerized lignins (DL) derived from the hydrotreatment of lignin, are still highly branched structures with intermediate molecular weight ($M_w \approx 1000-3000$) and abundant oxygen in the form of hydroxyl and ether bonds. Thus to make them useful sources for fuels and chemicals, further reduction of MW and oxygen content, through catalytic hydroprocessing or hydrodeoxygenation, is needed.

The majority of the catalysts studied for the hydrotreatment of both lignin and biomass-derived bio-oils, and subsequently lignin model compounds, have been either noble metals (e.g. Pt, Pd, Ru etc.) or Co- or Ni-promoted Mo sulfide catalysts borrowed from petroleum processing operations. (Zakzeski *et al.*, 2010) Ru catalysts, in particular, have been shown to be very active in the hydrodeoxygenation and hydrogenation of model compounds (e.g. phenol) as well as bio-oils. (Elliott and Hart, 2009; Gutierrez *et al.*, 2009; Lee *et al.*, 2012; Chang *et al.*, 2013) Mo has been the focus of much study, perhaps due to its use in petroleum hydrotreating operations. Although a few studies have investigated Mo in its reduced state as well as in oxide and even nitride forms, it has been mostly used in a sulfided state and in combination with Co or Ni and typically supported on alumina. (Senol *et al.*, 2007; Romero *et al.*, 2010; Saidi *et al.*, 2014) More recently, reductive depolymerization of lignin in the presence of hydrogen and metal catalysts especially late 3d and 4d transition metals (Fe, Co, Ni, Cu, Ru, Rh, Pd, and Ag) has been proposed. (Cateto *et al.*, 2009; Li *et al.*, 2011; Zhao *et*

al., 2011; Jin, 2014) A review of the literature also reveals that mixed noble metal-transition metal catalysts (e.g. Ru-Co, Rh-Cu and Rh-Ag) have been used, although not in the hydrotreatment of bio-oils. (Rouco and Haller, 1981; Zauwen *et al.*, 1989; Moura *et al.*, 2012)

Although alumina-supported catalysts are active in HDO reactions and catalyze methyl group transfer,(Gutierrez *et al.*, 2009) they also increase catalyst deactivation by promoting the formation and deposition of coke on the catalyst surface.(Centeno *et al.*, 1995; Prochazkova *et al.*, 2007; Elliott and Hart, 2009; Wildschutt *et al.*, 2009; Lin *et al.*, 2011) Centeno *et al.* (1995) proposed that it is the weak Lewis acid sites present in the alumina that promote the condensation reactions leading to coke formation. This effect was further seen in a comparison of Pt loaded onto alumina and acidified zeolite by Nimmanwudipong *et al.* (2011) who also found that the acidified support limited oxygen removal.

In order to avoid this phenomenon, researchers have investigated less-acidic support materials such as activated carbon and SiO₂ (Furimsky and Massoth, 1999; Reddy and Khan, 2005; Kersten *et al.*, 2007) as well as other less common supports e.g. ZrO₂ and MgO.(Senol *et al.*, 2007; Bui *et al.*, 2011) Yang *et al.* (2014) found that using carbon-supported catalysts resulted in yields equivalent to those of alumina-supported catalysts, but with lower proportions of oxygenated compounds.

The use of model compounds allows for the rapid determination of catalyst effectiveness. Most studies investigating lignin have used phenol as a model compound, (Popov *et al.*, 2011; Gandarias *et al.*, 2008) however the results of these studies may not be representative of lignin as a whole due to the presence of only one reactive oxygen group in phenol. In contrast, lignin contains much oxygen and research has shown that di-oxygenates such as guaiacol are more likely to undergo condensation reactions leading to coke formation and catalyst deactivation. (Asmadi *et al.*, 2011)

Therefore the performance of the metal catalysts varies significantly with the metal species and the support material used (Cateto *et al.*, 2009), as was evidenced in our previous chapter, and lignin hydroprocessing catalysts in particular need to be optimized in terms of their effectiveness in reduction of molecular weight and oxygen contents.

Thus, in this work, the hydrotreatment of guaiacol was investigated in the presence of several carbon-supported noble metal, transition metal and mixed noble metal-transition metal catalysts under hydrogen atmospheres for applications such as fuel additives and intermediates for chemicals and materials.

4.2 Experimental

4.2.1 Materials

Guaiacol, purchased from Sigma Aldrich, was used as a model compound for lignin or depolymerized lignin or lignin-derived bio-oil and was used as received. The ruthenium and molybdenum compounds, i.e. ruthenium (III) nitrosyl nitrate solution ($\text{Ru}(\text{NO})(\text{NO}_3)_3$) and ammonium molybdate tetrahydrate ($(\text{NH}_4)_6\text{Mo}_7\text{O}_{24}\cdot 4\text{H}_2\text{O}$), and phosphoric acid were ACS reagent grade and purchased from Sigma Aldrich as well. The solvents (e.g., methanol, acetone, etc.) used in the experiments were reagent grade and purchased from Canadawide Scientific. Activated carbon (AC) used as reference catalyst support and Ru/C catalyst used in this study as a reference catalyst were both purchased from Sigma-Aldrich and used as received.

For comparison, an in-house prepared biomass-derived activated charcoal (denoted as BAC-P) was prepared according to the following procedure: White pine sawdust was first suspended in distilled water with 2 wt.% phosphorus added as phosphoric acid. The suspension was stirred for 24 h after which the treated sawdust was dewatered and dried in an oven at 105 °C. After drying, the sawdust was carbonized in a muffle furnace at 550°C for 30 min and immediately placed in a desiccator under nitrogen to cool.

The other carbon-supported metal catalysts were prepared in-house by incipient wetness impregnation using AC or BAC-P as supports, ruthenium(III) nitrosyl nitrate solution ($\text{Ru}(\text{NO})(\text{NO}_3)_3$) and ammonium molybdate tetrahydrate ($(\text{NH}_4)_6\text{Mo}_7\text{O}_{24}\cdot 4\text{H}_2\text{O}$), as follows. The required amounts of the ruthenium compound and/or molybdenum salt dissolved in distilled water were added to a suspension of a carbon support in a 50% solution of methanol and distilled water. The mixture was agitated for more than 12 h and then dewatered by evaporation under vacuum. The dewatered catalysts were dried in air at 105 °C overnight and

cooled before storage. The catalysts were reduced at 550 °C for 5 h under 50 mL/min hydrogen. The cooled reduced catalysts were passivated by immersion in methanol before drying and storage. The following carbon-supported catalysts were prepared and tested in this study: Ru/C (reference catalyst), Ru/C(R) that was reduced under hydrogen at 550 °C for 5 h, Ru/BAC-P, Ru/AC, MoRu/AC, Mo/AC, and MoRu/BAC-P. The metal loading values (wt.%) in all catalysts, as well as their textural properties, are presented in Table 4.1. All of the catalysts were tested in the raw state without prior calcination or reduction, unless stated otherwise.

4.2.2 Experimental apparatus and procedure

The experiments were carried out batch-wise in a mini-reactor constructed from SS 316L stainless steel consisting of 5/8 inch Swagelok capped tubing, with an effective volume of ~12 mL. The guaiacol substrate and catalyst were added to the reactor which was then sealed. The air in the headspace was purged by repeated vacuuming and filling with high-purity nitrogen. After purging, the reactor was filled with 9 MPa high-purity hydrogen. The filled reactor was immersed in a fluidized sand bath set to the reaction temperature, which enabled rapid heating of the reactor to the specified reaction temperature. The reactor was affixed to a shaker arm operating at ~120 Hz to provide agitation. After the required reaction time had elapsed the reactor was removed from the sand bath and cooled in water to quench the reaction. After cooling, the gases in the reactor were collected in a sampling cylinder with a volume of 2.8 L. In order to facilitate micro-GC analysis, the pressure in the cylinder was brought to 1.2 bar with the injection of high purity nitrogen. The reactor contents were decanted from the reactor and combined with acetone wash solvent used to recover any catalyst and product remaining in the reactor. The catalyst and any solid products were separated from the liquid products by vacuum filtration through a Whatman #5 filter paper. The total mass of the filtrate was recorded and weighed samples were taken for later analysis. Each experiment was performed a minimum of two times to reduce the experimental error to $\pm 5\%$.

Gas product composition was measured with Agilent 3000 Micro-GC equipped with dual (Molecular Sieve and PLOT-Q) columns and thermal conductivity detectors. The system enabled analysis of gas species up to C₃, including O₂, N₂, H₂, CO, CO₂, CH₄, C₂H₄, C₂H₆, C₃H₈, and C₃H₆. The concentration of the major liquid products (methanol, cyclohexane,

phenol, benzene and methyl phenol) was analyzed by GC/FID (Shimadzu GCMS-QP2010 plus, equipped with an auto sampler/injector) using a 30 m \times 0.25 mm \times 0.25 μ m RTX-1701 column with a temperature program as follows: hold at 45 °C for 3 min followed by a 5 °C/min ramp to 220 °C followed by a 30 °C/min ramp to 250 °C with a 3 min hold. The peaks areas were integrated and compared to calibration curves constructed by the injection of standards of known concentrations. The XRD analyses were performed using a PANalytical X'Pert PRO X-ray diffractometer using Cu-K α radiation with a wavelength of 1.54187 Å. The thermal gravimetric analysis was performed using a TA Instruments TGA 2050 thermogravimetric analyzer. Approximately 10 mg of sample was placed in a platinum pan and heated to 900 °C at 10 °C/min in a flow of 50 mL/min air.

4.3 Results and Discussion

4.3.1 Fresh catalyst characterization

The textural analysis of the fresh catalysts used in this study is presented in Table 4.1. The two carbon support materials without metals loaded (AC and BAC-P) are presented for comparison. The BET specific surface areas, total pore volume and volumes of micro/meso-pores of the supported metal catalysts are generally lower than the respective support material likely due to the deposition of metal cations inside the pores. The BAC-P-supported catalysts exhibit higher surface area, which was expected given the greater surface area of the support material to begin with. The BAC-P also had a smaller average pore diameter due to a greater number of micropores (i.e. pores <2 nm). This is evident in the difference in the volume of the micropores (0.392 cm³) as compared to the volume of mesopores (0.236 cm³) which have a diameter of 2-50 nm.

Table 4.1 Textural analysis of fresh catalysts

Catalyst	Metal (wt.%)		BET S. Area (m ² /g)	Tot. Pore Vol. (cm ³)	Vol. of pores <2 nm (cm ³)	Vol. of pores 2-50 nm (cm ³)	Avg. Pore Dia. (nm)
	Mo	Ru					
Ru/C		5	837	0.691	0.190	0.423	3.30
Ru/C (R)		5	881	0.725	0.180	0.462	3.29
Ru/BAC-P		5	1127	0.537	0.355	0.181	1.91
Ru/AC		5	861	0.677	0.206	0.387	3.14
MoRu/AC	1	5	683	0.569	0.143	0.348	3.33
MoRu/BAC-P	1	5	1035	0.551	0.337	0.203	1.92
Mo/AC	10		678	0.546	0.127	0.384	3.36
AC support			977	0.749	0.224	0.428	3.11
BAC-P support			1303	0.63	0.392	0.236	1.90

4.3.2 Catalyst screening

Hydroprocessing of lignin or depolymerized lignin was investigated using neat guaiacol as a model compound in order to screen the performance of various carbon-supported catalysts. These new catalysts were tested in comparison to the commercial catalyst (Ru/C catalyst from Sigma Aldrich) that has been widely employed in literature.

The standard testing conditions for these runs were: 3 g guaiacol, 0.6 g catalyst (20 wt.% catalyst loading), 9 MPa cold hydrogen pressure, 350°C, 2 h reaction time. Two different carbon supports were tested relative to the reference catalyst - commercially available; activated carbon (AC) and a biomass-derived activated charcoal (BAC-P) prepared in-lab from sawdust and activated using H₃PO₄ prior to carbonization. The AC and BAC-P has a specific surface area of 975 m²/g and 1300 m²/g, respectively, as shown in Table 4.1. Ru is a very expensive catalyst metal, thus to investigate the effectiveness of cheaper catalysts, Mo was used as a co-catalyst with Ru or as a substitute for Ru in this study. Guaiacol conversion was calculated by determining the concentration of the feedstock in the solution obtained after rinsing the reactor. This value was compared to the concentration of the guaiacol loaded into the reactor. These results are presented in Figure 4.1. As is evident, the Ru/BAC-P catalyst resulted in much higher guaiacol conversion (almost 17 % greater) than the reference catalyst (Ru/C), while the Ru/AC resulted in very similar guaiacol conversion (approx. 70 %) to that of the reference catalyst.

The addition of 1 wt.% Mo to the Ru/AC catalyst as a co-catalyst was also found to drastically increase guaiacol conversion by 23% attaining 92% conversion as compared to the ~70% conversion achieved with Ru/C. In contrast to these results, adding 1 wt.% Mo to the Ru/BAC-P catalyst did not further affect guaiacol conversion perhaps because the guaiacol conversion with the Ru/BAC-P catalyst was already very high (84.1%). The Mo/AC catalyst led to similar guaiacol conversion as compared to the 5% Ru/BAC-P catalyst despite the fact that the former catalyst exhibited a lower surface area (743 m²/g vs. 1127 m²/g).

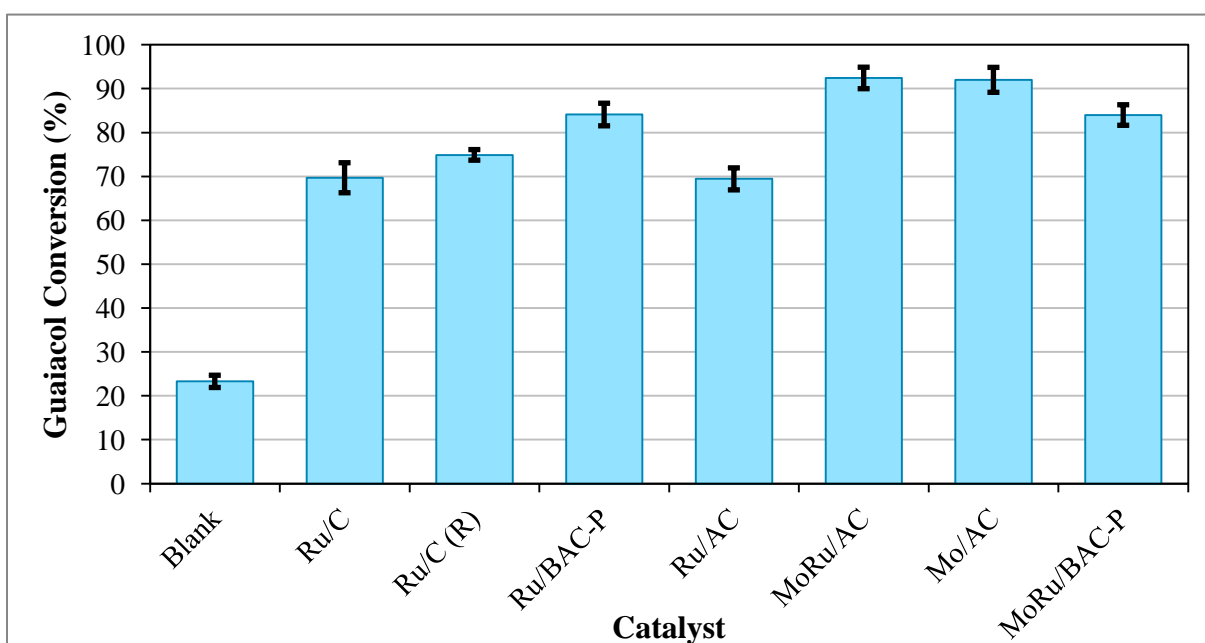


Figure 4.1 Conversion of guaiacol during hydroprocessing at 9 MPa cold hydrogen pressure, 350 °C, and 2 h reaction time

The performance of various carbon-supported catalysts is shown in Table 4.2.

Table 4.2 Guaiacol conversion and product yields from the guaiacol hydroprocessing experiments with various catalysts (2 h, 350°C with neat guaiacol, 9 MPa H₂)

	Blank	Ru/C	Ru/C (R)	Ru/ BAC-P	Ru/AC	MoRu/ AC	Mo/AC	MoRu/ BAC-P
GUA Conversion (%)	23.3 ±1.4	69.7 ±3.4	74.9 ±1.2	84.1 ±2.6	69.4 ±2.5	92.4 ±2.4	92.0 ±2.8	84.0 ±2.3
Coke yield (wt.%)	0.133 ±0.052	0.851 ±0.18	0.731 ±0.18	1.61 ±0.21	0.263 ±0.068	0.692 ±0.11	0.977 ±0.20	1.75 ±0.27
Gas yield (wt.%)	1.23 ±0.15	14.83 ±0.66	15.37 ±0.78	8.89 ±0.39	13.94 ±0.68	12.82 ±0.39	1.58 ±0.13	6.60 ±0.35
Methanol	4.6	14.8	4.9	11.3	12.3	10.7	8.67	12.3
Cyclohexane	n/d	2.99	24.2	1.13	8.86	6.59	n/d	n/d
Benzene	n/d	1.97	2.28	6.57	1.09	8.93	n/d	11.3
Phenol	6.03	15.1	16.4	15.6	14.9	34.4	24.9	21.1
Methyl Phenol	3.07	3.43	3.06	3.86	4.30	3.17	7.48	5.28
Unidentified	12.7	26.6	14.7	31.3	18.82	16.87	44.9	25.0
H ₂ Consumed (mol/kg GUA)	2.0 ±0.42	10.6 ±1.05	10.8 ±0.60	10.6 ±0.71	10.0 ±0.89	10.7 ±0.86	5.5 ±0.53	9.7 ±0.59

As can be seen, the main upgraded products from guaiacol are cyclohexane, benzene, phenol, methyl phenol and methanol as well as significant yield of unidentified compounds (ranging from 16-45% depending on the type of catalyst). The compounds identified are expected products of guaiacol deoxygenation and hydrogenation. The cumulative products that are listed as unidentified were not completely unknown, rather they were not definitively identified at >85% confidence using the GC/MS database.

The Ru/BAC-P catalyst significantly increased benzene yield while greatly decreasing cyclohexane yield relative to the Ru/C (reference catalyst) indicating that it was more active in deoxygenation as compared to hydrogenation. In contrast, even though the conversion of guaiacol in the presence of the Ru/AC catalyst was the same as for the reference catalyst, it resulted in significantly increased cyclohexane yield, accompanied with a decrease in benzene yield relative to the Ru/C, suggesting better activity of Ru/AC catalyst for hydrogenation, possibly due to the age of the catalyst. Partial reduction of Ru/C resulted in markedly higher cyclohexane and a significant drop in methanol yield. Thus, pre-reduction of the sup-

ported metal catalyst appears to improve its activity for hydrogenation rather than deoxygenation. The addition of Mo to the Ru/AC catalyst and Ru/BAC-P catalyst resulted in much higher benzene and phenol yields but a markedly decreased yield of cyclohexane. Thus, the addition of Mo co-catalyst enhances the hydrodeoxygenation activity of Ru catalyst rather than hydrogenation activity. In contrast, the Mo/AC catalyst produced mostly phenol and methyl phenol with no benzene or cyclohexane. This indicates that the Mo is very effective at oxygen removal, but only via scission of the aryl-O ether bond. Evidence of this can be seen in the increased phenol yields seen with the other two Mo-containing catalysts.

The above results suggest that the type of carbon support and the catalyst metals used exhibit significant but complex effects on both guaiacol conversion and product yields. As a general summary, catalyst reduction enhanced guaiacol conversion and markedly increased the catalyst's hydrogenation effects (leading to a higher cyclohexane yield) while addition of Mo to Ru catalysts generally increased the guaiacol conversion and more evidently enhanced guaiacol hydrodeoxygenation effects (producing more benzene and phenol compounds), rather than hydrogenation activity. To the best of the author's knowledge, the use of Mo-doped Ru catalysts has not been reported in the literature.

The cumulative molar yields of the liquid products resulting from the hydroprocessing of guaiacol are presented in Figure 4.2. The most striking result is that the Mo and Mo-doped Ru catalysts exhibit the equivalent or higher conversions of guaiacol than the best Ru catalyst as seen by how little unreacted guaiacol was detected by GC analysis.

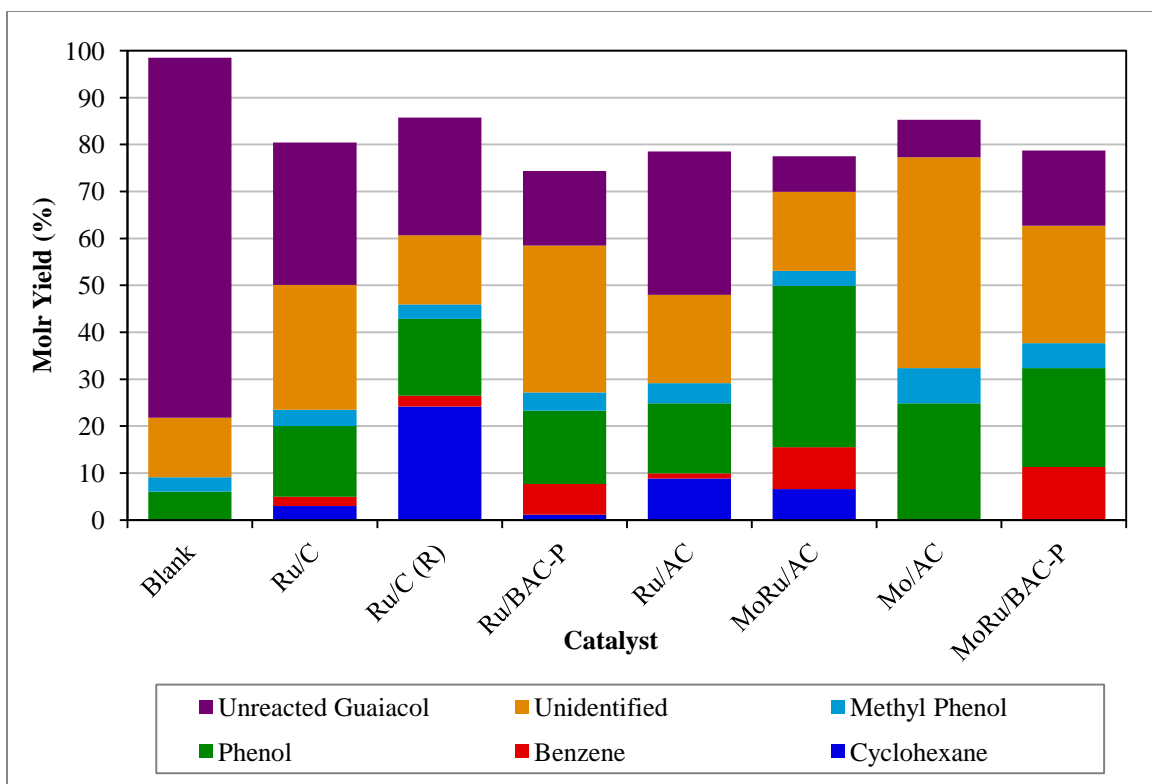


Figure 4.2 Molar yield of the liquid products after guaiacol hydroprocessing at 9 MPa cold hydrogen pressure, 350°C, and 2 h reaction time

Micro-GC gas analysis of the products showed that the major gaseous products of guaiacol hydroprocessing are CH_4 and CO_2 with much smaller quantities of, in order of decreasing prevalence, C_2H_6 , CO , C_3 and C_2H_4 gases. The molar yields of the main gas species and total molar C yield in gas from the guaiacol hydroprocessing experiments (2 h, 350°C with neat guaiacol, 9 MPa H_2) are presented in Table 4.3. Generally CH_4 was present in greater amount than CO_2 (mol ratio in the range of 0.92-2.0)

Table 4.3 Molar yields of main gas species and total molar C yield in gas from the guaiacol hydroprocessing experiments

	Blank	Ru/C	Ru/C (R)	Ru/ BAC-P	Ru/AC	MoRu/ AC	Mo/AC	MoRu/ BAC-P
Gas yield (wt.%)	1.23 ±0.15	13.9 ±0.68	14.8 ±0.66	15.4 ±0.78	8.89 ±0.39	12.8 ±0.39	1.58 ±0.13	6.60 ±0.35
Molar yields of gas species (mol/kg GUA)								
CH ₄	0.68	5.1	5.4	5.7	2.7	3.9	0.76	1.9
CO	n.d.	0.23	n.d.	0.0011	n.d.	n.d.	0.023	n.d.
CO ₂	0.009	2.1	2.4	2.4	2.1	2.8	0.095	1.7
C ₂ H ₄	n.d.	n.d.	n.d.	n.d.	n.d.	n.d.	n.d.	n.d.
C ₂ H ₆	0.001	0.46	0.51	0.56	0.23	0.46	0.009	0.13
C ₃ H ₆	n.d.	0.015	0.11	0.017	0.013	0.018	n.d.	0.006
C ₃ H ₈	n.d.	n.d.	n.d.	n.d.	n.d.	n.d.	n.d.	n.d.
Total molar C yield in gas (%)	0.6	14.9	15.5	8.9	13.9	12.8	6.6	1.2

Hydrogen consumption values during guaiacol hydroprocessing under 9 MPa cold hydrogen pressure, 350°C, and 2 h reaction are presented in Figure 4.3. As clearly shown in this Figure, the hydrogen consumption was almost constant around 10 mol H₂/kg-GUA for all of the catalysts except for Mo/AC which consumed about half as much hydrogen (5.5 mol H₂/kg-GUA) and the blank which consumed 2 mol H₂/kg-GUA. This result is not unexpected as Ru is known to be a hydrogenation catalyst. The lack of hydrogenation activity, as seen in the absence of cyclohexane in the products of guaiacol hydroprocessing with the Mo/AC catalyst, is in agreement with this finding.

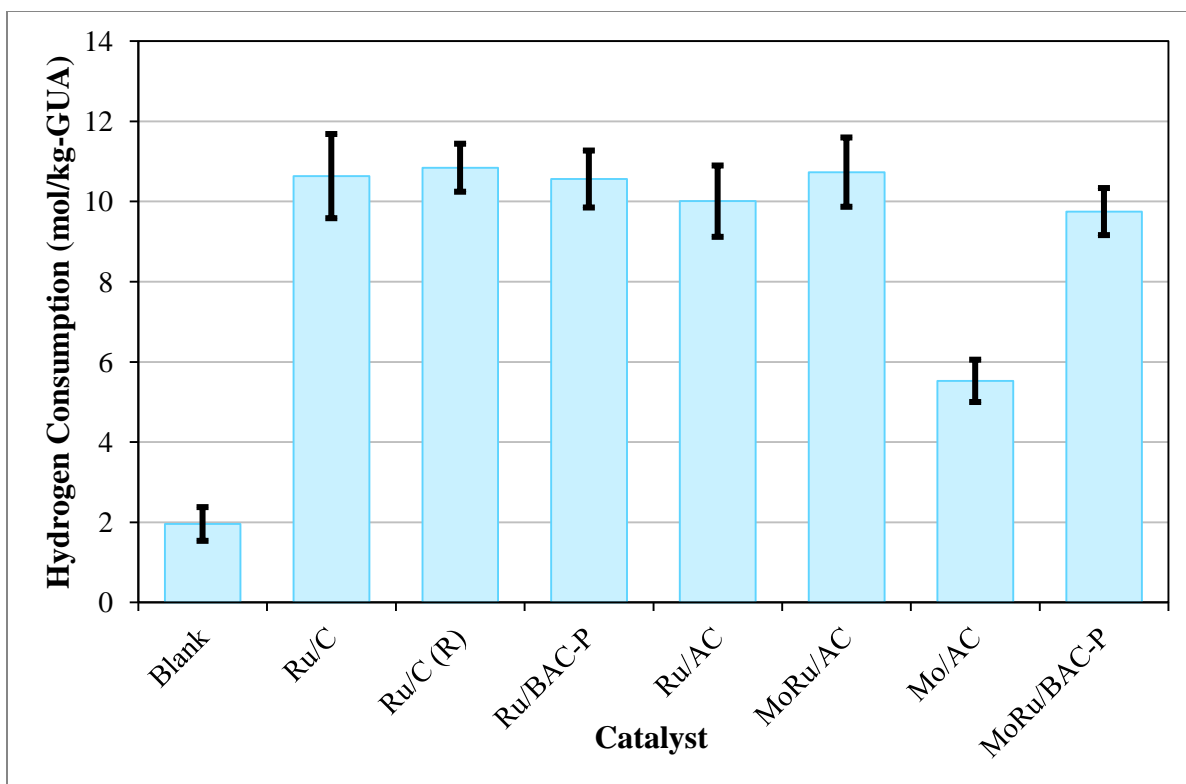


Figure 4.3 Hydrogen consumption during guaiacol hydroprocessing at 9 MPa cold hydrogen pressure, 350°C, and 2 h reaction time

The combined analyses of the solid, liquid and gaseous products allowed for determination of carbon balances for the catalysts tested. The mass of carbon in the solids was approximately calculated by assuming that all of the increase in mass of the catalyst was due to the deposition of pure carbon. The carbon present in the gases could be calculated by the ideal gas law, as the volume (2.8 L), pressure (1.2 bar) and temperature (25 °C) of the sample cylinder were known. The carbon in the liquid products was calculated based on the concentration of the liquid products in the diluted product stream. The carbon in the unknowns was approximated assuming that they contain seven carbons per mole and exhibit a similar FID response factor to guaiacol. The sum of these values was compared to the amount of carbon in the guaiacol loaded into the reactor. The cumulative carbon balances are presented in Figure 4.4, which clearly shows that there was generally good carbon recovery in all tests (~84-99%).

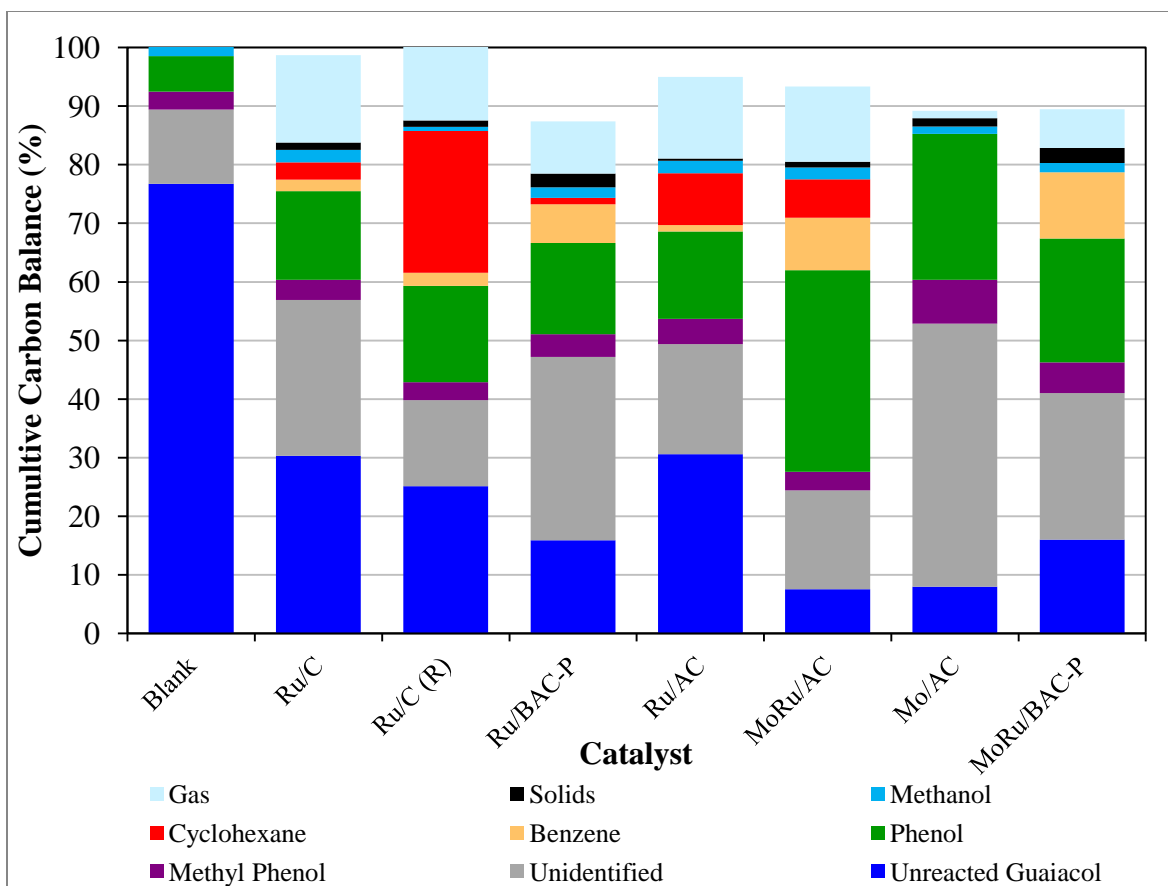


Figure 4.4 Cumulative carbon balances for the guaiacol hydroprocessing tests with various catalysts (2 h, 350°C, 9 MPa H₂)

4.3.3 Process Optimization

Given that it produced the highest guaiacol conversion, the MoRu/AC catalyst was initially chosen for the optimization study. However, for ease of catalyst preparation, this was changed to MoRu/C based on the similarity of the activity of the Ru/C and Ru/AC catalysts as discussed in the previous section. Thus, for simplicity 1 wt.% Mo was added to the commercially available Ru/C. After drying, the MoRu/C catalyst was reduced at 550°C for 4 h under flowing H₂ ~50 mL/min to maximize the availability of hydrogen for reaction with the guaiacol.

The variables for the optimization are: initial H₂ pressure, reaction time and reaction temperature. The initial H₂ pressures, 3, 6 and 9 MPa, were chosen to supply sub-, near- and

greater-than-stoichiometric hydrogen into the system. The different conditions were performed in a random order in order to avoid introducing a bias. GC/MS analyses from the first set of experiments completed indicated the presence of numerous compounds, but only a few (e.g. guaiacol, phenol, benzene) were identified with a high degree of confidence.

Figure 4.5 illustrates guaiacol conversion as a function of reaction time, temperature and initial H₂ pressure with MoRu/C catalyst. As can be clearly seen in the Figure, that at 30 min, guaiacol conversion ranges from a low of 46% at 3 MPa, 30 min, 300°C to as high as 98% at 9 MPa, 240 min, and 400°C. The curves for the runs at 3, 6, and 9 MPa initial hydrogen pressure show a remarkably solid trend, with guaiacol conversion appearing to plateau as reaction time reaches 240 min. However, extending the reaction time for the 3 MPa, 300°C condition to 240 min only increased conversion to ~63%, which was equivalent to the conversion at 3 MPa, at 350 °C and 30 min. At 400 °C, conversion at 3 MPa and 30 min was ~87%. Thus temperature and H₂ pressure appear to have a much greater effect on guaiacol conversion than does reaction time. Surprisingly, there was no difference in the conversion of guaiacol at less-than- and greater-than-stoichiometric concentrations of hydrogen. Rather, the difference was seen in the increased amount of coke deposited on the catalyst at low hydrogen pressure as well as an increase in the amount of unidentified compounds present in the liquid product.

Based on these results, it appears that longer reaction times may not be necessary provided that the experiments are performed at higher temperatures. The decreased duration may offset the higher energy cost. The yields of main liquid products (determined by GC/FID), solid residue and gas products along with guaiacol conversion from the above optimization tests are summarized in Table 4.4.

As can be seen, coke yields are low at lower temperatures and shorter reaction times regardless of hydrogen pressure. However, increased reaction times and temperatures result in increased coking, with more coking evident at high temperatures and lower hydrogen pressure. In the absence of sufficient hydrogen to cap reactive intermediates, these reactions are more likely to result in condensed products that deposit on the catalyst as coke. Extended reaction times greatly increased the amount of coke deposited on the catalyst (1.1 vs. 9.9 wt.%) even in the presence of greater-than-stoichiometric hydrogen. This is likely due to low reactivity of the molecular hydrogen.(Gosselink *et al.*, 2012) The amount and number of unknown

compounds also increased with extended reaction time from 6.8 to 18.6% owing to the increased residence time.

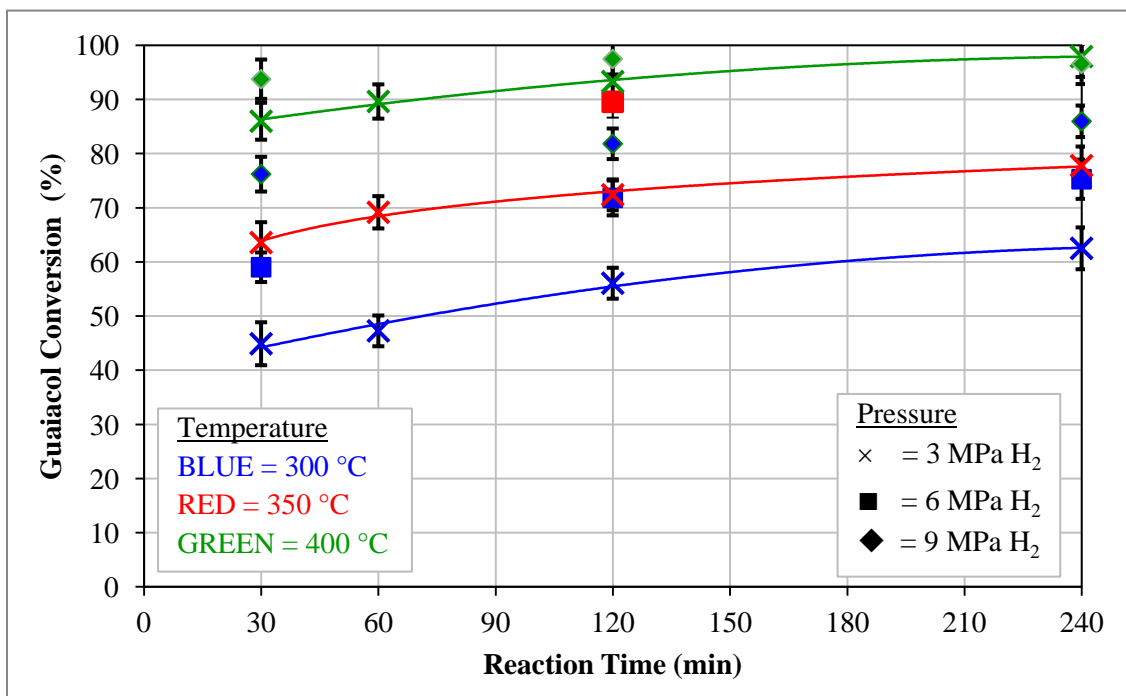


Figure 4.5 Guaiacol conversion as a function of reaction time, temperature and initial H₂ pressure with MoRu/C catalyst

The major gaseous products from the experiments were CH₄ and CO₂ with much smaller quantities of, in order of decreasing prevalence, C₂H₆, CO, C₃ and C₂H₄ gases. Generally, CH₄ was present in greater amount than CO₂ (mol ratio in the range of 0.92-2.0). Coke formation was generally negligible at lower temperatures and higher pressures but increased with increasing temperature and decreased hydrogen pressure. Hydrogen consumption varied from a low of 1.7 mol/kg-GUA to a high of 16.1 mol/kg-GUA.

Table 4.4 Guaiacol conversion and product yields from the guaiacol hydroprocessing experiments with MoRu/C catalyst at selected conditions

Reaction conditions			Guaiacol conv. (%)	Coke yield (wt.%)	Liquid Product Yield (wt.%)						mol H ₂ /kg GUA
Temp. (°C)	Time (min)	H ₂ Pressure (MPa)			Methanol	Cyclohexane	Benzene	Phenol	Methyl phenol	Unidentified	
300	30	3	44.9 ±4.0	0.2 ±0.02	2.62	1.61	2.18	8.41	0.78	2.28	1.7 ±0.34
300	30	6	59.0 ±2.7	0.3 ±0.06	4.52	2.79	3.76	14.53	1.34	3.01	2.4 ±0.33
300	30	9	76.2 ±3.2	0.2 ±0.04	7.54	4.65	6.27	24.23	2.23	3.87	3.5 ±0.21
300	30	3	44.9 ±4.0	0.2 ±0.12	2.62	1.61	2.18	8.41	0.78	2.28	1.7 ±0.34
300	120	3	56.1 ±2.9	1.0 ±0.21	4.08	2.52	3.39	13.12	1.21	3.50	4.1 ±0.28
300	240	3	62.5 ±3.9	1.4 ±0.27	5.07	3.13	4.22	16.30	1.50	4.64	6.5 ±0.30
300	30	3	44.9 ±4.0	0.2 ±0.12	2.62	1.61	2.18	8.41	0.78	2.28	1.7 ±0.34
350	30	3	63.6 ±3.8	7.7 ±1.3	5.24	3.24	4.36	16.86	1.55	4.22	3.8 ±0.22
400	30	3	86.0 ±3.4	12.4 ±1.3	9.59	5.92	7.98	30.84	2.84	4.97	6.7 ±0.47
400	30	9	93.8 ±3.2	1.1 ±0.29	11.40	7.03	9.48	36.66	3.38	6.83	9.9 ±0.72
400	240	9	96.6 ±3.8	9.9 ±1.1	11.75	7.25	9.77	37.76	3.48	18.60	16.1 ±1.3

4.3.4 Spent catalyst characterization

The results of TGA analysis are illustrated in Figures 4.6a and 4.6b. The analysis was performed on the fresh and spent Ru/AC and MoRu/AC catalysts heated from room temperature to 900°C in flowing air to evaluate the deposition of coke on the catalyst.

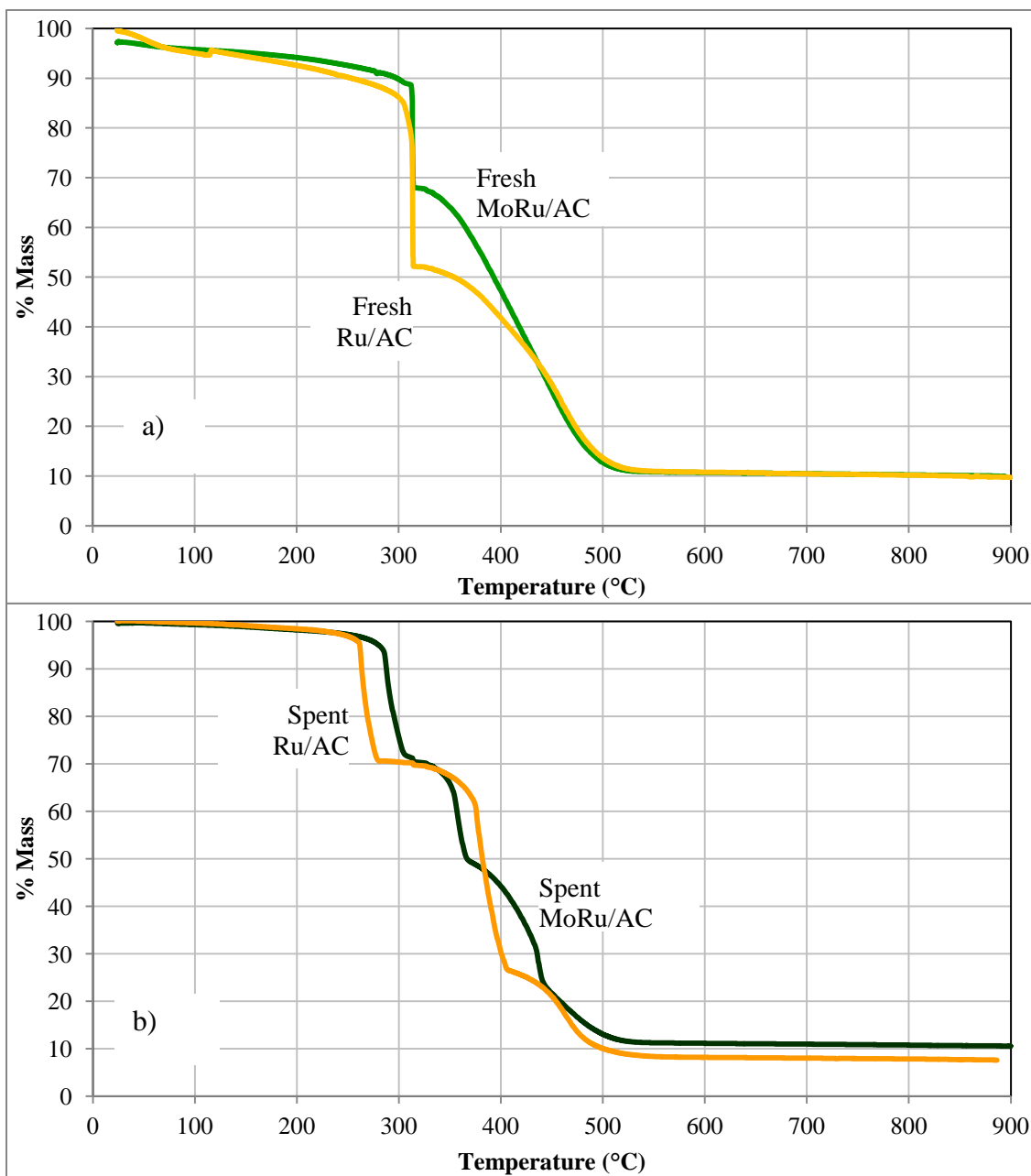


Figure 4.6 TGA plots for fresh (a) and spent (b) Ru/AC and MoRu/AC catalysts from the guaiacol hydroprocessing tests (2 h, 350°C, 9 MPa H₂)

It was noted that, unlike for mineral-supported catalysts like alumina, the carbon support material would also burn, thus necessitating a comparison between the fresh and spent catalyst. Figure 4.6b shows more mass decrease events in the TGA curves for the spent catalysts as compared to the fresh catalysts (Figure 4.6a), indicating the deposition of carbonaceous material on the spent catalysts. As was expected for both catalysts (MoRu/AC and Ru/AC), the fraction of mass remaining after burning of the fresh catalyst was unchanged and corresponds to the formation of metal oxides from the supported metals in these catalysts. The decreased mass of material remaining for the Ru/C catalyst in Figure 4.6b indicates that the metal oxides which remained after burning comprised a smaller fraction of the overall mass of the sample, indicating that this catalyst experienced increased coke deposition as compared to the MoRu/AC catalyst.

The dTGA curves presented in Figure 4.7 were constructed by taking the first derivative of the TGA plots, to evaluate the thermal stability of the carbonaceous materials (including the carbon support and the carbon deposits formed during the reactions). As is obviously shown in this Figure, the onset of two rapid mass loss peaks at around 250-350°C and 350-500°C, respectively, shifts to lower temperatures for the spent catalysts as compared to the fresh catalysts. This suggests deposition of carbonaceous materials (commonly called coke) during guaiacol hydroprocessing.

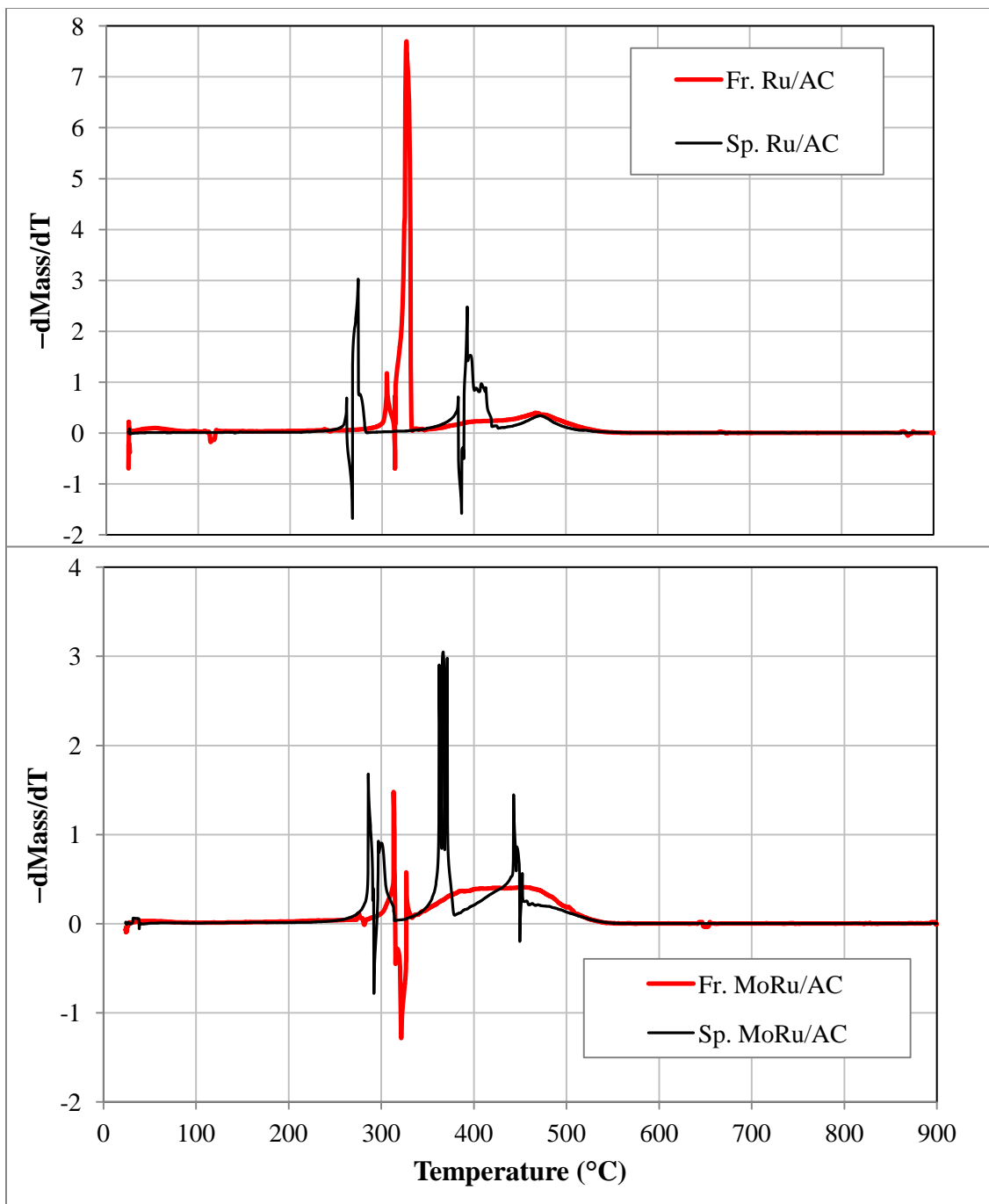


Figure 4.7 dTGA plots for fresh and spent Ru/AC and MoRu/AC catalysts from the guaiacol hydroprocessing tests (2 h, 350 $^{\circ}\text{C}$, 9 MPa H₂)

The XRD spectra of selected fresh and spent catalysts are presented in Figure 4.8. The catalysts all exhibit a broad peak centred on 22° and a smaller broad peak centred on 42° that are characteristic of amorphous carbon (Rajan *et al.*, 2014). The sharp peak at 26.5° is characteristic of the (002) plane of graphite. (Peng *et al.*, 2013) The smaller peak at $\sim 23^\circ$ may be attributed to the diffraction of the sample holder used in the XRD measurements. No XRD lines attributed to any metal species were detectable, likely due to the low metal loading (≤ 5 wt.%), or owing to the high dispersion states of the metals in the carbon supports (with a very high surface area and porosity).

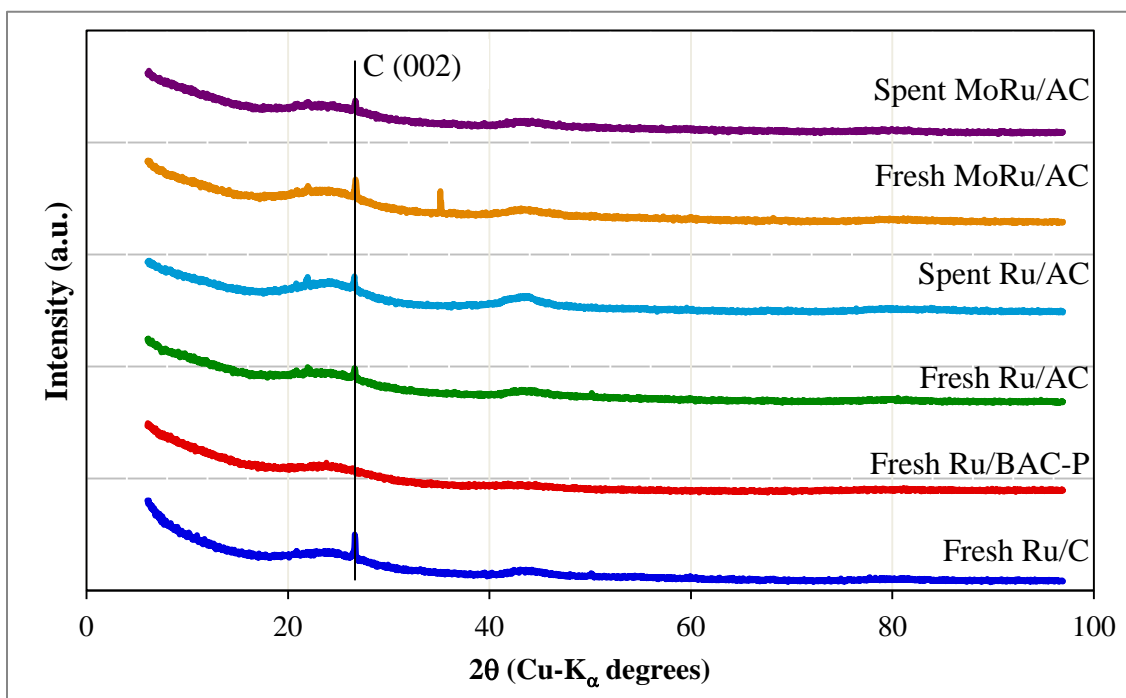


Figure 4.8 XRD spectra of selected fresh and spent catalysts

4.4 Conclusions

In this work, catalyst screening for the hydroprocessing of lignin or depolymerized lignin was investigated using guaiacol as a model compound. This study has demonstrated that the type of carbon support used to prepare Ru catalysts is an important factor in guaiacol conversion. The BAC-P-supported Ru catalyst exhibited ~14% greater conversion of guaiacol than the reference Ru catalyst. Catalyst reduction enhanced guaiacol conversion and markedly increased the catalyst's hydrogenation effects (leading to a higher cyclohexane yield) while the addition of Mo to Ru catalysts generally increased guaiacol conversion and more evidently enhanced guaiacol hydrodeoxygenation effectiveness (producing more benzene and phenol compounds), rather than hydrogenation activity. In addition, hydrogen consumption using Mo/AC catalyst was about half that of the catalysts containing Ru, indicating that Mo is not as efficient in hydrogenating guaiacol as the Ru catalysts. The increased conversion was, therefore, largely directed towards compounds of unknown composition. To the best of the author's knowledge, the use of Mo-doped Ru catalysts has not been reported in the literature.

The optimization study revealed that temperature and initial hydrogen pressure have a much greater effect on guaiacol conversion than does reaction time. For example, the conversion of guaiacol at 3 MPa, 240 min, and 300 °C was equivalent to the conversion at 3 MPa, 30 min and 350 °C. Thus longer reaction times may not be necessary provided that hydroprocessing is performed at higher temperatures (the decreased duration may offset the higher energy cost). The combination of high temperature (400 °C) and 9 MPa initial hydrogen pressure was even more effective, with conversion of ~94% after a reaction time of only 30 min. Coke formation was found to be negligible at lower reaction temperatures and short reaction times and increased at high reaction temperature, long reaction times and low initial hydrogen pressure.

4.5 References

- Asmadi M, Kawamoto H, Saka S. *J. Anal. Appl. Pyrol.*, 2011, 92, 88.
- Bui VN, Laurenti D, Delichere P, Geantet C. *Appl. Catal. B: Environ.*, 2011, 101, 246.
- Cateto CA, Barreiro MF, Rodrigues AE, Belgacem MN. *Ind. & Eng. Chem. Research*, 2009, 48, 2583.
- Centeno A, Laurent E, Delmon B. *J. Catal.*, 1995, 154, 288.
- Chakar FS, Ragauskas A. *J. Ind. Crops Prod.*, 2004, 20, 131.
- Chang J, Danuthai T, Dewiyanti S, Wang C, Borgna A. *Chem. Cat. Che.*, 2013, 5, 3041.
- Dournel P, Randrianalimanana E, Deffieux A, Fontanille M. *Eur. Polym. J.*, 1988, 24, 843.
- El Mansouri N-E, Yuan Q, Huang F. *BioResources*, 2011, 6, 2492.
- Elliott DC, Hart TR. *Energy Fuels*, 2009, 23, 631.
- Furimsky E, Massoth FE. *Catal. Today*, 1999, 52, 381.
- Gandarias I, Barrio VL, Requies J, Arias PL, Cambra JF, Gutierrez MB. *Int. J. of Hydrogen Energy*, 2008, 33, 3485.
- Gutierrez A, Kaila RK, Honkela ML, Siloor R, Krause AOI. *Catal. Today*, 2009, 147, 239.
- Gosselink RJA, Teunissen W, Van Dam JEG, Jong ED, Gellerstedt G, Scott EL, Sanders JPM. *Bioresour. Technol.*, 2012, 106, 173.
- Hirose S, Kobayashi M, Kimura H, Hatakeyama H. In: Kennedy JF, Phillips GO, Williams PA, Hatakeyama H. (Eds.), *Recent advances in environmentally compatible polymers*. Woodhead, Cambridge, 2001, 73.
- Jin Y, Ruan X, Cheng X, Lü Q. *Bioresour. Technol.*, 2011, 102, 3581.

Kersten SRA, van Swaaij WPM, Lefferts L, Seshan K. In: Centi G, van Santen RA. (Eds.), *Catalysis for Renewables—From Feedstocks to Energy Production*, Wiley-VCH, Weinheim, 2007, 119.

Lee CR, Yoon JS, Suh YW, Choi JW, Ha JM, Suh, Park YK. *Catal. Commun.*, 2012, 17, 54.

Li K, Wang R, Chen J. *Energy Fuels*, 2011, 25, 854.

Lin YC, Li CL, Wan HP, Lee HT, Liu CF. *Energy Fuels*, 2011, 25, 890.

Liu C, Wilson AK. Abstracts of Papers, 245th ACS National Meeting & Exposition, New Orleans, LA, United States, April 7-11, 2013, COMP-278.

Mahmood N, Yuan Z, Schmidt J, Xu C. *Bioresour. Technol.*, 2013, 139, 13.

Moura JS, Souza MOG, Bellido JDA, Assaf EM, Opportus M, Reyes P, do Carmo Rangel M. *Int. J. of Hydrogen Energy*, 2012, 37, 2985.

Nadji H, Bruzzese C, Belgacem MN, Benaboura A, Gandini A. *Macromol. Mater. Eng.* 2005, 290, 1009.

Nimmanwudipong T, Runnebaum RC, Block DE, Gates BC, *Catal. Lett.*, 2011, 141, 779.

Peng S, Fan X, Li S, Zhang J. *J. Chil. Chem. Soc.* 2013, 58, 2213.

Prochazkova D, Zamostny P, Bejblova M, Cerveny L, Cejka J. *Appl. Catal. A: Gen.*, 2007, 332, 56.

Rajan AS, Ashok SS, Shukla K. *Energy Environ. Sci.*, 2014, 7, 1110.

Reddy BM, Khan A. *Catal. Rev.*, 2005, 47, 257.

Romero Y, Richard F, Brunet S. *Appl. Catal. B: Environ*, 2010, 98, 213.

Rouco AJ, Haller GL. *J. Catal.*, 1981, 72, 246.

Saidi M, Samimi F, Karimipourfard D, Nimmanwudipong T, Gates BC, Rahimpour MR. *Energy Environ. Sci.*, 2014, 7, 103.

- Sasaki C, Wanaka M, Takagi H, Tamura S, Asada C, Nakamura Y. *Ind. Crops Prod.*, 2013, 43, 757.
- Senol OI, Ryymin E-M, Viljava T-R, Krause AOI. *J. Mol. Catal. A: Chem.*, 2007, 277, 107.
- Sigoillot J-C, Berrin J-G, Bey M, Lesage-Meessen L, Levasseur A, Lomascolo A, Record E, Uzan-Boukhris E. *Advances in Botanical Research*, 2012, 61(Lignins), 263.
- Tejado A, Pena C, Labidi J, Echeverria JM, Mondragon I. *Bioresour. Technol.*, 2007, 98, 1655.
- Vázquez G, Antorrena G, González J, Mayor J. *Bioresour. Technol.*, 1995, 51, 187.
- Wang M, Leitch M, Xu C. *Eur. Polym. J.*, 2009, 45, 3380.
- Wildschut J, Mahfud FH, Venderbosch RH, Heeres HJ. *Ind. Eng. Chem. Res.*, 2009, 48, 10324.
- Yang Y, Ochoa-Hernandez C, O'Shea VA, Pizarro P, Coronado JM, Serrano DP. *Appl. Catal. B: Environ.*, 2014, 45, 91.
- Yuan Z, Cheng S, Leitch M, Xu C. *Bioresour. Technol.*, 2010, 101, 9308.
- Zakzeski J, Bruijninx PC, Jongerius AL, Weckhuysen BM. *Chem. Rev.*, 2010, 110, 3552.
- Zauwen MN, Crucq A, Degols L, Lienard G, Frennet A, Mikhalenko N, Grange P. *Catal. Today*, 1989, 5, 237.
- Zhang L, Champagne P, Xu C. *Bioresour. Technol.*, 2011, 102, 8279.
- Zhao HY, Li D, Bui P, Oyama ST. *Appl. Catal. A: Gen.*, 2011, 391, 305.

Chapter 5

5 Hydrotreatment of organosolv lignin for aromatic chemicals and materials using carbon-based catalysts

5.1 Introduction

The depletion of fossil fuel reserves is an issue that has come to prominence in recent decades. Coupled with increased consumption from rising economies such as China and India, this has prompted an increased interest in the production of chemicals and fuels from alternative resources and is one of the major priorities of the 21st century.

Biomass is generally regarded as the most feasible alternative in this regard as it is widely available, renewable and generally carbon-neutral. Although it is possible to produce chemicals from crops such as corn etc., it is preferable to produce bio-products from non-food resources such as agricultural and forestry residues.

Of particular interest is lignin, which is the second most abundant naturally synthesized polymer after cellulose, comprising 25-40 % of dry wood and crop stems. (Tejado *et al.*, 2007) In addition, it is the most abundant natural source of aromatic compounds. More than 50 million tons of lignin in the form of Kraft lignin (KL) is generated annually as a by-product in the pulp and paper industry where it has historically been viewed as a waste material or a low value by-product. Consequently, it has been predominantly used as a low-energy content fuel in the recovery boilers of pulp/paper mills. However, the recovery boilers represent a bottleneck in a majority of the pulp/paper mills in North America. In addition to Kraft lignin, due to the recent increase and projected growth of bio-ethanol production, it is expected that large quantities of organosolv lignin (OL) and hydrolysis lignin (HL), as by-products of pre-treatment processes in cellulosic ethanol plants, will become available in the near future.

As an amorphous natural polymer of substituted propyl-phenols, lignin contains many polar hydroxyl groups, making it incompatible with most synthetic polymers due to its high polarity and broad glass transition temperature. (Chakar and Ragauskas, 2004) In addition, due to its highly branched structure and intermediate molecular weight, lignin alone is not strong

enough to be used as a structural material. Conversely, lignin's molecular weight is too high for it to be incorporated directly into fuel applications, not to mention its low energy content due to the abundance of oxygen in the polymer. Since lignin contains abundant ether linkages and aliphatic and phenolic hydroxyl groups, lignin depolymerization products of moderate molecular weight could be good candidates for raw material to replace petroleum based polyether polyols for the synthesis of polyurethane (PU) materials and replace petroleum phenol for the synthesis of phenol-formaldehyde (PF) (Vasquez *et al.*, 1995; Wang *et al.*, 2009) and epoxy resins. (Hirose *et al.*, 2001; Sasaki *et al.*, 2013)

Consequently, most of the research on the application of lignin is concentrated on converting lignin into chemicals and fuels via hydrolytic, oxidative and reductive depolymerization and pyrolysis. Most of these destructive methods suffer from the drawbacks of high energy input, low yields and difficulty in product separation. Fungal biodegradation of lignin has been intensively investigated, (Zhang *et al.*, 2011) but this process is slow and time consuming. Hydrolytic depolymerization has also been investigated, (Yuan *et al.*, 2010) but the yield is usually very low. To overcome these disadvantages, a more viable strategy might be moderate depolymerization of lignin under mild conditions to convert the lignin to oxygenated fuel additives and feedstock for various types of bio-materials.

Hydrogenation reactions are typically performed in the presence of noble metal catalysts. Ru catalysts, in particular, have been shown to be very active in the hydrogenation and hydrodeoxygenation of model compounds (e.g. phenol and guaiacol) as well as bio-oils. (Elliott and Hart, 2009; Gutierrez *et al.*, 2009; Lee *et al.*, 2012; Chang *et al.*, 2013) Co- or Ni-promoted Mo sulfide catalysts, typically supported on alumina, and borrowed from petroleum processing operations have also been used in the hydrotreatment of lignin and biomass-derived bio-oils. (Senol *et al.*, 2007; Romero *et al.*, 2010; Zakzeski *et al.*, 2010; Saidi *et al.*, 2014) More recently, reductive depolymerization of lignin in the presence of hydrogen and metal catalysts especially other late 3d and 4d transition metal (Fe, Co, Ni, Cu, Ru, Rh, Pd, and Ag) has been proposed. (Cateto *et al.*, 2009; Li *et al.*, 2011; Zhao *et al.*, 2011; Jin, 2014) A review of the literature also reveals that mixed noble metal-transition metal catalysts (e.g. Ru-Co, Rh-Cu and Rh-Ag) have been used, although not in the hydroprocessing of bio-oils. (Rouco and Haller, 1981; Zauwen *et al.*, 1989; Moura *et al.*, 2012)

Although alumina-supported catalysts are active in HDO reactions and catalyze methyl group transfer, (Gutierrez *et al.*, 2009) they also increase catalyst deactivation by promoting the formation and deposition of coke on the catalyst surface. (Centeno *et al.*, 1995; Prochazkova *et al.*, 2007; Elliott and Hart, 2009; Wildschutt *et al.*, 2009; Lin *et al.*, 2011) Centeno *et al.* (1995) proposed that it is the weak Lewis acid sites present in the alumina that promote the condensation reactions leading to coke formation.

In order to avoid coke formation, researchers have investigated less acidic supports such as activated carbon and SiO₂ (Furimsky and Massoth, 1999; Reddy and Khan, 2005; Kersten *et al.*, 2007) as well as other less common supports e.g. ZrO₂ and MgO. (Senol *et al.*, 2007; Bui *et al.*, 2011) Yang *et al.* (2014) found that using carbon-supported catalysts resulted in yields equivalent to those of alumina-supported catalysts, but with lower proportions of oxygenated compounds.

Previous work in our group has shown that Ru-based catalysts are effective in lignin depolymerization and that the addition of Mo to Ru catalysts increases catalyst effectiveness. In this work, several carbon-supported Mo-Ru catalysts, chosen based on the catalyst screening study reported in a previous chapter, were investigated for the hydroprocessing or reductive depolymerization of OL under hydrogen atmosphere for applications such as fuel additives and intermediates for chemicals and materials.

To the best of the author's knowledge, the investigation of lignin depolymerization via hydroprocessing using a mixed noble metal/transition metal catalyst has not been reported in the literature.

5.2 Experimental

5.2.1 Materials

The organosolv lignin (OL) used in this research was provided by Lignol, Canada and had a weight average molecular weight (M_w) of ~2,600 g/mol.

Different carbon-supported catalysts: $\text{Mo}_{0.01}\text{Ru}_{0.05}/\text{AC}$ (denoted as MoRu/AC), $\text{Mo}_{0.01}\text{Ru}_{0.05}/\text{AC-P}$ (MoRu/ACP), $\text{Mo}_{0.01}\text{Ru}_{0.05}/\text{C}$ (MoRu/C), $\text{Mo}_{0.1}/\text{AC}$ (Mo/AC) catalysts and the reference commercial catalyst $\text{Ru}_{0.05}/\text{C}$ (Ru/C), were used in this work. The names and textural analysis of these carbon-supported catalysts are shown later in Table 5.1.

The Ru/C reference catalyst was purchased from Sigma-Aldrich and used as provided, and carbon-supported MoRu catalysts were prepared in-house by incipient wetness impregnation of activated carbon with ruthenium (III) nitrosyl nitrate solution ($\text{Ru}(\text{NO})(\text{NO}_3)_3$) and ammonium molybdate tetrahydrate ($(\text{NH}_4)_6\text{Mo}_7\text{O}_{24}\cdot 4\text{H}_2\text{O}$). Solvents used included acetone and methanol. All were reagent grade and purchased from Sigma-Aldrich.

As an example, the MoRu/AC catalyst was prepared by suspending activated charcoal in a 50% solution of water and methanol. The calculated volume of the Ru solution was added to this solution. The Mo was added by dissolving the required amount of the Mo compound in some distilled water and adding the solution to the suspension. The suspension was then stirred for 24 h at ambient temperature. The catalyst was then dewatered by rotary evaporation under vacuum at 85°C and then dried overnight in an oven at 105°C . The catalyst was then loaded into a tube reactor and reduced under a flow of 50 mL/min hydrogen at 500°C for 4 h. The evolution of a brown gas at a temperature of $\sim 300^\circ\text{C}$ was evidence of the reduction taking place. After cooling to ambient temperature under nitrogen, the catalyst was decanted into a beaker of methanol, also under nitrogen, for passivation. After evaporation of the methanol at 65°C and cooling back to ambient, the catalyst was stored in an air-tight plastic bag before use.

To prepare MoRu/ACP catalyst, phosphorated activated charcoal was prepared. Briefly, the required amount of phosphoric acid was added to a suspension of activated charcoal in 50% water/methanol. The suspension was stirred for 24 h and then dewatered by rotary evaporation under vacuum at 85°C . The phosphorated support was then dried at 105°C overnight and stored after cooling, and used as a support to prepare MoRu/ACP catalyst in a similar method as described above for MoRu/AC .

In addition, MoRu/C catalyst was prepared by adding the calculated amount of the Mo compound dissolved in distilled water to a suspension of the reference Ru/C catalyst in 50:50

methanol/water. The remaining procedure was the same as for the MoRu/AC catalyst as explain above.

5.2.2 Experimental apparatus and procedure

The hydroprocessing/depolymerization of OL was carried out in a 100 mL stainless-steel autoclave reactor equipped with a stirrer. In a typical run, the reactor was loaded with 5 g of OL, 0.5 g of catalyst and 25 g of acetone. The reactor was sealed, purged with nitrogen and was subsequently pressurized to 5 MPa with hydrogen. The reactor was heated to the reaction temperature while stirring and kept at the desired temperature for 120 min before cooling. Once the reactor had cooled to room temperature, the gaseous products were sampled for analysis. The liquid products and solid residue (SR) were rinsed from the reactor with acetone and the resulting suspension was filtered under vacuum through a pre-weighed Whatman No. 5 filter paper. The SR, catalyst and filter paper were dried at 105 °C for 24 h before weighing. After a GC-MS sample was taken, the acetone (and maybe water formed during the hydroprocessing) was removed from the liquid product by rotary evaporation under vacuum at 40-50 °C. The yields of depolymerized OL (DOL) and SR were calculated relative to the mass of the OL loaded into the reactor. Each experiment was repeated to reduce the experimental error to $\pm 5\%$.

The relative molecular weights and their distributions of the OL feed and the hydroprocessed DOL were measured with a Waters Breeze GPC-HPLC (gel permeation chromatography-high performance liquid chromatography) instrument (1525 binary pump, UV detector at 270 nm; Waters Styrylgel HR1 column at a column temperature of 40 °C) using THF as the eluant at a flow rate of 1 mL/min. Linear polystyrene standards were used to generate a calibration curve for molecular weight estimation. ^1H NMR spectra were obtained on a 500 MHz Unity Inova NMR instrument at room temperature, wherein d_6 -dimethylsulfoxide was used as solvent. FT-IR spectra were collected on a Bruker Tensor 37 FTIR spectrophotometer in the range of 550-4000 cm^{-1} with ATR accessory. The volatile components of the DOLs were identified by GC-MS (HP 6890 GC and HP 5972 MS) using a silicon column with temperature programming from an initial temperature of 50 °C for 2 min hold at 10 °C/min to a final temperature of 280 °C for 2 min hold. CHNS (carbon, hydrogen, nitrogen, and sulfur) ele-

mental analysis was conducted on a Flash EA 1112 Series elemental Analyzer. The BET surface area analysis was performed on a Micrometrics ASAP 2010 instrument. The samples were degassed at 150 °C until a stable static vacuum of less than 5×10^{-3} Torr was achieved prior to analysis. The gas composition was measured on an Agilent 3000 Micro-GC equipped with dual columns (Molecular Sieve and PLOT-Q) and thermal conductivity detectors. The GC system employed in this work enabled analysis of gas species up to C₃, including O₂, N₂, H₂, CO, CO₂, CH₄, C₂H₄, C₂H₆, C₃H₈, and C₃H₆.

5.3 Results and Discussion

5.3.1 Catalyst characterization

The textural analysis of all catalysts prepared is presented in Table 5.1. There was no great difference in the surface areas, pore volumes and pore diameters of the catalysts, therefore the differences in catalyst performance must be due to the supported metals.

Table 5.1 Textural analysis of the carbon-supported catalysts

Catalyst	Metal cont. (wt.%)		BET S. Area (m ² /g)	Tot. Pore Vol. (cm ³)	Vol. of pores <2 nm (cm ³)	Vol. of pores 2-50 nm (cm ³)	Avg. pore dia. (nm)
	Mo	Ru					
Ru/C	0	5	893	0.852	0.034	0.507	3.61
MoRu/C	1	5	865	0.826	0.045	0.514	3.62
MoRu/AC	1	5	875	0.786	0.034	0.442	3.58
MoRu/ACP	1	5	771	0.704	0.032	0.405	3.67
Mo/AC	10		678	0.656	0.027	0.400	3.62

5.3.2 DOL Yields

The OL was depolymerized at standard reaction conditions of 5 g OL dissolved in 25 g acetone, 0.5 g catalyst, 5 MPa initial hydrogen pressure and 1 h reaction time at 300 °C unless otherwise noted. The yields of DOL at different temperatures are presented in Figure 5.1.

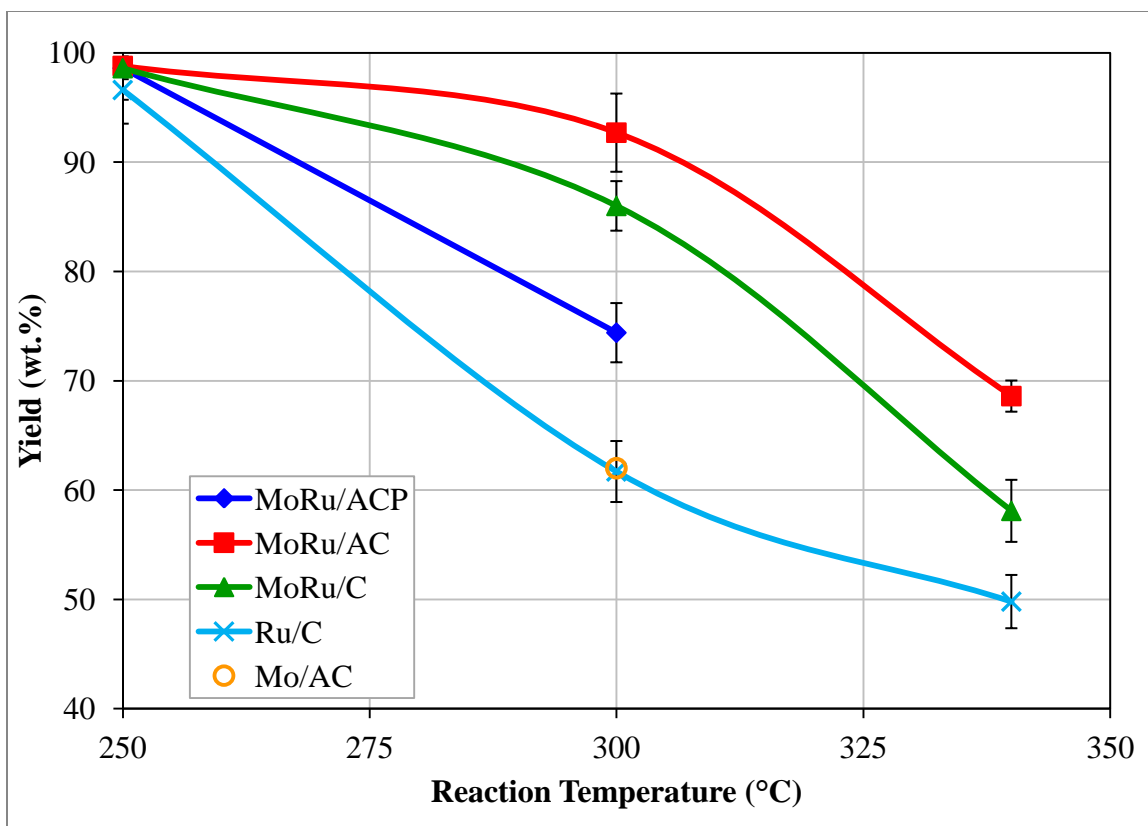


Figure 5.1 Yield of DOL as a function of reaction temperature

The DOL yields for all four Ru-based catalysts were very high (<95 wt.%) at 250 °C but were found to decrease with increased temperature. The yield of DOL for MoRu/AC catalyst at 300 °C was still ~95 wt.% but the other catalysts exhibited marked decreases. At 340 °C, the DOL yields with all catalysts were <70 wt.% due to increased char (solid residue, SR) formation.

It is interesting to note that the yield of DOL for the Mo/AC catalyst at 300 °C was equivalent to that of the Ru/C reference catalyst. Due to this poor showing, further tests with this catalyst were not performed.

The yields of DOL, solid residue (SR or char), and gas are presented in Table 5.2 and Figure 5.2. As can be seen, the amount of SR obtained increases with increasing temperature. This is reasonable, as increased fragmentation of the lignin macromolecule presents greater opportunity for reactive moieties to recombine and form solid residue/char. As expected, the amount

gas products from the hydroprocessing of OL also increased with increasing temperature. The yield of water, produced as a consequence of hydrodeoxygenation reactions, was obtained simply based on mass difference. As clearly shown in Table 5.2, the formation of water was not very evident at lower temperatures but became more evident at higher temperatures as the more refractive C-O bonds began to break.

Table 5.2 DOL and product yields

Catalyst	Temp. (°C)	DOL (wt.%)	Char (wt.%)	Gas (wt.%)	Water* (wt.%)	Sum (wt.%)
MoRu/ACP	250	98.6 ±2.2	1.2 ±0.4	0.04 ±0.2	0.16	100.0
	300	74.4 ±2.7	25.5 ±0.73	0.30 ±0.03	0.0	100.2
MoRu/AC	250	99.2 ±3.1	1.5 ±0.29	1.8 ±0.08	0.0	102.5
	300	94.7 ±3.6	1.5 ±0.12	6.1 ±0.21	0.0	102.3
	340	68.6 ±1.4	15.7 ±0.73	8.3 ±0.42	7.4	100
MoRu/C	250	98.6 ±1.0	1.9 ±0.22	1.7 ±0.07	0.0	102.2
	300	86 ±2.3	6.4 ±0.48	6.5 ±0.30	1.1	100
	340	58.1 ±2.8	27.7 ±0.87	7.8 ±0.44	6.4	100
Ru/C	250	96.6 ±3.1	3.1 ±0.27	1.1 ±0.09	0.0	100.8
	300	61.7 ±2.8	31.4 ±0.76	5.5 ±0.64	1.4	100
	340	49.8 ±2.4	30.8 ±0.97	15.7 ±0.69	3.7	100
Mo/AC	300	62.0	36.4	2.4	0.0	100.8

Reaction Conditions: 5 g OL:25 g acetone, 0.5 g catalyst, 5 MPa cold hydrogen, 1 h reaction time at temperature

* Values determined by mass difference.

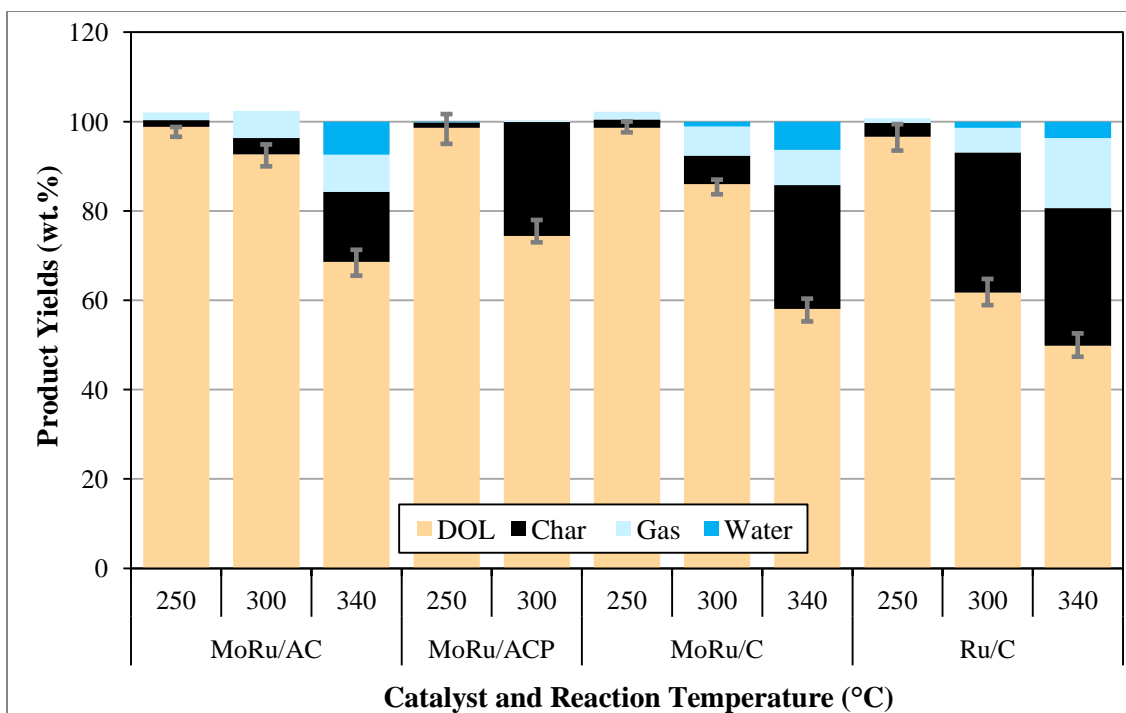


Figure 5.2 Cumulative DOL Product Yields

MoRu/ACP catalyst was not tested at elevated temperature due to the drastically reduced yield of DOL at 300 °C accompanied by a sharp increase in char formation. In addition, the DOL product obtained with MoRu/ACP catalyst at 300 °C was of poor quality: it was a brittle solid, whereas the DOL products with other catalysts at 300 °C were viscous liquids. This difference was confirmed by GPC as will be examined later.

The decrease in DOL yields with increasing temperature is likely due to the deactivation of the catalyst at a higher temperature caused by carbon/coke deposition, leading to drastically decreased surface area of the catalyst. A comparison of the textural properties of the fresh and spent MoRu/AC catalysts is given in Table 5.3. Taking MoRu/AC catalyst as an example, the surface area of the spent catalysts decreases greatly with increasing temperature. This indicates that solid residue produced by condensation reactions at elevated temperatures was deposited on the catalyst surface, deactivating the active sites on the surface and preventing access to active sites in the interior of the catalyst by blocking pores.

Table 5.3 Comparison of textural properties of MoRu/AC catalyst after reaction at different temperatures

Reaction temperature (°C)	BET S. Area (m ² /g)	Tot. Pore Vol. (cm ³)	Vol. of pores <2 nm (cm ³)	Vol. of pores 2-50 nm (cm ³)	Avg. pore dia. (nm)
fresh	875	0.786	0.034	0.442	3.58
250	209	0.275	0.010	0.191	3.63
300	128	0.162	0.004	0.107	3.56
340	14.8	0.019	0.0004	0.008	3.54

More generally, Table 5.4 displays comparison of textural properties of fresh and spent catalysts at 300 °C, from which there seems to exhibit a strong correlation between the DOL yield and the textural properties (e.g., specific surface area and pore volume) of the spent catalysts. The MoRu/AC, which produced the highest yield of DOL, has the largest remaining surface area and pore volume. The surface area of the reference Ru/C catalyst, producing the lowest yields of DOL at 300 °C, was reduced to only 13.6 m²/g. Similarly, the pore volume of this catalyst was also greatly reduced.

Table 5.4 Comparison of textural properties of fresh and spent catalysts at 300 °C

Catalyst and reaction condition	BET S. Area (m ² /g)	Tot. Pore Vol. (cm ³)	Vol. of pores <2 nm (cm ³)	Vol. of pores 2-50 nm (cm ³)	Avg. pore dia. (nm)
MoRu/AC fresh	875	0.786	0.034	0.442	3.58
MoRu/AC 300	158	0.162	0.004	0.107	3.60
Ru/C fresh	893	0.852	0.034	0.507	3.61
Ru/C 300	13.6	0.013	0.001	0.008	3.65
MoRu/C fresh	865	0.826	0.045	0.514	3.62
MoRu/C 300	128	0.151	0.005	0.091	3.56
MoRu/ACP fresh	771	0.704	0.032	0.405	3.67
MoRu/ACP 300	40.4	0.045	0.002	0.024	3.57

The gases produced during the reactions were analyzed by Micro-GC. The volume of the gas produced was accurately determined using a 2.8 L gas cylinder equipped with a pressure

gauge. The product gas compositions are presented in Table 5.5. As expected, the amounts of gaseous product increased with increasing temperature. The most obvious trend is the increase in methane concentration. The formation of methane from lignin hydroprocessing is believed to be due to the decomposition/cleaving of the methoxy linkages in the lignin (Chatterjee, *et al.*, 2013; He *et al.*, 2014) or from methanation of C, CO or CO₂ (e.g. $C + H_2 \rightarrow CH_4$; CO (or CO_2) + $H_2 \rightarrow CH_4 + H_2O$). The amount of CO and CO₂ produced also increased with increasing temperature as can be seen with the reference catalyst, suggesting a greater extent of gasification reactions (e.g. $C + H_2O \rightarrow CO + H_2$; $CO + H_2O \rightarrow H_2 + CO_2$) occurring. Surprisingly, for the MoRu/AC and MoRu/C catalysts, the amount of CO₂ at 340 °C decreased when compared with that at 300 °C. This result is perhaps indicative of increased methanation of CO₂ ($CO_2 + 4 H_2 \rightarrow CH_4 + 2 H_2O$) in the presence of the mixed Mo/Ru catalysts at elevated temperatures as compared to the catalyst composed of only Ru.

Table 5.5 Composition of gaseous products (vol. %) from OL hydroprocessing with different catalysts and at different temperatures

Catalyst	MoRu/ACP		MoRu/AC			MoRu/C			Ru/C		
	250	300	250	300	340	250	300	340	250	300	340
CH ₄	2.0	9.2	4.0	11.7	21.4	4.1	11.2	20.1	3.9	11.3	36.2
CO	0.3	1.0	0.1	0.2	0.3	0.1	0.2	0.4	0.7	2.3	4.0
CO ₂	0.4	7.0	1.4	6.2	1.1	1.0	6.0	1.1	1.0	4.8	9.9
C ₂ H ₄	-	-	-	-	-	-	-	0.001	-	-	0.002
C ₂ H ₆	0.1	1.5	0.3	1.3	2.6	0.3	1.2	2.5	0.1	0.8	2.6
C ₃ H ₈	-	0.3	-	0.1	0.2	-	0.1	0.2	-	-	0.2
Propylene	0.0	-	0.08	0.3	0.5	0.1	0.3	0.4	0.03	0.06	0.1
1,2-Propadiene	-	-	-	-	0.2	-	-	-	-	-	-
Methyl Acetylene	-	0.1	-	-	-	-	0.19	-	-	-	0.16

Quantification of the different gaseous products allowed for determination of the amount of OL that was gasified. Based on the ideal gas law, with known volume, pressure and temperature of the gas, the number of moles of each gas species was calculated. The number of

moles of each carbon species present in the gas was multiplied by the number of carbon atoms in each molecule to determine the total number of moles of carbon present in the gas, and hence the mass of carbon in the gas. The sum of these values was compared to the mass of carbon present in the OL feed (as determined by CHNS analysis) which in turn allowed for the calculation of the amount of OL that was converted into gaseous species, assuming negligible gasification of the carbon support or the solvent during the hydroprocessing process. The results are presented in Table 5.6.

As expected, and in agreement with the composition of the gaseous products (Table 5.5), very little OL was gasified at low temperatures and the amount gasified increased with increased reaction temperature. This was especially evident with the reference catalyst. Ru/C is well known as a gasification catalyst and consequently resulted in greater gasification of the feed, especially at a high temperature (i.e. 340 °C).

Table 5.6 Gasification of OL

Temp. (°C)	MoRu/ACP		MoRu/AC			MoRu/C			Ru/C		
	250	300	250	300	340	250	300	340	250	300	340
mol C in gas	0.003	0.025	0.007	0.025	0.034	0.007	0.024	0.032	0.005	0.023	0.065
mass C in gas	0.041	0.296	0.087	0.303	0.413	0.081	0.289	0.386	0.054	0.277	0.785
% C gasified	1.1	8.3	2.4	8.5	11.5	2.3	8.1	10.8	1.5	7.7	21.9
% OL gasified	0.82	5.92	1.73	6.06	8.25	1.63	5.78	7.72	1.08	5.54	15.70

5.3.3 Hydrogen consumption during OL hydroprocessing

Micro-GC analysis also allowed for the calculation of amount of hydrogen that was consumed during the hydroprocessing operation. The amount of hydrogen introduced into the reactor as determined based on the volume of head space above the reaction mixture and the initial pressure of hydrogen (5 MPa), which was confirmed by Micro-GC analysis of gas sampled prior to reaction and determined to be greater than stoichiometric. Therefore the hydrogenation and hydrodeoxygenation of the OL is not hydrogen-limited.

The hydrogen consumption during hydroprocessing of OL with different catalysts and various temperatures is presented in Figure 5.3. For three of the MoRu catalysts (MoRu/AC,

MoRu/C and MoRu/ACP), ~20 mol/kg OL of hydrogen was consumed regardless of the reaction temperature, implying that the OL hydrogenation/hydrodeoxygenation reactions do not appear to require elevated temperatures and proceed to a constant extent. Surprisingly, the amount of hydrogen consumed in the reactions with the Ru/C catalyst is much lower than with the MoRu catalysts. This is likely due to the fact that Ru/C is a gasification catalyst and could produce hydrogen (Barati *et al.*, 2014), which would balance the hydrogen consumed in the OL hydrogenation/hydrodeoxygenation reactions. The increased consumption at elevated temperature indicates that hydrogen consumption increases relative to production. This is evident in the increased amount of CH₄, CO and CO₂ present in the gas phase.

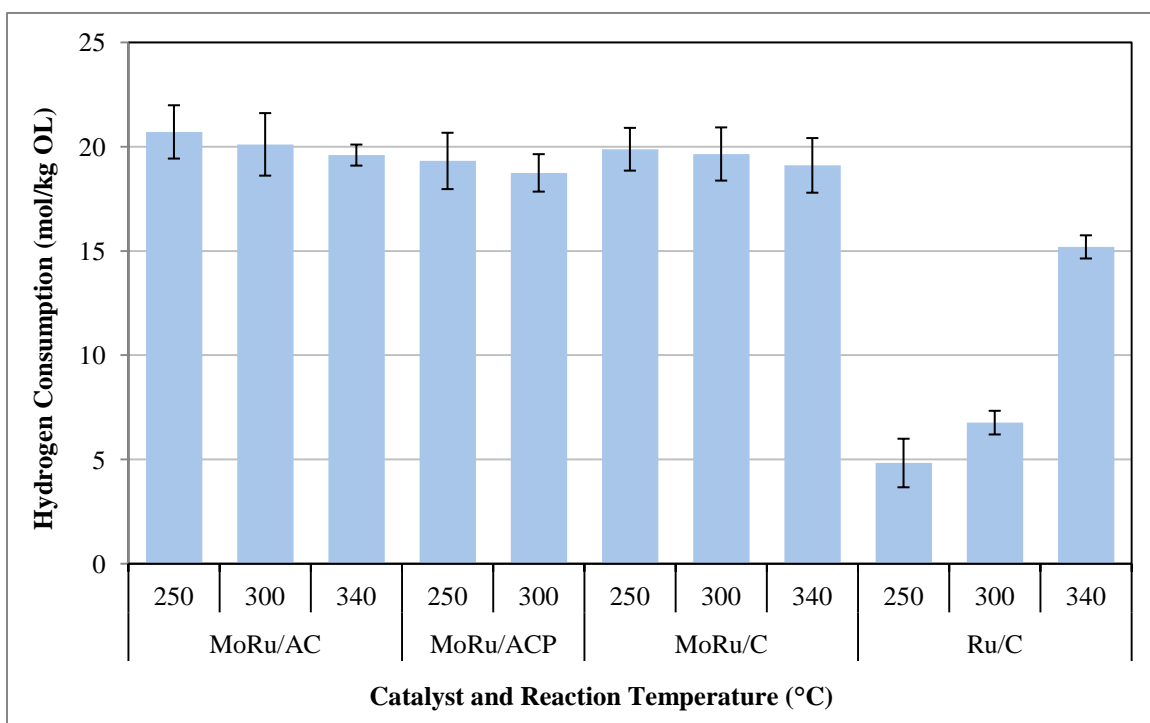


Figure 5.3 Hydrogen consumption during OL hydroprocessing

5.3.4 DOL product characterization

The molecular weights of the DOL products as presented in Table 5.7 and Figures 5.4 and 5.5. As mentioned previously, the DOL obtained with MoRu/ACP catalyst at 250 °C was

solid. The molecular weight of the DOL was actually higher than the OL feed (2,770 vs. 2,600 g/mol). This is consistent with other work that was performed in our group which determined that condensation reactions occur at lower temperatures than do hydrogenation/hydrodeoxygenation reactions. (Chen and Falconer, 1994; Mahmood *et al.*, 2013) This increase in molecular weight was only observed with the MoRu/ACP catalyst, indicating that the addition of phosphorus, which has been seen to decrease char yields in the hydroprocessing of model compounds (DeCanio *et al.*, 1991; Yang *et al.*, 2009) had a detrimental effect in the presence of a more complex feed. It is possible that residual phosphoric acid was present and since acidity is known to promote condensation reactions, this resulted in the increase in molecular weight. The molecular weights of DOL produced at 250 °C with the other catalysts were reduced from 2600 g/mol to ~1900-2100 g/mol. At 300 °C, the DOL products showed a marked decrease in molecular weight. Again, MoRu/ACP performed poorly with a molecular weight ~60% greater than the most effective catalyst. Due to these results, further tests with MoRu/ACP were not performed. The molecular weight of the DOL obtained from the Mo/AC catalyst was equivalent to that of the reference Ru/C catalyst.

Table 5.7 DOL molecular weight as a function of catalyst and reaction temperature

OL Feed (g/mol)	MoRu/ACP		MoRu/AC			MoRu/C			Ru/C			Mo/AC	
	Temp (°C)		Temp (°C)			Temp (°C)			Temp (°C)			Temp (°C)	
	250	300	250	300	340	250	300	340	250	300	340	300	
M_n	750	700	390	580	330	230	620	350	240	700	330	230	300
M_w	2600	2770	1175	1870	730	460	1930	810	516	2110	910	540	907
PDI	3.47	3.96	2.33	3.22	2.21	2.00	3.11	2.31	2.25	3.01	2.91	2.24	3.02

The molecular weights for the DOL products obtained with MoRu catalysts at 300 °C (730 g/mol for MoRu/AC and 810 g/mol for MoRu/C) are lower than the molecular weight obtained with Ru/C or Mo/AC catalysts (910 and 907 g/mol), suggesting a synergistic effect of the presence of the Mo and Ru in depolymerization of OL. Further increasing the reaction temperature to 340 °C resulted in DOL products with a very low M_w (460-540 g/mol) that were much less viscous than the products produced at 300 °C, with the MoRu/AC, MoRu/C and Ru/C catalysts producing liquid DOL that remained fluid at temperatures below 0 °C.

The viscosity of these DOLs at 340 °C was measured to be 29, 31 and 32 cP, respectively.

The GPC curves for the DOL obtained using different catalysts at 300 °C are presented in Figure 5.4. Although the peaks for all curves occur at relatively the same elution volume, the shapes of the curves account for the differences in molecular weight.

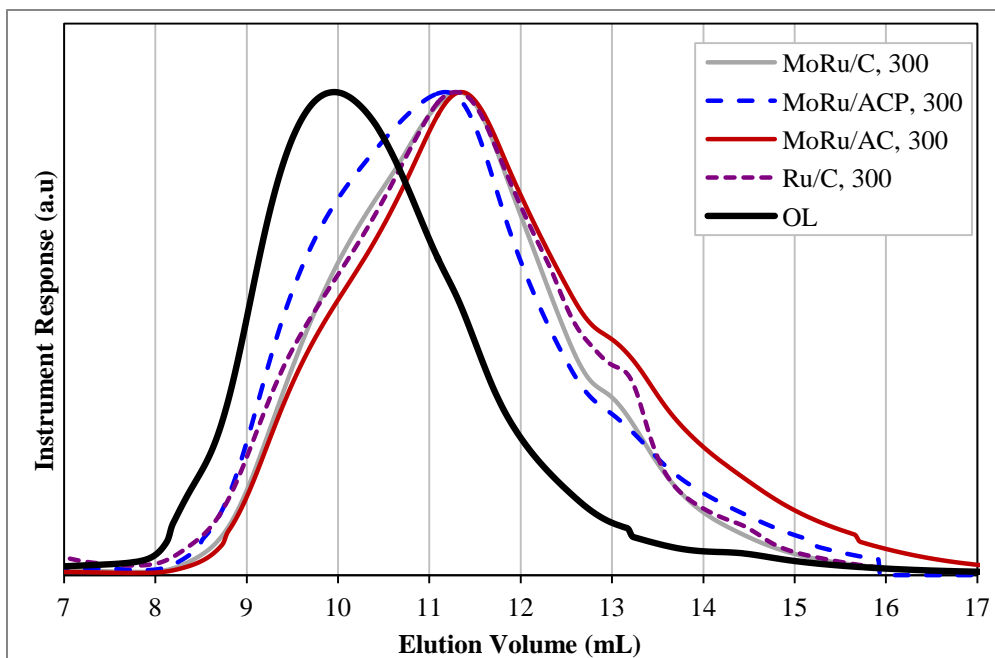


Figure 5.4 GPC curves for DOL obtained at 300 °C using different catalysts

The effect of reaction temperature on DOL molecular weight can be more clearly seen in Figure 5.5. The shift of the GPC peaks to the right at a higher temperature with both MoRu/AC (Figure 5.5a) or Ru/C catalyst (Figure 5.5b) indicates reduced molecular weight.

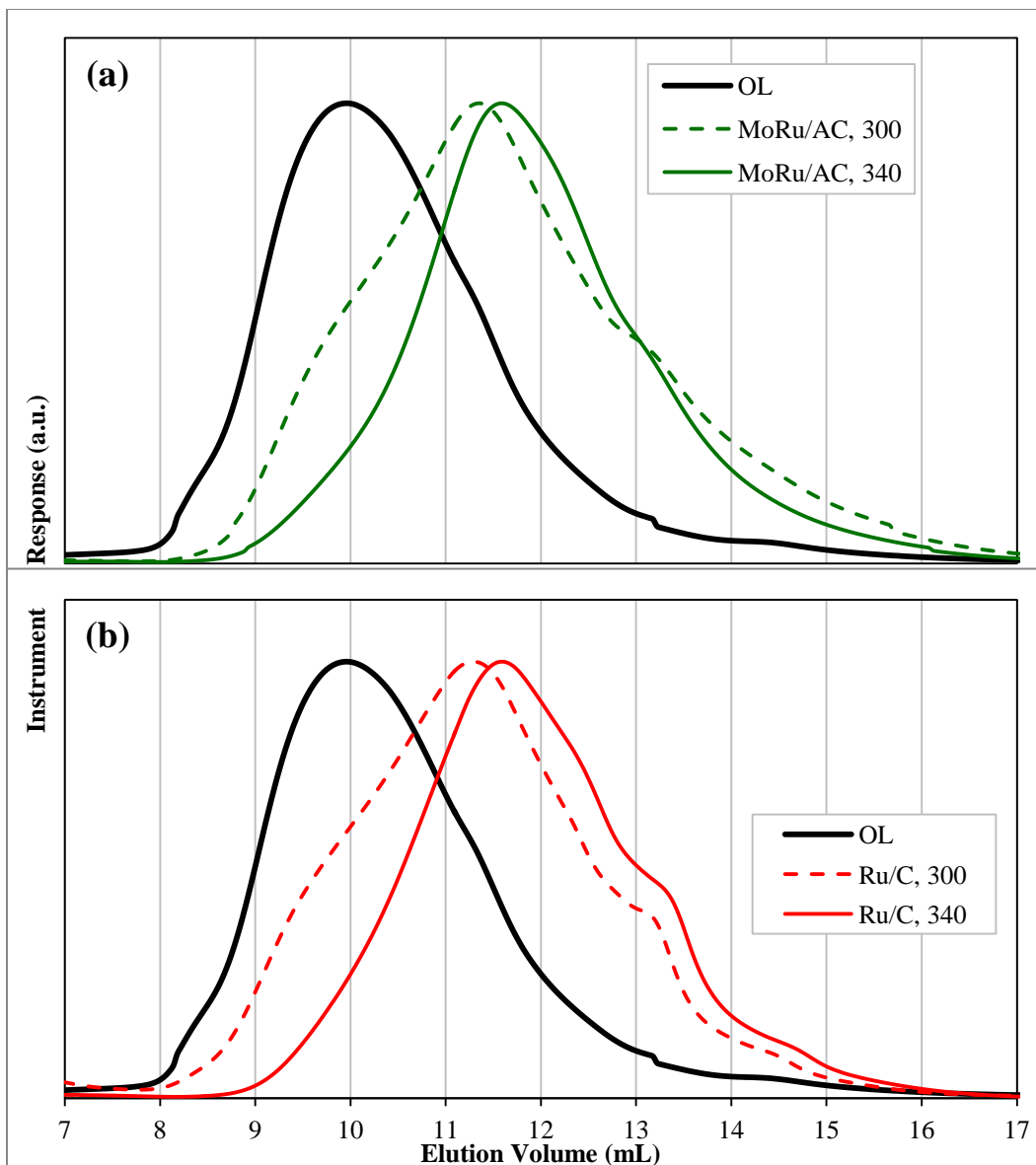


Figure 5.5 GPC curves for DOL obtained at different temperatures using MoRu/AC (a) and Ru/C (b)

5.3.5 Elemental analysis of DOL

Elemental analysis performed on the DOL products showed that catalysts used in this study were moderately effective in the deoxygenation and hydrogenation of the OL feed as seen in Tables 5.8 and 5.9. From the results at 300 °C with different catalysts, the average decrease in O content was ~30%, with MoRu/AC being the most effective catalyst at 34.4% reduction.

The Ru/C catalyst performed poorly and was only able to remove ~25% of the oxygen present. A similar trend was observed with the increase in hydrogen content of the DOL product although the differences between various catalysts were not significant. Again, MoRu/AC performed the best with a ~40% increase in H content.

Table 5.8 Elemental analysis of DOL produced using different catalysts at 300 °C

	C	H	N	S	O*	% increase in H	% decrease in O
OL Feed	64.3	5.60	0.15	0.01	29.9		
MoRu/AC	72.6	7.81	0.01	0.00	19.6	39.5	34.4
Ru/C	69.8	7.66	0.01	0.00	22.5	36.8	24.8
MoRu/C	71.6	7.78	0.02	0.00	20.6	39.0	31.0
MoRu/ACP	71.4	7.68	0.00	0.00	21.0	37.1	30.0
Mo/AC	70.9	7.74	0.13	0.00	21.3	38.3	29.0

The van Krevelen plot for these values is illustrated in Figure 5.6, from which it is shown that DOL products with various catalysts have similar H/C ratio of ~1.3 and O/C ratio of ~0.23, compared with H/C ratio of ~1.05 and O/C ratio of ~0.35 for the OL feed.

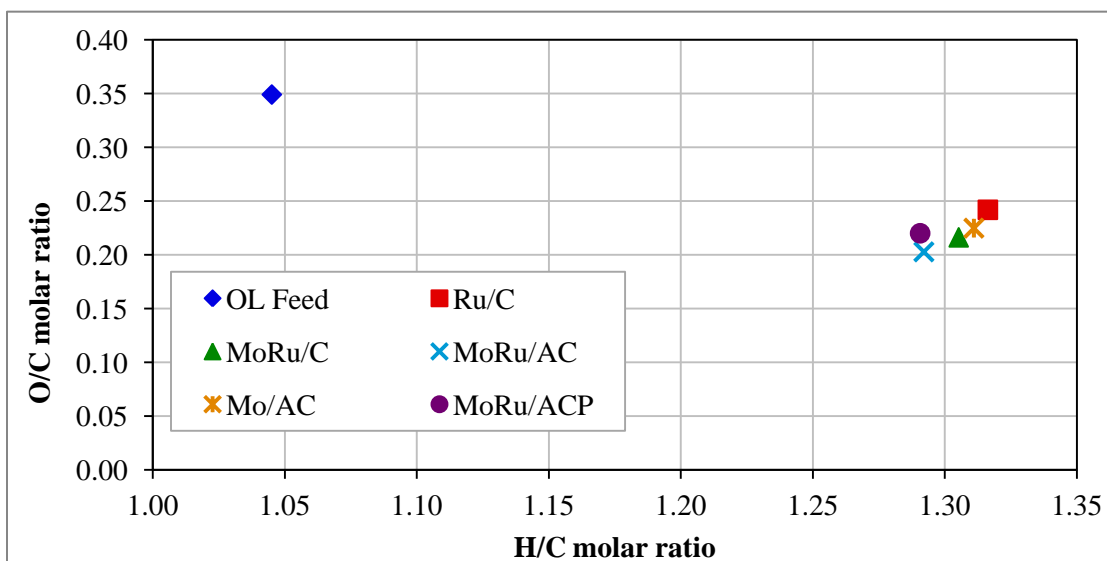


Figure 5.6 Van Krevelen plot for DOL produced by different catalysts at 300 °C

Elemental composition of the DOL products obtained at different temperatures is compared in Table 5.9 and presented graphically in Figure 5.7. As expected, the effectiveness of O removal and H addition increased with increasing temperature. Although the reference Ru/C catalyst and MoRu/AC catalysts performed approximately equally well in terms of hydrogen addition at 300 °C, the Ru/C performed much better at 340 °C, increasing H content by 50% as compared to ~42% (MoRu/AC). However, the MoRu/AC catalyst was more effective in oxygen removal than Ru/C (~38% vs. ~25% at 340 °C).

Table 5.9 Elemental analysis of DOL produced at different temperatures using different catalysts

	OL Feed	MoRu/AC			MoRu/C			Ru/C		
		250	300	340	250	300	340	250	300	340
H	5.60	7.19	7.81	7.93	6.73	7.78	7.93	6.81	7.66	8.41
N	0.15	0.00	0.01	0.01	0.00	0.02	0.00	0.01	0.01	0.02
C	64.30	69.00	72.55	73.44	66.59	71.55	71.75	68.04	69.81	69.13
S	0.01	0.00	0.00	0.01	0.01	0.00	0.01	0.00	0.00	0.01
O*	29.94	23.81	19.63	18.61	26.68	20.65	20.30	25.14	22.53	22.43
% decrease in O		20.5	34.4	37.8	10.9	31.0	32.2	16.0	24.8	25.1
% increase in H		28.3	39.5	41.6	20.1	39.0	41.7	21.6	36.8	50.2

* Value determined by mass difference

The trends in these data can be better presented in a van Krevelen plot as seen in Figure 5.7. At 250 °C (red markers), the MoRu/AC catalyst was the most effective in both hydrogen addition and oxygen removal. Increasing the temperature to 300 °C (green markers) resulted in a further decrease in the O content for all three catalysts, with MoRu/AC being the most effective, but the increase in H content for MoRu/C and Ru/C improved relative to the MoRu/AC. When further increasing the temperature to 340 °C (blue markers), there was only a slight improvement in the removal of O and in H addition for the DOL with MoRu/AC as compared to 300 °C. A similar trend was observed in the O removal for the MoRu/C or Ru/C catalysts. However, the level of hydrogen addition increased markedly with increasing temperature for the Ru/C catalyst, likely owing to the fact that Ru/C is a hydrogenation catalyst. (Kluson and Cerveny, 1995; Genet, 2003) These results indicate that there appears to be a significant fraction of C-O bonds that are refractory to the action of Ru/C catalyst even at

elevated temperatures. The addition of Mo to the Ru catalyst increased the extent of O removal (decreased O/C ratio), but also decreased the extent of hydrogenation (decreased H/C ratio) of the DOL product at higher temperature. Thus, as mentioned previously, there are still a number of oxygen bonds that these catalysts are unable to sever, although the MoRu catalyst is able to break more of these bonds than the Ru catalyst alone. In addition, Mo appears to hinder the hydrogenation efficiency of the Ru catalyst.

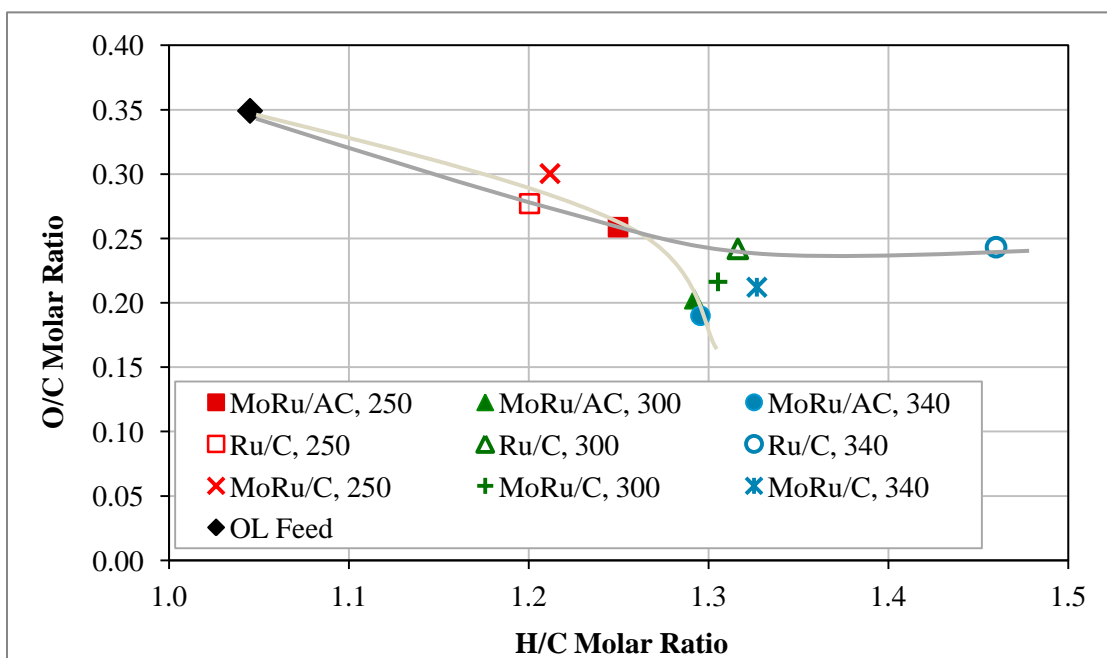


Figure 5.7 Van Krevelen plot for DOL produced by different catalysts at different temperatures

5.3.6 GC/MS analysis of DOL

The volatile components of the DOL products were analyzed by GC-MS. The identified compounds are mainly substituted phenolic compounds and aromatic hydrocarbons as can be seen in Table 5.10. The shaded cells indicate that no compounds were evident at a particular retention time and catalyst/temperature condition. As is evident, fewer volatile compounds are present in DOL products at lower temperatures, which is consistent with the larger M_w for the DOL products at 250°C (Table 5.7). Consistent with the elemental analysis results of the DOL products in which the oxygen content decreased with increased temperature, the com-

pounds detected in the DOL products at 340 °C are generally less-oxygenated than the compounds present in the DOL products at lower temperatures e.g. cresol vs. creosol, 2-methyl-3-ethyl phenol and 2-propyl phenol vs. 4-ethyl-2-methoxy phenol, 2-methoxy-4-propyl phenol and 2,6-dimethoxyphenol. These results are consistent with results reported in the literature, that at elevated temperatures, the ether bonds can be cleaved more easily, forming less-oxygenated compounds (Chakar and Ragauskas, 2004). Although there are differences in the yields and deoxygenation/hydrogenation performance of the MoRu/AC and Ru/C catalysts, as presented previously, the compounds present in the DOL with these catalysts are similar regardless of the reaction temperature and the type of catalyst used. A plot of the GC/MS spectra showing the differences in volatile components with respect to reaction temperature is presented in Figure 5.8

Table 5.10 Comparison of compounds found in DOL with MoRu/AC and Ru/C at different temperatures

RT (min)	250 °C		300 °C		340 °C	
	MoRu/AC	Ru/C	MoRu/AC	Ru/C	MoRu/AC	Ru/C
2.37			Methyl Isobutyl Ketone			
3.22	3-Hexen-2-one			3-Penten-2-one, 4-methyl-		
4.13			2-Pentanone, 4-hydroxy-4-methyl-			
7.86					Phenol	
8.62					Phenol, 2-methyl-	
8.69				Phenol, 2-methoxy-		
9.05				<i>p</i> -Cresol		
9.67			Phenol, 2,4-dimethyl-			
9.84			Creosol			
10.01					Phenol, 3-ethyl-	
10.61			Phenol, 4-ethyl-2-methoxy-			
10.76					Phenol, 2-propyl-	
11.13			1,2-Benzenediol, 3-methoxy-			
11.28			Phenol, 2-methoxy-4-propyl-			
11.62			Phenol, 2,6-dimethoxy-			
11.81				Phenol, 3,4-dimethoxy-		
12.22			1,2,3-Trimethoxybenzene			
12.65					4-Ethylbiphenyl	
12.67	2-Methoxybenzyl alcohol		Benzene, 1,2,3-trimethoxy-5-methyl-		5-tert-Butylpyrogallol	
13.13			4-Propyl-1,1'-diphenyl			

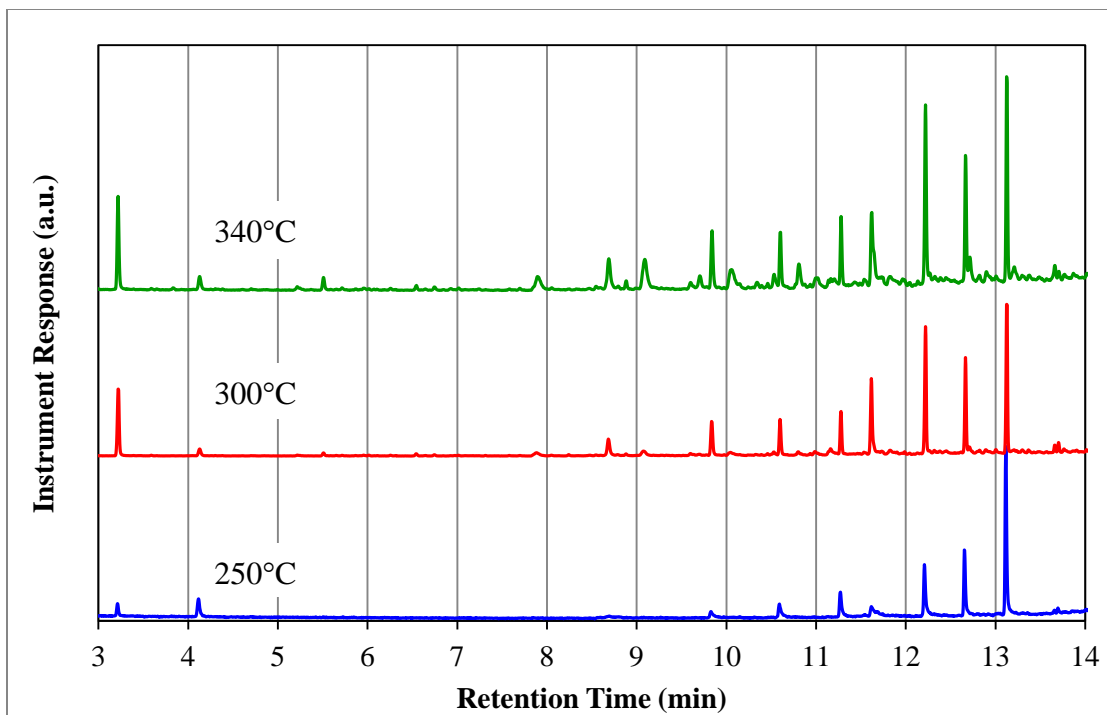


Figure 5.8 GC/MS plots for DOL obtained at 250 °C (bottom), 300 °C (middle) and 340 °C (top)

5.3.7 FTIR analysis of DOL

FTIR analysis was performed on the DOL products to elucidate the changes in functional groups. Figure 5.9 compares the FTIR spectra of OL feed and DOL products obtained with MoRu/AC at different temperatures. Immediately evident is the relative increase in absorption in the OH region ($3,500\text{-}3,000\text{ cm}^{-1}$) which may be attributed to newly formed OH groups resulting from the scission of the ether bonds present in the OL. Also evident is increased -CH_3 bend which could be the result of the cleavage of methylene bridges followed by hydrogenation. The peaks at 1200 , 1100 and 1025 cm^{-1} , indicative of phenolic or acyl C-O and ether C-O bonds, respectively, show that these bonds were relatively unaffected by the hydroprocessing at temperatures $< 300\text{ }^\circ\text{C}$. Similarly, the response of carbonyl bonds at 1700 cm^{-1} decreased in all DOL products suggesting deoxygenation of the OL, in particular at $340\text{ }^\circ\text{C}$. These results combined with the results of the elemental analysis, indicate that deoxygenation of the OL feed increased with increasing temperature.

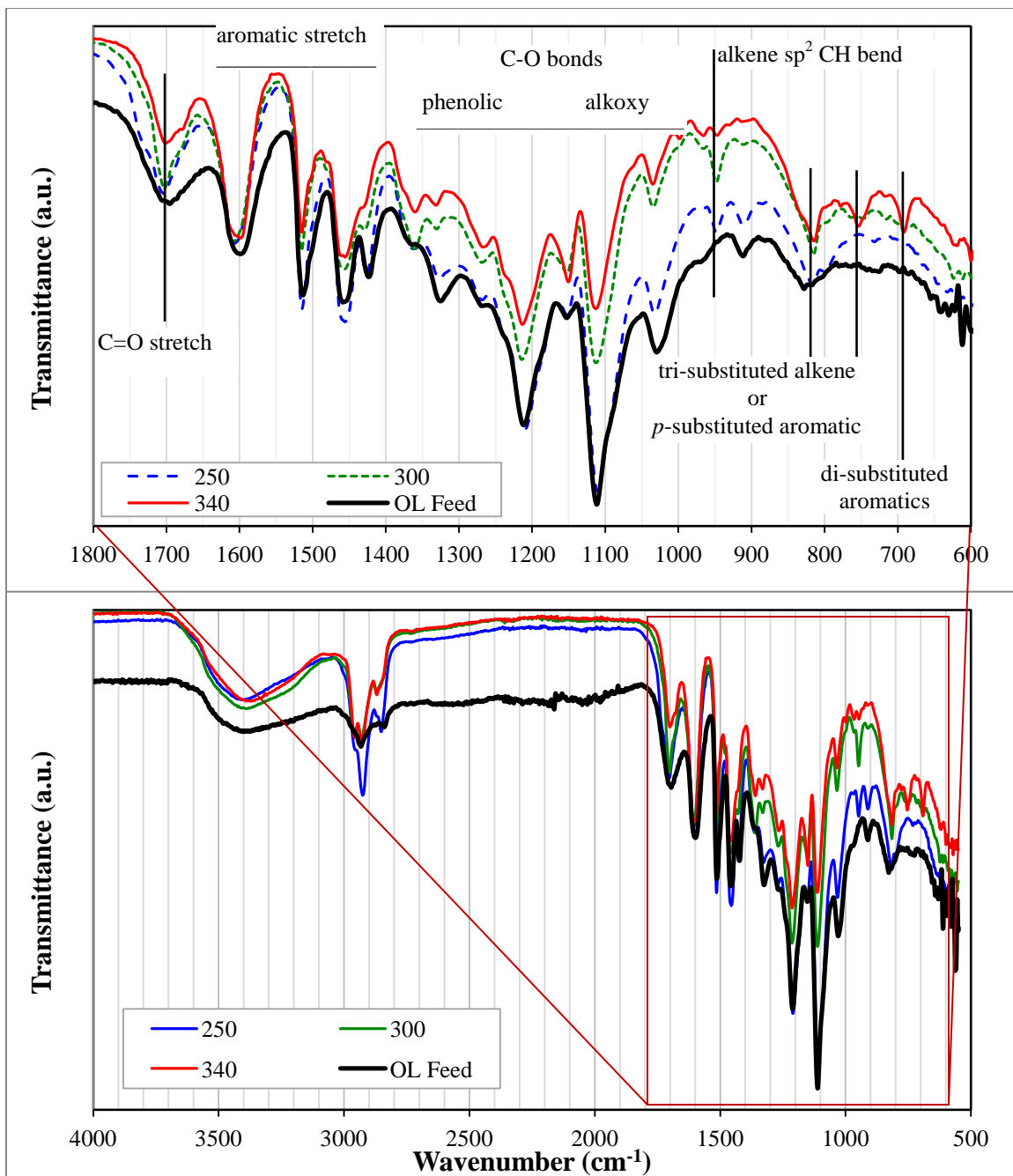


Figure 5.9 FTIR spectra of OL feed and DOL products obtained at different temperatures with MoRu/AC and the expanded fingerprint region (top).

The appearance of the peaks at $\sim 690\text{--}820\text{ cm}^{-1}$ at 340 °C is indicative of mono- and di-substituted aromatic rings, which is consistent with the GC/MS analysis of the DOL at this temperature. It also indicates that the complex bonds between the aromatic rings are being cleaved and that the vacant positions are being hydrogenated.

5.3.8 NMR analysis of DOL

The changes in composition of DOL as a result of hydrogenation/hydrodeoxygenation can also be revealed by H-NMR spectroscopy. Figure 5.10 illustrates the NMR spectra for OL feed (bottom) and MoRu/AC DOL at 300 °C (middle) and 340 °C (top). It should be noted that DOL is not a pure compound, but rather a complex mixture of many related compounds; therefore it is very difficult to assign peaks to a single species with a high degree of certainty. It is more convenient to discuss the changes in broad rather than specific terms. The peak at 2.5 ppm is due to the deuterated dimethylsulfoxide solvent. The three NMR spectra in this Figure reveal a number of interesting changes. The peaks in the range of 9-10 ppm, which correspond to aldehydic C-H bonds, virtually disappear at elevated reaction temperature. This agrees with the decrease in carbonyl bonds observed in the FTIR spectra. The number and intensity of the peaks in the range of 6-8 ppm, corresponding to aromatic C-H bonds, are higher in DOL products than for the OL feed. A similar trend is observed in the range of 0.5-2 ppm which corresponds to the response due to C-H present in the form of sp^3 bonds. The response in this region shifts to the left according to the sequence $CH > CH_2 > CH_3$. As can be seen, at a reaction temperature of 300 °C, the number of $-CH_2$ groups that are present increases compared to the OL feed and as the temperature increases to 340 °C, both the number and intensity of the peaks in this region increase and shift to the right, indicating a greater abundance of $-CH_3$ groups. The signals corresponding to the proton in alcohol $-OH$ groups can appear over a broad range of 1-5 ppm. The peaks present in the range of 2.0-2.5 ppm may be due to $-OH$ groups that form from the cleavage of ether bonds followed by hydrogenation of the oxygen.

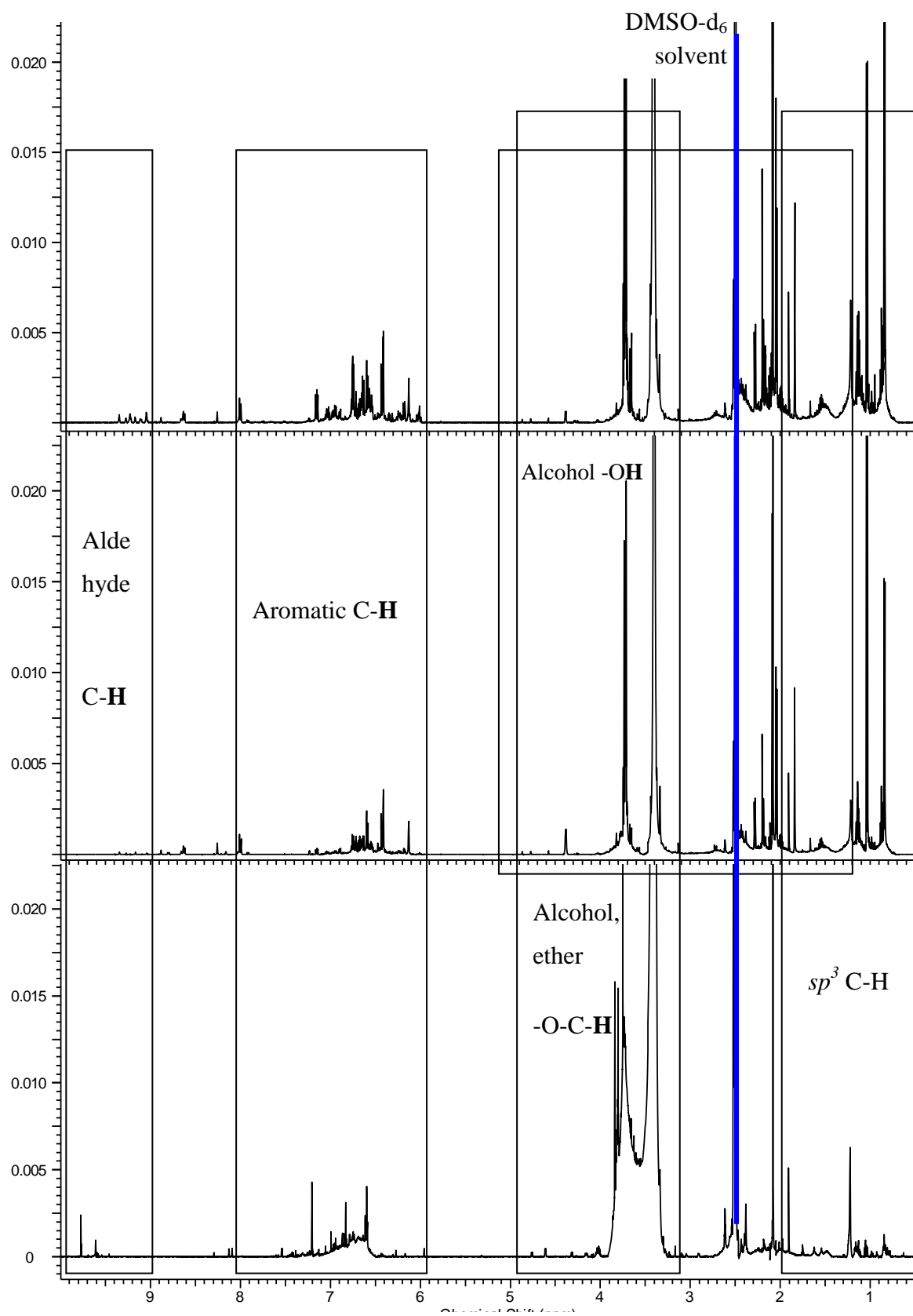


Figure 5.10 NMR spectra for OL feed (bottom) and MoRu/AC DOL at 300 °C (middle) and 340 °C (top)

5.4 Conclusions

All of the catalysts tested were effective in the depolymerization and hydrotreatment of organosolv lignin. However, the presence of phosphorus in the catalyst, which is known to decrease solid residue and improve product yields in previous studies using model compounds, was found to inhibit the depolymerization of the organosolv lignin, perhaps due to residual acidity. The catalysts tested were able to greatly decrease the molecular weight of the OL feed from ~2600 to 460 g/mol at 340°C with the most effective MoRu/AC catalyst. The MoRu/C and reference Ru/C catalysts resulted in DOL with molecular weights of 516 and 540 g/mol at the same condition, respectively. All three of these DOL products obtained from the hydroprocessing at 340°C remained liquid even at temperatures below 0 °C. The oxygen content of DOL obtained with MoRu/AC at 340 °C was found to have decreased by ~38% as compared to ~25% for Ru/C, indicating that the presence of Mo in Ru catalysts has a synergistic effect in oxygen removal. At the same temperature, the hydrogen content of the DOL with Ru/C catalyst was found to increase by ~50% as compared to 42% with the MoRu/AC. The addition of Mo to carbon-supported Ru catalysts therefore produced a more effective catalyst for the reductive depolymerization of OL under hydrogen atmosphere for applications such as fuel additives and intermediates for chemicals and materials. More work needs to be done to develop MoRu catalysts capable of further increasing oxygen removal and maintaining the hydrogenation efficiency of the Ru catalyst.

5.5 References

- Barati M, Babatabar M, Tavasoli A, Dalai AK, Das U. *Fuel Proc. Technol.*, 2014, 123, 140.
- Bui VN, Laurenti D, Delichere P, Geantet C. *Appl. Catal. B: Environ.*, 2011, 101, 246.
- Cateto CA, Barreiro MF, Rodrigues AE, Belgacem MN. *Ind. & Eng. Chem. Research*, 2009, 48, 2583.
- Centeno A, Laurent E, Delmon B. *J. Catal.*, 1995, 154, 288.
- Chakar FS, Ragauskas AJ. *Ind. Crops Prod.*, 2004, 20, 131.
- Chang J, Danuthai T, Dewiyanti S, Wang C, Borgna A. *Chem. Cat. Che.*, 2013, 5, 3041.
- Chatterjee M, Ishizaka T, Suzuki A, Kawanami H. *Chem. Commun.*, 2013, 49, 4567.
- Chen BS, Falconer JL. *J. Catal.*, 1994, 147, 72.
- Decanio EC, Edwards JC, Scalzo TR, Storm DA, Bruno JW. *J. Catal.*, 1991, 132, 498.
- Elliott DC, Hart TR. *Energy Fuels*, 2009, 23, 631.
- Furimsky E, Massoth FE. *Catal. Today*, 1999, 52, 381.
- Genet JP. *Acc. Chem. Res.*, 2003, 12, 908.
- Gutierrez A, Kaila RK, Honkela ML, Siloor R, Krause AOI. *Catal. Today*, 2009, 147, 239.
- He J, Zhao C, Mei D, Lercher JA. *J. Catal.*, 2014, 309, 280.
- Hirose S, Kobayashi M, Kimura H, Hatakeyama H. In: Kennedy JF, Phillips GO, Williams PA, Hatakeyama H. (Eds.), *Recent advances in environmentally compatible polymers*. Woodhead, Cambridge, 2001, 73.
- Jin Y, Ruan X, Cheng X, Lü Q. *Bioresour. Technol.*, 2011, 102, 3581.

Kersten SRA, van Swaaij WPM, Lefferts L, Seshan K. In: Centi G, van Santen RA. (Eds.), *Catalysis for Renewables—From Feedstocks to Energy Production*, Wiley-VCH, Weinheim, 2007, 119.

Kluson P, Cervený L. *Appl. Catal. A: Gen.*, 1995, 128, 13.

Lee CR, Yoon JS, Suh YW, Choi JW, Ha JM, Suh, Park YK. *Catal. Commun.*, 2012, 17, 54.

Li K, Wang R, Chen J. *Energy Fuels*, 2011, 25, 854.

Lin YC, Li CL, Wan HP, Lee HT, Liu CF. *Energy Fuels*, 2011, 25, 890.

Mahmood N, Yuan Z, Schmidt J, Xu C. *Bioresour. Technol.*, 2013, 139, 13.

Moura JS, Souza MOG, Bellido JDA, Assaf EM, Opportus M, Reyes P, do Carmo Rangel M. *Int. J. of Hydrogen Energy*, 2012, 37, 2985.

Prochazkova D, Zamostny P, Bejblova M, Cervený L, Cejka J. *Appl. Catal. A: Gen.*, 2007, 332, 56.

Reddy BM, Khan A. *Catal. Rev.*, 2005, 47, 257.

Romero Y, Richard F, Brunet S. *Appl. Catal. B: Environ.*, 2010, 98, 213.

Rouco AJ, Haller GL. *J. Catal.*, 1981, 72, 246.

Saidi M, Samimi F, Karimipourfard D, Nimmanwudipong T, Gates BC, Rahimpour MR. *Energy Environ. Sci.*, 2014, 7, 103.

Sasaki C, Wanaka M, Takagi H, Tamura S, Asada C, Nakamura Y. *Ind. Crops Prod.*, 2013, 43, 757.

Senol OI, Ryymin E-M, Viljava T-R, Krause AOI. *J. Mol. Catal. A: Chem.*, 2007, 277, 107.

Tejado A, Pena C, Labidi J, Echeverria JM, Mondragon I. *Bioresour. Technol.*, 2007, 98, 1655.

Vázquez G., Antorrena G, González J, Mayor J. *Bioresour. Technol.*, 1995, 51, 187.

Wang M, Leitch M, Xu C. *Eur. Poly. J.*, 2009, 45, 3380.

Wildschut J, Mahfud FH, Venderbosch RH, Heeres HJ. *Ind. Eng. Chem. Res.*, 2009, 48, 10324.

Yang Y, Gilbert A, Xu C. *Appl. Catal. A: Gen.*, 2009, 360, 242.

Yang Y, Ochoa-Hernandez C, O'Shea VA, Pizarro P, Coronado JM, Serrano DP. *Appl. Catal. B: Environ.*, 2014, 45, 91.

Zakzeski J, Bruijninx PC, Jongerius AL, Weckhuysen BM. *Chem. Rev.*, 2010, 110, 3552.

Zauwen MN, Crucq A, Degols L, Lienard G, Frennet A, Mikhalenko N, Grange P. *Catal. Today*, 1989, 5, 237.

Zhao HY, Li D, Bui P, Oyama ST. *Appl. Catal. A: Gen.*, 2011, 391, 305.

Chapter 6

6 Reductive depolymerization of hydrolysis lignin for aromatic chemicals and fuels

6.1 Introduction

As our society starts to focus more and more on environmental and economical sustainability, renewable bio-energy and bio-materials from non-food resources, especially wood, are drawing increasing attention from consumers, governments, industries, and research institutes (Li and Ragauskas, 2012). Agricultural residues such as cornstalks, wheat straw, and corn and nut shells are abundant and renewable, as are forestry residues, from logging and pulp and paper manufacturing. Furthermore, they are produced in mass quantities in many countries, especially in Canada, Russia, China, India and Brazil.

The main components of these residues are cellulose, hemicellulose and lignin (Xu *et al.*, 2012). Lignin represents 30% of all non-fossil organic carbon on Earth and its availability exceeds 300 billion tons (Smolarski, 2012). Thus large quantities of lignin are available from the numerous pulping mills and bio-refinery industries (such as cellulosic ethanol plants). In pulp and paper mills, most of the residues (lignin) is burned directly or discarded. These approaches not only waste precious bioresources, but also cause air pollution.

Recently, transforming agricultural residues into bio-ethanol, functional polysaccharides or bio-gas by means of enzymatic conversion has attracted much attention in many countries (Demirbas *et al.*, 2006; Champagne, 2007). In these conversion processes, most of cellulose is fully utilized, leaving behind hydrolysis lignin (HL) - a by-product from the pre-treatment processes such as in cellulosic ethanol plants, which is mainly utilized as a low-value fuel. But large-scale development of these biomass conversion projects is limited by the high cost of cellulose enzymes and process equipment.(Jin *et al.*, 2011) Finding effective ways to make full use of the lignin present in the process residues for value-added energy and chemical products is critical in improving the process economics.

HL is expected to become more widely available and in large quantities as projects producing cellulosic sugar-based chemicals or ethanol are realized. HL is a solid residue from the en-

zymatic hydrolysis of lignocellulosic biomass and is composed mainly of lignin (~60 wt.% or higher), unreacted cellulose and mono & oligosaccharides.(Sazanov *et al.*, 2010) Compared with sulfur-containing Kraft lignin, the by-product of most wood pulping operations, HL is sulfur-free and therefore a much easier biomass to work with. As a consequence of processing conditions, hydrolysis lignin has undergone extensive acid condensation reactions and therefore is insoluble in water. Extensive research was undertaken in the former Soviet Union to find uses for this material. After extensive modification, the uses developed ranged from soil additives to dispersants, i.e. environment protection, soil quality improvement, crop farming, live stock farming, leather processing, recycling of valuable chemicals by waste water treatment etc. The majority of the hydrolysis lignin was disposed of because the required modifications were either too expensive or the material did not function well enough in application. These are the same problems facing today's researchers who are looking for a use for hydrolysis lignin (Monica, 2005). Thus, further research into the effective and efficient utilization of HL is needed.

Due to its aromatic components, HL is a potential source of phenol and other aromatic compounds. One means of making use of this resource is to depolymerize the macromolecular HL into oligomers and monomers via hydrothermal depolymerization. This will dissociate the lignin and carbohydrates and partially cleave the primary and secondary ether bonds in both lignin and high molecular weight carbohydrates (cellulose and hemicellulose) into lower molecular weight compounds and, depending on the process parameters used, decreased oxygen content.(Xu *et al.*, 2012) As a result, the solid lignocellulosic biomass (e.g. HL) can be converted into a product which can potentially be used as fuel and/or chemicals.

The hydrotreatment of lignin has typically been performed in the presence of sulfided Co- or Ni-promoted Mo catalysts, typically supported on alumina, borrowed from petroleum processing operations.(Senol *et al.*, 2007; Romero *et al.*, 2010; Zakzeski *et al.*, 2010; Saidi *et al.*, 2014) Noble metal catalysts have also been used in the hydroprocessing of lignin and biomass-derived bio-oils. Ru catalysts, in particular, have been shown to be very active in the hydrogenation and hydrodeoxygenation of model compounds (e.g. phenol and guaiacol) as well as bio-oils. (Elliott and Hart, 2009; Gutierrez *et al.*, 2009; Lee *et al.*, 2012; Chang *et al.*, 2013) More recently, reductive depolymerization of lignin in the presence of hydrogen and other late 3d and 4d transition metals (e.g. Fe, Co, Ni, Cu, Ru, Rh, Pd, and Ag) has been pro-

posed.(Cateto *et al.*, 2009; Li *et al.*, 2011; Zhao *et al.*, 2011; Jin, 2014) A review of the literature also reveals that mixed noble metal-transition metal catalysts (e.g. Ru-Co, Rh-Cu and Rh-Ag) have been used, although not in the hydroprocessing of bio-oils.(Rouco and Haller, 1981; Zauwen *et al.*, 1989; Moura *et al.*, 2012)

Although alumina-supported catalysts have been found to be active in HDO, they also increase catalyst deactivation by promoting the formation and deposition of coke on the catalyst surface.(Centeno *et al.*, 1995; Prochazkova *et al.*, 2007; Elliott and Hart, 2009; Wildschutt *et al.*, 2009; Lin *et al.*, 2011) Centeno *et al.* (1995) proposed that it is the weak Lewis acid sites present in the alumina that promote the condensation reactions leading to coke formation.

In order to avoid coke formation, researchers have investigated less-acidic supports such as activated carbon and SiO₂ (Furimsky and Massoth, 1999; Reddy and Khan, 2005; Kersten *et al.*, 2007) as well as other less common supports e.g. ZrO₂ and MgO.(Senol *et al.*, 2007; Bui *et al.*, 2011) Yang *et al.* (2009) found that using carbon-supported catalysts in the hydrotreatment of phenol as a lignin model compound resulted in yields equivalent to those of alumina-supported catalysts, but with lower proportions of oxygenated compounds.

Horáček *et al.* (2012) investigated direct conversion of HL into chemicals in a semi-continuous process using high loadings (C/L = 0.25-1.0) of sulfided NiMo (30% metal loading) and NiMoP (20% metal loading) catalyst supported on γ -Al₂O₃. They produced a binary phase product composed mainly of aromatics, naphthenes and phenols but experienced high gas and char production. More recently, Mahmood *et al.* (2013) performed a comparative study on the depolymerization of HL under acid, basic and neutral conditions employing water, ethanol, and water-ethanol mixtures.

The objective of this study was the reductive depolymerization (i.e. depolymerization and hydrotreatment) of hydrolysis lignin in supercritical acetone and in the presence of MoRu/AC catalyst under a hydrogen atmosphere to obtain low molecular weight compounds. Acetone was chosen as the solvent because both the aromatic components of HL (as evidenced by the solubility of both organosolv and Kraft lignin in acetone) as well as the aliphatic compounds produced are expected to be soluble in acetone. The catalysts used in this

study (Ru/C, Mo/AC and MoRu/AC) have been shown to be effective in the hydroprocessing of organosolv lignin as seen in the author's own research reported in the previous chapter. To the best of the author's knowledge, the depolymerization and hydroprocessing of HL in the presence of a mixed noble/transition metal catalyst has not been reported in the literature.

6.2 Experimental

6.2.1 Materials

The hydrolysis lignin (HL) used in this study, derived from hardwood, was provided by FPInnovations, and contains 56.7 wt.% lignin, 29.8 wt.% carbohydrates, 1.2 wt.% ash and 12.3 wt.% unknowns. The HL's chemical and elemental composition is provided in Table 6.1. The HL was insoluble in THF and several other common organic solvents including ethanol, methanol and acetone etc. due to the cross-linking between cellulose and lignin in the structure. Therefore, it was not possible to determine the weight average molecular weight (M_w) of the HL by GPC-UV. (Yuan *et al.*, 2012) The molecular weight of original HL is believed to be >20,000 g/mol, and its pH was neutral.

Table 6.1 Chemical and elemental composition (d.a.f) of hydrolysis lignin (HL)

Component	Mass fraction (%)
Lignin ¹	56.7
Carbohydrates ¹	29.8
Ash ¹	1.2
Others ³	12.3
Elemental analysis (wt.%) ²	
Carbon	49.8
Hydrogen	7.1
Nitrogen	0.58
Others	42.5

¹ On a dry basis; ² On a dry and ash-free basis (d.a.f.); ³ by difference

The reference catalyst used in this study was Ru/C, a commercial catalyst containing 5 wt.% Ru supported on activated carbon, purchased from Sigma-Aldrich and used as provided. The MoRu/AC (containing 1 wt.% Mo and 5 wt.% Ru) and Mo/AC (containing 10 wt.% Mo) catalysts were prepared in-house by incipient wetness impregnation from activated charcoal (AC), ruthenium (III) nitrosyl nitrate solution ($\text{Ru}(\text{NO})(\text{NO}_3)_3$) and/or ammonium molybdate tetrahydrate ($(\text{NH}_4)_6\text{Mo}_7\text{O}_{24}\cdot 4\text{H}_2\text{O}$). These chemicals and the solvents used (acetone and methanol) were reagent grade and purchased from Sigma-Aldrich.

The MoRu/AC catalyst was prepared by suspending the activated charcoal in a 50% solution of deionized water and methanol. The required volume of the $\text{Ru}(\text{NO})(\text{NO}_3)_3$ solution was added to the suspension. The Mo was added by dissolving the required amount of the Mo compound in some distilled water and adding the solution to the suspension. The suspension was then stirred for 24 h at ambient temperature. The catalyst was then dewatered by rotary evaporation under vacuum at 85 °C. The catalyst was dried overnight in an oven at 105 °C. The catalyst was then loaded into a tube reactor and reduced under a flow of 50 mL/min hydrogen at 500 °C for 4 h. The evolution of a brown gas at a temperature of ~300 °C followed by the evolution of ammonia was evidence of reduction taking place. After cooling to ambient temperature under nitrogen, the catalyst was decanted into a beaker of methanol, also under nitrogen, for passivation. After evaporation of the methanol at 65 °C and cooling back to ambient, the catalyst was stored in an air-tight plastic bag before use. The Mo/AC catalyst was prepared according to the same procedure as the MoRu/AC catalyst.

The textural properties of the catalysts used in this study are presented in Table 6.2 below along with the textural analysis of the AC support, for comparison. The addition of the catalyst metals does not appear to have greatly decreased the surface area except in the case of the Mo/AC catalyst which was loaded with 10 wt.% of the metal. The volume of micropores however was greatly reduced (~85%) due to the deposition of metal(s). In contrast, the volume of mesopores was relatively unchanged indicating that the metal loading blocked the very smallest pores mainly. This is confirmed by the ~15% increase in average pore diameter. This change in pore size and volume did not affect the reaction due to the large size of the component compounds comprising the HL, which are too large to enter the micropore structure of the catalyst.

Table 6.2 Textural properties of the carbon-supported catalysts and activated charcoal support

Catalyst	Metal Loading (wt.%)		BET S. Area (m ² /g)	Tot. Pore Vol. (cm ³)	Vol. of pores <2 nm (cm ³)	Vol. of pores 2-50 nm (cm ³)	Avg. pore dia. (nm)
	Mo	Ru					
Ru/C		5	893	0.852	0.034	0.507	3.61
MoRu/AC	1	5	875	0.786	0.034	0.442	3.58
Mo/AC	10		678	0.656	0.027	0.400	3.62
AC support			963	0.749	0.224	0.405	3.11

6.2.2 Method and apparatus

The hydroprocessing of HL was carried out in a 100 mL stainless-steel autoclave reactor equipped with a stirrer. Unless otherwise noted, the following conditions were used for all of these reactions. In a typical run, the reactor was loaded with 5 g of HL, 0.5 g of catalyst and 25 g of acetone. The reactor was sealed, purged with hydrogen three times and was subsequently pressurized to 5 MPa with hydrogen. The reactor was heated to the reaction temperature while stirring and kept at the desired temperature for 60 min before cooling. Once the reactor had cooled to room temperature, the gaseous products were collected for analysis in a 2.8 L gas cylinder equipped with a pressure gauge. The liquid products and solid residue (SR) were rinsed from the reactor with acetone and the resulting suspension was filtered under vacuum through a pre-weighed Whatman No. 5 filter paper. The SR, catalyst and filter paper were dried at 105 °C for 24 h before weighing. After a GC-MS sample was taken, the acetone was removed from the liquid product by rotary evaporation under vacuum at 45 °C. The yields of DHL and SR were calculated relative to the mass of the HL loaded into the reactor. Each experiment was performed a minimum of two times to reduce the experimental error to $\pm 5\%$.

The relative molecular weights and their distributions of the original and de-polymerized lignin samples were measured with a Waters Breeze GPC-HPLC (gel permeation chromatography-high performance liquid chromatography) instrument (1525 binary pump, UV detector at 270 nm; Waters Styrylgel HR1 column at a column temperature of 40 °C) using THF as the eluant at a flow rate of 1 mL/min. Linear polystyrene standards were used to generate a calibration curve for molecular weight estimation. H1 NMR spectra were obtained on a 500

MHz Unity Inova NMR instrument at room temperature, wherein chloroform-*d* was used as solvent. FT-IR spectra were collected on a Bruker Tensor 37 FTIR spectrophotometer in the range of 550-4000 cm^{-1} with ATR accessory. The volatile components of the DOL and DAL were identified by GC-MS (HP 6890 GC and HP 5972 MS) using a silicon column with temperature programming from an initial temperature of 50 °C for 2 min hold at 10 °C/min to a final temperature of 280 °C for 2 min hold. Elemental analysis of CHNS (carbon, hydrogen, nitrogen, and sulfur) was conducted on a Flash EA 1112 Series elemental Analyzer. The BET surface area analysis was performed on a Micrometrics ASAP 2010 instrument. The samples were degassed at 150 °C until a stable static vacuum of less than 5×10^{-3} Torr was achieved prior to analysis.

6.3 Results and Discussion

Hydrolysis lignin was successfully depolymerized into a liquid bio-oil under the conditions outlined above. All of the bio-oils were clear amber liquids that remained liquid even when stored at temperatures below freezing. The viscosity of the oils was measured and found to be in the range of 14-19 cP at 50 °C.

6.3.1 Effect of catalyst and temperature on HL bio-oil yields

The effects of temperature and catalyst on the yield of HL bio-oil are presented in Figure 6.1. At 200 °C and after 1 h reaction time in the presence of MoRu/AC catalyst, the yield of bio-oil was ~34 wt.% and increased monotonically to ~84 wt.% at 300 °C. Increasing the temperature to 350 °C only increased the yield to ~88 wt.%.

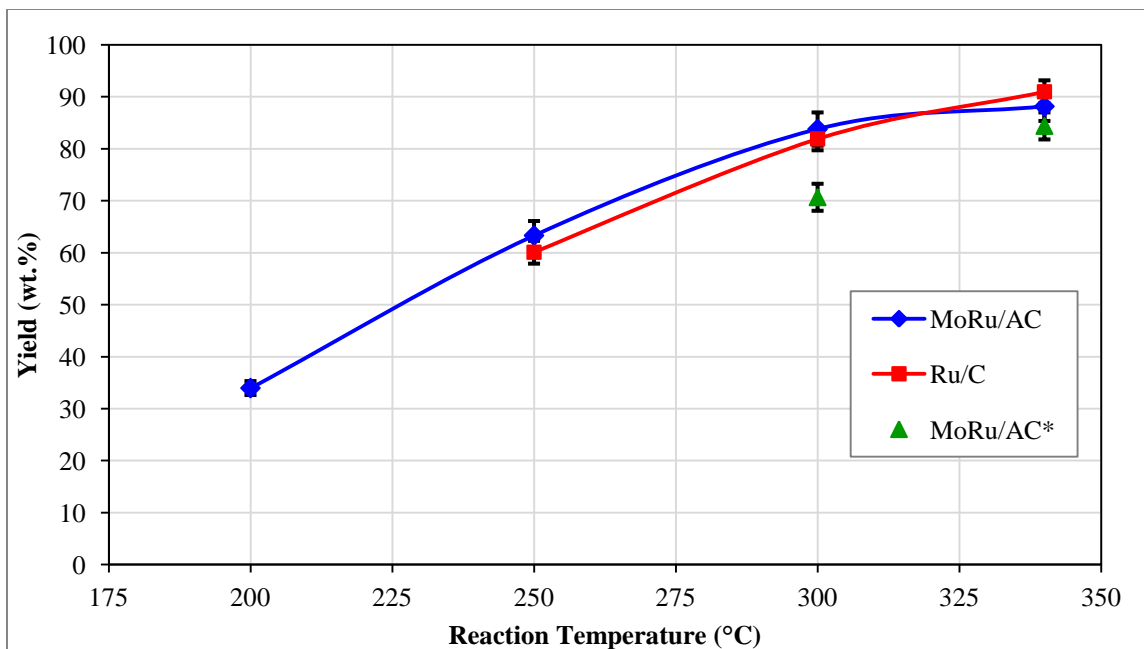


Figure 6.1 HL bio-oil yields as a function of temperature

A similar trend was observed with the Ru/C catalyst indicating that the two catalysts exhibited approximately equivalent activity in HL depolymerization/liquefaction.

The data points in the figure indicated with asterisks were obtained with MoRu/AC catalyst in experiments which were purposely stopped as soon as the reactor reached the reaction temperature. Comparing these results to those obtained at the same reaction temperatures (300 and 340 °C), but after 60 min reaction time at temperature, shows that the extended soak did not increase the yields much, suggesting that the liquefaction of HL occurs rapidly under the conditions tested and that extended reaction times are not required to obtain adequate bio-oil yields. In contrast, in the work of Horáček *et al.* (2012), after 4 h online, they obtained oil yields of ~3-6 wt.% with an aqueous phase comprising 25-30 wt.% of the HL.

The effects of reaction time on bio-oil yields are shown in Figure 6.2. As can be seen, at 300 °C the yield of bio-oil obtained after the ~30 min heating time was ~70 wt.% indicating that the decomposition of HL into bio-oil occurs very rapidly and at lower temperatures.

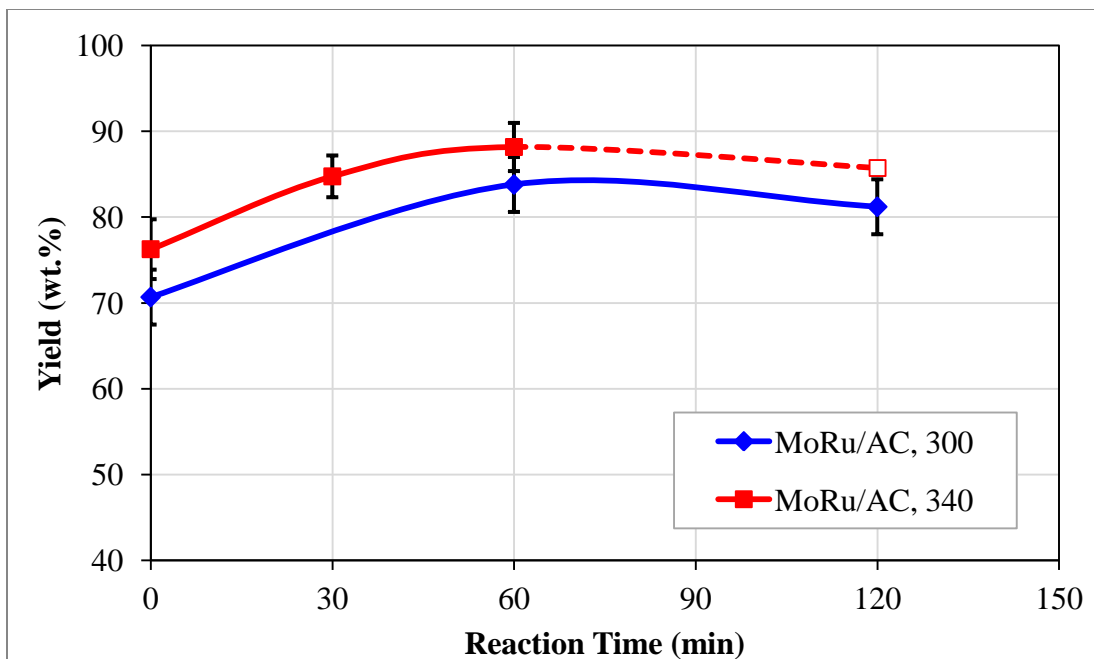


Figure 6.2 HL bio-oil yields as a function of soaking time at reaction temperature

The extended runs at 300 °C did not improve the yield of bio-oil. A similar experiment performed at 340 °C revealed that the yield of HL bio-oil was ~76 wt.% after heating to reaction temperature and had increased to ~85 wt.% after only 30 min reaction time. This yield is very similar to the yield of bio-oil of ~88 wt.% obtained after 60 min. Therefore at elevated temperature, even 60 min reaction time may not be necessary to obtain maximum bio-oil yields. Consistent with the increasing yields of bio-oil, the amount of solid residue remaining after reaction decreased with increased reaction time (5.6, 4.8 and 3.7 wt.% at 300 °C respectively and 3.2, 1.9 and 1.8 wt.% at 340 °C).

In comparison, the conversion of HL by Horáček *et al.* (2012) at 320 °C resulted in an oil yield of ~7 wt.%, aqueous phase yield of ~16 wt.%, gas yield of around 30 wt.%, and a char yield of ~43 wt.%. At elevated temperature (380 °C), the yields of oil and aqueous phase increased to ~11 and ~29 wt.%, respectively, and char yield decreased to ~25 wt.% with gas formation unchanged.

Figure 6.3 shows the cumulative product yields for the hydrothermal liquefaction of HL. As is immediately evident, the yield of solid residue (SR) at lower temperatures (up to 250 °C) is

very high, but decreased drastically with increased temperature and is negligible at 340 °C. It should be noted here that only at 340 °C can the SR actually be considered char. At lower temperatures, the SR was a fluffy mass of unreacted HL mixed with the catalyst as shown in Figure 6.4.

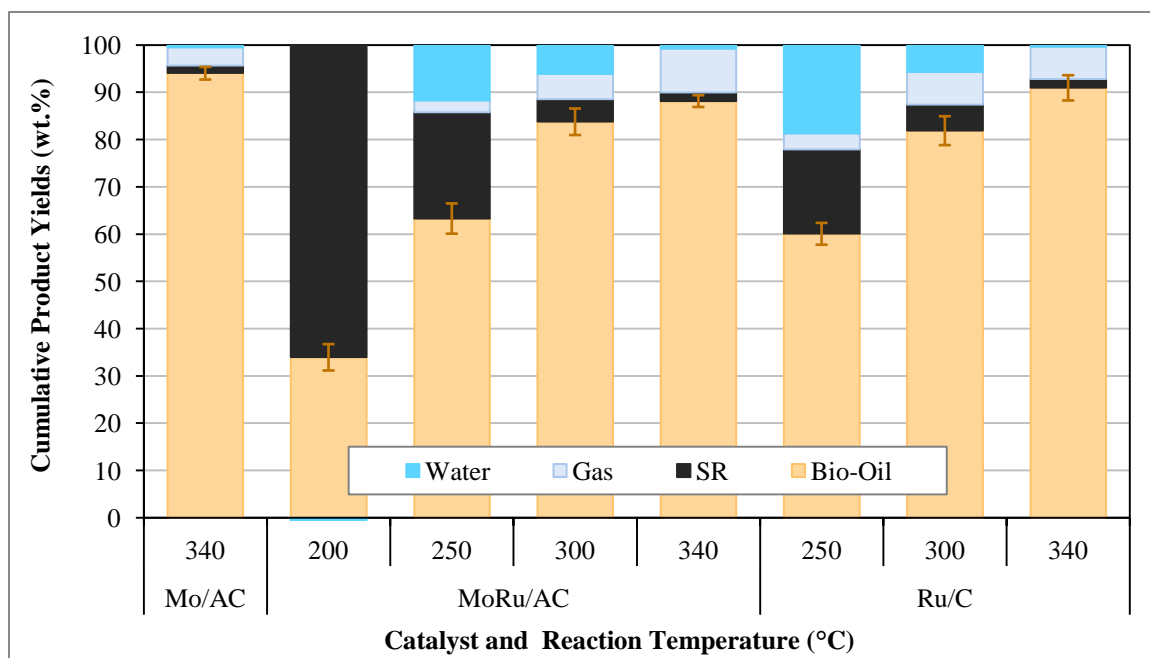


Figure 6.3 Cumulative product yields as a function of reaction temperature and catalyst

Water can be produced by dehydration reactions that occur during HL depolymerization. The yield of water, as presented in Figure 6.3, was calculated by difference. As is also evident, formation of water was negligible at 200 °C, but became substantial (12 and 19 wt.% with MoRu/AC and Ru/C, respectively) at 250 °C, indicating that dehydration reactions were occurring to a great extent at these temperatures. Increasing the reaction temperature further resulted in decreased water content but increased gas yields, which might be due to the reaction of some of the water to produce gaseous compounds at elevated temperatures. As is clearly shown in the figure, at 340°C the water yield was negligible.



Figure 6.4 Photographs of solid residue from HL depolymerization at 200 °C with MoRu/AC catalyst (left) and HL feed before reaction (right)

6.3.2 Elemental analysis of HL bio-oils

Elemental analysis was performed on the bio-oil samples, and the results are presented in Table 6.3 and Figures 6.5-6.7. The results reveal that deoxygenation of the HL is possible at very low temperatures using MoRu/AC catalyst. For instance, the oxygen content of the bio-oil produced with MoRu/AC at 200 °C contained ~14% less O than the HL feed. This was accompanied by a modest 2.2% increase in hydrogen content. Increasing reaction temperature drastically increased the hydrogen content of the bio-oils relative to the feed, owing to enhanced hydrogenation reactions at higher temperatures and, at 340 °C, the H content with MoRu/AC catalyst increased by ~50%. This was accompanied by a large (~44%) decrease in O content. The MoRu/AC catalyst generally performed similarly to the Ru/C reference catalyst. However, at 340 °C, the MoRu/AC catalyst produced a bio-oil with greatly increased hydrogen content (~50% increase compared to ~30% increase in H with Ru/C), suggesting better hydrogenation/hydrodeoxygenation activity of the MoRu/AC. As also shown in Table 6.3, the Mo/AC catalyst exhibited good hydrogenation/hydrodeoxygenation activity as well, leading to an increase in H content by 28.5% at 340 °C. The above results suggest that Mo on its own is an effective hydrogenation/deoxygenation catalyst of HL under the conditions tested. The use of Mo catalysts in HDO of bio-oils has been widely reported by other researchers in literature, but usually in sulfided form. (Meier, *et al.*, 1992; Ryymin *et al.*, 2009) or promoted form. (Yang *et al.*, 2008; Shabtai *et al.*, 1999) The combination of Mo and Ru

exhibits a synergistic effect in this regard, as was also observed in the studies reported in previous chapters. The extent of oxygen removal at 340 °C was approximately the same for all three catalysts, as also clearly displayed by O/C molar ratios of all bio-oils presented in van Krevelen plots in Figures 6.6 and 6.7. The extent of hydrogenation however was largely dependent on the catalyst used, leading to 28.5, 30 and 50% increases in H content with Mo/AC, Ru/C and MoRu/AC, respectively (Table 6.3 and Figure 6.5).

Table 6.3 Elemental composition of HL-derived bio-oils

Sample	Temp.(°C)	% N	% C	% H	%O*	Increase in %H	Decrease in %O
HL Feed		0.58	49.8	7.1	42.5		
MoRu/AC	200	0.46	55.6	7.3	36.6	2.2	13.8
MoRu/AC	250	0.47	58.9	7.6	33.0	7.1	22.3
MoRu/AC	300	0.53	62.5	8.5	28.5	20.0	33.0
MoRu/AC	340	0.54	65.0	10.6	23.9	49.6	43.9
Ru/C	250	0.54	61.6	7.4	30.4	4.7	28.4
Ru/C	300	0.5	63.7	8.7	27.1	22.9	36.2
Ru/C	340	0.5	65.2	9.2	25.0	30.1	41.1
Mo/AC	340	0.47	66.3	9.1	24.1	28.5	43.3

* determined by mass difference

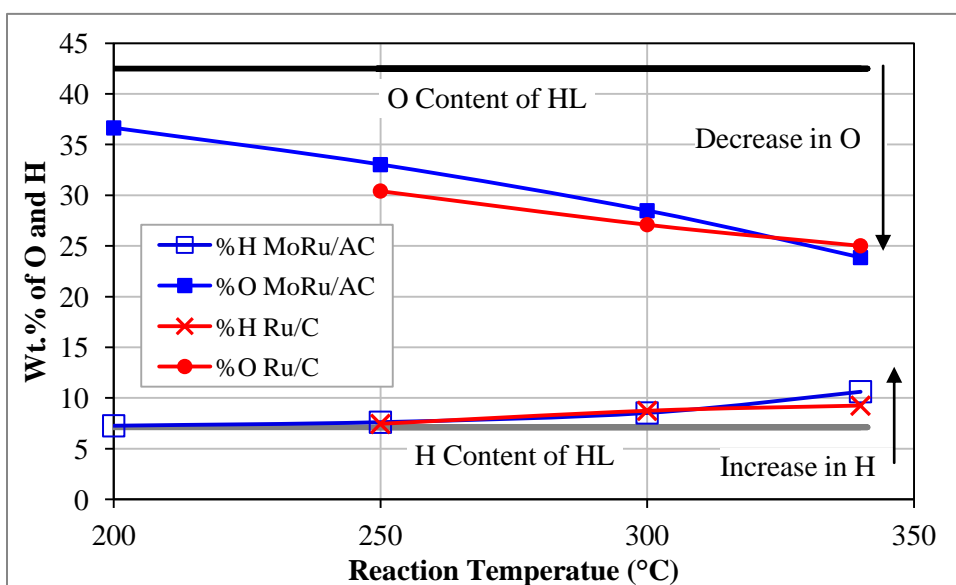


Figure 6.5 Hydrogen and oxygen contents in HL bio-oils produced at different temperatures

Van Krevelen plots, illustrated in Figures 6.6 and 6.7, reveal interesting trends in the performance of the different catalysts in deoxygenation and hydrogenation of the HL at various temperatures. Figure 6.6 compares the O/C and H/C molar ratios for bio-oils obtained at 340 °C using different catalysts. As discussed previously, all three catalysts were approximately equally effective in reducing the O/C ratio of the bio-oils relative to the HL feed. However, the H/C ratios reveal a different trend. The H/C ratios for the Mo/AC actually decreased with respect to the HL feed, suggesting condensation reactions, e.g. dehydration reactions forming condensed products and water (as evidenced in Figure 6.3), as has been reported in many bio-oil HDO studies. (Mortensen *et al.*, 2011; Wildschut, *et al.* 2009) Only the MoRu/AC catalyst exhibited superior activity in the hydrogenation of HL, producing bio-oils with a substantially increased H/C ratio.

Figure 6.7 plots the O/C vs. H/C ratios for bio-oils obtained at different temperatures. In all experiments, the O/C ratios decreased relative to the HL, as expected owing to the HDO effects of the catalysts. However, in most of the experiments (except for those with MoRu/AC catalyst at 340°C), the H/C ratios decreased relative to the feed, even though the hydrogen content of the bio-oils increased, possibly due to condensation reactions, e.g. dehydration reactions forming condensed products and water (as evidenced in Figure 6.3).

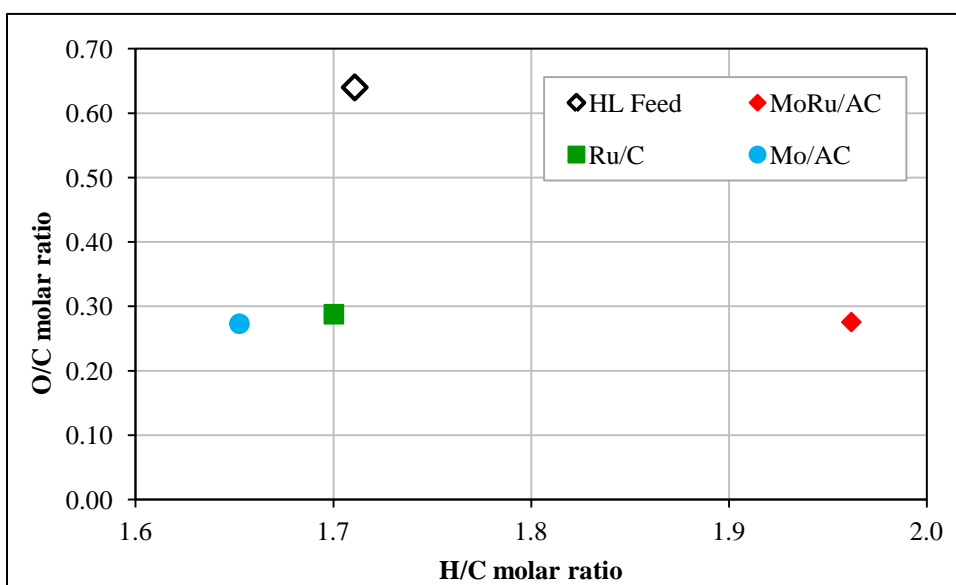


Figure 6.6 van Krevelen plot for HL bio-oils obtained at 340 °C

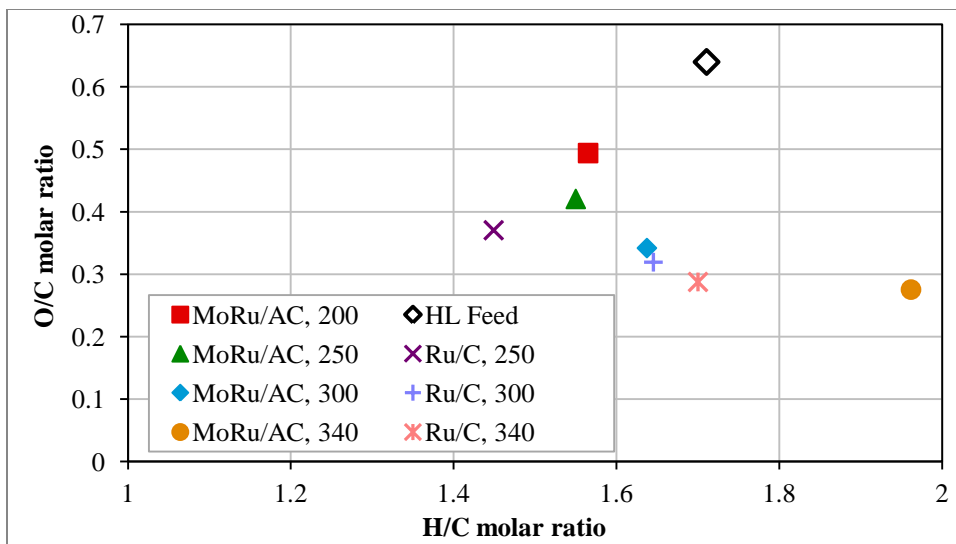


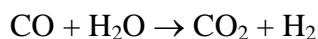
Figure 6.7 van Krevelen plot for HL bio-oils obtained at different temperatures

6.3.3 Formation of gaseous products and hydrogen consumption during HL hydroprocessing

The gaseous products of HL liquefaction were collected and analyzed by GC-TCD. The concentration of the carbonaceous gases produced from experiments with different catalysts and temperatures is shown in Table 6.4. As is evident, and was expected, the amounts of the methane and CO₂ increased with increasing temperature. Moreover, the MoRu/AC catalyst produced over 50% more methane than the reference Ru/C catalyst at 340 °C. This result implies that the Mo acts as a promoter for Ru/AC, enhancing the activity of the catalyst in lignin demethanation and methanation of CO/CO₂ at higher temperatures according to the following reaction:



The above mechanism is likely supported by the variation of CO concentration with temperature which peaked at a reaction temperature of 250 °C and decreased with increasing temperature. The reduction of CO coincides with the increase in CO₂ and corresponding decrease in water, suggesting the occurrence of the water-gas shift reaction:



The work of Horáček *et al.* (2012) showed that they obtained ~30-35 wt.% gasification of the HL. The major gaseous product evolved during their reactions was CO₂ (15-35 wt.% depending on reaction temperature) accompanied by approximately equal amounts of CO and CH₄ (maximum ~8 wt.%).

Table 6.4 Composition of gaseous products (vol.%) from experiments with different catalysts and temperatures

Catalyst	MoRu/AC				Ru/C			Mo/AC
	200	250	300	340	250	300	340	340
Temp. (°C)								
CH ₄	0.21	3.24	7.67	16.1	4.79	10.8	10.8	3.09
CO	0.12	1.45	0.87	0.45	3.96	3.67	1.30	1.49
CO ₂	0.254	3.51	8.57	13.4	2.76	8.43	10.28	3.04
C ₂ H ₄	-	0.001	-	-	0.001	0.001	0.002	0.039
C ₂ H ₆	0.023	0.383	0.95	1.89	0.344	0.866	0.838	0.274
C ₃ H ₈	-	0.046	0.051	0.095	0.032	0.083	0.205	0.15
Propylene	-	0.020	0.061	0.147	0.007	0.035	0.039	0.072
Tot. mol C in gas	0.0007	0.0105	0.0222	0.0396	0.0141	0.0288	0.0285	0.0102
Mass C in gas	0.0087	0.1263	0.2668	0.4753	0.1698	0.3451	0.3421	0.1229
% C gasified	0.3	5.1	10.7	19.1	6.8	13.9	13.7	4.9
% HL gasified	0.17	2.5	5.3	9.5	3.4	6.9	6.8	2.5

Hydrogen consumption was also determined by GC-TCD analysis. The amount of hydrogen initially present before reaction was calculated based on the free headspace in the reactor after it was loaded with the solvent, catalyst and feed. The volume of the headspace was calculated by subtracting the volume of solvent and feed from the total volume of the reactor when empty. Figure 6.8 shows hydrogen consumption in hydroprocessing of with various catalysts and catalysts.

Hydrogen consumed generally increased with increasing temperature but not as much as might be expected given the increasing amount of methane that was observed (due to methanation reactions) (Table 6.4). However, the hydrogen consumption values are all in a narrow range of 15-20 mol/kg, irrespective of temperature and the type of catalyst. A possible reason for this is the generation of hydrogen during the water-gas shift reaction offsetting the hydrogen consumed by hydrogenation and HDO reactions, as discussed previously.

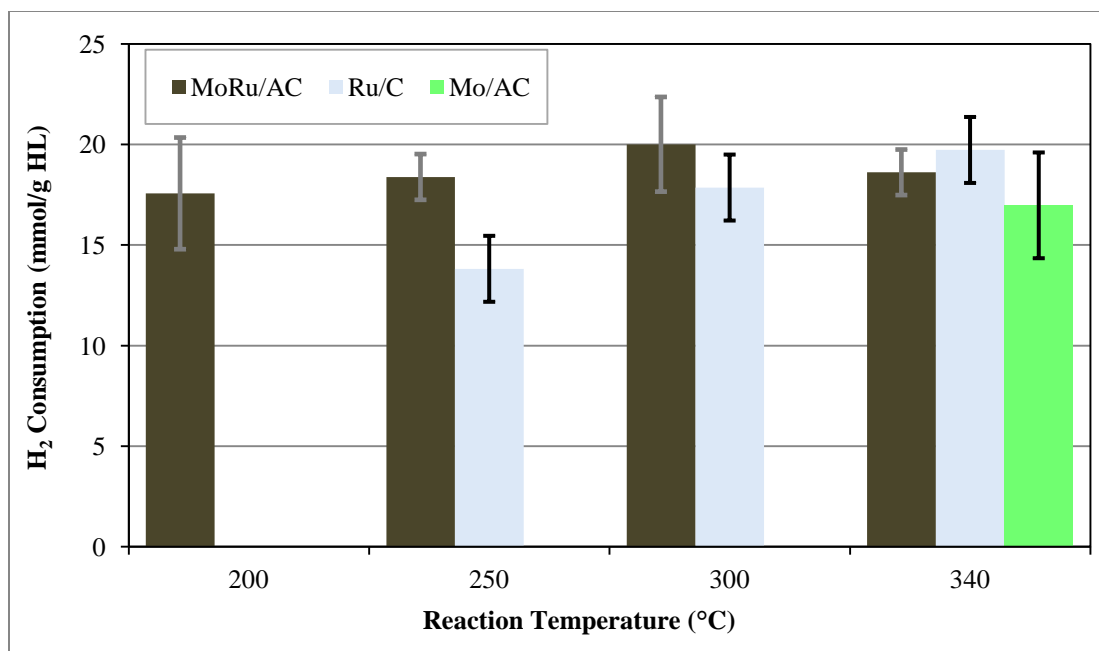


Figure 6.8 HL hydrogen consumption vs. temperature

The hydrogen consumption from the hydroprocessing of HL with MoRu/AC catalyst for extended reaction times is presented in Figure 6.9. An extended reaction time increases hydrogen consumption slightly, but levelled off at approx. 60 min, which follows the similar trends observed in the bio-oil yields vs. reaction time (Figure 6.2). After 60 min, the hydrogen consumption slightly dropped with further increasing time, which might also be accounted for by the trade-off between hydrogen consumed and hydrogen generated due to water-gas shift reaction.

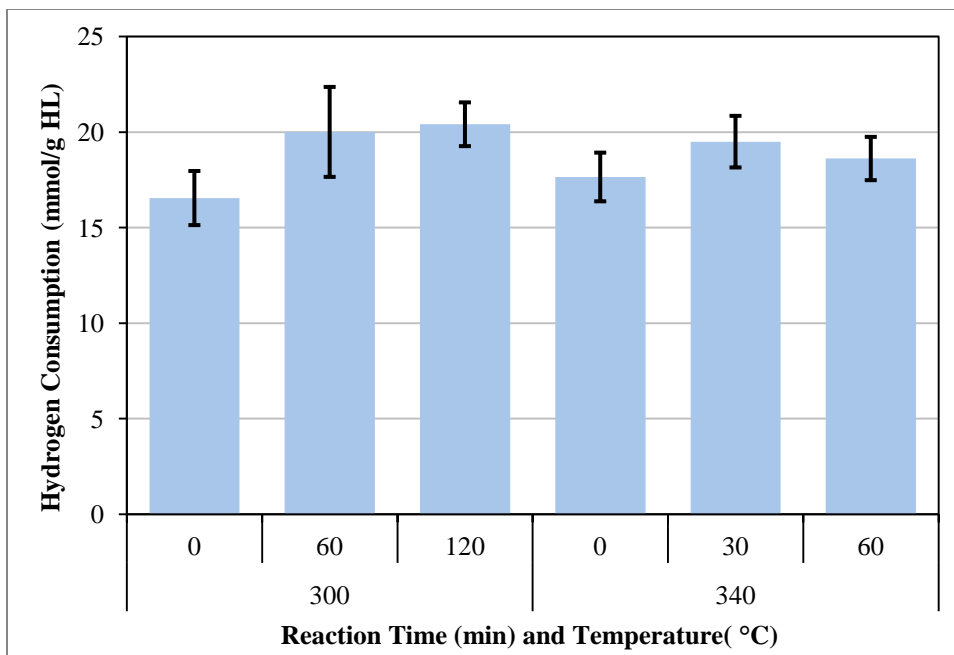


Figure 6.9 Hydrogen consumption vs. reaction time and temperature during hydroprocessing of HL with MoRu/AC catalyst

6.3.4 GPC analysis of HL bio-oils

GPC analysis was performed to determine the molecular weights of the various bio-oils. The GPC curves for bio-oils obtained from the HL hydroprocessing at 340 °C in the presence of different catalysts are presented in Figure 6.10. The plots reveal all of metal catalysts produced bio-oils with approximately the same molecular weights ($M_w \approx 400$ g/mol).

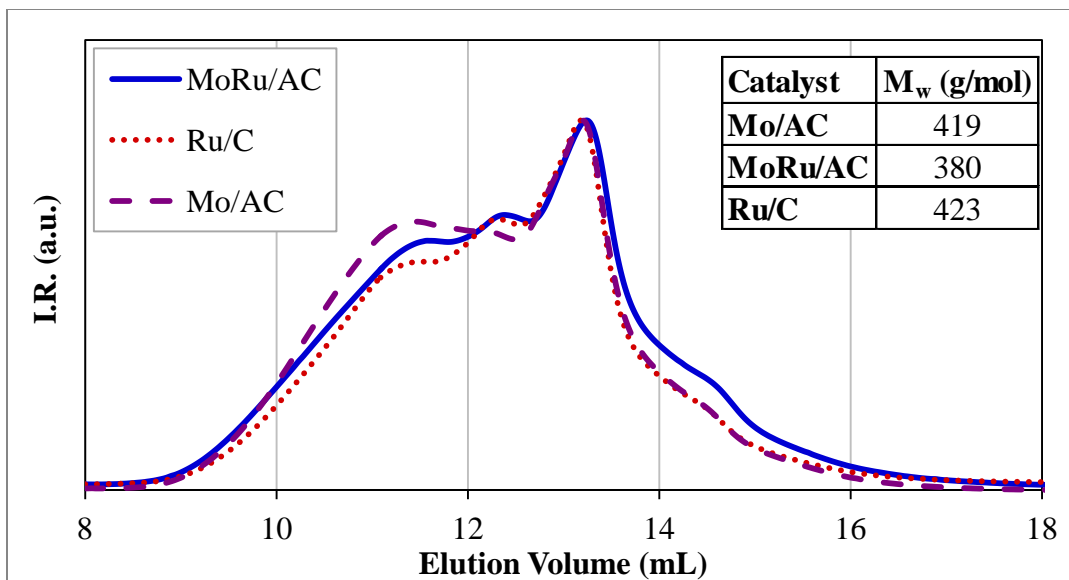


Figure 6.10 GPC curves for bio-oils obtained at 340 °C and different catalysts

The GPC curves in Figure 6.11 show the effect of reaction temperature on the molecular weight of the bio-oils. At 200 °C, the weight-average molecular weight (M_w) of the bio-oil is ~560 g/mol and this value increases to ~630 g/mol at 250 °C.

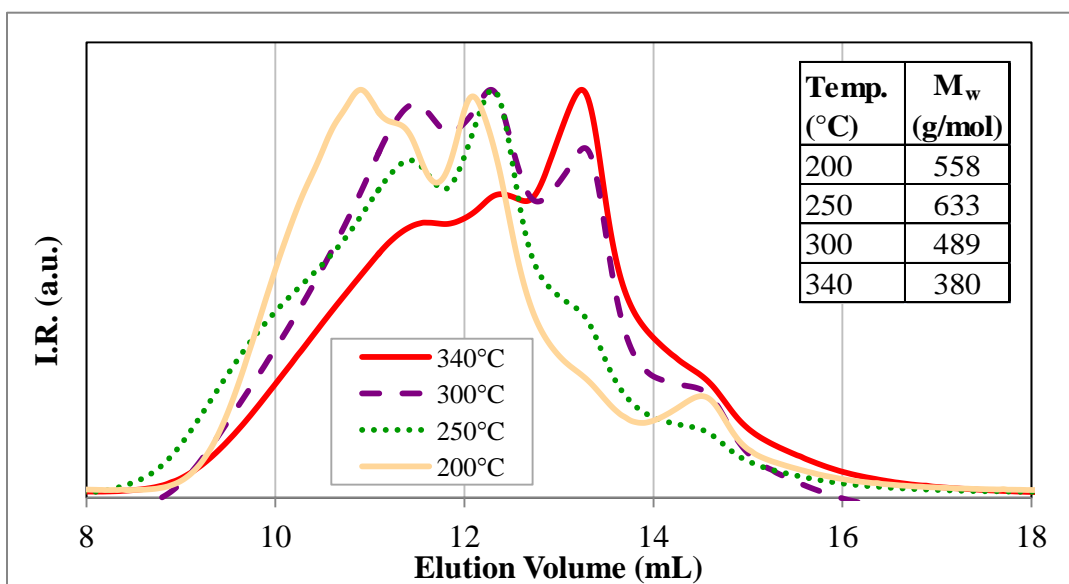


Figure 6.11 GPC curves for HL at different reaction times

This is perhaps due to the scission of bonds that are easily cleaved which released larger components into solution. The lower temperatures did not provide enough energy to break the more resistant bonds as indicated by the lower molecular weights obtained at higher temperatures.

The changes in molecular weight due to reaction time are presented in Table 6.5. As is reasonably expected, the molecular weight of the bio-oils was found to decrease with increased reaction time. At 300 °C and 60 min reaction time, there was sufficient energy and time for the resistant bonds to break, decreasing the molecular weight of the bio-oil. Extended reaction time did not materially affect the molecular weight, indicating that under these conditions, it is not possible to break the remaining bonds and further decrease bio-oil molecular weight.

At higher temperature, 340 °C, sufficient energy was applied to the reaction system to thermodynamically promote depolymerization reactions: Increasing the reaction time resulted in a further decrease in bio-oil molecular weight, reaching 380 g/mol at 60 min reaction time.

Table 6.5 Effects of reaction time and temperature on molecular weight and distribution of bio-oils from the hydroprocessing of HL in the presence of MoRu/AC catalyst

Reaction Temperature (°C)	Reaction Time (min)	M _w (g/mol)	M _n (g/mol)	PDI
300	0	698	233	2.99
	60	489	190	2.58
	120	477	204	2.34
340	0	478	208	2.29
	30	429	177	2.42
	60	380	154	2.47

6.3.5 FTIR analysis of HL bio-oils

FTIR analysis was performed on the HL-derived bio-oils to determine how the functional groups present were affected by the catalysts used as well as the reaction conditions.

Figure 6.12 presents the FTIR spectra of bio-oils obtained after 1 h reaction time at different temperatures using MoRu/AC catalyst. The spectra have been normalized with respect to the aromatic peak at 1620 cm^{-1} . It is immediately evident that the response the -OH region ($3,600\text{-}3,000\text{ cm}^{-1}$) decreases with increasing temperature, indicating that the number of OH bonds present in the bio-oils was greatly reduced when subjected to increased temperatures. A possible reason for this decrease in -OH groups, in addition to the loss of oxygen in the form of CO and CO₂, is hydrodeoxygenation reactions affecting the carbohydrate fraction of the HL which form water as a product.

Looking at the expanded fingerprint region, there is an increase in response around 1700 cm^{-1} , indicative of C=O stretch, which is unexpected given that the reactions took place under a reducing atmosphere. However, given that a large fraction of the HL is composed of carbohydrates, it is possible that the associated OH groups could have reacted to form carbonyl groups. The peak at $\sim 1680\text{ cm}^{-1}$ can be attributed to the formation of quinone structures.

The peaks between 1520 and 1450 cm^{-1} , which are due to aromatic stretch, exhibit a decreased response at elevated temperatures, possibly due to hydrogenation of the aromatic ring.

It is interesting to note that the decrease in response in this region was not uniform. The peak at 1520 cm^{-1} did not decrease until the reaction temperature was $340\text{ }^{\circ}\text{C}$, whereas the peaks at ~ 1460 and 1425 cm^{-1} decreased in step as the temperature increased. This indicates that the amount of energy required to affect the structures responsible for the response at 1520 cm^{-1} was greater than those at the smaller wavenumber. The peak at 1375 cm^{-1} ($\text{sp}^3\text{ CH}$ bend) decreased when the temperature increased from 200 to $250\text{ }^{\circ}\text{C}$ but did not decrease further, indicating that some of the structures with CH_3 bonds were easily cleaved even at lower temperatures.

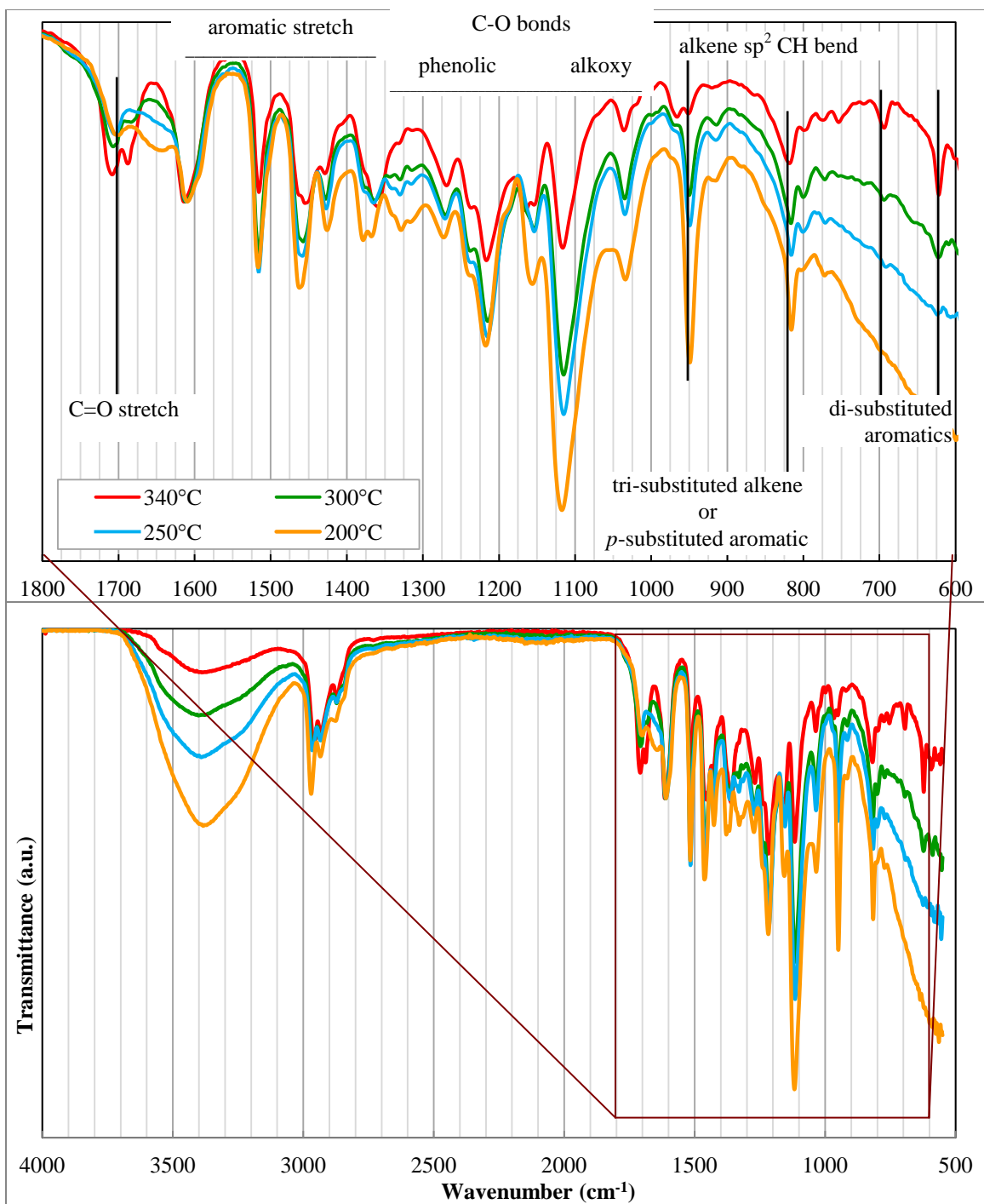


Figure 6.12 Normalized FTIR spectra for HL bio-oils as a function of reaction temperature with the fingerprint region expanded

The response in the range $1325\text{--}1000\text{ cm}^{-1}$, indicative of C-O stretch, shows similar differences in response to temperature. Some of the peaks exhibit incremental decreases as the temperature increased (1325 , 1120 and 1030 cm^{-1}), while others (1220 cm^{-1}) were not af-

ected until 340 °C indicating that these structures required greater energy to break. The appearance of peaks in the range of 690-590 cm^{-1} at 340 °C is indicative of the presence of substituted benzene rings, indicating that higher temperatures were required to cleave the structures bonded to the aromatic rings leaving behind simpler mono- and di-substituted compounds.

The expanded fingerprint region of the FTIR spectra for bio-oils obtained using the different catalysts at 340 °C is presented in Figure 6.13. Similarly, the spectra have been normalized with respect to the aromatic peak at 1620 cm^{-1} . Generally the IR spectra were not affected by type of catalyst and the IR response in the -OH region (3,600-3,000 cm^{-1}) for all catalysts (not shown in this figure) was approximately the same, indicating that the bio-oils obtained from the catalytic depolymerization of HL at a same temperature (340 °C) are all similar in chemical structure.

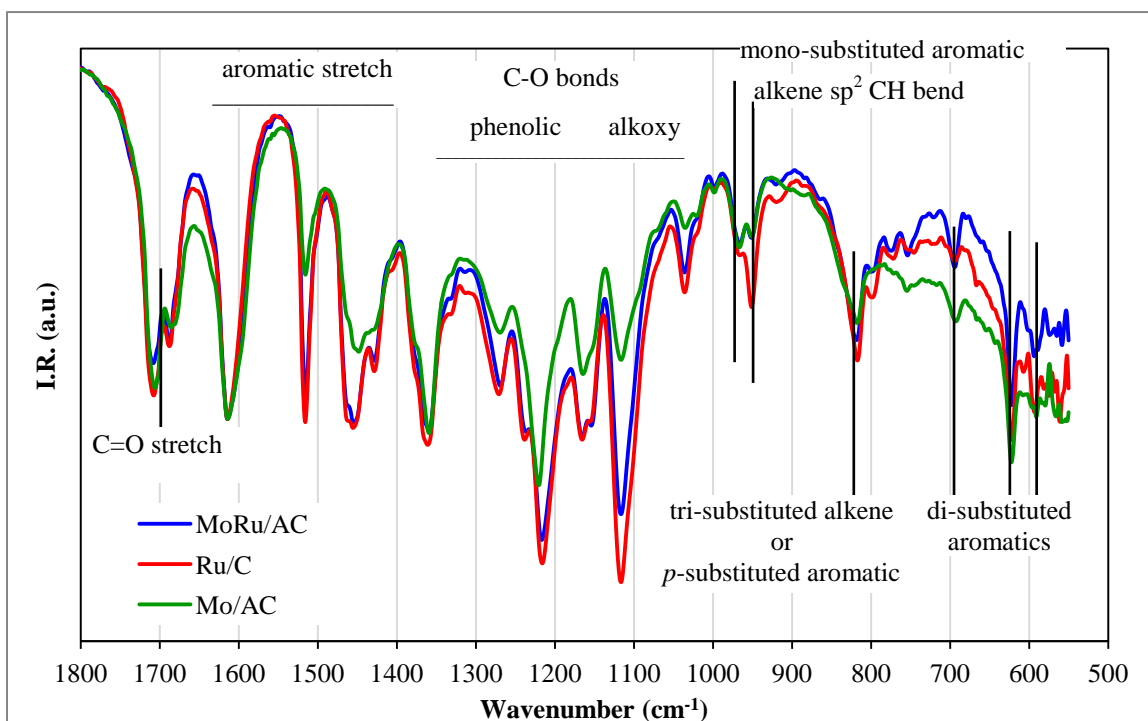


Figure 6.13 Normalized FTIR spectra (expanded fingerprint region) for HL-derived bio-oils obtained at 340 °C with different catalysts

6.3.6 GC/MS analysis of HL bio-oils

The analysis of HL-derived bio-oil by GC/MS elucidated the volatile compounds present in the bio-oil. Peaks with small areas and low confidence were omitted from the analysis. Figure 6.14 and Table 6.6 present the GC chromatograms and composition of the bio-oils obtained at 340 °C for 1 h reaction with different catalysts. Again, all oils at the same temperature although obtained with different catalysts have similar composition, as evidenced previously by the FTIR analysis.

As shown in Table 6.6, the first few compounds that eluted are ketones that can form from the dimerization of the acetone solvent as well as decomposition of the hydrocarbon component of HL. As expected, compounds that were identified by GC/MS are primarily phenolic compounds derived from lignin, indicating that de-polymerization/de-gradation of the lignin present in the HL was readily achieved at 340°C. Note that the shaded cells indicate that no compounds were evident at a particular retention time and catalyst/temperature condition.

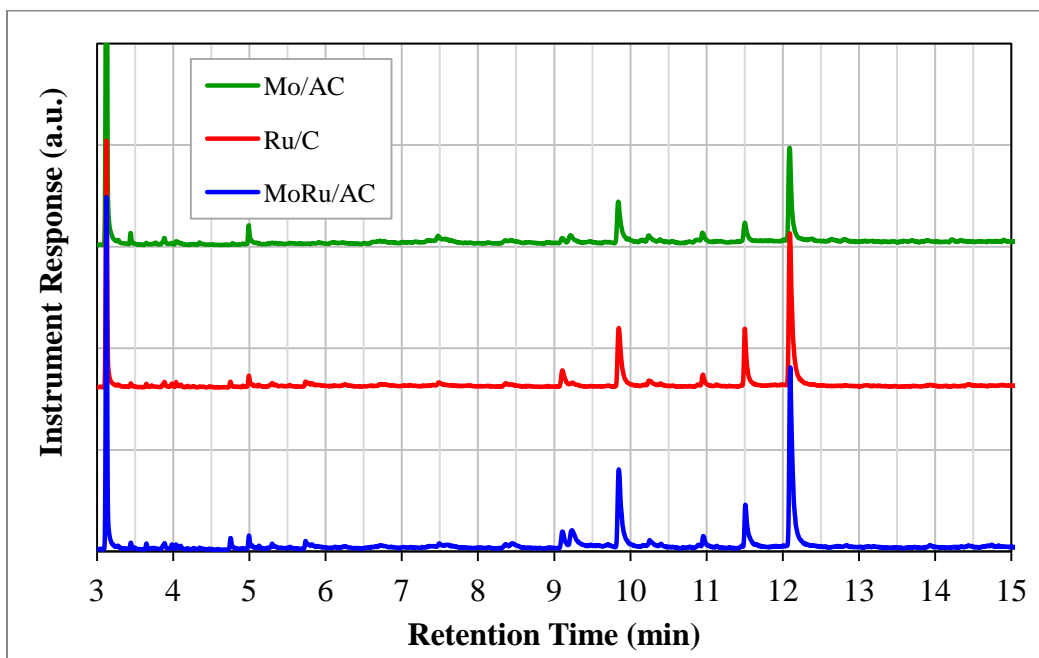


Figure 6.14 GC/MS plots for HL bio-oils produced at 340 °C with different catalysts

Table 6.6 Composition of HL bio-oils produced at 340 °C with different catalysts

RT (min)	Catalyst		
	MoRu/AC	Mo/AC	Ru/C
3.1	3-Penten-2-one, 4-methyl-/3-Hexen-2-one		
3.4	Cyclopentanone	2-Cyclohexen-1-one, 3,5-dimethyl-	Cyclopentanone
3.6	2-Hexanone, 4-methyl-	Cyclopentanone	2-Hexanone, 5-methyl-
4.0	Cyclopentanone, 2-methyl-		
5.0	Mesitylene/Benzene, 1,2,4-trimethyl-		
7.5	2-Cyclohexen-1-one, 4,5-dimethyl-/	2-Cyclohexen-1-one, 3,6-dimethyl-6-(1-methylethyl)-	2,5,5-Trimethylcyclohex-2-enone
8.3	Creosol		
8.4	Phenol, 3-ethyl-	Phenol, 3,5-dimethyl-	
9.1	Phenol, 4-ethyl-2-methoxy-		
9.2	Phenol, 2-propyl-	Phenol, 3-propyl-	
9.9	Phenol, 2-methoxy-4-propyl-		
10.3	Phenol, 2,6-dimethoxy-		
11.0	1,2,4-Trimethoxybenzene		
11.5	1,1'-Biphenyl, 2-ethyl-	5-tert-Butylpyrogallol	
12.1	4-Propyl-1,1'-diphenyl		

The composition of the HL-derived bio-oil obtained after 1 h reaction with MoRu/AC catalyst at different temperatures was analyzed by GC/MS, and the results are presented in Figure 6.15 and Table 6.7. The results show that increasing reaction temperature results in an increase in the variety of compounds present in the bio-oils, as is expected, and that the abundance of the compounds detected (mainly phenolics) depended strongly on temperature. At lower temperatures, these compounds are more oxygenated and even contain double bonds e.g. 2,6-dimethoxy-4-(2-propenyl)-phenol. At increased temperatures, the compounds containing double bonds are reduced while alkyl-substituted phenolic compounds increase and some completely deoxygenated aromatics e.g. 2-ethyl-1,1'-biphenyl form.

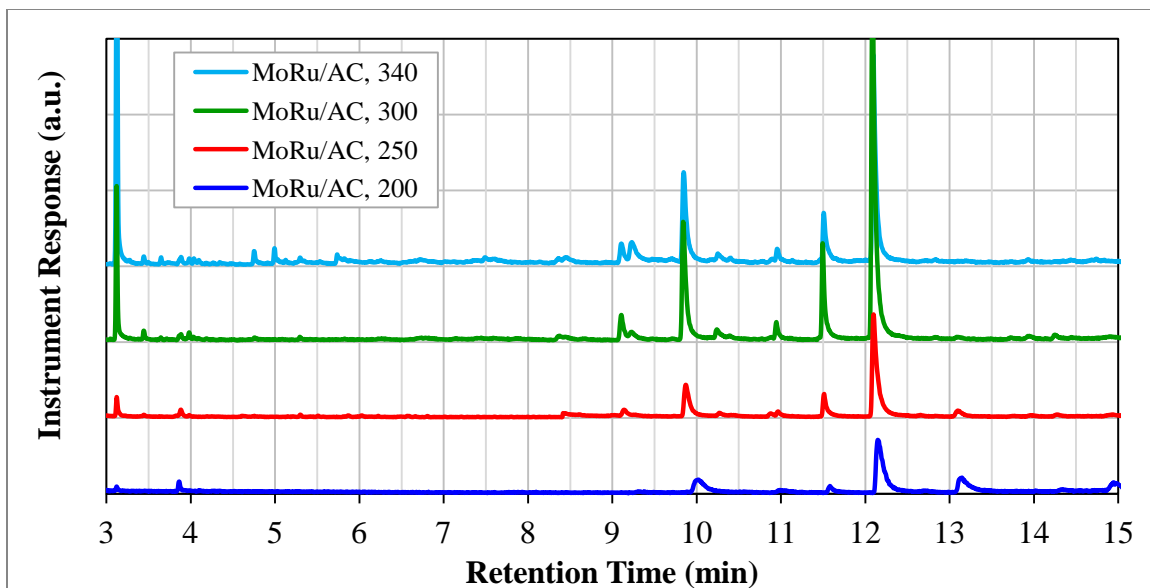


Figure 6.15 GC/MS plots for HL bio-oils produced with MoRu/AC catalyst at different temperatures

Table 6.7 Composition of HL bio-oils produced with MoRu/AC catalyst at different temperatures

RT (min)	Reaction Temperature (°C)			
	200	250	300	340
3.1		2-Pentene, 3,4-dimethyl-		3-Penten-2-one, 4-methyl-
3.4				Cyclopentanone
3.6				2-Hexanone, 4-methyl-
3.9		2-Pentanone, 4-hydroxy-4-methyl-		Cyclopentanone, 2-methyl-
5.0				Mesitylene
7.5				2-Cyclohexen-1-one, 4,5-dimethyl-
8.4				Creosol
8.5				Phenol, 3-ethyl-
9.1			Phenol, 4-ethyl-2-methoxy-	
9.2				Phenol, 2-propyl-
9.9		Phenol, 2-methoxy-4-propyl-		
10.3			Phenol, 2,6-dimethoxy-	
11.0			1,2,4-Trimethoxybenzene	
11.5	Benzene, 1,2,3-trimethoxy-5-methyl-	5-tert-Butylpyrogallol		1,1'-Biphenyl, 2-ethyl-
12.1	Benzaldehyde, 4-[[4-(acetyloxy)-3,5-dimethoxyphenyl]methoxy]-3-methoxy-		4-Propyl-1,1'-diphenyl	
13.1	Phenol, 2,6-dimethoxy-4-(2-propenyl)-			

The HL-derived bio-oils obtained at 340 °C after different lengths of reaction time were also analyzed, although the results are not presented here. As shown previously, the compounds in all of the oils are largely phenolics. Similar to what observed with increasing temperature, increasing reaction time allowed for the hydrogenation of the double bonds present in the phenolics. Similar results were observed for bio-oils obtained with extended reaction times at 300 °C.

6.3.7 NMR analysis of HL-derived bio-oils

NMR analysis was performed to help elucidate the changes that occurred during reaction and NMR spectra of HL bio-oils after 1 h reaction using MoRu/AC at 200 °C and 340 °C are illustrated in Figure 6.16. Several differences are evident between the two spectra shown in this Figure. In the oil obtained at a higher temperature, there is a decrease in intensity in the region of 5-3.3 ppm which corresponds to protons associated with ether bonds, accompanied by a corresponding increase in intensity in the region of 2.6-1.5 ppm, corresponding to the hydroxyl proton. As is commonly agreed upon, ether bonds can be cleaved readily by H₂ scission during the hydroprocessing operation (Lin *et al.*, 2001; Ryymin *et al.*, 2009). If the ether –O– is capped with hydrogen, an alcohol is produced. As is seen in the Figure, the peak at ~1.2 ppm decreases and the peak at 0.9 ppm increases. This indicates that the abundance of CH₂ moieties in the bio-oils decreases with increased temperature, accompanied by more CH₃ groups, as would be expected as ether and other functional groups are cleaved and are hydrogenated.

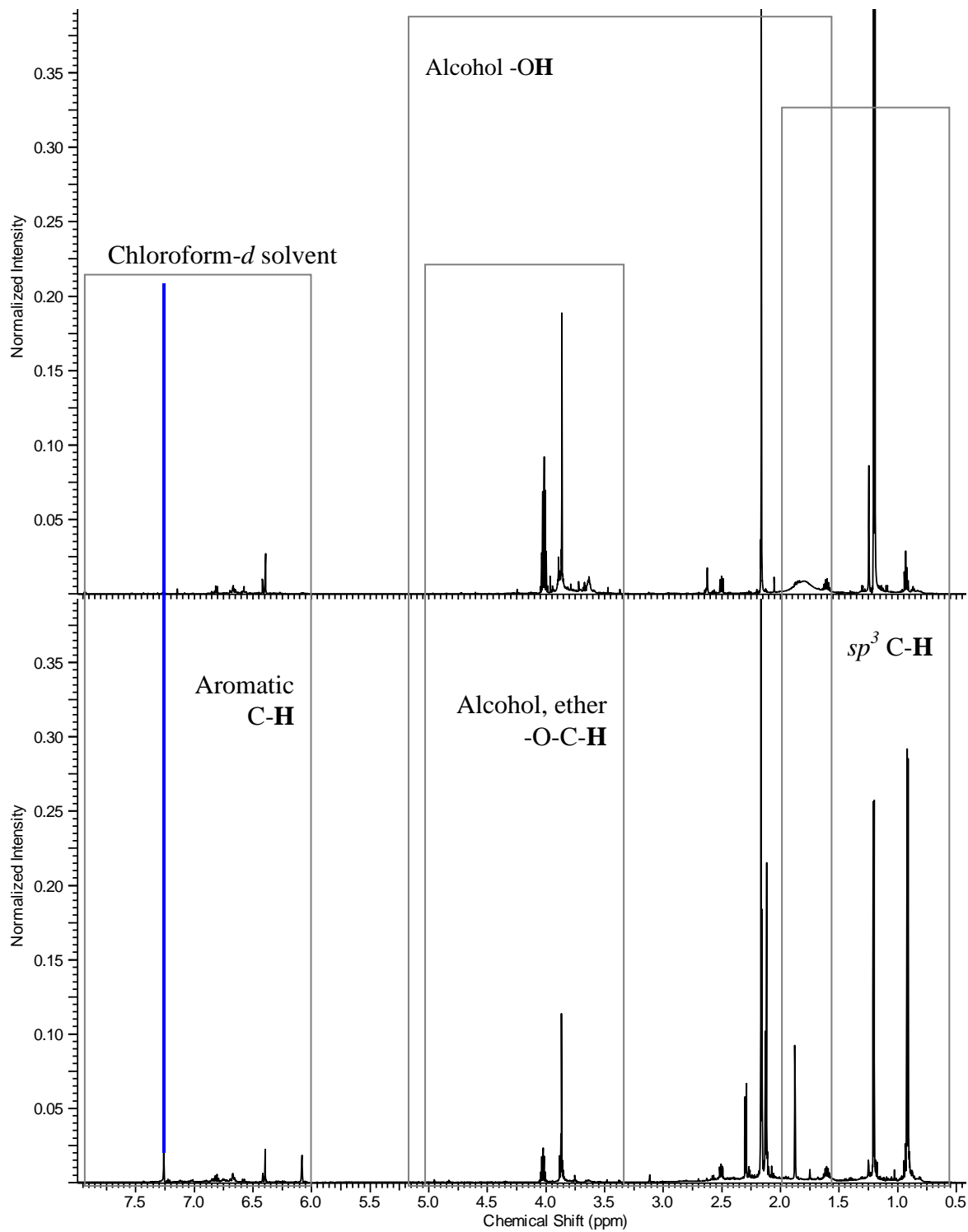


Figure 6.16 $^1\text{H-NMR}$ spectra of HL bio-oil obtained after 1 h reaction using MoRu/AC at 200 °C (top) and 340 °C (bottom)

6.4 Conclusions

Hydrolysis lignin was successfully depolymerized (or liquefied) in the presence of hydrogen, a carbon-supported metal catalyst and acetone solvent, producing low molecular weight bio-oils (as low as 380 g/mol) with high yields around 85 wt.%. The HL-derived bio-oils remained liquid at temperatures slightly below freezing. At 340 °C and with MoRu/AC catalyst, the yield of solid residue was less than 2 wt.%. Deoxygenation of HL was found to be largely thermally driven - the yields and M_w as well as chemical composition of the bio-oils are strongly dependent on the reaction temperature. Hydrogenation highly promoted by the presence of the MoRu/AC catalyst at 340 °C, resulting in a bio-oil with a remarkable 50% increase in hydrogen content relative to the HL feed. GC/MS analysis of the bio-oils revealed that in addition to the presence of ketones from the decomposition of the carbohydrates present in the HL feed, the bio-oils were largely composed of phenolic compounds. This indicates that the lignin component of HL can easily be depolymerized or liquefied at temperatures between 200 and 340 °C.

6.5 References

- Bui VN, Laurenti D, Delichere P, Geantet C. *Appl. Catal. B: Environ.*, 2011, 101, 246.
- Cateto CA, Barreiro MF, Rodrigues AE, Belgacem MN. *Ind. & Eng. Chem. Research*, 2009, 48, 2583.
- Centeno A, Laurent E, Delmon B. *J. Catal.*, 1995, 154, 288.
- Champagne P. *Resources, Conservation and Recycling*, 2007, 50, 211.
- Chang J, Danuthai T, Dewiyanti S, Wang C, Borgna A. *Chem. Cat. Che.*, 2013, 5, 3041.
- Demirbas A, Pehlivan E, Altun T. *Int. J. of Hydrogen Energy*, 2006, 31, 613.
- Elliott DC, Hart TR. *Energy Fuels*, 2009, 23, 631.
- Furimsky E, Massoth FE. *Catal. Today*, 1999, 52, 381.
- Gutierrez A, Kaila RK, Honkela ML, Siloor R, Krause AOI. *Catal. Today*, 2009, 147, 239.
- Horáček J, Homola F, Kubičková I, Kubička D. *Catal. Today*, 2012, 179, 191.
- Jin S, Xiao Z, Li C, Chen X, Wang L, Xing J, Li W, Liang C. *Catal. Today*, 2014, 234, 125.
- Jin Y, Ruan X, Cheng X, Lü Q. *Bioresour. Technol.*, 2011, 102, 3581.
- Kersten SRA, van Swaaij WPM, Lefferts L, Seshan K. In: Centi G, van Santen RA. (Eds.), *Catalysis for Renewables—From Feedstocks to Energy Production*, Wiley-VCH, Weinheim, 2007, 119.
- Lee CR, Yoon JS, Suh YW, Choi JW, Ha JM, Suh, Park YK. *Catal. Commun.*, 2012, 17, 54.
- Li K, Wang R, Chen J. *Energy Fuels*, 2011, 25, 854.
- Li Y, Ragauskas AJ. *RSC Advances*, 2012, 2, 3347.
- Lin L, Yao Y, Shiraishi N. *Holzforschung*, 2001, 55, 617.

- Lin YC, Li CL, Wan HP, Lee HT, Liu CF. *Energy Fuels*, 2011, 25, 890.
- Mahmood N, Yuan Z, Schmidt J, Xu C. *Bioresour. Technol.*, 2013, 139, 13.
- Meier D, Ante R, Faix O. *Bioresour. Technol.*, 1992, 40, 171.
- Monica, E. The Status of Applied Lignin Research, Report No. 2, 2005, Processum.
- Mortensen PM, Grunwaldt JD, Jensen PA, Knudsen KG, Jensen AD. *Appl. Catal. A: Gen.*, 2011, 407, 1.
- Moura JS, Souza MOG, Bellido JDA, Assaf EM, Opportus M, Reyes P, do Carmo Rangel M. *Int. J. of Hydrogen Energy*, 2012, 37, 2985.
- Prochazkova D, Zamostny P, Bejblova M, Cerveny L, Cejka J. *Appl. Catal. A: Gen.*, 2007, 332, 56.
- Reddy BM, Khan A. *Catal. Rev.*, 2005, 47, 257.
- Romero Y, Richard F, Brunet S. *Appl. Catal. B: Environ.*, 2010, 98, 213.
- Rouco AJ, Haller GL. *J. Catal.*, 1981, 72, 246.
- Ryymyn E-M, Honkela ML, Viljava TR, Krause AO. *Appl. Catal. A: Gen.*, 2009, 358, 42.
- Saidi M, Samimi F, Karimipourfard D, Nimmanwudipong T, Gates BC, Rahimpour MR. *Energy Environ. Sci.*, 2014, 7, 103.
- Senol OI, Ryymyn E-M, Viljava T-R, Krause AOI. *J. Mol. Catal. A: Chem.*, 2007, 277, 107.
- Shabtai JS, Zmierczak WW, Chornet E, Johnson DK. Am. Chem. Soc. Div. Fuel. Chem. Prepr. 1999, 44, 267
- Smolarski N. Paris: Frost & Sullivan, 2012, 15.
- Wildschut J, Mahfud FH, Venderbosch RH, Heeres HJ. *Ind. Eng. Chem. Res.*, 2009, 48, 10324.
- Xu J, Jiang J, Hse C, Shupe TF. *Green Chem.*, 2012, 14, 2821.

Yang Y, Gilbert A, Xu C. *Appl. Catal. A: Gen.*, 2009, 360, 242.

Yang YQ, Tye CT, Smith KJ. *Catal. Commun.*, 2008, 9, 1364.

Yuan Z, Browne CT, Zhang X. World patent 2012, WO2011057413A1. Retrieved December 2014 from, <http://www.google.com/patents/WO2011057413A1?cl=en>.

Zakzeski J, Bruijninx PC, Jongerius AL, Weckhuysen BM. *Chem. Rev.*, 2010, 110, 3552.

Zauwen MN, Crucq A, Degols L, Lienard G, Frennet A, Mikhalenko N, Grange P. *Catal. Today*, 1989, 5, 237.

Zhao HY, Li D, Bui P, Oyama ST. *Appl. Catal. A: Gen.*, 2011, 391, 305.

Chapter 7

7 Hydrotreatment of depolymerized hydrolysis lignin

7.1 Introduction

The awareness of the impending depletion of fossil fuel resources in recent decades has resulted in the growth of interest into the effective utilization of biomass resources as alternative feedstocks for bio-chemicals and bio-materials (Cheng *et al.*, 2010). The use of biomass has the advantages of: (1) being renewable and widely available, (2) containing negligible sulfur and other detrimental elements, and (3) it can be regarded as a carbon-neutral resource as the utilization of biomass does not result in a net increase in the CO₂ concentration in the atmosphere (Tymchyshyn and Xu, 2010).

Lignocellulosic biomass consists of three major components: cellulose, hemicelluloses and lignin. Cellulose is a homo-polymer of D-glucose units, joined by β -O-4 glycosidic linkages and comprises from 30-50% of biomass (MacLellan, 2010). Polysaccharides, i.e. cellulose and different hemicelluloses, are the primary constituents of wood and wood pulps. Hemicelluloses are heteroglycans containing several different types of neutral (pentose and hexose) and acidic (uronic acid) monosaccharides as structural elements.

A well-established approach to obtain chemicals from lignocellulosic biomass is enzymatic hydrolysis of wood and pulps. During hydrolysis, enzymes break down the polysaccharides in the woody biomass into simpler molecules. Thus, the reaction is generally not hindered by the presence of either lignin or lipophilic extractives. This allows for the removal of most of the lignin and extractives from the fibers and enhances the swelling and porosity of the fibers. The cellulose and hemicelluloses in these chemical pulps can then be effectively hydrolyzed into their monosaccharide components by the enzymes. In some cases however, delignification or acid pre-hydrolysis may be required in order for the enzymes to access the degradable cellulosic components. If enzymatic hydrolysis is performed without such pretreatment, then much of the lignin remains in the hydrolyzed product. The solid residues which remain after the enzymatic hydrolysis of wood are known as hydrolysis lignin (HL) or hydrolyzed wood biomass and are composed of unreacted cellulose, mono and oligosaccharides, and lignin, with lignin comprising 50 to 55% of the mass. (Dahlman *et al.*, 2000; San-

tos *et al.*, 2012)

Conventionally, lignin is regarded as a low value waste product and is used to produce heat via direct combustion. However, due to its structure, lignin is a promising source of phenols and aromatics. Lignin is a complex aromatic biopolymer composed of three basic phenyl-propanol building blocks, i.e., *p*-hydroxyl-phenyl propanol, guaiacyl-propanol and syringyl-propanol (Tejado *et al.*, 2007). These phenyl-propanols are linked mainly by two types of linkages: condensed linkages such as 5-5 and β -1 linkages and ether bonds such as α -O-4 and β -O-4 linkages. The ether linkages are more reactive and, under proper reaction conditions, are more easily cleaved than the more stable C-C bonds, (Chakar and Ragauskas, 2004) and as a result, solid lignin can be converted into a product which can potentially be used as fuels and/or chemicals.

Typically, the hydroprocessing of lignin-derived bio-oils (to remove oxygen and hydrogenate the product) has been performed in the presence of noble metal catalysts. Ru catalysts, in particular, have been shown to be very active in the hydrogenation and hydrodeoxygenation of model compounds (e.g. phenol and guaiacol) as well as bio-oils. (Elliott and Hart, 2009; Gutierrez *et al.*, 2009; Lee *et al.*, 2012; Chang *et al.*, 2013) Co- or Ni-promoted Mo sulfide catalysts, typically supported on alumina, borrowed from the petroleum industry have also been used in the hydroprocessing of lignin and biomass-derived bio-oils, especially from Kraft lignin. (Senol *et al.*, 2007; Romero *et al.*, 2010; Zakzeski *et al.*, 2010; Saidi *et al.*, 2014) More recently, reductive depolymerization of lignin in the presence of hydrogen and metal catalysts especially other late 3d and 4d transition metal (e.g. Fe, Co, Ni, Cu, Ru, Rh, Pd, and Ag) has been proposed. (Cateto *et al.*, 2009; Li *et al.*, 2011; Zhao *et al.*, 2011; Jin, 2014) A review of the literature also reveals that mixed noble metal/transition metal catalysts (e.g. Ru-Co, Rh-Cu and Rh-Ag) have been used, although not in the hydroprocessing of bio-oils. (Rouco and Haller, 1981; Zauwen *et al.*, 1989; Moura *et al.*, 2012)

Although the typical alumina-supported catalysts have been found to be active in HDO, they also increase catalyst deactivation by promoting the formation and deposition of coke on the catalyst surface. (Centeno *et al.*, 1995; Prochazkova *et al.*, 2007; Elliott and Hart, 2009; Wildschutt *et al.*, 2009; Lin *et al.*, 2011) Centeno *et al.* (1995) proposed that it is the weak Lewis acid sites present in the alumina that promote the condensation reactions leading to coke

formation.

In order to avoid coke formation, researchers have investigated less-acidic supports such as activated carbon and SiO₂ (Furimsky and Massoth, 1999; Reddy and Khan, 2005; Kersten *et al.*, 2007) as well as other less common supports e.g. ZrO₂ and MgO. (Senol *et al.*, 2007; Bui *et al.*, 2011) Yang *et al.* (2009) found that using carbon-supported catalysts resulted in yields equivalent to those of alumina-supported catalysts, but with lower proportions of oxygenated compounds.

The major objective of this work was the catalytic hydrotreatment of depolymerized hydrolysis lignin (DHL) - obtained by the depolymerization of hydrolysis lignin, itself a by-product from pre-treatment processes in cellulosic ethanol plants, in super-critical acetone and investigating the effects of reaction temperature and time on process yields. To the best of the author's knowledge no systematic study of the catalytic hydroprocessing of DHL has been reported in the literature.

7.2 Experimental

7.2.1 Materials

The hydrolysis lignin (HL) used in this study was provided by FPIInnovations and was insoluble in THF and several other common organic solvents including ethanol, methanol and acetone due to the cross-linking between cellulose and lignin present in the material. Therefore, it was not possible to determine the weight average molecular weight (M_w) of the HL by GPC-UV.(Yuan *et al.*, 2012) The pH value of original hydrolysis lignin was neutral.

This hydrolysis lignin was depolymerized via a proprietary process at 150-300 °C for 30-120 min under operating pressure of ~300 psig at a substrate concentration of 5-30 wt.%. The process resulted in a moderately high yield of DHL (~70 wt.%) with a solid residues (SR) yield of ~ 10 wt.%. The detailed operating conditions are protected due to a patent application. This depolymerized material was precipitated from solution, neutralized to a pH greater than 5.5, filtered, rinsed and dried before use.

The Ru/C catalyst used in this study was purchased from Sigma-Aldrich and used as pro-

vided. The MoRu/AC catalyst was prepared in house by incipient wetness impregnation from activated charcoal, ruthenium (III) nitrosyl nitrate solution ($\text{Ru}(\text{NO})(\text{NO}_3)_3$) and ammonium molybdate tetrahydrate ($(\text{NH}_4)_6\text{Mo}_7\text{O}_{24}\cdot 4\text{H}_2\text{O}$). Solvents included acetone and methanol. All were reagent grade and purchased from Sigma-Aldrich.

To prepare the MoRu catalyst activated charcoal was suspended in a 50% solution of water and methanol. The calculated volume of the Ru nitrate solution was added to this solution. The Mo was added by dissolving the required amount of the Mo compound in some distilled water and adding the solution to the suspension. The suspension was then stirred for 24 h at ambient temperature. The catalyst was then dewatered under vacuum and rotary evaporation at 85 °C. The catalyst was then dried overnight in an oven at 105 °C. The catalyst was then loaded into a tube reactor and reduced under a flow of 50 mL/min hydrogen at 500°C for 4 h. The evolution of a brown gas at a temperature of ~300°C and ammonia was evidence of the reduction taking place. After cooling to ambient temperature under nitrogen, the catalyst was decanted into a beaker of methanol, also under nitrogen, for passivation. After evaporation of the methanol at 65°C and cooling back to ambient, the catalyst was stored in an air-tight container.

7.2.2 Method and apparatus

The hydroprocessing of the DHL was carried out in a 100 mL stainless-steel autoclave reactor equipped with a stirrer. In a typical run, the reactor was loaded with 5 g of DHL, 0.5 g of catalyst and 25 g of acetone. The reactor was sealed, purged with hydrogen three times and was subsequently pressurized to >5 MPa hydrogen. After a 5 min leak check, the reactor pressure was vented to obtain 5 MPa. The reactor was heated to the reaction temperature while stirring and kept at the desired temperature for 60 min before cooling. Once the reactor had cooled to room temperature, the gaseous products were sampled for analysis. The liquid products and solid residue (SR) were rinsed from the reactor with acetone and the resulting suspension was filtered under vacuum through a pre-weighed Whatman No. 5 filter paper. The SR, catalyst and filter paper were dried at 105 °C for 24 h before weighing. After a GC-MS sample was taken, the acetone was removed from the liquid product by rotary evaporation under vacuum at 45 °C. The yields of the hydroprocessed DHL and SR were calculated

relative to the mass of the DHL loaded into the reactor. Each experiment was performed a minimum of two times to reduce the experimental error to $\pm 5\%$.

The relative molecular weights and their distributions of the DHL feed and resulting bio-oils were measured with a Waters Breeze GPC-HPLC (gel permeation chromatography-high performance liquid chromatography) instrument (1525 binary pump, UV detector at 270 nm; Waters Styrylgel HR1 column at a column temperature of 40 °C) using THF as the eluant at a flow rate of 1 mL/min. Linear polystyrene standards were used to generate a calibration curve for molecular weight estimation. ^1H NMR spectra were obtained on a 500 MHz Unity Inova NMR instrument at room temperature, wherein chloroform-*d* was used as solvent. FT-IR spectra were collected on a Bruker Tensor 37 FTIR spectrophotometer in the range of 550-4000 cm^{-1} with ATR accessory. The volatile components of the DHL bio-oils were identified by GC-MS (HP 6890 GC and HP 5972 MS) using a silicon column with temperature programming from an initial temperature of 50 °C for 2 min hold at 10 °C/min to a final temperature of 280 °C for 2 min hold. CHNS (carbon, hydrogen, nitrogen, and sulfur) elemental analysis was conducted on a Flash EA 1112 Series elemental Analyzer. The BET surface area analysis was performed on a Micrometrics ASAP 2010 instrument. The samples were degassed at 150 °C until a stable static vacuum of less than 5×10^{-3} Torr was achieved prior to analysis.

7.3 Results and Discussion

7.3.1 Catalyst characterization

The textural analysis of these catalysts is presented in Table 7.1. There was no great difference in the surface areas, pore volumes and pore diameters of the catalysts, therefore the differences in catalyst performance must be due to the catalyst metals.

Table 7.1 Catalyst textural properties

Catalyst	Metal Loading (wt.%)		BET Surface Area (m ² /g)	Tot. Pore Vol. (cm ³)	Vol. of pores <2 nm (cm ³)	Vol. of pores 2-50 nm (cm ³)	Avg. pore dia. (nm)
	Mo	Ru					
	Ru/C	5					
MoRu/AC	1	5	875	0.786	0.034	0.442	3.58

7.3.2 Effect of catalyst and temperature

The DHL was hydrotreated at standard reaction conditions of 5 g DHL dissolved in 25 g acetone, 0.5 g catalyst, 5 MPa initial hydrogen pressure and 1 h reaction time unless otherwise noted. The bio-oils produced as a result of these experiments were thick and viscous. It was not possible to measure their viscosity even at 80 °C. Evidence of the nature of the bio-oils was observed during the removal of the char and catalyst by filtration, where the filtration of ~250 mL of suspension required more than 2 hours under vacuum.

The yields of hydrotreated DHL (referred to as bio-oil for convenience) are presented in Figure 7.1. As can be seen, the yields of bio-oil started at a maximum of ~83 wt.% and decreased with increasing reaction temperature to a low of ~40 wt.% due to increasing char (solid residue) formation. A similar trend was seen in work performed in our group using these catalysts to hydroprocess organosolv lignin, and reported in previous chapters, but not to the same extent. The MoRu/AC catalyst performed better than the reference Ru/C catalyst by ~12 wt.% regardless of reaction temperature. At shorter reaction times, the yields of hydroprocessed DHL were smaller than at 60 min, however, the differences were not significant.

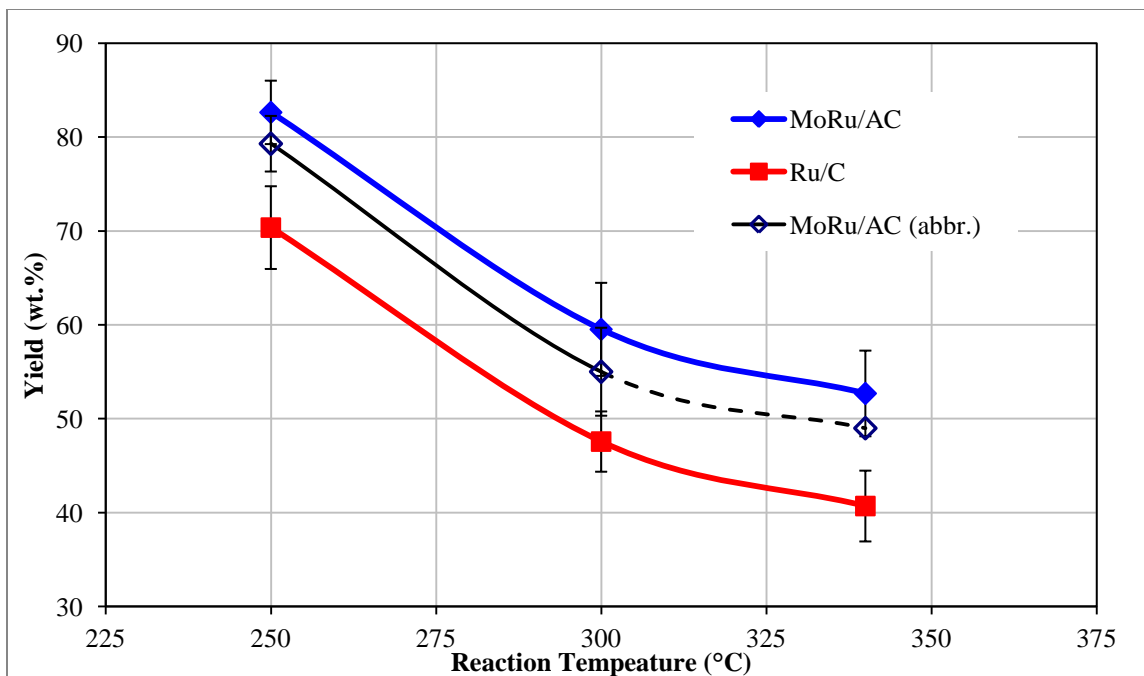


Figure 7.1 Yields of DHL bio-oil vs. temperature and catalyst

The cumulative product yields for these experiments are presented in Table 7.2 and Figure 7.2. As is evident, the decrease in bio-oil yield is accompanied by an increase in the amount of solid residue (char) that was produced. Gasification of the DHL feed was not a significant factor in the yields being less than 4 wt.% for all conditions tested.

Although unexpected, the large amount of char that formed can be explained by the fact that the DHL feed had previously been processed at 250 °C in the presence of H₂SO₄. Reaction with such a strong acid would have greatly reduced the number of reactive (e.g. ether) bonds present in the DHL, leaving behind the more refractory bonds. Thus, when the DHL feed was subjected to further hydrothermal treatment, a portion of the fragments of the macromolecule were able to combine and condense into acetone-insoluble compounds. Increased reaction times were found to slightly reduce the amount of char present, but not significantly. This is likely due to hydrogenation of the condensed products. As reported in previous chapters, the formation of char leads to decreased bio-oil yields by deposition of carbon on the catalyst, thus decreasing the catalyst surface area due to deactivation of active sites on the catalyst surface as well as preventing access to active sites in the interior of the catalyst by blocking pores.

The formation of water during the reactions was insignificant.

Table 7.2 DHL hydrotreatment product yields

Catalyst	Temperature (°C)	Bio-Oil (wt.%)	Char (wt.%)	Gas (wt.%)	Sum
MoRu/AC	250*	79.3 ±3.0	21.4 ±2.4	0.1 ±0.01	100.8
	250	82.6 ±1.7	18.2 ±2.1	0.2 ±0.03	101.1
	300*	55.0 ±4.7	47.2 ±3.9	1.0 ±0.08	103.2
	300	59.5 ±3.1	41.2 ±4.1	1.7 ±0.09	102.4
	340	52.7 ±2.8	48.5 ±4.3	3.7 ±0.13	104.9
Ru/C	250	70.4 ±2.6	30.2 ±3.5	0.2 ±0.03	100.7
	300	47.6 ±1.8	50.5 ±4.6	1.8 ±0.08	99.9
	340	40.7 ±2.1	53.9 ±4.2	4.0 ±0.15	98.6

Reaction Conditions: 5 g OL:25 g acetone, 0.5 g catalyst, 5 MPa cold hydrogen, 1 h reaction time at temperature

* indicates abbreviated runs where the reaction was stopped upon reaching the set temperature.

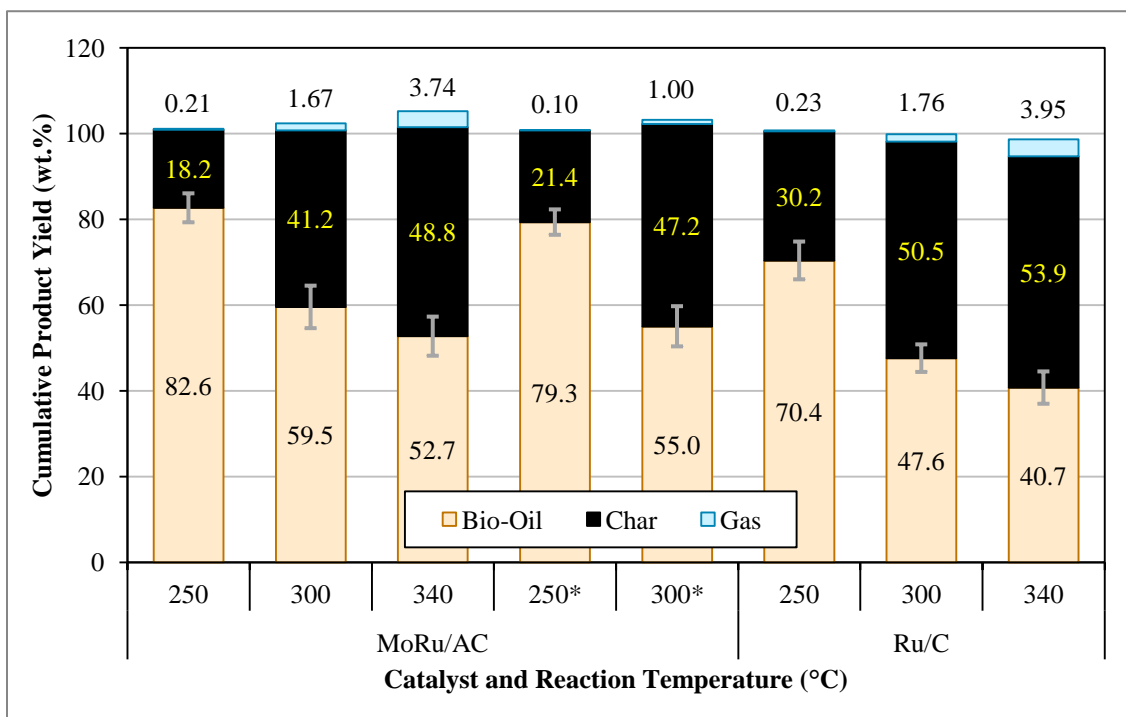


Figure 7.2 Cumulative product yields for hydroprocessed DHL

7.3.3 DHL gasification

The formation of gas during lignin depolymerization reactions is due to the cleavage of the aliphatic propane chain and removal of ring substituents (Gosselink *et al.*, 2012). The typical composition of the gases produced is presented in Table 7.3. The values in the table show that the amount of carbon gases present increased with increasing temperature, as is expected, with methane comprising the bulk of the gas. The methane is due to the decomposition/cleaving of the methoxy linkages in DHL (Chatterjee, *et al.*, 2013; He *et al.*, 2014) or from the methanation of C, CO or CO₂ ($C + H_2 \rightarrow CH_4$; $CO \text{ (or } CO_2) + H_2 \rightarrow CH_4 + H_2O$).

The gasification of DHL was calculated using the mol fraction of the various carbon species in the gas to determine the amount of gasified carbon present. This was possible because the gases were collected in a sample cylinder of known volume and pressure. Using the ideal gas law, it was possible to determine the total mol of gas in the sample. The mass of the carbon in the gases was then compared to the mass of carbon fed into the reactor with the DHL, as determined by CHNS analysis and assuming negligible gasification of the carbon support or the solvent during the hydrotreatment process. These results are presented in Table 7.4 and Figure 7.3.

As expected, and in agreement with the composition of the gaseous products (Table 7.3), very little DHL was gasified at low temperatures and the amount gasified increased with increased reaction temperature.

Table 7.3 Typical DHL hydroprocessing gas composition (mol%) vs. temperature and catalyst

Catalyst	MoRu/AC					Ru/C			
	Temp. (°C)	250	300	340	250*	300*	250	300	340
CH ₄		0.3	3.1	7.2	0.1	1.9	0.3	3.5	8.1
CO		0.15	0.9	1.6	0.1	0.7	0.1	0.6	1.3
CO ₂		0.2	1.0	2.3	0.1	0.6	0.4	1.5	2.7
C ₂ H ₄		0.0	0.0	0.0	0.0	0.0	0.0	0.0	0.0
C ₂ H ₆		0.0	0.3	0.7	0.0	0.1	0.0	0.3	0.8
C ₃ H ₈		0.0	0.2	0.3	0.0	0.1	0.0	0.1	0.15
Propylene		0.0	0.0	0.2	0.0	0.0	0.0	0.0	0.05

* indicates abbreviated runs stopped as soon as the reaction reached the specified temperature.

Table 7.4 DHL gasification during hydroprocessing vs. temperature and catalyst

Catalyst	MoRu/AC					Ru/C		
	250	300	340	250*	300*	250	300	340
Temp.								
CH ₄ (mol)	0.0003	0.0036	0.0082	0.0001	0.0022	0.0003	0.0041	0.0094
CO	0.0002	0.001	0.0018	8E-05	0.0009	0.0001	0.0007	0.0014
CO ₂	0.0002	0.0011	0.0026	0.0001	0.0007	0.0004	0.0017	0.0031
C ₂ H ₄	3E-06	2E-05	2E-05	1E-06	2E-05	5E-06	2E-05	3E-05
C ₂ H ₆	4E-05	0.0003	0.0008	2E-05	0.0002	3E-05	0.0003	0.0009
C ₃ H ₈	3E-06	0.0002	0.0004	0	8E-05	0	7E-05	0.0002
Propylene	2E-05	2E-05	4E-05	0	5E-06	0	9E-06	5E-05
mol C in gases	0.0009	0.007	0.0156	0.0004	0.0044	0.0009	0.0073	0.0165
mass C in gases	0.0106	0.0837	0.1869	0.0043	0.0523	0.0114	0.0878	0.1977
% C gasified	0.3	2.4	5.3	0.1	1.5	0.3	2.5	5.6
wt.% DHL gasified	0.21	1.67	3.74	0.09	1.05	0.23	1.76	3.95

* indicates abbreviated runs stopped as soon as the reaction reached the specified temperature.

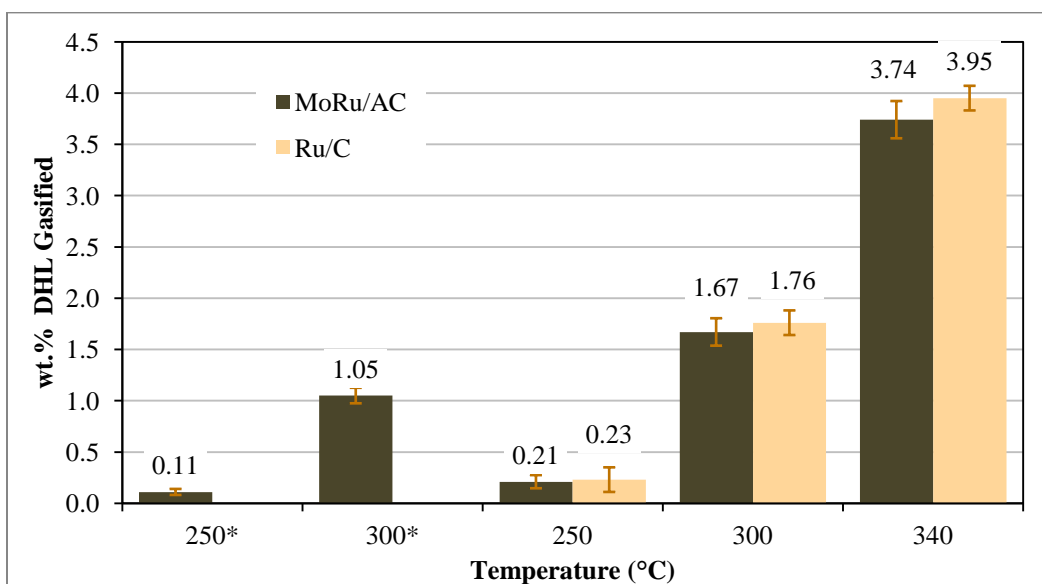


Figure 7.3 DHL gasification during hydroprocessing

* indicates abbreviated runs stopped when the reaction mixture reached the reaction temperature.

7.3.4 DHL hydrogen consumption

In a similar manner as was done for the carbon gases, the amount of hydrogen in the sample cylinder allowed for the determination of hydrogen consumed during the reaction. The amount of hydrogen fed into the reactor was determined by calculating the volume of the

headspace over the reaction mixture and the initial pressure of the hydrogen (5 MPa). The calculated amount of hydrogen introduced into the reactor was confirmed by Micro-GC analysis.

The hydrogen consumption is presented in Figure 7.4. As can be seen, the hydrogen consumed increased with increasing reaction time, as expected. Also evident is that hydrogen consumption was much greater for the MoRu/AC catalyst than for the Ru/C catalyst. Other work with this catalyst has revealed that Mo-doped Ru catalysts are more active, therefore it is expected that more hydrogen would be consumed during hydroprocessing reactions. Ru/C is also known as a hydrogenation catalyst and can therefore produce hydrogen (Barati *et al.*, 2014). Thus, the decreased hydrogen consumption could be the result of hydrogen production during the depolymerization.

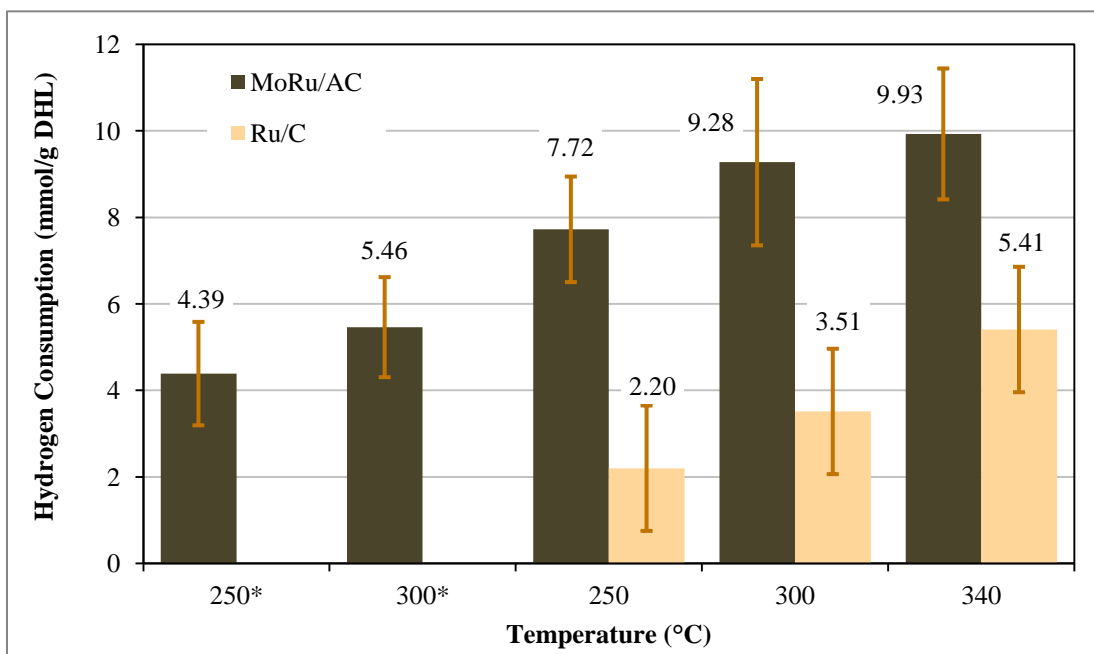


Figure 7.4 Hydrogen consumption during DHL hydroprocessing vs. reaction temperature and time

* indicates abbreviated runs stopped when the reaction mixture reached the reaction temperature.

Hydrogen consumption for the abbreviated runs was about half that for the runs that ran for 60 min, indicating that insufficient time has elapsed to allow the hydrogen consuming reactions to occur to the same extent as after 60 min reaction time. That being said, the extended reaction time resulted in only a doubling of the hydrogen consumed. The hydrogenation reactions must therefore begin occur as the reaction mass is heating up.

7.3.5 Elemental analysis of hydroprocessed DHL

The elemental composition of the bio-oils was determined by CHNS analysis and is shown in Table 7.5. The small amount of sulfur present in the DHL bio-oils was due to residual sulfate present in the feed material as a consequence of the depolymerization process that was used and was evident by the sulfurous odour of the bio-oils. As can be seen, hydrogenation of the DHL was moderately effective. The H content of the DHL feed was ~6% and, as expected, the hydrogen contents of the bio-oils increased with increased reaction time and temperature. This is in agreement with the fact that Ru/C is a hydrogenation catalyst. (Genet, 2003; Kluson and Cervený, 1995)

Unexpectedly, the O content of the bio-oils produced at 250 °C were greater than that of the DHL feed. The only source of oxygen in the system was the acetone solvent and, as seen with these catalysts in previous chapters, acetone can react to form dimers. Therefore, in order for the increase in O content to have occurred, the intermediates of acetone must have reacted with the DHL feed. This was confirmed by FTIR analysis as will be discussed later. This may also explain, in part, the increase in H content of the bio-oils, as acetone is ~10% H by mass. The slight decrease in hydrogen content between runs at 300 and 340 °C may be due to the removal of grafted acetone fragments at higher temperature. To the best of the author's knowledge, acetone grafting to DHL has not been reported in the literature.

The presence of free acetone in the bio-oils was ruled out as the bio-oils had been isolated by rotary evaporation at -0.8 bar vacuum and 45 °C. The boiling point of acetone at -0.8 bar vacuum (~150 mmHg) is ~18 °C. Most of the water present would also have been removed during solvent evaporation but to ensure that no residual water was present, the mostly dry bio-oils were further dried over night in a vacuum oven at 55 °C.

Table 7.5 Elemental composition of DHL and DHL-derived bio-oils

Sample	Elemental Analysis (mass %)					% Increase in H	% Increase in O
	C	H	S	N	O*		
DHL feed	69.1	6.03	0.21	0.57	24.1		
MoRu/AC, 250 °C*	67.7	6.40	0.17	0.40	25.3	6.09	5.15
MoRu/AC, 250 °C	64.2	6.83	0.11	0.40	28.4	13.3	18.2
MoRu/AC, 300 °C*	67.1	7.08	0.11	0.45	25.3	17.3	5.20
MoRu/AC, 300 °C	69.3	7.20	0.17	0.48	22.9	19.3	-4.97
MoRu/AC, 340 °C	72.4	7.55	0.15	0.47	19.5	25.2	-19.0
Ru/C, 250 °C	66.3	6.92	0.10	0.36	26.3	14.7	9.34
Ru/C, 300 °C	69.1	7.77	0.11	0.38	22.6	28.9	-6.03
Ru/C, 340 °C	71.7	7.74	0.25	0.47	19.9	28.4	-17.3

* indicates abbreviated runs stopped when the reaction mixture reached the reaction temperature.

A closer look at the oxygen contents of the bio-oils shows that the O content of the abbreviated MoRu/AC run at 250 °C increased by ~5%. Since the O content of the bio-oil produced after 60 minutes using the same catalyst and temperature had an O content of ~18%, this indicates that the low value is due simply in insufficient residence time. Increasing the reaction temperature to 300 °C resulted in a similar O content for the abbreviated run. However, extended reaction time at 300 °C resulted in a decrease in O content of ~5%. This change in behaviour can be explained by thermodynamics. At lower temperatures, condensation reactions are favoured and involved acetone. But at higher temperatures, smaller molecules are more energetically favourable, thus hydrogenation reactions leading to depolymerization and deoxygenation become more dominant. Further evidence for this is that the O content of the DHL bio-oil resulting from 60 min reaction at 340 °C had decreased by 19%. It is believed that reaction at still higher temperatures would have further reduced the oxygen content. It is also believed that extended reaction time would also result in decreased O content.

The differences in DHL bio-oil can be better visualized in a van Krevelen plot as presented in Figure 7.5. The figure clearly shows that the molar hydrogen/carbon ratio of the DHL bio-oils increased relative to the DHL feed. The larger increase at 250 °C is due to the large fraction of oxygen present in that sample which decreased the relative amount of carbon present and so skewed the point to the right (increased H/C). Also clearly seen is the decrease in O content relative to carbon content with increased temperature.

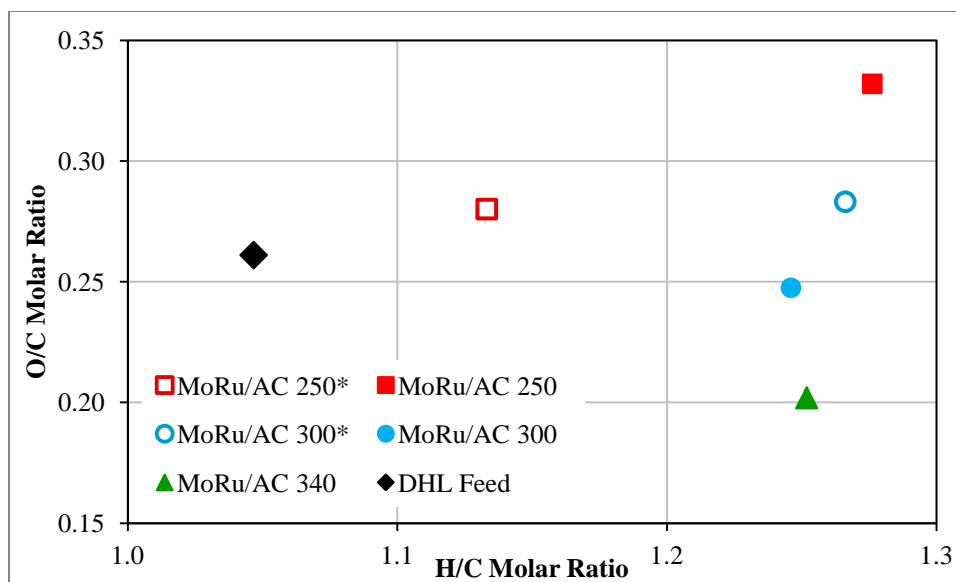


Figure 7.5 van Krevelen plot of DHL hydroprocessed at different temperatures

* indicates abbreviated runs stopped when the reaction mixture reached the reaction temperature.

At 250 °C the Ru/C catalyst also produced bio-oils with increased O content, but increase was only half that seen with the MoRu/AC catalyst (9.3 vs. ~18.2%). At 300 °C, the O content of the bio-oil had decreased by ~6% as compared to ~5%, and at elevated temperature the O content had decreased by ~17% as compared to 19%. This indicates that at lower temperatures, the addition of Mo to the Ru catalyst resulted in increased incorporation of O into the bio-oil (possibly due to increased activation and grafting of acetone). With increased reaction temperature, this effect was negated and possibly reversed at still higher reaction temperature.

These differences can be seen in the van Krevelen plot presented in Figure 7.6. The shift of the points to the right shows that all of the bio-oils exhibited increased H content relative to the DHL feed. The increased O content at lower temperature is evident by the vertically displaced points in red. At 300 °C, the O content of the bio-oils is only slightly lower than that of the feed, and the increased hydrogenation activity of the Ru/C can be seen by the greater shift to the right as compared to the MoRu/AC catalyst. This difference in hydrogen content between the two catalysts is diminished at 340 °C. The smaller O/C values at this temperature are evidence that deoxygenation of DHL requires higher energy.

Despite consistently higher yields, the MoRu/AC catalyst was slightly less effective in hydrogenating the DHL than the reference Ru/C catalyst. It is possible that optimization of the ratio of Mo to Ru could improve the hydroprocessing efficiency of the MoRu/AC catalyst.

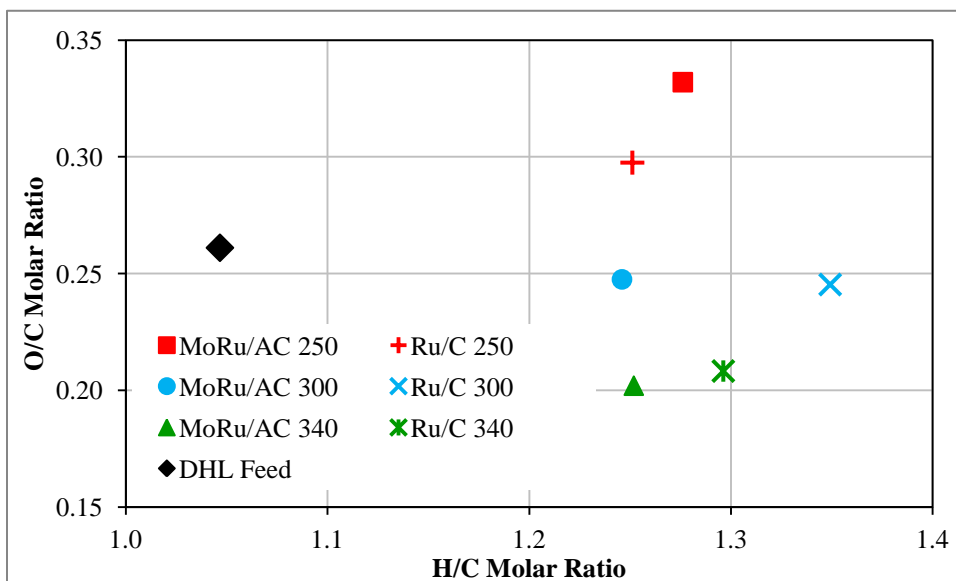


Figure 7.6 van Krevelen plot of DHL and DHL hydroprocessed with different catalysts

7.3.6 GPC analysis of hydroprocessed DHL

The relative molecular weights of the DHL bio-oils as well as the DHL feed were measured by gel permeation chromatography (GPC). The results of this analysis are presented in Table 7.6.

The GPC curves comparing the feed to the bio-oils for reaction and different temperatures and with different catalysts are presented in Figure 7.7. As can be seen, the GPC curves for the bio-oils produced at 250 °C are very similar to the curve for the DHL feed and the molecular weights of these bio-oils is slightly higher than the DHL 1,784 and 1,820 g/mol for Ru/C and MoRu/AC, respectively, vs. 1,695 g/mol for the DHL feed.

Table 7.6 Hydroprocessed DHL molecular weights

Catalyst	Temp. (°C)	Mw (g/mol)
MoRu/AC	250*	1,560
	250	1,820
	300*	940
	300	808
	340	631
Ru/C	250	1784
	300	775
	340	577
DHL Feed		1,695

* indicates abbreviated runs stopped when the reaction mixture reached the reaction temperature.

This is despite the fact that the O content of the bio-oils had increased significantly as discussed previously. In contrast, the molecular weight of the abbreviated run decreased relative to the feed (1,560 g/mol). This is an indication that residence time had a minor effect on the extent of condensation at low temperature. In comparison, the abbreviated run at 300 °C exhibited a marked lower molecular weight of 940 g/mol. Thus the depolymerization of the DHL into smaller molecules is dominant over the condensation reactions at elevated temperature (Chen and Falconer, 1994; Mahmood *et al.*, 2013).

A possible reason for the initial increase in molecular weight could be the presence of residual acid in the DHL feed. As was explained in the materials section, the DHL was produced by treating hydrolysis lignin with sulfuric acid. As is well known, acidity catalyzes condensation reactions. Thus, it is possible that insufficient time was given during the neutralization step for the residual acid adsorbed in the DHL to be neutralized before the solution was filtered to obtain the DHL. Any residual acid present would have acted as a condensation catalyst and this would explain the unexpected increase in molecular weight after reaction at 250 °C. Due to the small amount of acid residual, its effect would be limited and hydrogenation reactions would come to dominate at higher temperatures.

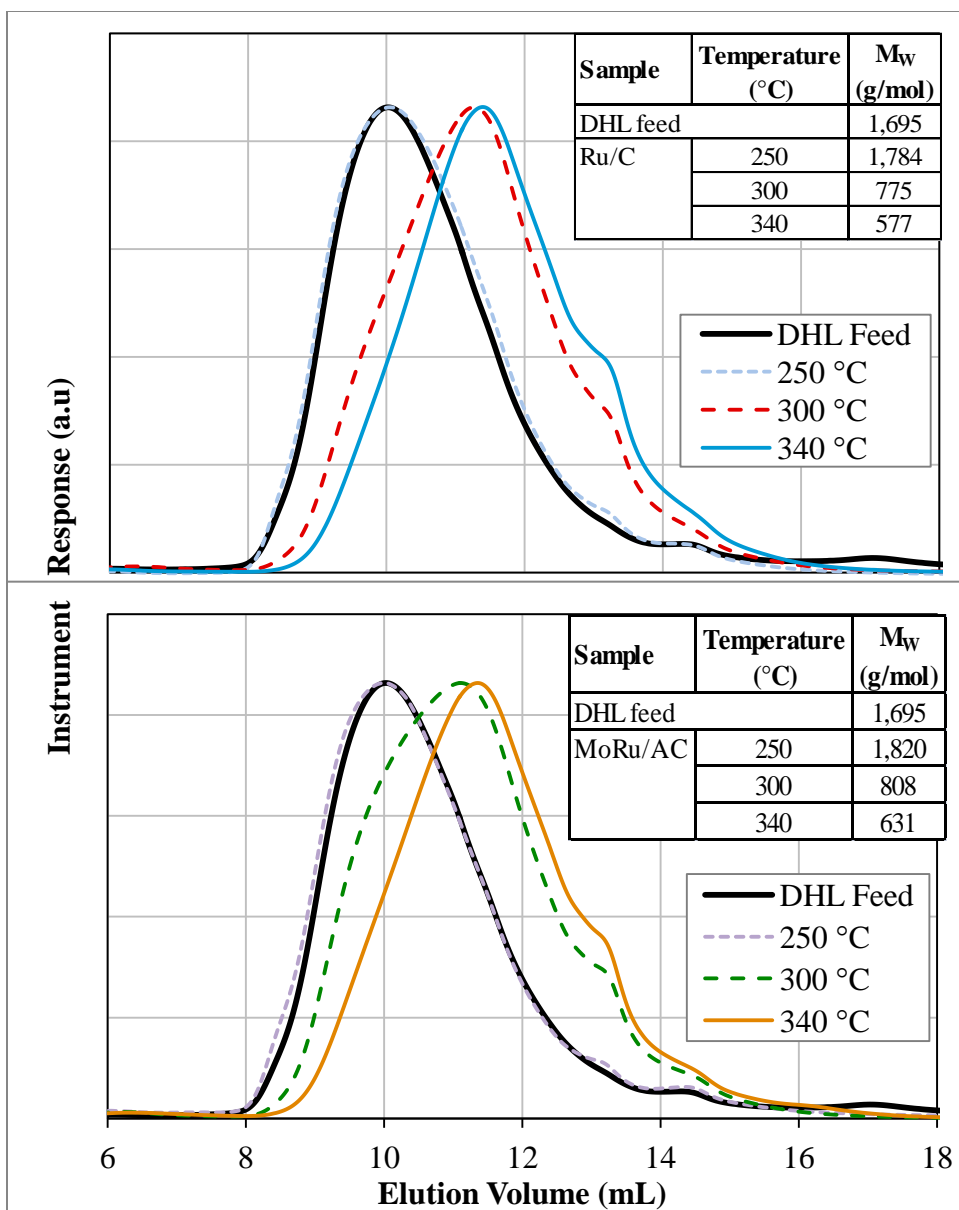


Figure 7.7 GPC curves for DHL at different reaction temperatures for Ru/C (top) and MoRu/AC catalyst (bottom)

The bio-oils resulting from 60 min reaction at 300 °C had molecular weights of 775 and 808 g/mol for Ru/C and MoRu/AC, respectively. These values are about half of the molecular weight of the original DHL. Increasing the reaction temperature to 340 °C resulted in a further decrease in molecular weight to 577 and 631 g/mol, respectively. Despite these relatively low molecular weights, these bio-oils were viscous, almost gummy, substances that did

not flow well. This is in sharp contrast to work done in our group with these catalyst (to be submitted for publication) where organosolv lignin ($M_w = \sim 2,600$ g/mol) was depolymerized into bio-oil of similar molecular weight but which was much less viscous and flowed at temperatures below freezing. This difference between the previous bio-oils and the bio-oils in this study must be due to the composition and functional groups present in these bio-oils.

Further evidence that the depolymerization reactions were occurring as the reaction temperature was increased can be seen in Figure 7.7. The molecular weight of the bio-oil obtained after quenching the reaction immediately upon reaching temperature exhibits a greatly reduced molecular weight (940 vs. ~ 1700 g/mol). Extended reaction time only decreased the molecular weight to ~ 810 g/mol. Therefore, extended reaction times do decrease molecular weight, but likely only to a certain point. Higher reaction temperature has a greater effect in reducing molecular weight. Unfortunately it was not possible to investigate this due to temperature limitations of the reactor used.

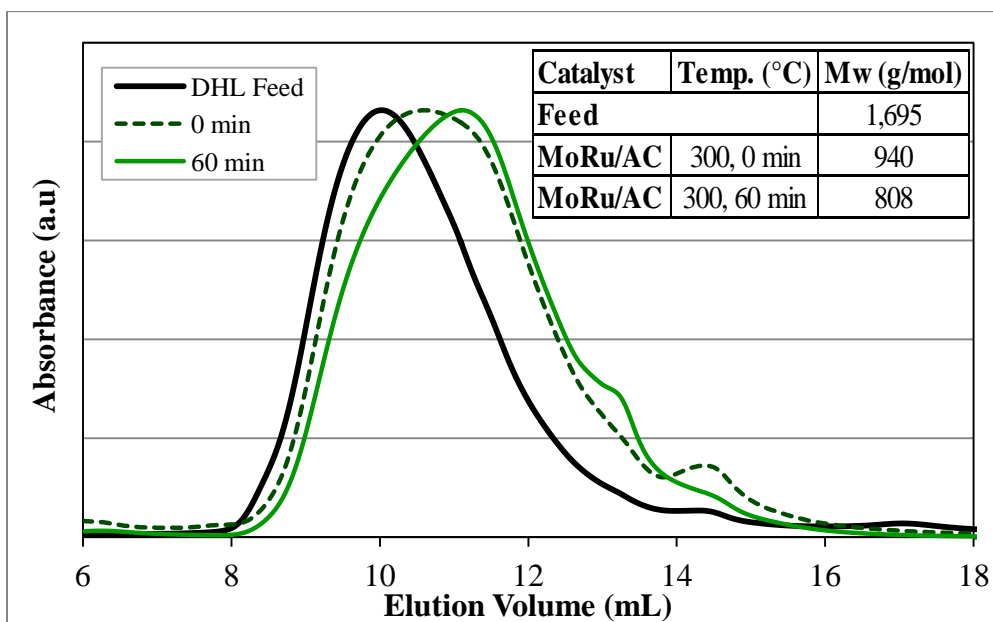


Figure 7.8 GPC curves of MoRu/AC-derived DHL bio-oil at different reaction times

7.3.7 GC/MS analysis of hydroprocessed DHL

The volatile components of the bio-oils obtained from the hydroprocessing of DHL were analyzed by GC/MS. Note that the samples analyzed were taken before the solvent was removed from the bio-oils. The plot of the MoRu/AC bio-oils after 60 min reaction at different temperatures is presented in Figure 7.8. The plots for the bio-oils obtained with the reference Ru/C catalyst were nearly identical.

As can clearly be seen, very few volatile compounds are evident in the plot for 250 °C. This is consistent with the absence of depolymerization/hydrogenation reactions occurring and the large molecular weight of these bio-oils. The two peaks at 3.1 and 3.9 min retention time were identified as 4-methyl-3-penten-2-one and 2-4-hydroxy-4-methyl-pentanone. These are dimers of acetone and are present in all of the bio-oils. Analysis of the recovered solvent (not presented) revealed that several more dimers of acetone are present in addition to trace amounts of phenol and lighter phenolic compounds.

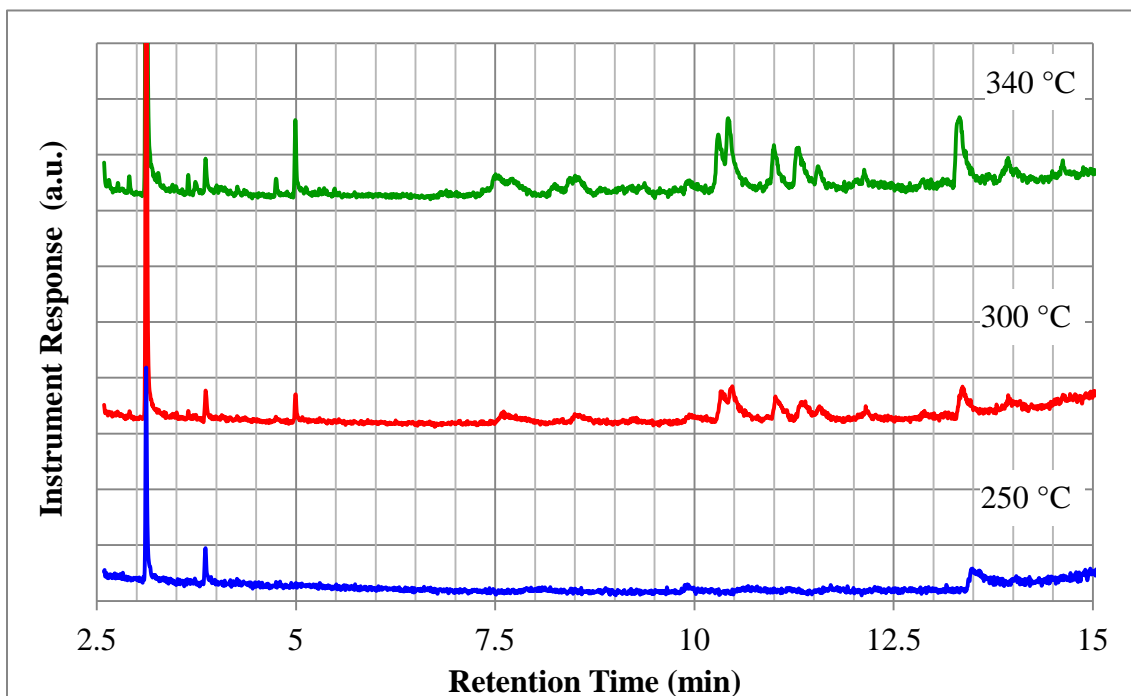


Figure 7.9 Comparison of the GC spectra for hydroprocessed DHL obtained with MoRu/AC catalyst at different temperatures

Increased reaction temperature to 300 °C increased the number of volatile compounds present and this effect was enhanced at 340 °C. Table 7.7 presents an abridged list of the compounds in the bio-oils. Only those compounds identified with greater than 85% certainty and peak areas greater than 2% are included. The shaded cells indicate that no compounds were evident at a particular retention time and catalyst/temperature condition. As can be seen, almost all of the compounds are phenolic in nature. This is expected as the DHL feed had been processed to remove a majority of the carbohydrates initially present. Despite the difference in bio-oil yields between the catalysts, the compounds present in the Ru/C bio-oils are almost exactly the same as listed here, indicating that there virtually is no difference in product selectivity between them.

Table 7.7 Comparison of hydroprocessed DHL composition vs. temperature

RT (min)	MoRu/AC		
	250 °C	300 °C	340 °C
3.1	3-Penten-2-one, 4-methyl-	3-Hexen-2-one	3-Penten-2-one, 4-methyl-
3.9		2-Pentanone, 4-hydroxy-4-methyl-	
5.0		Benzene, 1,2,3-trimethyl-	Mesitylene
7.5			Ethanone, 1-(1-cyclohexen-1-yl)-
10.3		Phenol, 2,6-dimethoxy-	
10.4		Phenol, 3,4-dimethoxy-	
11.0		4-Methoxy-2-methyl-1-(methylthio)benzene?	
11.3			Dodecanoic acid??
11.5		5-tert-Butylpyrogallol	
13.3		4-Hydroxy-1-methyloctahydro-2(1H)-quinolinone	

7.3.8 FTIR analysis of hydroprocessed DHL

FTIR analysis was performed on the DHL bio-oils to determine how the functional groups present were affected by the catalysts used as well as the reaction conditions. It should be noted that these bio-oils are complex mixtures of many compounds and therefore exhibit many more peaks and broader peaks than would be present in the spectra of pure compounds. This makes analysis of these spectra more difficult.

Figure 7.9 presents the FTIR spectra of bio-oils obtained at different temperatures using MoRu/AC catalyst. The spectra have been normalized with respect to the aromatic peak at 1610 cm^{-1} and are virtually identical to the spectra obtained with the Ru/C catalyst except as noted.

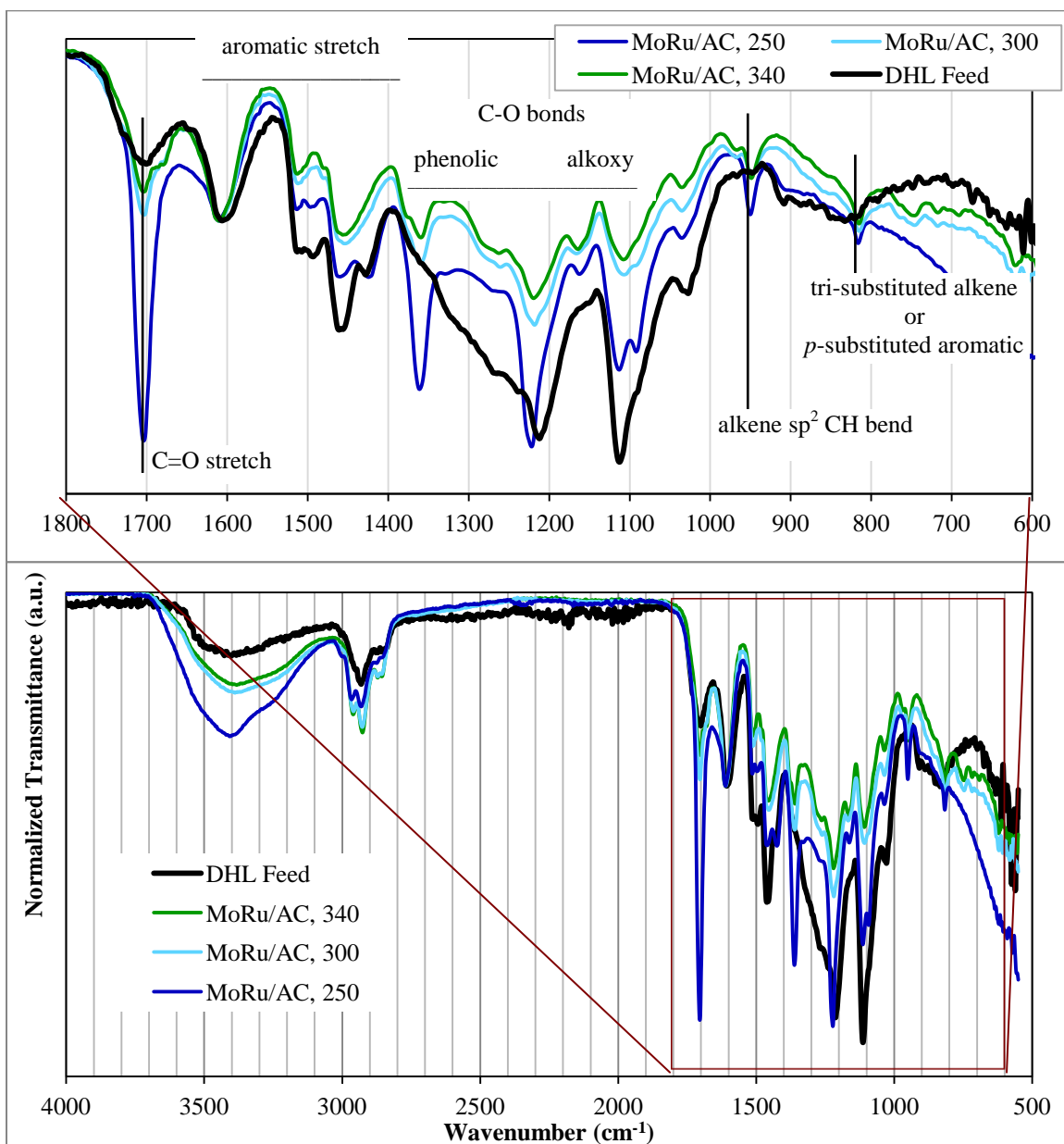


Figure 7.10 FTIR spectra of DHL bio-oils obtained using MoRu/C catalyst at different temperatures

It is immediately evident from the response in the -OH region (3,600-3,000 cm^{-1}) that the number of OH bonds in the bio-oils has increased relative to the DHL feed. This is consistent with the increased O content of the bio-oils as determined by elemental analysis. Increasing reaction temperature decreased the number of OH bonds. The loss of oxygen corresponds with the increased in oxygen-containing gaseous species (CO and CO₂) as well as any traces of water that may have been carried over with the acetone solvent during solvent removal under vacuum. The response at 3,000-2,850 cm^{-1} assigned to -CH stretch increased, as would be expected if acetone has been incorporated into the structure of the bio-oil.

Looking at the expanded fingerprint region, there is a large increase in response around 1700 cm^{-1} , indicative of C=O stretch, at 250 °C which is again expected if acetone were to have reacted with the DHL feed. The decrease in response with increased temperature is in agreement with the decreased O content at 300 and 340 °C. The peaks between 1520 and 1450 cm^{-1} , which are due to aromatic stretch, exhibit a decreased response with increasing temperature, possibly due to hydrogenation of the aromatic rings. The peak at 1375 cm^{-1} (due to *sp*³ CH bend) increased markedly at 250 °C and is consistent with grafted acetone introducing methyl groups into the bio-oil structure. At increased temperature, this peak decreased, possibly indicating that the acetone fragments had decomposed and partitioned into the gas or solid phase. The response in the range 1225-1000 cm^{-1} , indicative of C-O stretch, indicates that these bonds were present in the DHL feed. No change was observed in the peak at 1220 cm^{-1} at 250 °C, but rather at increased temperature, indicating that these bonds required more energy to break, as is consistent with aromatic C-O bonds (Chakar and Ragauskas, 2004). In contrast, the peaks at 1120 and 1030 cm^{-1} , which are indicative of aliphatic C-O bonds, decreased in intensity even at low temperature, indicating that these C-O bonds were more easily broken than the C-O bonds at 1220 cm^{-1} . The peaks at 950 and 815 cm^{-1} are due to alkene C-H bend and tri-substituted alkene C-H bend, respectively, and appear after reaction at 250 °C. Increased temperature led to the disruption of the alkene bonds and resulted in decreased response. It is interesting to note that these peaks are absent in the spectrum of bio-oil produced using Ru/C at 250 °C, but appeared at elevated temperatures.

The appearance of peaks in the range of 750-690 cm^{-1} at 300 and 340 °C is indicative of the presence of substituted benzene rings, indicating that higher temperatures were required to

cleave the structures bonded to the aromatic rings leaving behind simpler mono- and di-substituted compounds.

7.3.9 NMR analysis of hydroprocessed DHL

NMR analysis was performed to help elucidate the changes that occurred during reaction and are presented in Figure 7.10. Several differences are evident between the three plots. Moving from left to right, the first difference that can be seen is the great increase in the peaks in the 8-6 ppm range between the bio-oil produced at 340 °C (top) and the bio-oil produced and 250 °C (middle) and the DHL feed (bottom). These peaks can be attributed to aromatic protons and indicate that reaction at elevated temperature has greatly increased the number of free aromatic sites on the ring structures that are present in the bio-oil. The region between 5 and 3.3 ppm corresponds to the protons associated with ether bonds, but also overlaps the region attributed to alcoholic protons (5.2-1.5 ppm). Regardless, the peaks in this region appear to decrease slightly after reaction at lower temperature but increase greatly after reaction at elevated temperatures. There is a corresponding increase in intensity in the region of 3-2 ppm. This region is representative of both hydroxyl protons, benzylic and alpha carbonyl protons, and allylic protons. In concert with the other analyses, it is possible to eliminate hydroxyl protons as being responsible for this increase in response as the oxygen content of the bio-oils was found to decrease with increasing reaction temperature (confirmed by FTIR analysis). Thus this response must be due to protons associated with benzylic, carbonyl and allylic bonds. The peak at ~2.35 ppm, which decreases with increasing temperature, is more likely to be due to hydroxyl protons. Similarly, the response in the region of 2.0-0.5 ppm, which corresponds to sp^3 C-H bonds, changes in both intensity and chemical shift. The change in chemical shift depends on the number of hydrogen atoms bonded to the carbon atom. As the number of hydrogen atoms increases, the shift decreases and follows the trend $CH > CH_2 > CH_3$. As is seen in the figure, the peaks at ~1.2 ppm and especially at 0.9 ppm increase with increased reaction temperature. This indicates that the abundance of both CH_2 and CH_3 moieties in the bio-oils increases with increased reaction temperature. The peak at 0.1 ppm could not be identified but can be seen to have decreased greatly after reaction at low temperature and almost completely disappears after reaction at high temperature. Not

surprisingly, due to prior processing, there was no evidence of aldehydic protons in the spectrum of the DHL feed.

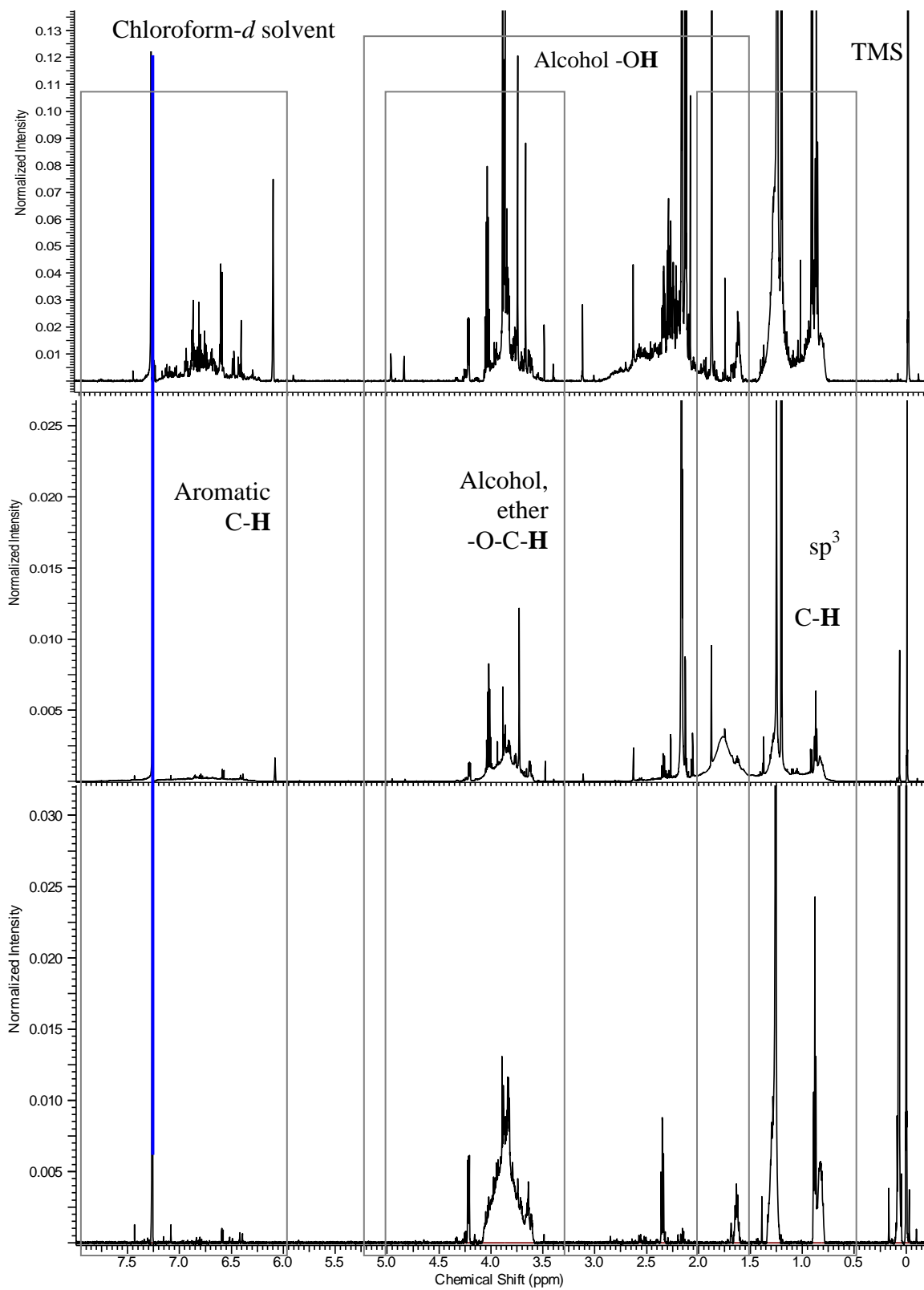


Figure 7.11 $^1\text{H-NMR}$ spectra of DHL (bottom) and DHL bio-oils obtained at 250 (middle) and 340 °C (top)

7.4 Conclusions

DHL was successfully depolymerized into lower molecular weight bio-oils after reaction with MoRu/AC and Ru/C catalysts under hydrogen. The yields were reasonably high (83 wt.%) at lower temperatures (250 °C) but decreased with increasing temperature. Hydrotreatment with the MoRu/AC catalyst resulted in consistently greater yields of bio-oil than the reference Ru/C catalyst (by ~12 wt.%) regardless of reaction temperature. Gasification of the DHL feed was found not to be significant, amounting to less than 4 wt.% at most. The yield of solid residue or char was high and increased in step with the decrease in bio-oil yields. Elemental analysis revealed that the acetone solvent was reacting with the DHL feed and increasing the oxygen content of the bio-oils. Despite the decreased yields of bio-oil that were obtained after reaction at higher temperatures, the molecular weights of the resulting bio-oils were found to have decreased by ~65% relative to the DHL (600 vs. 1700 g/mol).

Despite the decrease in molecular weight, these bio-oils were very viscous, and even though the present catalysts were able to effect a promising reduction in molecular weight, the poor yields of bio-oil and high yields of char indicate that more work needs to be done to obtain useful bio-oils from DHL.

7.5 References

- Barati M, Babatabar M, Tavasoli A, Dalai AK, Das U. *Fuel Proces. Technol.*, 2014, 123, 140.
- Bui VN, Laurenti D, Delichere P, Geantet C. *Appl. Catal. B: Environ.*, 2011, 101, 246.
- Cateto CA, Barreiro MF, Rodrigues AE, Belgacem MN. *Ind. & Eng. Chem. Research*, 2009, 48, 2583.
- Centeno A, Laurent E, Delmon B. *J. Catal.*, 1995, 154, 288.
- Chakar FS, Ragauskas AJ. *Ind. Crops Prod.*, 2004, 20, 131.
- Chang J, Danuthai T, Dewiyanti S, Wang C, Borgna A. *Chem. Cat. Che.*, 2013, 5, 3041.
- Chatterjee M, Ishizaka T, Suzuki A, Kawanami H. *Chem. Commun.*, 2013, 49, 4567.
- Chen BS, Falconer JL. *J. Catal.*, 1994, 147, 72.
- Cheng S, D'cruz I, Wang M, Leitch M, Xu C. *Energy Fuels*, 2010, 24, 4659.
- Dahlman O, Jacobs A, Liljenberg A, Olsson AI. *J. Chrom. A*, 2000, 891, 157.
- Elliott DC, Hart TR. *Energy Fuels*, 2009, 23, 631.
- Furimsky E, Massoth FE. *Catal. Today*, 1999, 52, 381.
- Genet JP. *Acc. Chem. Res.*, 2003, 12, 908.
- Gosselink RJA, Teunissen W, VanDam JEG, Jong ED, Gellerstedt G, Scott EL, Sanders JPM. *Bioresour. Technol.*, 2012, 106, 173.
- Gutierrez A, Kaila RK, Honkela ML, Siloor R, Krause AOI. *Catal. Today*, 2009, 147, 239.
- He J, Zhao C, Mei D, Lercher JA. *J. Catal.*, 2014, 309, 280.
- Jin S, Xiao Z, Li C, Chen X, Wang L, Xing J, Li W, Liang C. *Catal. Today*, 2014, 234, 125.

Kersten SRA, van Swaaij WPM, Lefferts L, Seshan K. In: Centi G, van Santen RA. (Eds.), *Catalysis for Renewables—From Feedstocks to Energy Production*, Wiley-VCH, Weinheim, 2007, 119.

Kluson P, Cervený L. *Appl. Catal. A: Gen.*, 1995, 128, 13.

Lee CR, Yoon JS, Suh YW, Choi JW, Ha JM, Suh, Park YK. *Catal. Commun.*, 2012, 17, 54.

Li K, Wang R, Chen J. *Energy Fuels*, 2011, 25, 854.

Lin YC, Li CL, Wan HP, Lee HT, Liu CF. *Energy Fuels*, 2011, 25, 890.

MacLellan J. *MMG 445 Basic Biotechnol.* 2010, 6, 31.

Mahmood N, Yuan Z, Schmidt J, Xu C. *Bioresour. Technol.*, 2013, 139, 13.

Moura JS, Souza MOG, Bellido JDA, Assaf EM, Opportus M, Reyes P, do Carmo Rangel M. *Int. J. of Hydrogen Energy*, 2012, 37, 2985.

Prochazkova D, Zamostny P, Bejblova M, Cervený L, Cejka J. *Appl. Catal. A: Gen.*, 2007, 332, 56.

Reddy BM, Khan A. *Catal. Rev.*, 2005, 47, 257.

Romero Y, Richard F, Brunet S. *Appl. Catal. B: Environ.*, 2010, 98, 213.

Rouco AJ, Haller GL. *J. Catal.*, 1981, 72, 246.

Saidi M, Samimi F, Karimipourfard D, Nimmanwudipong T, Gates BC, Rahimpour MR. *Energy Environ. Sci.*, 2014, 7, 103.

Santos RB, Lee JM, Jameel H, Chang HM, Lucia LA. *Bioresour. Technol.*, 2012, 110, 232.

Sazanov YN, Popova EN, Sumerskii IV, Mokeyev MV, Kulikova EM, Litvinova LS, Kevery EE, Krutov SM, Griбанov AV. *Russ. J. of Appl. Chem.*, 2010, 83, 1607.

Senol OI, Ryymin E-M, Viljava T-R, Krause AOI. *J. Mol. Catal. A: Chem.*, 2007, 277, 107.

Tejado A, Peña C, Labidi J, Echeverria JM, Mondragon I. *Bioresour. Technol.*, 2007, 98, 1655.

Tymchyshyn M, Xu C. *Bioresour. Technol.*, 2010, 101, 2483.

Wildschut J, Mahfud FH, Venderbosch RH, Heeres HJ. *Ind. Eng. Chem. Res.*, 2009, 48, 10324.

Yang Y, Gilbert A, Xu C. *Appl. Catal. A: Gen.*, 2009, 360, 242.

Yuan Z, Browne CT, Zhang X. World patent 2012, WO2011057413A1. Retrieved December 2014 from <http://www.google.com/patents/WO2011057413A1?cl=en>.

Zakzeski J, Bruijninx PC, Jongerius AL, Weckhuysen BM. *Chem. Rev.*, 2010, 110, 3552.

Zauwen MN, Crucq A, Degols L, Lienard G, Frennet A, Mikhalenko N, Grange P. *Catal. Today*, 1989, 5, 237.

Zhao HY, Li D, Bui P, Oyama ST. *Appl. Catal. A: Gen.*, 2011, 391, 305.

Chapter 8

8 Conclusions and Future Work

8.1 Conclusions

The aim of this work was to investigate the depolymerization and hydroprocessing of several different types of lignin (Kraft lignin, organosolv lignin, and hydrolysis lignin) in the presence of catalysts and supercritical acetone to obtain lower molecular weight and deoxygenated compounds suitable for use as substitutes for fuels and chemicals from fossil resources.

In the first study, a number of different metal catalysts and support materials were successfully employed in the depolymerization and hydroprocessing of Kraft and organosolv lignin. Carbon-supported catalysts were found to outperform catalysts supported on alumina.

The effectiveness of novel mixed noble metal/transition metal MoRu catalysts was investigated using guaiacol as a model compound for lignin. Guaiacol conversion was most effective in the presence of activated carbon-supported MoRu catalyst. Based on this work, the depolymerization and hydroprocessing of organosolv lignin using these MoRu catalysts was investigated. OL was successfully hydroprocessed and depolymerized into DOLs composed of aromatic compounds with increased hydrogen contents, decreased oxygen contents and greatly decreased molecular weights.

Further work investigated the effectiveness of the mixed noble metal/transition metal MoRu catalyst on the hydroprocessing and depolymerization of hydrolysis lignin and resulted in bio-oils composed of aromatic compounds with increased hydrogen contents, decreased oxygen contents and greatly reduced molecular weights. Continuing this work, the hydroprocessing of depolymerized hydrolysis lignin (hydrolysis lignin that had been hydrolyzed in the presence of a strong acid) was moderately successful in producing bio-oils of reduced molecular weight.

The following detailed conclusions can be drawn from this work:

- (1) Ru metal is a much more effective catalyst in the hydroprocessing of Kraft lignin (KL) and organosolv lignin (OL) in supercritical acetone than Ni metal. Additionally,

the carbon-supported Ru (and NiMoW-based FHUDES-2) catalyst performed better than alumina-supported Ru catalyst. This difference may be due to the acidic nature of the alumina support. The molecular weights of the hydroprocessed DKL and DOL were markedly lower than the lignin feeds (~1,000 vs. 2,600 and 10,200 g/mol for OL and KL, respectively). The molecular weight of organosolv lignin decreased monotonically with increased temperature but temperatures greater than 300 °C were required to materially decrease the molecular weight of Kraft lignin. In addition, after hydroprocessing, the sulfur content of the DKL was found to have decreased by ~95% relative to the KL feed. The modest decrease in oxygen content of 20-30% may be due to the difference in strength of C-O bonds (358 kJ/mol) relative to C-S bonds (272 kJ/mol) in addition to difference in bond strength between aromatic and aliphatic C-OH bonds.

- (2) A systematic study of the effectiveness of carbon-supported Ru and novel noble metal/transition metal MoRu catalysts on the hydroprocessing of guaiacol revealed that activated carbon-supported MoRu and Mo catalyst were more effective than the reference Ru/C catalyst, exhibiting greater than 90% guaiacol conversion. However, the Mo catalyst produced fewer deoxygenated compounds and more unidentified compounds. The MoRu catalyst also exhibited greater gasification of the guaiacol feed.

Based on these findings MoRu catalyst was used for further optimization work. Hydroprocessing temperature and initial hydrogen pressure were found to have a much greater effect on guaiacol conversion than reaction duration. Thus, longer reaction times may not be necessary provided that hydroprocessing is performed at higher temperatures: the decreased duration may offset the higher energy cost.

- (3) All of the catalysts tested in the depolymerization and hydroprocessing of organosolv lignin in supercritical acetone were effective. However, the presence of phosphorus in the catalyst, which is known to decrease solid residue and improve product yields in

model compounds, was found to inhibit the depolymerization of the organosolv lignin, perhaps due to residual acidity. The yields of depolymerized organosolv lignin were found to decrease with increasing reaction temperature, in contrast to previous work. At 250 °C, the yields were equivalent to work presented a previous chapter (>96 wt.%), however, at 300 °C, while the yields with the MoRu/AC catalyst remained high (~93 wt.%), only ~62 wt.% of DOL was produced using the reference Ru/C catalyst. At 340 °C, the yield of Ru/C DOL had decreased further to ~50 wt.%, and the DOL yield with MoRu/AC catalyst experienced a large decrease to ~62 wt.%. It is believed that this difference is due mainly to the difference in initial hydrogen pressure (5 MPa in this study vs. 9 MPa in the previous work) as well as differences in heat and mass transfer effects between the different autoclave reactors that were used (100 vs. 500 mL).

The catalysts tested resulted in DOL products with greatly decreased molecular weights. The molecular weight of DOL hydroprocessed at 340 °C in the presence of the most effective MoRu/AC catalyst was reduced from ~2,600 g/mol for the OL feed to 460 g/mol. Under similar reaction conditions, the MoRu/C and reference Ru/C catalysts produced DOLs with molecular weights of 516 and 540 g/mol, respectively. All three of these DOL products remained liquid even at temperatures below 0 °C.

GC/MS analysis of the DOL revealed the presence of a large variety of substituted phenolic and benzene compounds, consistent with the depolymerization of the aromatic structures of OL. Unexpectedly, the acetone solvent was found to have reacted and formed a number of dimers.

The oxygen content of the DOL obtained with MoRu/AC catalyst at 340 °C was found to have decreased by ~38% as compared to ~25% for Ru/C, indicating that the addition of Mo to the Ru catalyst had a synergistic effect in oxygen removal. In contrast, the Ru/C catalyst was found to have increased hydrogen content by ~50% as compared to ~42% for the MoRu/AC. The addition of Mo to carbon-supported Ru catalysts was therefore an effective means of increasing the yield of DOL and improving its quality.

- (4) Hydrolysis lignin (HL) was successfully depolymerized (liquefied) in the presence of hydrogen, carbon-supported mixed noble metal/transition metal catalysts and supercritical acetone solvent, producing low molecular weight bio-oils (as low as 380 g/mol) with high yields around 85 wt.%, that remained liquid at temperatures below freezing. The yields of HL bio-oil were found to increase with increasing temperature. At 340 °C and with MoRu/AC catalyst, the yield of solid residue was less than 2 wt.%.

Deoxygenation of HL was found to be largely thermally driven - the yields and M_w as well as the chemical composition of the bio-oils were strongly dependent on the reaction temperature. Hydrogenation was highly promoted by the presence of the MoRu/AC catalyst at 340 °C, resulting in a bio-oil with a remarkable 50% increase in hydrogen content relative to the HL feed. GC/MS analysis of the bio-oils revealed that in addition to the presence of ketones from the decomposition of the carbohydrates present in the HL feed, the bio-oils were largely composed of phenolic compounds. This indicates that, in the presence of the MoRu catalyst, the lignin component of HL can easily be depolymerized at temperatures between 200 and 340 °C.

- (5) Depolymerized hydrolysis lignin (DHL), produced by processing HL in the presence of ethylene glycol and H_2SO_4 , was successfully hydroprocessed and further depolymerized into lower molecular weight products after reaction with MoRu/AC and Ru/C catalysts in supercritical acetone under hydrogen. The yields were reasonably high (~83 wt.%) at lower temperatures (250 °C) but decreased with increasing temperature. Hydroprocessing with the MoRu/AC catalyst resulted in consistently greater yields of bio-oil than with the reference Ru/C catalyst (by ~12 wt.%) regardless of reaction temperature. The yield of solid residue, or char, was high and increased in step with the decrease in bio-oil yields. Gasification of the DHL feed was found not to be significant, amounting to less than 4 wt.% at most.

Elemental analysis of the hydroprocessed DHL revealed an increase in oxygen content at 250 °C that was attributed to the acetone solvent reacting with the DHL feed. The increase in O content decreased with increased reaction temperature indicating

that the reaction between the acetone and DHL occurred very rapidly and at lower temperatures. Despite the decreased yields of bio-oil that were obtained after reaction at higher temperatures, the molecular weights of the resulting bio-oils were found to have decreased by ~65% relative to the DHL feed (~600 vs. ~1,700 g/mol). However, despite the decrease in molecular weight, these bio-oils were very viscous and unsuitable for use without further processing.

8.2 Future Work

- (1) Carbon-supported Ru catalysts were found to be very effective in the hydroprocessing of various lignins, and the addition of 1 wt.% Mo to 5 wt.% Ru catalyst resulted in improved catalytic performance. However, at 5 wt.% Ru, this is a very expensive catalyst. More work needs to be done in order to determine the most effective combination of Mo and Ru and reduce the cost of the catalyst. This has to be done without sacrificing catalyst effectiveness in terms of lignin depolymerization as well as deoxygenation and hydrogenation. The effectiveness of additional promoters, e.g. Co, should also be investigated.
- (2) Hydroprocessing of Kraft lignin (KL) should be investigated with the MoRu/AC catalyst to determine if this catalyst retains its excellent performance, as seen with OL. This work should be performed in a high-pressure reactor with OL as well as KL, as this would determine if the differences in catalyst performance that were observed are indeed due to higher initial hydrogen pressure.
- (3) The hydroprocessing of hydrolysis lignin (HL) resulted in very high yields of low molecular weight bio-oils. It would be interesting to see if optimization of process conditions could further reduce HL bio-oil molecular weight and oxygen content.
- (4) Despite the promising reduction in molecular weight obtained with the MoRu/AC catalyst, the poor yields of product from the DHL feed and high yields of char indicate that more work needs to be done to obtain useful products from the hydroprocessing of DHL. Ensuring that residual acidity from the initial hydrolysis step is vital,

as acidity is well known for promoting condensation reactions. The trends in DHL deoxygenation indicate that O removal improves with increased temperature. Therefore, further hydroprocessing studies of DHL should be performed in a reactor capable of withstanding elevated temperatures and the correspondingly higher pressures. A corollary to this study would be hydroprocessing of DHL at higher initial hydrogen pressures and lower temperatures.

- (5) The purpose of producing DHL was to convert HL into a product with reduced molecular weight for use as a substitute for the polyol feed in the production of bio-polyurethane foams. However, the solid DHL product had to be oxypropylated in order to be used. In contrast, the hydroprocessing of HL in this work resulted in very low molecular weight bio-oils that remained liquid at temperatures below freezing. It would be interesting to investigate if these bio-oils could serve as a viable substitute for oxypropylated DHL in the production of bio-polyurethane foams.
- (6) Most industrial processes run on a continuous or semi-continuous basis, therefore the hydroprocessing of lignin using the MoRu/Ac catalyst used in these experiments should be investigated under continuous or semi-continuous conditions to facilitate scale-up.

Curriculum Vitae

Name: Matthew Alexander Tymchyshyn

Post-secondary Education and Degrees:

Sheridan College of Applied Arts and Technology
Brampton, Ontario, Canada
1997-2000 Chemical Environmental Engineering Technologist Diploma

Lakehead University
Thunder Bay, Ontario, Canada
2005-2008 B.Eng. in Chemical Engineering

Lakehead University
Thunder Bay, Ontario, Canada
2008-2010 M.Sc.Eng. in Environmental Engineering

The University of Western Ontario
London, Ontario, Canada
2011-2015 Ph.D. Chemical Engineering

Honours and Awards:

Sheridan College, Canadian Society for Chemistry Silver Medal
2000

Lakehead University Transfer Student Scholarship
2005

Lakehead University Returning Student Bursary
2006-2007

Lakehead University Dr. Joseph Swartz Memorial Scholarship
2010

UWO Dean's Scholarship
2011

Mitacs-Accelerate Internship
2014-15

**Related Work
Experience**

Research Technician, OSB Technical Service
Dynea Canada Ltd.
2000-2004

Summer Research Student
Lakehead University Green Energy Laboratory
2007

Graduate Assistant
Lakehead University
2008-2010

Graduate Researcher
Lakehead University Green Energy Laboratory
2010

Teaching Assistant
The University of Western Ontario
2011-2012

Publications:

Tymchyshyn, Matthew and Xu, Charles. Liquefaction of biomass in hot compressed water for the production of phenolic compounds, *Bioresour. Technol.*, 2010, 101(7), 2483-2490.

Tymchyshyn, Matthew; Yuan, Zhongshun and Xu, Charles. Reforming of glycerol into bio-crude: A parametric study, *IJCRE*, 2013, 11(1), 1-13.

Tymchyshyn, Matthew; Yuan, Zhongshun and Xu, Charles. Direct conversion of glycerol into bio-oil via hydroprocessing using supported metal catalysts, *Fuel*, 2013, 112, 193-202.

Huang, Shanhua; Mahmood, Nubla; **Tymchyshyn, Matthew**; Yuan, Zhongshun; Xu, Chunbao (Charles). Reductive De-polymerization of Kraft Lignin for Chemicals and Fuels using Formic Acid as an In-situ Hydrogen Source, *Bioresour. Technol.*, 2014, 171, 95-102.

Reyhantash, Ehsan; **Tymchyshyn, Matthew**; Yuan, Zhongshun; Albion, Katherine; van Rossum, Guus; Xu, Chunbao (Charles). Upgrading Fast Pyrolysis Oil via Hydrodeoxygenation and Thermal Treatment: Effects of Catalytic Glycerol Pretreatment. *Energy Fuels*, 2014, 28(2), 1132-1138.

Xu, Chunbao (Charles); Shao, Yuanyuan; Yuan, Zhongshun; Cheng, Shuna; Feng, Shanghuang; Nazari, Laleh; **Tymchyshyn, Matthew**. Hydrothermal liquefaction of biomass in hot-compressed water, alcohols and alcohol-water co-solvents for bio-crude production, Application of Hydrothermal Reactions to Biomass Conversion, Springer Berlin Heidelberg, 2014, 171-187.

Xu, Chunbao (Charles); Reyhantash, Ehsan; van Rossum, Guus; Yun, Yang; Yuan, Zhongshun; Ahmadi, Shima; Guo, Cheng; Rohani, Sohrab; **Tymchyshyn, Matthew**; Albion, Katherine; Yang, Linxi; He, Quan (Sophia); Shui, Hengfu. Fast Pyrolysis Oils and Hydrothermal Liquefaction Bio-crude Oils: Composition and Upgrading, Reaction Pathways and Mechanisms in Thermocatalytic Biomass Conversion, Springer Berlin Heidelberg, 2015.

Submitted for Publication:

Tymchyshyn, Matthew; Yuan, Zhongshun; Xu, Charles C. Reductive depolymerization of Kraft lignin and organosolv lignin for aromatic chemicals and materials, In submission.

Huang, Shanhua; **Tymchyshyn, Matthew**; Mahmood, Nubla; Yuan, Zhongshun; Xu, Chunbao (Charles). Catalytic Reductive De-polymerization of Kraft Lignin into Bio-chemicals & Fuels, In submission.

Mahmood, Nubla; Yuan, Zhongshun; **Tymchyshyn, Matthew**; Schmidt, John; Xu, Chunbao (Charles). Hydrolytic Depolymerization of Hydrolysis Lignin for the Preparation of Bio-based Rigid Polyurethane Foam, In submission.

Zhang, Yongsheng; Nanda, Malaya; **Tymchyshyn, Matthew**; Yuan, Zhongshun; Xu, Charles C. Thermal, Physical and Mechanical Properties of HMTA-Cured Phenol-Hydroxymethylfurfural (PHMF) Resin-based Glass Fiber Reinforced Composites - Effects of

Amount of the Curing Agents, In submission.

To be Submitted:

Tymchyshyn, Matthew; Yuan, Zhongshun; Xu, Chunbao (Charles). Screening of carbon-supported catalysts for lignin hydroprocessing using guaiacol as a model compound, To be submitted.

Tymchyshyn, Matthew; Yuan, Zhongshun; Xu, Chunbao (Charles). Hydroprocessing of organosolv lignin for aromatic chemicals and materials using carbon-supported MoRu catalysts, To be submitted.

Tymchyshyn, Matthew; Nanda, Malaya; Yuan, Zhongshun; Xu, Chunbao (Charles). Reductive depolymerization of hydrolysis lignin for aromatic chemicals and fuels, To be submitted.

Tymchyshyn, Matthew; Nanda, Malaya; Mahmood, Nubla; Yuan, Zhongshun; Xu, Chunbao (Charles). Hydroprocessing of depolymerized hydrolysis lignin, To be submitted.

Nanda, Malaya; **Tymchyshyn, Matthew;** Yuan, Zhongshun; Qin, Wensheng; Xu, Chunbao (Charles). Crude glycerol: A liability or an evolving opportunity, To be submitted.

Reyhanitash, Ehsan; **Tymchyshyn, Matthew;** Yuan, Zhongshun; Albion, Katherine; van Rossum, Guus; Xu, Chunbao (Charles). Effects of catalytic alcohol pre-treatment using various alcohols on hydrodeoxygenation of fast pyrolysis oil, To be submitted.